Defining the Role of IL-18 in the Renal Inflammation Leading to Hypertension

Jordyn Michele Thomas

B. BiomedSc. (Hons)

A thesis submitted in total fulfilment of the requirements of the degree of

DOCTOR OF PHILOSOPHY

Department of Physiology, Anatomy and Microbiology

School of Life Sciences

College of Science, Health and Engineering

La Trobe University, Victoria, Australia

June 2021

© Copyright by Jordyn M Thomas (2021)

All Rights Reserved.

Except as provided in the Copyright Act 1968, this thesis may not be reproduced in any form without the written permission of the author.

I certify that I have made all reasonable efforts to secure copyright permissions for third-party content included in this thesis and have not knowingly added copyright content to my work without the owner's permission.

Table of Contents

Table of Contents III

List of Figures IX

List of Tables XII

Abstract XIII

Statement of Authorship XV

Acknowledgements XVII

Publications Arising from this Work XIX

Conference Presentations XX

Abbreviations XXIII

Chapter 1: Introduction **1**

1.1 Abstract 2

1.2 Introduction 3

1.3 IL-18 production in the kidneys 4

1.4 Targets of IL-18 in the kidneys 10

1.5 Evidence for pathogenic roles of IL-18 signalling in kidney disease: Preclinical studies 17

1.6 IL-18 mechanisms of action in the kidney 18

1.6.1 Classical IL-18 signalling: IL-18 the "IFN-γ-inducing factor" (IGIF) 18

1.6.2 IL-18 signalling via JAK-STAT pathways: IL-17 production 19

1.6.3 IL-18 signalling via NFκB pathways 19

1.6.4 IL-18 signalling via Src/ERK pathways 21

1.6.5 IL-18 signalling via PI3K/Akt and JNK pathways 21

1.6.6 Autocrine/paracrine IL-18 signalling 22

1.7 Targeting IL-18R1 signalling in preclinical studies 22

1.8 IL-18 as a biomarker for kidney injury 23

1.8.1 IL-18 as a biomarker for AKI 24

1.8.2 IL-18 as a biomarker for AKI in the paediatric population 25

1.8.3 IL-18 as a biomarker for cardiovascular risk and mortality in CKD 25

1.8.4 Future directions 26
1.9 Targeting IL-18 in the clinic 26
1.10 Conclusion 27
1.11 Hypothesis and aims of the thesis 28
1.12 References 30
Chapter 2: General Methods 47
2.1 Animals 48
2.2 Generation of IL-18RAP-deficient mice 48
2.3 Induction of hypertension 49
2.4 Bone marrow transplantation 50
2.5 Adoptive transfer of T cells 51
2.6 Bolus saline challenge to assess renal function and urine metabolites 51
2.7 Blood pressure measurements 52
2.7.1 Tail cuff plethysmography 52
2.7.2 Radiotelemetry 53
2.8 Measurement mRNA expression levels 54
2.9 Flow cytometric analysis 56
2.9.1 Intracellular Cytokine Detection 57
2.10 Histopathology staining 58
2.11 Immunohistochemistry 59
2.12 Statistics 59
2.13 References 61
2.14 Tables 62
2.15 Figures 64
Chapter 3: Interleukin-18 Produced by Renal Tubular Epithelial Cells Promotes Hypertension and Kidney Damage Induced by Deoxycorticosterone Acetate/Salt in Mice 66
3.1 Summary 67
3.2 Graphical abstract 68
3.3 Introduction 69
3.4 Methods 71

3.4.1 Transparency and Openness Promotion 71
3.4.2 Animals 71
3.4.3 Induction of hypertension 71
3.4.4 Bone marrow cell transplantation 72
3.4.5 Saline challenge to assess fluid volume loading and renal injury 72
3.4.6 Blood pressure measurements 73
3.4.7 Measurement mRNA expression levels 73
3.4.8 Flow cytometric analysis 73
3.4.9 Histopathology staining 74
3.4.10 Immunohistochemistry 75
3.4.11 Statistics 75
3.5 Results 77
3.5.1 IL-18$^{-/-}$ mice are protected from 1K/DOCA/salt-induced hypertension 77
3.5.2 IL-18$^{-/-}$- mice are protected from 1K/DOCA/salt-induced renal inflammation 77
3.5.3 IL-18$^{-/-}$ mice are protected from 1K/DOCA/salt-induced renal fibrosis and histopathology 78
3.5.4 IL-18$^{-/-}$ mice are protected from 1K/DOCA/salt-induced volume overload and kidney dysfunction 79
3.5.5 T cells and tubular epithelial cells are likely targets of IL-18 in hypertensive kidneys 80
3.5.6 IL-18 is produced by renal tubular epithelial cells 81
3.5.7 Non-bone marrow-derived IL-18 causes renal fibrosis and injury in 1K/DOCA/salt-induced hypertension 82
3.6 Discussion 83
3.6.1 Perspectives 88
3.7 References 89
3.8 Figures 95
3.9 Supplementary Methods 101
3.9.1 Animals 101
3.9.2 Induction of hypertension 101

3.9.3 Bone marrow cell transplantation 102

3.9.4 Saline challenge to assess fluid volume loading and renal injury 102

3.9.5 Blood pressure measurements 103

3.9.6 Measurement mRNA expression levels 103

3.9.7 Flow cytometric analysis 104

3.9.8 Intracellular Cytokine Detection 105

3.9.9 Histopathology staining 106

3.9.10 Immunohistochemistry 107

3.9.11 Statistics 107

3.10 Supplementary Tables 108

3.11 Supplementary Figures 110

Chapter 4: Interleukin-18 Receptor 1 Positive T Cells are not Essential to Kidney Inflammation and Damage Induced by Deoxycorticosterone Acetate/Salt in Mice 121

4.1 Summary 122

4.2 Introduction 124

4.3 Methods 125

4.3.1 Animals 125

4.3.2 Induction of hypertension 125

4.3.3 Adoptive transfer of T cells 126

4.3.4 Blood pressure measurements 126

4.3.5 Measurement mRNA expression levels 127

4.3.6 Flow cytometric analysis 127

4.3.7 Histopathology staining 129

4.3.8 Immunohistochemistry 129

4.3.9 Statistics 129

4.4 Results 131

4.4.1 IL-18R1$^{-/-}$ mice are protected from 1K/DOCA/salt-induced hypertension but have a higher incidence of abdominal aortic aneurysms 131

4.4.2 IL-18R1-deficiency does not prevent immune cell accumulation and activation in the kidneys of 1K/DOCA/salt-treated mice 132

4.4.3 T cell-specific IL-18R1 deficiency provides protection against 1K/DOCA/salt-induced hypertension 132

4.4.4 T cell-specific IL-18R1 deficiency does not confer protection against 1K/DOCA/salt-induced renal inflammation 134

4.4.5 RAG1$^{-/-}$ mice that receive WT, or IL-18R1$^{-/-}$ T cells are not protected from 1K/DOCA/salt-induced kidney fibrosis 135

4.5 Discussion 137

4.6 References 141

4.7 Figures 144

4.8 Supplementary Tables 155

4.9 Supplementary Figures 157

Chapter 5: Interleukin-18 Receptor Accessory Protein Is Not Required for the Development of Renal Inflammation and Elevated Blood Pressure in 1 Kidney /DOCA/Salt-Induced Hypertension in Mice 158

5.1 Summary 159

5.2 Introduction 161

5.3 Methods 163

5.3.1 Animals 163

5.3.2 Generation of IL-18RAP-deficient mice 163

5.3.3 Induction of hypertension 164

5.3.4 Blood pressure measurements 164

5.3.5 Measurement mRNA expression levels 165

5.3.6 Flow cytometric analysis 165

5.3.7 Measurement of T cell IFN-γ production 167

5.3.8 Histopathology staining 167

5.3.9 Immunohistochemistry 168

5.3.10 Statistics 168

5.4 Results 169

5.4.1 Effect of IL-18RAP gene deletion on IL-18 signalling and IL-18 receptor expression in the kidneys 169

5.4.2 IL-18RAP gene-deficiency does not protect against 1K/DOCA/salt-induced hypertension 169

5.4.3 IL-18RAP-deficiency does not influence the incidence of abdominal aortic aneurysms or mortality rate 170

5.4.4 IL-18RAP-deficiency does not alter the expression of inflammatory genes in the kidney of 1K/DOCA/salt-treated mice 171

5.4.5 IL-18RAP-deficiency does not alter renal immune cell infiltration in 1K/DOCA/salt-treated mice 171

5.4.6 IL-18RAP-deficiency does not alter renal fibrosis in 1K/DOCA/salt-treated mice 172

5.4.7 Neither male nor female IL-18RAP deficient mice are afforded protection from renal injury associated with 1K/DOCA/salt hypertension 172

5.5 Discussion 173

5.6 References 178

5.7 Figures 181

5.8 Supplementary Tables 192

5.9 Supplementary Figures 193

Chapter 6: General Discussion 196

6.1 Summary of key findings 197

6.2 IL-18-IL-18R1-IL-18RAP signalling axis in CKD 197

6.3 Stimuli for IL-18 production 205

6.4 Potential mechanisms for IL-18-mediated Na^+ reabsorption and increase in BP 209

6.5 Inhibition of IL-18 213

6.6 Overall conclusion 216

6.7 References 218

List of Figures

Figure 1.1 Cellular sources of IL-18 in the kidney 6

Figure 1.2 Schematic representation of DAMPs/PAMPs that initiate inflammasome activation in the kidney 8

Figure 1.3 Schematic representation of IL-18, IL-37 IL-18R1, IL-18RAP and IL-1R8 structure and binding 12

Figure 1.4 Schematic representation of IL-18 pro-inflammatory signalling in kidney injury 13

Figure 1.5 IL-18BP isoforms a, b, c and d and their affinity to neutralise IL-18 15

Figure 2.1 Gating strategy for flow cytometric analysis 64

Figure 2.2 Gating strategy for intracellular cytokine detection using flow cytometric analysis. 65

Figure 3.1 1K/DOCA/salt-induced hypertension is blunted in IL-18$^{-/-}$ mice 95

Figure 3.2 IL-18$^{-/-}$ mice are protected from 1K/DOCA/salt-induced renal immune cell infiltration and inflammatory gene expression. 96

Figure 3.3 IL-18$^{-/-}$ mice are protected from renal fibrosis and damage associated with 1K/DOCA/salt hypertension 97

Figure 3.4 IL-18R1 is localised to T cells and tubular epithelial cells in kidneys of 1K/DOCA/salt-treated mice 98

Figure 3.5 Tubular epithelial cells are the main source of IL-18 in the kidneys of 1K/DOCA/salt-treated mice 99

Figure 3.6 Bone marrow-derived cells are not responsible for IL-18-mediated fibrosis and tubular damage in 1K/DOCA/salt-induced hypertension 100

Supplementary Figure 3.1 Gating strategy for flow cytometric analysis 110

Supplementary Figure 3.2 Gating strategy for intracellular cytokine detection using flow cytometric analysis 111

Supplementary Figure 3.3 Radiotelemetry heart rate measurements in 1K/DOCA/salt-treated WT and IL-18$^{-/-}$ mice 112

Supplementary Figure 3.4 1K/DOCA/salt-induced upregulation of the IL-18 signalling system is blunted in IL-18$^{-/-}$ mice 113

Supplementary Figure 3.5 IL-18$^{-/-}$ mice are protected from 1K/DOCA/salt-induced T cell infiltration of the kidney 114

Supplementary Figure 3.6 IL-18$^{-/-}$ mice are protected from 1K/DOCA/salt-induced upregulation of renal collagen gene expression 115

Supplementary Figure 3.7 IL-18-deficiency protects against 1K/DOCA/salt-mediated volume loading and renal injury 116

Supplementary Figure 3.8 Proportion of CD45^{+} immune cell subsets expressing IL-18R1 in 1K/placebo- and 1K/DOCA/salt-treated wild-type mice 117

Supplementary Figure 3.9 Percentage of IL-18R1-expressing $CD3^+$ T cells in 1K/placebo- and 1K/DOCA/salt-treated wild-type mice 118

Supplementary Figure 3.10 IL-18-induced IFN-γ production in T cells isolated from 1K/placebo- and 1K/DOCA/salt-treated WT mouse kidneys 119

Supplementary Figure 3.11 Immunolocalisation of IL-18 and aquaporin 1 (AQP-1) in 1K/DOCA/salt-treated mouse kidney sections 120

Figure 4.1 1K/DOCA/salt-induced hypertension is blunted in IL-18R1$^{-/-}$ mice at day 21, but IL-18R1$^{-/-}$ mice are more susceptible to abdominal aortic aneurysms 144

Figure 4.2 IL-18R1-deficiency prevents the accumulation of IL-18R1$^+$ in the kidneys of 1K/DOCA/salt-treated mice 145

Figure 4.3 IL-18R1$^{-/-}$ mice are not protected from 1K/DOCA/salt-induced renal immune cell infiltration 146

Figure 4.4 IL-18R1 staining is absent in IL-18R1$^{-/-}$ mice and localised to T cells and tubular epithelial cells in the kidney of 1K/DOCA/salt-treated WT mice 148

Figure 4.5 1K/DOCA/salt-induced hypertension is blunted in mice with T cell specific IL-18R1-deficiency 149

Figure 4.6 Mice with T cell specific IL-18R1-deficiency are not protected from 1K/DOCA/salt-induced renal immune cell infiltration 150

Figure 4.7 Mice with T cell specific IL-18R1-deficiency are not protected from 1K/DOCA/salt-induced renal inflammatory gene expression 152

Figure 4.8 Mice with T cell specific IL-18R1-deficiency are not protected from 1K/DOCA/salt-induced renal fibrosis 154

Supplementary Figure 4.1 Gating strategy for intracellular cytokine detection using flow cytometric analysis 157

Figure 5.1 IL-18RAP gene dose influences IL-18-mediated cytokine production 181

Figure 5.2 Neither male nor female IL-18RAP$^{-/-}$ mice are afforded protection from 1K/DOCA/salt-induced increases in BP 182

Figure 5.3 Genetic and protein gene dosing effect is present in 1K/DOCA/salt-treated IL-18RAP$^{+/+}$, IL-18RAP$^{+/-}$ and IL-18RAP$^{-/-}$ mice 183

Figure 5.4 Neither male nor female IL-18RAP$^{-/-}$ mice are afforded protection from 1K/DOCA/salt-induced mortality due to the development and rupture of abdominal aortic aneurysms 185

Figure 5.5 Neither male nor female IL-18RAP$^{-/-}$ mice are afforded protection from 1K/DOCA/salt-induced expression of inflammatory genes in the kidney 186

Figure 5.6 Neither male nor female IL-18RAP$^{-/-}$ mice are afforded protection from 1K/DOCA/salt-induced renal immune cell infiltration 187

Figure 5.7 Neither male nor female IL-18RAP$^{-/-}$ mice are afforded protection from renal fibrosis associated with 1K/DOCA/salt hypertension 188

Figure 5.8 Neither male nor female IL-18RAP$^{-/-}$ mice are afforded protection from renal tubular damage in 1K/DOCA/salt-induced hypertension 190

Supplementary Figure 5.1 Gating strategy for intracellular cytokine detection using flow cytometric analysis 193

Supplementary Figure 5.2 Gating strategy for intracellular cytokine detection using flow cytometric analysis 194

Supplementary Figure 5.3 Genotype results for IL-18RAP knockout mice 195

Figure 6.1 Immunolocalisation of IL-18R1 in the papilla of 1K/DOCA/salt-treated mouse kidney sections 203

Figure 6.2 Hypothetical mechanism by which IL-18 regulates sodium (Na^+) homeostasis in the kidney 204

Figure 6.3 Schematic representation of DAMPs/PAMPs that initiate inflammasome activation in tubular epithelial cells (TECs) 208

Figure 6.4 Mechanisms by which pro-inflammatory cytokines regulate sodium (Na^+) reabsorption in the kidney 212

List of Tables

Table 1.1 Cellular sources of IL-18 in the kidney 7

Table 1.2 Renal inflammasome expression 10

Table 2.1 Mice treated with 1K/DOCA/salt or 1K/placebo 62

Table 2.2 Mice used for bone marrow (BM) transplant study 62

Table 2.3 Mice used for T cell transfer study 63

Table 2.4 Antibody panel for flow cytometry 63

Table 2.5 Immunohistochemistry antibodies 63

Table 3.1 Mice used for 1K/DOCA/salt vs. 1K/placebo studies 107

Table 3.2 Mice used for bone marrow transplant studies 107

Table 3.3 Antibodies used for flow cytometry 108

Table 3.4 Antibodies used for flow cytometry experiments to detect T cell-derived IFN-γ 108

Table 4.1 Mice used for this study 154

Table 4.2 Antibody panel for flow cytometry 155

Table 5.1 Mice used for this study 191

Table 5.2 Antibody panel for flow cytometry 191

Table 6.1 Drugs that inhibit inflammasome activity 215

Abstract

Previous work from our lab has demonstrated that the NLRP3 inflammasome is critical to the development of renal inflammation and elevated blood pressure in experimental models of hypertension. The NLRP3 inflammasome is responsible for activating the cytokines, interleukin (IL)-1β and IL-18, which then stimulate cognate receptors on neighbouring cells to initiate inflammatory signalling cascades. It is established that IL-18 is elevated in the circulation of patients with hypertension; however, whether this cytokine plays a causal role in the pathogenesis of hypertension and renal inflammation remains unknown. The aims of this thesis were to establish if IL-18, and its cognate receptor complex, are required for the development of hypertension and kidney disease in a model of low-renin hypertension in mice involving removal of a kidney and treatment with deoxycorticosterone and salt (1K/DOCA/salt).

In Chapter 3, I demonstrated that 1K/DOCA/salt-induced hypertension in mice is associated with upregulation of IL-18 on renal tubular epithelial cells, and accumulation of IL-18 receptor (IL-18R1)-expressing leukocytes in the kidneys. I further showed that IL-18 acts on T cells to cause the production of IFN-γ in hypertension. Global gene deletion of IL-18 was protective against the development of kidney inflammation, fibrosis, and high blood pressure in 1K/DOCA/salt-treated mice. Bone marrow (BM) transplant studies suggested that non-BM cell-derived IL-18 was driving 1K/DOCA/salt-induced chronic kidney disease (CKD) and related pathologies.

In Chapter 4, I demonstrated that global and T cell restricted IL-18R1-deficiency is protective against the development of 1K/DOCA/salt-induced hypertension in mice. However, IL-18R1$^{-/-}$ mice were susceptible to the development and rupture of abdominal aortic aneurysms in response to 1K/DOCA/salt-treatment and global and T cell restricted IL-18R1-deficiency was not protective against 1K/DOCA/salt-induced kidney inflammation.

In Chapter 5, I used IL-18 receptor accessory protein (RAP)$^{-/-}$ mice (generated specifically for this project) to determine the role of this subunit of the IL-18 receptor complex in the development of hypertension and kidney disease in 1K/DOCA/salt-treated mice. IL-18RAP$^{-/-}$ mice developed a similar level of hypertension, renal inflammation and damage following 1K/DOCA/salt treatment as observed in wild type mice. Therefore, IL-18 likely mediates its pro-hypertensive and renal-damaging effects through IL-18R1 and non-cognate signalling mechanisms distinct from IL-18RAP.

In conclusion, these findings provide evidence that the inflammasome-derived cytokine IL-18 is a crucial mediator of elevated blood pressure, kidney inflammation, fibrosis, and dysfunction during hypertension. Interestingly, the hypertensive and renal inflammatory effects of IL-18 appear to be mediated by non-cognate signalling pathways that are partially reliant on IL-18R1, but independent of IL-18RAP. Further understanding of these non-cognate IL-18 signalling mechanisms may unearth novel targets for future therapies against hypertension and chronic kidney disease.

Statement of Authorship

Except where reference is made in the text of the thesis, this thesis contains no material published elsewhere or extracted in whole or in part from a thesis accepted for the award of any other degree or diploma. No other person's work has been used without due acknowledgment in the main text of the thesis. This thesis has not been submitted for the award of any degree or diploma in any other tertiary institution.

This work was supported by an Australian Government Research Training Program Scholarship.

All research procedures reported in this thesis were carried out with the approval of the

La Trobe University Animal Ethics Committee (AEC16-93).

This thesis includes (1) original paper under review at a peer reviewed journal and (1) review article and (2) unpublished publications. The core theme of this thesis is 'Defining the role of IL-18 in the renal inflammation leading to hypertension'. The ideas, development and writing up of all the papers in this thesis were the principal responsibility of myself, the candidate, working within the Department of Physiology, Anatomy and Microbiology under the supervision of Prof Grant Drummond (primary supervisor), Dr Brooke Huuskes (co-supervisor) and Dr Antony Vinh (co-supervisor). The inclusion of co-authors reflects the fact that the work came from active collaboration between researchers and acknowledges input into team-based research.

In the case of Chapters 1, 3, 4 and 5 my contribution to the work involved the following:

Thesis Chapter	Publication title	Publication status	Nature and extent of contribution
1	The IL-18/IL-18R Signalling Axis: Diagnostic and Therapeutic Potential in Hypertension and Chronic Kidney Disease	Manuscript completed	Wrote the review paper with assistance from co-authors: Christopher G Sobey, Antony Vinh, Brooke M Huuskes, Grant R. Drummond

3	Interleukin-18 Produced by Renal Tubular Epithelial Cells Promotes Hypertension and Kidney Damage Induced by Deoxycorticosterone Acetate/Salt in Mice	Under review	Conducted all experiments and data analysis, except for radiotelemetry, T cell stimulation and blinded scoring of haematoxylin and eosin staining. Prepared figures and wrote the manuscript, with intellectual advice and assistance from co-authors: Yeong H Ling, Brooke M Huuskes, Prerna Sharma, Narbada Saini, Dorota M Ferens, Henry Diep, Shalini M Krishnan, Barbara K Kemp-Harper, Paul M O'Connor, Eicke Latz, Thiruma V Arumugam, Tomasz J Guzik, Michael J Hickey, Ashley Mansell, Christopher G Sobey, Antony Vinh, Grant R Drummond.
4	Inhibition of Interleukin-18R1-Mediated Signalling in T cells Prevents Hypertension but Does Not Supress Renal Inflammation	Manuscript completed	Conducted all experiments and data analysis, prepared figures and wrote the manuscript, with intellectual advice and assistance from co-authors: Brooke M Huuskes, Christopher G Sobey, Antony Vinh, Grant R Drummond.
5	Interleukin-18 Receptor Accessory Protein Is Not Required for the Development of Renal Inflammation and Elevated Blood Pressure in 1 Kidney /DOCA/Salt-Induced Hypertension in Mice	Manuscript completed	Conducted all experiments and data analysis, except for PCR in naïve mice and blinded scoring of haematoxylin and eosin staining. Prepared figures and wrote the manuscript, with intellectual advice and assistance from co-authors: Quynh Nhu Dinh, Hericka Bruna Figueiredo Galvao, Brooke M Huuskes, Narbada Saini, Christopher G Sobey, Antony Vinh, Grant R Drummond.

Jordyn Thomas

9 June 2021

Acknowledgements

I would like to offer my sincerest thanks to everyone who has made it possible to conduct the research to complete this thesis.

First and foremost, I would like to thank my brilliant supervisory team, who have always gone above and beyond to offer me advice, mentor, challenge, support and encourage me within research and extracurricular endeavours. Grant, I am so grateful that you have always made time in your heavy workload to help and mentor me when I have needed it, I am always in awe of your enthusiasm for science, and your immense knowledge of all things cardiovascular and immune. I am also so thankful for your leadership in the department, and for creating an enriching research culture for HDR students. Bill, I would like to thank you so much for always encouraging me to try new things, take on new opportunities, and for making time to teach me new techniques. It has been an absolute joy to learn from you and have a good chat while we are at it! I would also like to thank Brooke for her help, especially in learning more about kidney structure, staining and immunofluorescence, and her encouragement to participate in extracurricular societies and communication activities. I am so grateful for our keeping-on-track meetings, and for her tremendous enthusiasm for kidneys!

I would like to offer an enormous thank you to the members of the Vascular Biology and Immunopharmacology Group. I am incredibly fortunate to have completed my honours year and PhD in a research group that values excellent science, support for one another, good food and fun. I am so grateful to Chris, Grant, and the theme leaders of our lab, for fostering this environment, and to everyone for sustaining it, and helping each other out when needed. I would like to say an additional thank you to Narbada, for being a lovely presence in the lab, and for her help with injury scoring. Furthermore, I would like to thank Quynh and Henry for making me feel welcome and comfortable at La Trobe when we were

just starting out, and since. I would like to further thank Henry for his help with experiments and for going out of his way to keep things running.

I am also grateful for the mentorship of Karla Helbig, who has been immensely helpful in providing advice, especially during COVID-19. Thank you, Karla, for helping me out on days where you were feeling the strain of the situation yourself, and for making time for me in your busy schedule.

I have been so privileged to complete my PhD with a wonderful HDR student cohort, who have worked hard to provide academic and social opportunities for students within the Physiology, Anatomy and Microbiology department, and made it a welcoming and pleasant place to work. A very special thank you to Ebony, Steph and Haylo for their friendship, support and for being excellent Shut Up and Write buddies. An extra special thanks to Vivian, who has been the most amazing friend to endure a PhD alongside. I am so grateful for her generosity, help and kindness, and her encouragement for everyone around her. I cannot wait to see what you all accomplish next!

I would like to extend a big thanks to my beautiful friends Ashley, Adelaide, and Maddie, I am so grateful for your patience, support, and advice while I have been doing my PhD.

I would like to acknowledge my family, who have given me every opportunity to succeed in my 20+ years of learning. They have always been models of hard work, persistence, and resilience, and have been kinder to me and more supportive of me than I could ever deserve. I would also like to thank Daphne, Scarlett, Audrey, and Lucy for tolerating all the pats, walks and cuddles that have gotten me through my PhD.

Finally, I would like to acknowledge my brilliant husband, Nick, who has been my biggest support and cheerleader, and has stuck with me through it all. Thank you for always making me laugh and helping me put things in perspective. I am beyond lucky to have you in my life.

Publications Arising from this Work

Publications resulting from work in this thesis:

Jordyn M Thomas, Yeong H Ling, Brooke Huuskes, Prerna Sharma, Narbada Saini, Dorota M Ferens, Henry Diep, Shalini M Krishnan, Barbara K Kemp-Harper, Paul M O'Connor, Eicke Latz, Thiruma V Arumugam, Tomasz J Guzik, Michael J Hickey, Ashley Mansell, Christopher G Sobey, Antony Vinh, Grant R Drummond. (2021). Interleukin-18 Produced by Renal Tubular Epithelial Cells Promotes Hypertension and Kidney Damage Induced by Deoxycorticosterone Acetate/Salt in Mice (*Under review at Hypertension (IF 7.71)*). This publication is related to Chapter 3 of this thesis*

**JM Thomas contributed significantly to the conception, design, drafting and revision of these manuscripts as evidenced by her first authorship.*

Conference Presentations

Physiology, Anatomy and Microbiology Higher Degree Research Student Research Symposium (December 2020). Title: Interleukin-18 receptor accessory protein is not required for the development of renal inflammation & elevated BP in 1 kidney/DOCA/salt-induced hypertension. **Oral presentation**. *Awarded Highly Commended 10-minute talk.*

High Blood Pressure Research Council of Australia Annual Scientific Meeting (December 2020). Title: Interleukin-18 receptor accessory protein is not required for the development of renal inflammation & elevated BP in 1 kidney/DOCA/salt-induced hypertension. **Mini Oral presentation**. *Student award session.*

Victorian Infection and Immunity Network Young Investigator Symposium (October 2020). Title: Interleukin-18 is crucial to the development of 1 kidney/DOCA/salt-induced renal inflammation and elevated blood pressure. **Poster presentation.**

High Blood Pressure Research Council of Australia Winter School (July 2020). Title: Urine Trouble! The Role of IL-18 in kidney inflammation and hypertension. **Mini Oral presentation**.

Baker-La Trobe Cardiovascular Research Symposium (January 2020). Title: Interleukin-18 is crucial to the development of 1 kidney/DOCA/salt-induced renal inflammation and elevated blood pressure. **Oral presentation**. *Awarded Best 10-minute talk.*

Physiology, Anatomy and Microbiology Higher Degree Research Student Research Symposium (December 2019). Title: Renal tubular epithelial cell derived interleukin-18 is crucial to the development of renal inflammation and elevated BP in 1 kidney/DOCA/salt-

induced hypertension. **Oral and poster presentation**. *Awarded Highly Commended 10-minute talk.*

Asian-Pacific Congress of Hypertension (November 2019). Title: Renal Tubular epithelial cell-derived Interleukin-18 is crucial to the development of renal inflammation and elevated BP in 1K/DOCA/salt-induced hypertension. **Oral presentation**. *Awarded Judith Whitworth Women in High Blood Pressure Research Award.*

La Trobe Institute for Molecular Science (LIMS) Early Career Researcher Symposium (November 2019). Title: The role of the interleukin-18 receptor in experimental kidney disease. **Poster presentation.**

Australasian Society of Clinical and Experimental Pharmacologists and Toxicologists Cardiovascular Special Interest Group Student Symposium (October 2019). Title: Renal tubular epithelial cell derived interleukin-18 is crucial to the development of renal inflammation and elevated BP in 1 kidney/DOCA/salt-induced hypertension. **Oral presentation**. *Awarded Highly Commended 10-minute talk.*

International Society of Nephrology World Congress of Nephrology (April 2019). Title: The role of the interleukin-18 receptor in experimental kidney disease. **Poster presentation.**

Physiology, Anatomy and Microbiology Higher Degree Research Student Research Symposium (December 2018). Title: A Crucial Role for Interleukin-18/IL-18R Signalling Axis in the Development of Renal Inflammation in 1K/DOCA/Salt-Induced Hypertension. **Oral and poster presentation**.

Australian and New Zealand Society of Nephrology Annual Scientific Meeting (September 2018). Title: A crucial role for interleukin-18/IL-18R signalling axis in the development of renal inflammation in 1K/DOCA/salt-induced hypertension. **Oral presentation**. *Young Investigator award session.*

La Trobe – Baker Institute Cardiovascular Research Symposium (April 2018). Title: A crucial role for interleukin-18/IL-18R signalling axis in the development of renal inflammation and elevated blood pressure in 1 kidney/DOCA/salt-induced hypertension. **Poster presentation.**

Experimental Biology (April 2018). Title: A crucial role for interleukin-18/IL-18R signalling axis in the development of renal inflammation and elevated blood pressure in 1 kidney/DOCA/salt-induced hypertension. **Oral and poster presentation.**

Australasian Society of Clinical and Experimental Pharmacologists and Toxicologists Cardiovascular Special Interest Group Student Symposium (October 2017). Title: Interleukin-18 is crucial for the development of renal inflammation and elevated blood pressure during 1 kidney/DOCA/salt-induced hypertension. **Oral presentation.**

Abbreviations

AAA	Abdominal aortic aneurysm
AIM1	Absent in melanoma 1
AIM2	Absent in melanoma 2
AKI	Acute kidney injury
ANCA	Anti-neutrophil cytoplasmic antibodies
Ang II	Angiotensin II
ANOVA	Analysis of variance
AP-1	Activator protein 1
Apo-E	Apolipoprotein E
AQP	Aquaporin
ARC	Animal Resources Centre
ASC	Apoptosis-associated speck like protein containing a caspase recruitment domain
ATP	Adenosine triphosphate
BM	Bone marrow
BP	Blood pressure
BUN	Blood urea nitrogen
CBP	Cardiopulmonary bypass
CCL	Chemokine (C-C) motif ligand
CD11b	Cluster of differentiation 11b
CD3	Cluster of differentiation 3
CD4	Cluster of differentiation 4
CD44	Cluster of differentiation 44
CD45	Cluster of differentiation 45
CD69	Cluster of differentiation 69
CD8	Cluster of differentiation 8
cDNA	Complementary de-oxy ribonucleic acid
CKD	Chronic kidney disease
Cl	Chloride
CRISPR	Clustered regularly interspaced short palindromic repeats
Ct	Cycle threshold
CXCL	Chemokine (C-X-C motif) ligand
DAMP	Danger associated molecular pattern
DAPI	4',6-Diamidino-2-Phenylindole
DGF	Delayed graft function
DNA	Deoxyribonucleic acid
DOCA	Deoxycorticosterone acetate
DPX	Dibutyl phthalate polystyrene xylene
eGFR	Estimated glomerular filtration rate
ELISA	Enzyme-linked immunoassay
EMMPRN/BSG	Extracellular matrix metalloproteinase inducer/Basigin
ENaC	Epithelial sodium channels
ERK	Extracellular receptor kinase
ESRD	End-stage renal disease
FoxP3	Forkhead box P3
FSC	Forward scatter

GAPDH	Glyceraldehyde 3-phosphate dehydrogenase
GFR	Glomerular filtration rate
ICAM	Intercellular adhesion molecule 1
ICU	Intensive care unit
IFN-γ	Interferon-γ
Ig	Immunoglobulin
IgG	Immunoglobulin G
IGIF	Interferon-gamma-inducing factor
IKK	IκB kinase
IL	Interleukin
IL-12	Interleukin-12
IL-12R	Interleukin-12 receptor
IL-17	Interleukin-17
IL-18	Interleukin-18
IL-18BP	Interleukin-18 binding protein
IL-18R1	Interleukin-18 receptor
IL-18RAP	Interleukin-18 receptor accessory protein
IL-1R8	Interleukin-1 receptor 8
IL-1β	Interleukin-1β
IL-23a	Interleukin-23a
IL-23R	Interleukin-23 receptor
IL-33	Interleukin-33
IL-37	Interleukin-37
IL-6	Interleukin-6
iNOS	Inducible nitric oxide synthase
IRI	Ischemia reperfusion injury
JAK	Just another kinase (aka Janus Kinase)
K	Potassium
Kd	Dissociation constant
LARTF	La Trobe Animal Research and Teaching Facility
LPS	Lipopolysaccharide
mAb	Monoclonal antibody
MAP	Mean arterial pressure
MAPK	Mitogen-activated protein kinase
MARP	Monash Animal Research Platform
MCP-1	Monocyte chemoattractant protein-1
MEK/ERK	Mitogen-activated protein kinase extracellular signal-regulated kinase
MIP-1	Macrophage inflammatory proteins
mmHg	Millimetres of mercury
MMP	Matrix metalloproteinases
M.O.M	Mouse on mouse
MR	Mineralocorticoid receptor
mRNA	Messenger ribonucleic acid
MyD88	Myeloid differentiation factor 88
Na	Sodium
NCC	Sodium chloride cotransporter
NFAT	Nuclear factor of activated T-cells
NFκB	Nuclear factor κB

NHE3	Sodium/hydrogen exchanger 3
NK	Natural killer
NKCC2	Sodium-potassium-two chloride
NLRC	Nucleotide-binding oligomerization domain-like receptor C4
NLRP3	Nucleotide-binding oligomerization domain-like receptor family pyrin domain-containing protein
NO	Nitric oxide
NOD	Nucleotide-binding oligomerization domain
PAMP	Pathogen associated molecular pattern
PBS	Phosphate-buffered saline
PCR	Polymerase chain reaction
PI3K/Akt	Phosphoinositide-3-kinase–protein kinase B/Akt
PRR	Pattern recognition receptor
RAAS	Renin-angiotensin-aldosterone system
RAG	Recombination activating gene
RBC	Red blood cell
ROS	Reactive oxygen species
SCr	Serum creatinine
SEM	Standard error of the mean
sgRNA	Single guide RNA
SNP	Single-nucleotide polymorphism
SOCS	Suppressors of cytokine signalling
SPF	Specific pathogen-free
STAT	Signal transducer and activator of transcription
STAT3	Signal transducer and activator of transcription 3
T2DM	Type 2 diabetes mellitus
TCR-β	T cell receptor β
TEC	Tubular epithelial cells
Th1	T-helper 1
Th17	T-helper 17
TIR	Toll/interleukin-1 receptor
TLR	Toll-like receptor
TNF-α	Tumour necrosis factor α
UUO	Unilateral ureteral obstruction
VCAM	Vascular adhesion molecule 1
WT	Wild type
XIAP	X-linked inhibitor of apoptosis protein

Chapter 1

Introduction: The IL-18/IL-18R1 Signalling Axis: Diagnostic and Therapeutic Potential in Hypertension and Chronic Kidney Disease

1.1 Abstract

Chronic kidney disease (CKD) is inherently an inflammatory condition, which ultimately results in the development of end stage renal disease (ESRD) or cardiovascular events. Low grade inflammatory diseases such as hypertension and diabetes are leading causes of CKD,[1] where there is also a concomitant decrease in renal function and increase in circulating pro-inflammatory cytokines interleukin (IL)-1β, IL-6 and tumour necrosis factor (TNF)-α in patients with these diseases.[2] The inflammasome is an important inflammatory signalling platform that has been associated with the aforementioned low-grade chronic inflammatory diseases, hypertension and type-2 diabetes mellitus (T2DM).[3, 4] Notably, activation and assembly of the inflammasome causes the auto cleavage of pro-caspase-1 into its active form, which then processes the pro-inflammatory cytokines pro-IL-1β and pro-IL-18 into active IL-1β and IL-18.[5] Currently, the nod-like receptor pattern recognition receptor (NLRP)-3 inflammasome has been implicated in the development of CKD in both pre-clinical and clinical settings,[6, 7] and the ablation or inhibition of inflammasome components have been shown to be reno-protective in a mouse model of CKD.[3] While clinical trials have demonstrated that neutralisation of IL-1β signalling by the drug anakinra lowers inflammatory markers in haemodialysis patients,[8] ongoing pre-clinical studies are showing that this ability is limited in progressive models of kidney disease,[9] even though fibrosis is ameliorated.[10] These results suggest a potential predominant role for IL-18 in the development of CKD. This review will discuss the role of the inflammasome and its pro-inflammatory product IL-18 in the development of renal fibrosis and inflammation that contribute to the pathophysiology of CKD. Furthermore, we will demonstrate that the inflammasome and the downstream pro-inflammatory cytokine IL-18 are likely targets for future CKD therapies and examine the potential of the IL-18 signalling axis as an anti-inflammatory target and its usefulness as diagnostic biomarker to predict acute kidney injury (AKI).

1.2 Introduction

Chronic kidney disease (CKD) is estimated to affect 11-13% of people globally.[11] As the precursor to ESRD, and a major risk factor for cardiovascular disease, CKD is recognised by the World Health Organisation as one of the top 20 leading causes of death worldwide.[12] It is characterised by a decrease in glomerular filtration rate that persists for greater than three months[13] and by pathological features such as albuminuria, proteinuria, haematuria and volume overload.[14] CKD is graded in 5 stages, with the majority of cases not being detected until stage 3 or beyond, when GFR is already severely reduced (i.e. by > 30% of normal or < 60mL/minute/1.73m^2) and significant damage to the kidneys has already occurred. Current treatment guidelines for CKD include lifestyle interventions and concurrent therapy with drugs that suppress the activity of the renin-angiotensin-aldosterone system (RAAS).[15] The major goal of RAAS inhibition is to reduce filtration pressure on the kidneys, in part by lowering systemic blood pressure and by promoting intrarenal efferent vasodilation.[16, 17] While this approach is effective at reducing proteinuria, it is not curative and merely delays disease progression. Hence, patients remain at heightened risk for cardiovascular events and ESRD.[18-23] Clearly, there is an urgent need for earlier diagnosis of CKD and more efficacious therapies that directly target the underlying disease mechanisms.

The two most common causes of CKD — hypertension and diabetes — are present in almost two thirds of patients with CKD.[24, 25] The remaining one-third of cases can be attributed to genetic diseases such as polycystic kidney disease, autoimmune conditions such as lupus, glomerulonephritis, or to stimuli that cause AKI. Such injurious stimuli include ischemia-reperfusion injury due to septic shock or major surgery; urinary obstructions by kidney stones, tumours or an enlarged prostate; infections; or drugs such as the chemotherapeutic agent, cisplastin.[17] A unifying feature of all of these conditions — whether acute or chronic — is that they result in the formation of 'danger signals' (see below) and a persistent sterile, low-grade

inflammation within the kidneys, which is thought to ultimately give rise to the vascular, glomerular and tubular damage that conspire to cause CKD. Hence, a major focus of the global research effort in the area over the past decade has been on elucidating the mechanisms that trigger, amplify, and maintain this inflammatory response. From this work, evidence has emerged for a crucial role of the pro-inflammatory cytokine, IL-18, both as one of the early initiators of renal inflammation, and as a key determinant of the amplification and maturation of the immune response that maintains a state of chronic inflammation. In this review, we will provide a brief overview of the biochemistry of IL-18 formation and the pharmacology that governs its pro-inflammatory signalling properties. We will summarise the evidence implicating IL-18 in the pathogenesis of CKD and highlight the opportunities that this knowledge affords in terms of new therapeutics and biomarkers for the early diagnosis of CKD.

1.3 IL-18 production in the kidneys

IL-18 is a member of the IL-1 family of cytokines, which also includes IL-1β and IL-33. IL-18 is formed intracellularly as a 24 kDa inactive precursor protein, pro-IL-18, which requires processing into its active form via the proteolytic actions of a family of innate signalling complexes termed inflammasomes.[26-28] Inflammasomes serve as platforms for the detection of pathogen- or host-derived danger signals, and the subsequent activation of pro-inflammatory caspase-1. Inflammasomes are comprised of a pattern recognition receptor (PRR) domain, which is usually a member of the nod-like receptor family (except in the case of absent in melanoma 1; AIM1). The PRR is linked either directly or indirectly via the adapter protein ASC (Apoptosis-associated Speck like protein containing a Caspase recruitment domain) to pro-caspase-1, which upon maturation into caspase-1, cleaves IL-18 at Asp,[35] forming an 18kD active protein.[29]

IL-18 was first shown to be produced by macrophages and their precursors, monocytes, following viral infection,[30] and it would seem that these cell types are at least one of the important sources of IL-18 within the kidneys following injury and disease (Figure 1.1). IL-18 expression is increased in macrophages in human transplanted kidneys undergoing T cell mediated rejection,[31] and was localised by immunoperoxidase staining to interstitial macrophages in biopsies of patients with anti-neutrophil cytoplasmic antibody (ANCA)-associated vasculitis.[32] Similarly, in a rat model of renal transplant allograft rejection, IL-18 production was greatest in allograft-transplant recipient animals compared to isograft-transplant recipient animals, and this increase was blunted with macrophage-depleting clodronate treatment.[33]

However, macrophages are not the only source of IL-18 in the kidneys. Indeed, in a unilateral ureteral obstruction (UUO) model of CKD, macrophage-depletion failed to abrogate IL-18 production. Instead, IL-18 and its receptor, IL-18R1, were shown to be colocalised to renal tubular epithelial cells (TECs; Figure 1.1).[34] Likewise, TECs were identified as the primary source of IL-18 in kidney transplant patients with a confirmed polyomavirus infection.[31] Liang *et al.,* also demonstrated that the expression of IL-18 and its receptor was increased in renal TECs in biopsy samples from patients with CKD, and were colocalised to atrophic tubules, compared to control subjects who displayed minimal renal IL-18 expression.[35] In the same study, cultured human renal TECs were shown to produce IL-18 in a dose-dependent manner following lipopolysaccharide (LPS) challenge.[35] Furthermore, in a preclinical model of lupus nephritis, it was shown that TEC expression levels of IL-18 were increased in proportion with disease severity.[36] It was also evident that both pro- and active IL-18 were produced by TECs in this disease model.[36]

Other kidney cell types have also been reported to produce IL-18 in preclinical and clinical pathological settings as summarised in the table below (Figure 1.1; Table 1.1). Briefly, these

include mesangial cells, glomerular podocytes, myofibroblasts and distal tubular epithelial cells, whilst in healthy human subjects IL-18 was shown to be expressed in the intercalated cells of the distal tubule, connecting tubule, and collecting duct of the kidneys.[37] Overall, this evidence suggests that the source of IL-18 in the kidneys varies depending on the type of injury or disease condition.

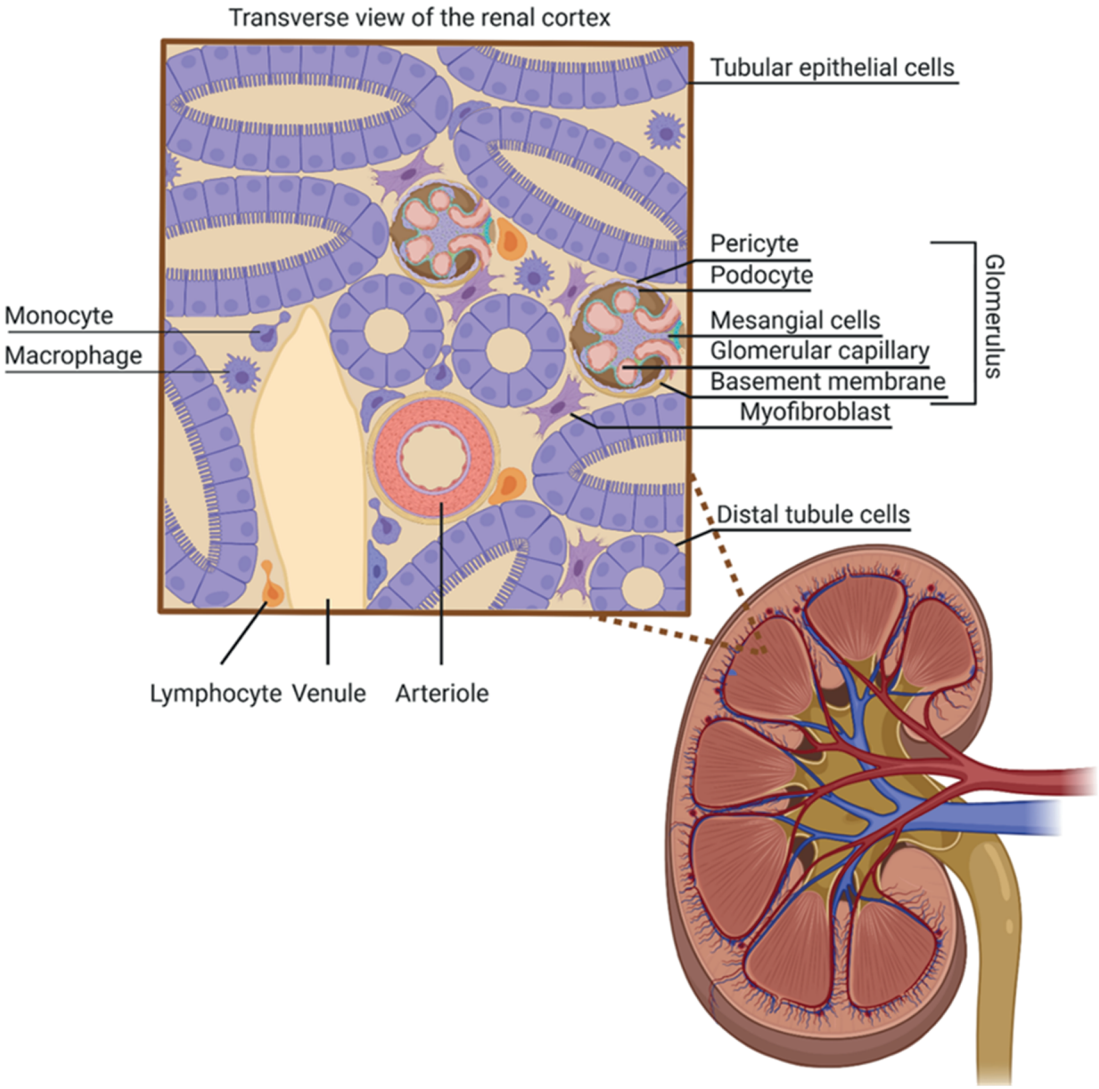

Figure 1.1 Cellular sources of IL-18 in the kidney. Cell types that produce IL-18 in the kidney are coloured in purple and include tubular epithelial cells (TECs), pericytes, podocytes, mesangial cells, distal TECs, myofibroblasts, intercalated cells of the distal tubule, connecting tubule, collecting duct cells, and macrophages have been identified in the clinic and in pre-clinical models as sources of IL-18 in kidney disease. Created with BioRender.com.

Table 1.1 Kidney cell types that produce IL-18 in healthy and disease settings

Kidney cell type	Sample/Disease model
Pericyte	*In vitro* LPS and ATP stimulation[38]
Glomerular podocytes	Anti-neutrophil cytoplasmic antibodies (ANCA)- associated vasculitis patients[32] High fat diet-induced renal inflammation and injury[39]
Mesangial cells	Mouse model of LPS accelerated lupus nephritis[40] patients with lupus nephritis[41]
Myofibroblasts	ANCA- associated vasculitis patients[32]
Distal TECs	
Intercalated cells of the distal tubule	Healthy human subjects[37]
Connecting tubule	
Collecting duct	
Macrophages	Human transplanted kidneys undergoing T-cell mediated rejection[31] Patients with ANCA-associated vasculitis[32] Rat model of renal transplant allograft rejection[33]
TECs	Mouse model UUO[34] Kidney transplant patients with a confirmed polyomavirus infection[31] Biopsy samples from patients with CKD and cultured human renal TECs following LPS challenge[35] Preclinical model of lupus nephritis[36]

As mentioned above, the initiating stimuli for IL-18 production are 'danger signals'. Danger signals are molecular signatures that are recognised by PRRs as 'non-self' and may be either pathogen- or host-derived. Pathogen-associated molecular patterns (PAMPs) include bacterial LPS, lipooligosaccharides, pore-forming toxins and viral DNA and protein, whereas host-derived molecular signatures — so-called danger-associated molecular patterns (DAMPs) — are indicative of cellular damage or metabolic disturbances. In the context of inflammasome activation during chronic kidney disease, a number of candidate PAMPs/DAMPs have been proposed including LPS,[39] reactive oxygen species (ROS),[40] albumin[41-43] and microcrystals of uric acid or calcium.[44, 45] In addition to these more "traditional" PRR activators, other signals

such as high interstitial salt concentrations, aldosterone, and hypoxia have been shown to initiate inflammation in the kidney (Figure 1.2).[46-48\]

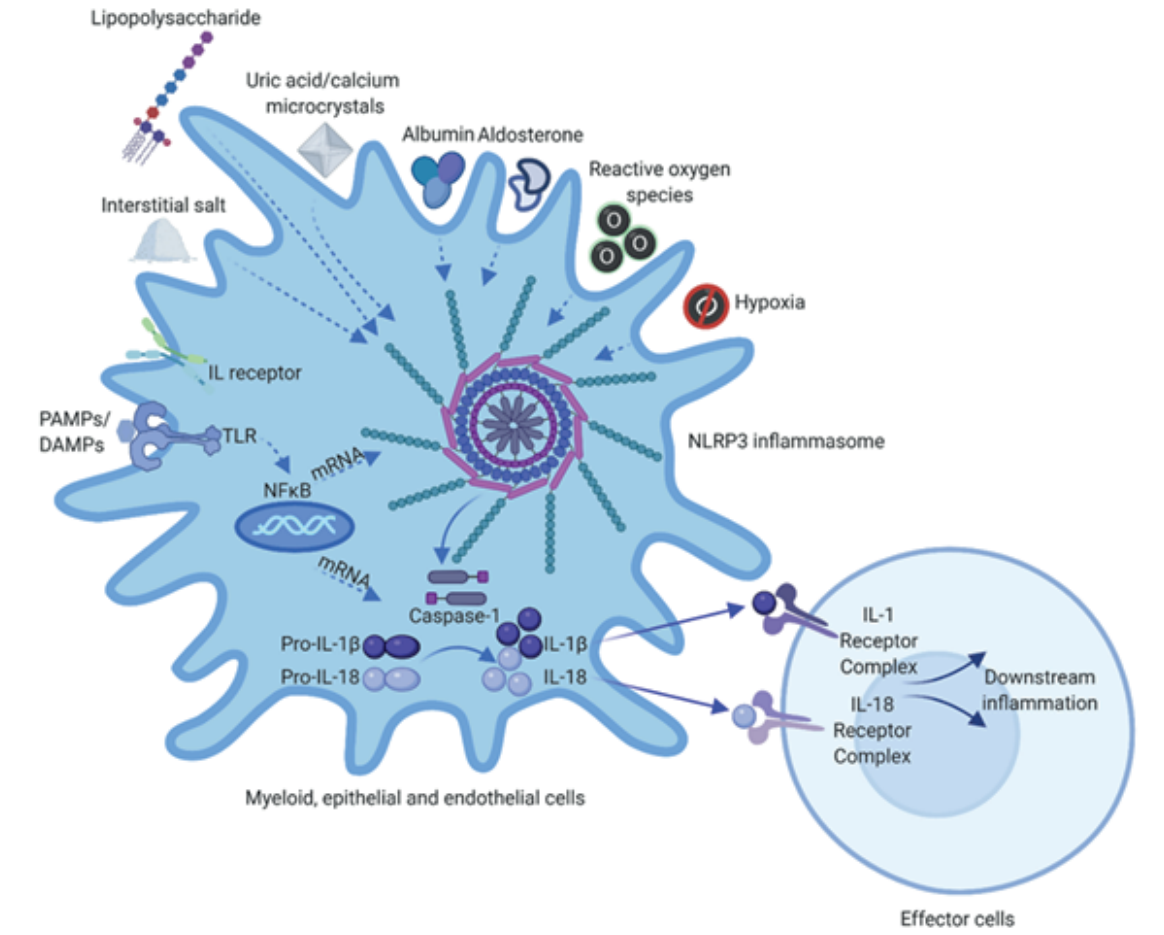

Figure 1.2 Schematic representation of DAMPs/PAMPs that initiate inflammasome activation in the kidney. Inflammasomes are comprised of a pattern recognition receptor (PRR) domain, the adapter protein ASC and pro-caspase-1. 'Danger signals' or danger associated molecular patterns (DAMPs), including: LPS; reactive oxygen species; albumin; microcrystals of uric acid or calcium; high interstitial salt concentrations; aldosterone; and hypoxia, initiate inflammasome activation in the kidney, which causes the production of mature IL-18. Created with BioRender.com.

At least 8 inflammasome subtypes are expressed in the kidneys (Table 1.2), but the majority of evidence to date points to the NLRP3 inflammasome as the key driver of the renal

inflammation, pathology and dysfunction that occurs in CKD.[49-51] Firstly, NLRP3 is highly expressed in macrophages and tubular epithelial cells — two key cell types in the pathogenesis of CKD — and moreover, NLRP3 expression was shown to be elevated in kidney biopsies of patients with AKI and CKD,[7] as well as in a mouse model of CKD involving removal of a kidney and treatment with deoxycorticosterone-acetate (DOCA) and salt (1K/DOCA/salt).[3, 52] Importantly, mice that are genetically deficient in either NLRP3, ASC or caspase-1 are profoundly protected from renal inflammation, damage and/or dysfunction caused by a variety of stimuli including UUO, 5/6 nephrectomy, crystal nephropathy, or cisplatin-induced kidney injury. [3, 53-55] Even more recently, we provided evidence that MCC950 — a small molecule inhibitor of NLRP3 activity — is highly effective at limiting renal damage in mice, even when administered two weeks after the induction of kidney injury via 1K/DOCA/salt treatment.[3, 52]

Collectively, the above findings highlight inflammasomes and the DAMPs that activate them as crucial mediators of CKD and promising targets for future therapies. Indeed, these concepts have been covered in detail in several recent reviews[62-64] and will thus not be discussed further here. Instead, we will return our focus to the pathogenic and therapeutic implications of the events that occur downstream of inflammasome activation as a result of IL-18 production.

Table 1.2 Renal inflammasome expression

Inflammasome type	Setting
NLRC4	Increased renal and gene expression following IRI[56]
NLRP3	Activated in podocytes in a model of diabetic nephropathy[57] Increased renal expression in a model of oxalate nephropathy[45] Increased expression in uric acid treated TECs[45]
NLRP1	Single-nucleotide polymorphisms (SNPs) in NLRP1- measured in peripheral blood mononuclear cells (PBMCs)- are protective in patients with diabetic kidney disease[58] Increased expression in mice with cisplatin induced AKI[51]
NOD1/2	Expressed in tubular epithelial cells and knockout mice are protected from renal IRI[59]
NLRP2, -6, -10 and -12	mRNA is expressed in mouse kidneys[60]
AIM2	Increased expression in renal macrophages in an apopDNA-induced mouse model of lupus[61] IFN-γ induces expression in macrophages from renal biopsies of patients with kidney transplant rejection[50] Expressed in glomeruli, upregulated in tubules and renal leukocytes of patients with diabetic nephropathy and hypertension nephrosclerosis[49] Expressed in tubules and glomeruli of mice subjected to UUO[49]

1.4 Targets of IL-18 in the kidneys

IL-18 mediates its effects by forming a complex with two membrane-bound receptor subunits — the IL-18 receptor-1 (IL-18R1) and the IL-18 receptor accessory protein (IL-18RAP). IL-18R1 and IL-18RAP belong to the immunoglobulin-like family of interleukin-1 receptors. Each receptor subunit contains immunoglobulin-like C2-types 1 and 2 domains. In addition, IL-18R1 contains a type-3 domain, as well as a toll/interleukin-1 receptor (TIR) domain (Figure 1.3). Engagement of IL-18 with the receptor complex initially involves its binding to the IL-18R1 subunit. This is a relatively low affinity interaction (Kd of 11 nM) and on its own is insufficient to induce activation of intracellular second messenger pathways (Figure 1.3).[65] Rather, the bound IL-18 must then recruit IL-18RAP to which it binds with markedly higher affinity (Kd of 0.4 nM; Figure 1.3).[65-67] Once assembled, the hetero-trimeric complex of IL-18/IL-18R1/IL-18RAP attracts the cytosolic adapter TRAM to the intracellular TIR domain,

which recruits Myeloid differentiation primary response 88 (MyD88) and subsequently forms a "Myddosome" complex with IRAK and TRAF6 (Figure 1.4).[68] TRAF6 then ubiquitinates IκBα, which is broken down to form active NFκB.[69] NFκB is then free to translocate to the nucleus to cause the transcription of pro-inflammatory cytokines, chemokines and adhesion molecules downstream of IL-18 signalling (Figure 1.4). IL-18 receptor complex activity can also lead to activation of a number of alternative signalling pathways. This includes the activation of mitogen activated protein kinases (MAPK), phosphoinositide 3-kinase/AKT serine/threonine kinase (PI3K/AKT) and non-receptor tyrosine kinases (Src) -which triggers signalling via the Ras/Raf pathway (Figure 1.4). Additionally, IL-18 can signal through ERK1/2, resulting in AP-1 activation, Jnk/Sp1 and MMP-9 signalling via EMMPRIN/BSG and MAPK pathways, and p38-MAPK phosphorylation resulting in nitric oxide synthase expression (Figure 1.4).[68] These IL-18 signalling pathways will be described in more detail below in relation to their role in the development of kidney disease.

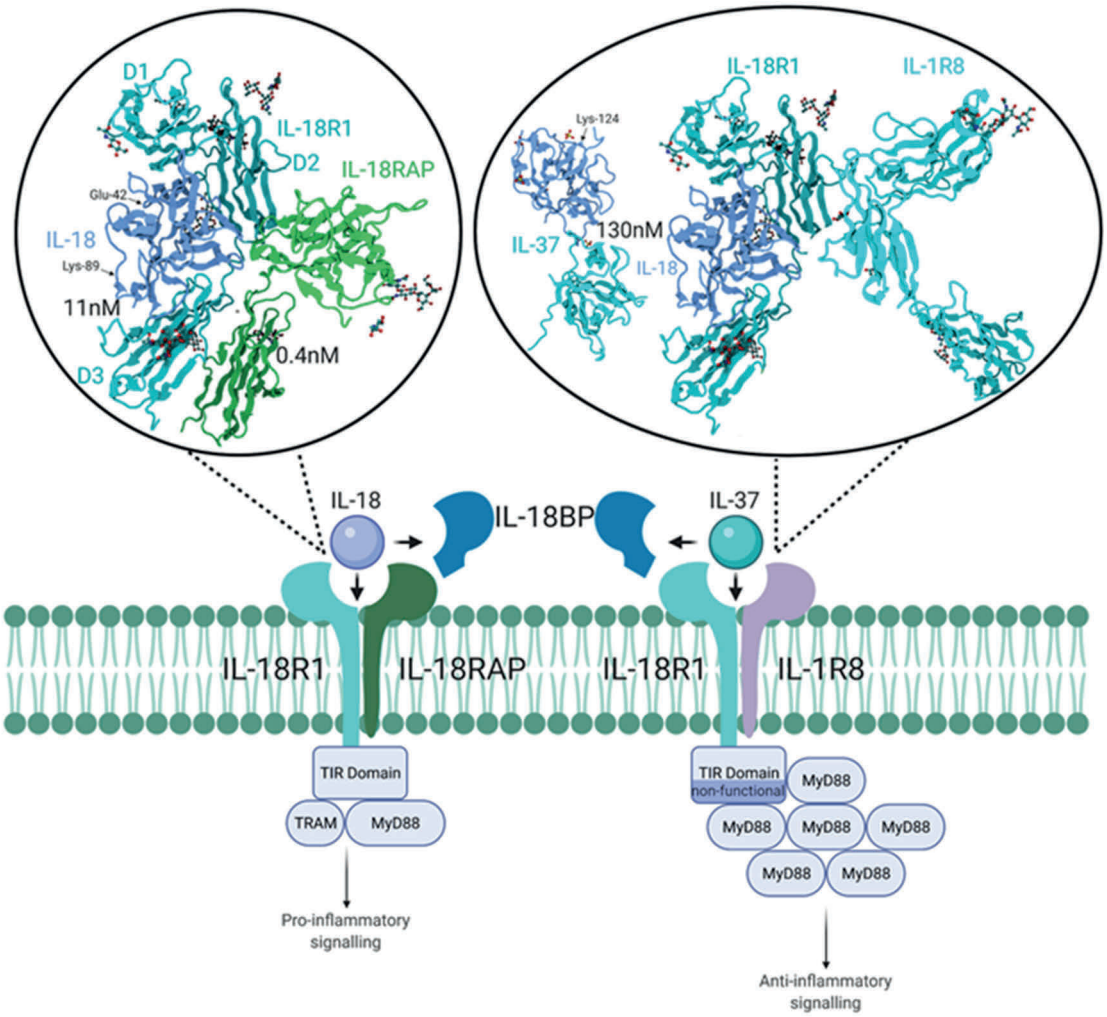

Figure 1.3 Schematic representation of IL-18, IL-37, IL-18R1, IL-18RAP and IL-1R8 structure and binding. IL-18 mediates its effects by forming a complex with two membrane-bound receptor subunits — the IL-18 receptor-1 (IL-18R1) and the IL-18 receptor accessory protein (IL-18RAP). IL-18 binds IL-18R1 with relatively low affinity (Kd= 11 nM) which causes the recruitment of IL-18RAP for high affinity binding (Kd= 0.4 nM). This receptor complex initiates the recruitment of TRAM/MyD88 signalling pathways which activates pro-inflammatory signalling. IL-37 may modulate IL-18 activity by binding to IL-18R1 with low affinity (Kd= 130 nM), causing the recruitment of IL-1R8 which has a non-functional TIR domain preventing the engagement of the proinflammatory signalling pathway. Created with BioRender.com.

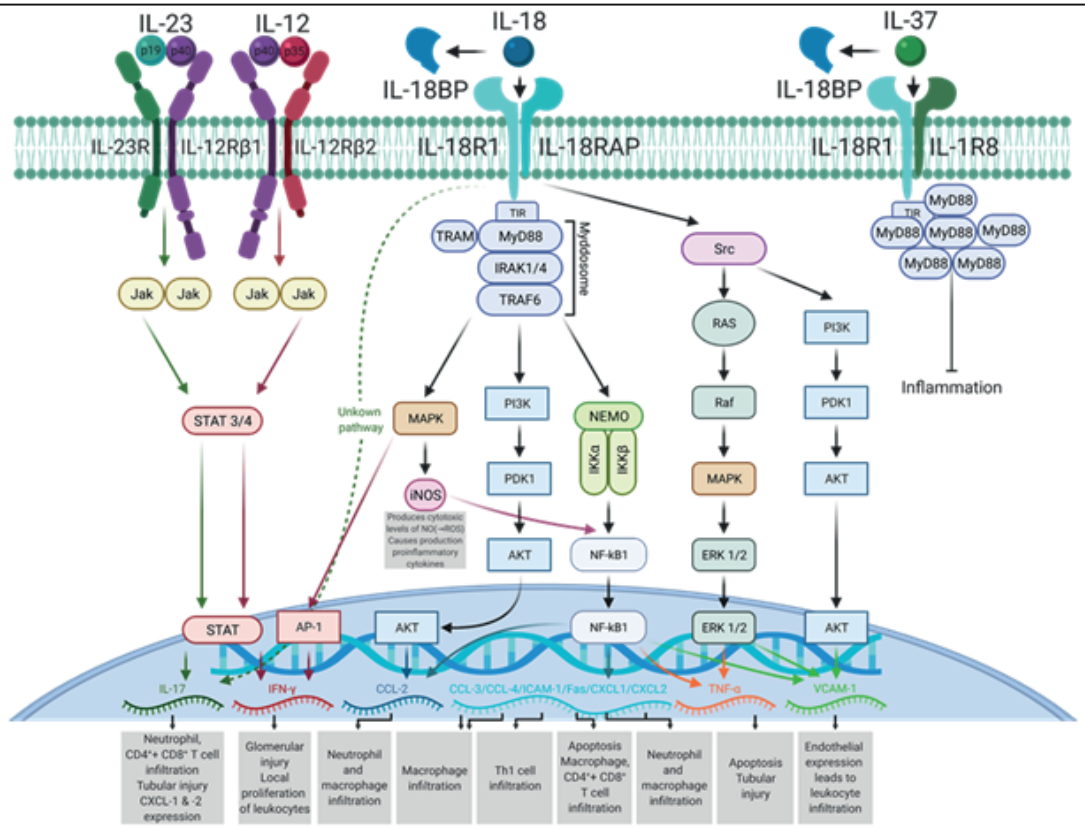

Figure 1.4 Schematic representation of IL-18 pro-inflammatory signalling in kidney injury. IL-18 mediates its effects by activating: the Myddosome; mitogen activated protein kinases (MAPK); phosphoinositide 3-kinase/AKT serine/ threonine kinase (PI3K/AKT); non-receptor tyrosine kinases (Src); Ras/Raf pathway; and MAPK pathways, to cause the production of IL-17, IFN-γ, CCLs2-4, ICAM-1, VCAM-1, Fas, CXCL1, CXCL2, and TNF-α to cause inflammation, fibrosis and apoptosis in the kidney. Created with BioRender.com.

IL-18 signalling through IL-18R1/IL-18RAP can be negatively modulated by two separate mechanisms. The first involves regulation of the bioavailability of IL-18 by an endogenous binding protein, IL-18 binding protein (IL-18BP). IL-18BP binds with high affinity to IL-18 in the circulation, neutralising its pro-inflammatory actions (Figure 1.5).[28] IL-18BP acts as a soluble receptor that is distinct from the IL-1 family of receptors in that it contains only a single immunoglobulin (Ig)-like domain (as opposed to the three Ig-like domain structure of IL-1 family members).[70] IL-18BP is produced from a precursor that can be alternatively spliced to form four isoforms (*a*-*d*; Figure 1.5). Isoforms *a* and *c* bind and neutralise IL-18 activity with a Kd of 400 pM and 2.94 nM, respectively (Figure 1.5). While the human IL-18BP*b* and *d* isoform are unable to neutralise IL-18 activity, the murine *d* isoform is capable of neutralising not only mouse, but also human IL-18.[71, 72] IL-18BP*a* is constitutively expressed in the spleen, colon, small intestine and prostate, and is present in the serum of healthy subjects at levels of 2,000-4,000 pg/mL,[73] at least an order of magnitude higher than the average serum levels of IL-18 in healthy subjects (i.e. 80-120 pg/mL).[73] The expression of IL-18BP is regulated by interferon (IFN)-γ, which creates a negative feedback loop to limit IL-18 activity, i.e. increased IL-18 expression causes increased IFN-γ production and therefore increased IL-18BP expression.[74] It has been shown that patients with chronic renal insufficiency and/or on haemodialysis have significantly higher plasma levels of IL-18BP than patients with normal kidney function.[75] Paradoxically, patients on haemodialysis also have greater plasma levels of unbound IL-18.[75] Disease pathology often arises from imbalances of IL-18 and IL-18BP,[28] or from altered IL-18BP splicing which favours the formation of the non-functional IL-18BP isoforms IL-18BP*b* and *d* resulting in increased levels of circulating unbound IL-18.[72]

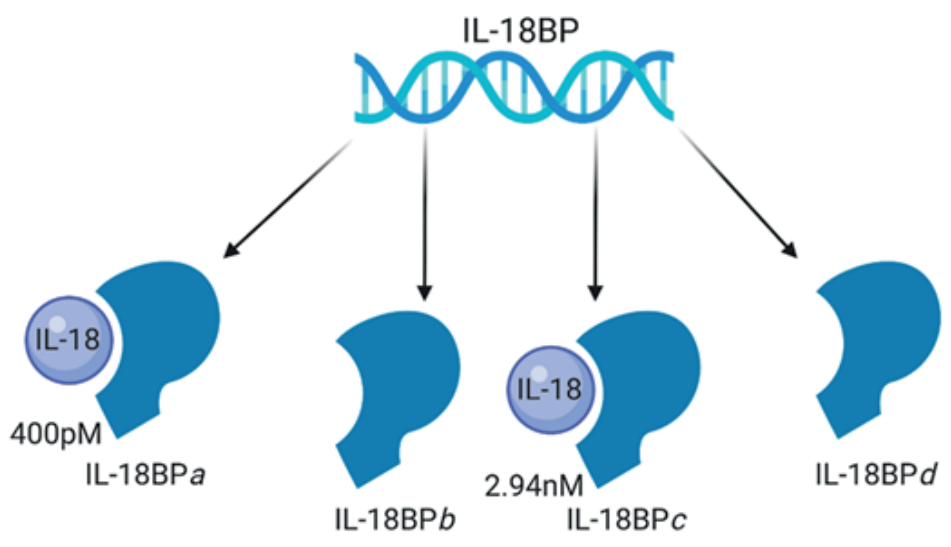

Figure 1.5 IL-18BP isoforms a, b, c and d and their affinity to neutralise IL-18. IL-18BP isoforms *a* and *c* are able to bind and neutralise the pro-inflammatory activity of IL-18, and IL-18BP isoforms *b* and *d* are unable to neutralise IL-18 activity. Created with BioRender.com.

The second mechanism by which IL-18 signalling may be modulated is through the actions of another IL-1 family member, namely IL-37. IL-37 levels are increased in autoimmune diseases including Graves' disease, rheumatoid arthritis and systemic lupus erythematosus, among others,[76-78] and it has been suggested that this may be evoked as a compensatory mechanism to counter the pro-inflammatory effects of IL-18.[79] Like IL-18, IL-37 is processed into its active form by caspase-1 and shares the β-barrel structure that is characteristic of the IL-1 family of cytokines (Figure 1.3).[80, 81] IL-37 can be spliced into five alternative isoforms (IL-37*a*-*e*), with isoforms *a*, *b* and *d* sharing exons 4-6, which are crucial to IL-37 signalling.[82] IL-37*b* is the most prevalent IL-37 isoform and the only one that is expressed in the kidney.[81] IL-37*b* shares as little as 19% homology with IL-18, and yet can bind to both IL-18BP, and to IL-18R1 as its primary receptor (Figure 1.3).[83] To date, binding studies suggest that IL-37 binds to IL-18R1 via the conserved amino acids Glu-35 and Lys-124, which are similarly present in IL-18 at position 42 and 89,

respectively, and are the key residues that allow IL-18 to bind to IL-18R1 and IL-18BP (Figure 1.3).[84] Recently, this binding hypothesis has been questioned, as IL-37 binds to IL-18R1 with only low affinity (Kd= 130 nM), compared to IL-18 (Kd= 11 nM; Figure 1.3).[85] This difference in binding profiles, as well as the finding that the addition of increasing concentrations of IL-37 to NK cells pre-stimulated with IL-18 had no effect on reducing the production of IFN-γ,[84] suggests that IL-37 might not be an orthostatic antagonist of IL-18 binding, but rather may bind to a separate, as yet undetermined binding site on IL-18R1.[82] Regardless of its precise binding properties, it has been demonstrated that IL-37 binds to the third domain of IL-18R1 and causes the recruitment of yet another member of the immunoglobulin-like family of interleukin-1 receptors, IL-1R8 or SIGRR (as opposed to IL-18RAP; Figure 1.3).[79] Formation of this receptor complex results in the recruitment of Myd88, but, because IL-1R8 has a non-functional TIR domain, the inflammatory intracellular signalling cascade is not engaged (Figure 1.3).[86, 87] In essence, IL-1R8 acts as a decoy for both IL-18R1 and Myd88 thereby inhibiting IL-18 signalling (Figure 1.3).

In addition to acting as a decoy for IL-18R1/MyD88, there is evidence to suggest that IL-37 binding to IL-18BP may increase the ability of IL-18BP to neutralise IL-18 by greater than 25%,[84] which could boost the efficacy of future IL-18BP therapies that target IL-18.

A major limiting factor to preclinical IL-37 research is, surprisingly, the apparent absence of IL-37 in rodents.[82] This spurred the creation of a transgenic mouse model where human IL-37 is expressed, which has provided some insight into the likely role of IL-37 in kidney disease. Indeed, IL-37 transgenic mice were found to be protected from the development of kidney inflammation, injury and dysfunction in a model of renal ischemia reperfusion injury (IRI).[88] These mice also displayed blunted expression of pro-inflammatory cytokines TNF-α, IL-6 and IL-1β. Consistent with an anti-inflammatory action, treatment of peripheral blood mononuclear cells from patients with systemic lupus erythematosus with exogenous IL-37, similarly resulted in decreased expression of TNF-α, IL-6 and IL-1β.[76,

[88] Collectively the previous findings imply that exogenous treatment with IL-37 may represent a new frontier for reducing IL-18-induced disease pathology in the kidneys.

1.5 Evidence for pathogenic roles of IL-18 signalling in kidney disease: Preclinical studies

There is substantial evidence that manipulation of IL-18 signalling, either by ablation of IL-18 production, antibody-mediated neutralisation or by overexpression of its endogenous inhibitor IL-18BP, results in protection from renal dysfunction in preclinical studies of kidney damage. In models of bilateral IRI dysfunction, wild type mice display increased serum creatinine (SCr) and blood urea nitrogen (BUN) levels compared to sham-operated mice, with both of these indices of kidney dysfunction attenuated in caspase-1$^{-/-}$ and IL-18BP-overexpressing mice.[89-91] Mice treated with anti-IL-18 serum prior to being subjected to IRI were also shown to be protected from kidney damage as measured by reduced SCr levels and tubular necrosis scores.[92] Furthermore, IL-18$^{-/-}$ mice subjected to bilateral IRI were protected from the increase in renal mRNA expression of pro-inflammatory cytokines TNF-α, MIP-2 and MCP-1, as well as tubular injury that was evident in wild type mice, 24 and 72 hours post-IRI.[91] Pre-treatment of mice with exogenous IL-18BP similarly reduced kidney dysfunction, tubular damage and renal expression of pro-inflammatory markers in response to bilateral IRI.[91] Transgenic IL-18BP-overexpressing mice were also protected from increased renal collagen expression, renal macrophage accumulation, and renal pro-inflammatory cytokine expression that resulted from UUO.[93] IL-18$^{-/-}$ mice were similarly protected from increased renal expression of pro-inflammatory cytokines and collagen, renal macrophage infiltration, and from severe glomerular injury that develops in a model of crescentic glomerulonephritis induced by treatment with sheep anti-glomerular basement membrane antibodies.[94] Additionally, caspase 1-deficiency attenuates albuminuria in a model of diabetic nephropathy.[95] Hence, it is clear that IL-18 plays a significant role in kidney inflammation and injury, as protection from macrophage infiltration, pro-

inflammatory chemokine and cytokine signalling and kidney injury has been demonstrated in mouse models of IRI, UUO, glomerulonephritis and diabetic nephropathy.[91, 93-95]

1.6 IL-18 mechanisms of action in the kidney

While the exact mechanism by which IL-18 causes kidney pathology in the aforementioned studies is unclear, several mechanisms have been suggested in the literature. These include promoting the production and release of cytokines, chemoattractants and adhesion molecules, the infiltration by immune cells, kidney cell apoptosis, and deposition of collagen in the kidneys (Figure 1.4). This section of the review will explain in detail the possible pathways and mechanisms by which IL-18 mediates kidney inflammation, fibrosis, and dysfunction in response to kidney injury as summarised in Figure 1.4.

1.6.1 Classical IL-18 signalling: IL-18 the "IFN-γ-inducing factor" (IGIF)

Initially, IL-18 was defined as the "IFN-γ-inducing factor" (IGIF) due to its ability to act in concert with IL-12 to potently increase the production of IFN-γ by NK cells and Th1 T cells.[96] IL-12 stimulation of the IL-12 receptor complex — which is comprised of IL-12 receptor (IL-12R) β1 and IL-12Rβ2 — results in activation of Janus kinase (JAK) signal transducer and activator of transcription proteins (STAT) or Activator Protein 1 (AP-1) pathways, which in turn promote the transcription of IFN-γ (Figure 1.4).[97, 98] IL-12 also sensitises IFN-γ-producing cells to IL-18 by causing an increase in the expression of IL-18R1. Indeed, stimulation of T cells with a combination of IL-12 and IL-18 causes a 20-fold increase in IFN-γ production compared to stimulation with IL-12 alone.[99] IL-18 activity at its receptor complex results in activation of MyD88 and MAPK-ERK pathways which contribute to the transcription and protein stabilisation of IFN-γ.[100, 101] Indeed, in models of renal IRI, IL-18 mRNA expression in the kidney is upregulated 24 hours post-injury, preceding the increase in IFN-γ and IL-12 expression, which occurs 6-days post-perfusion.[102] IL-18 upregulation also precedes increases in IL-12 and IFN-γ expression in models of lupus nephritis[36] and it is clear that the combined actions of IL-18 and IL-12 are

essential for the production of IFN-γ in the kidney during IRI, as a combination of IL-18 and IL-12 neutralisation *in vivo* caused a reduction in renal IFN-γ production.[102] Furthermore, in the setting of preclinical glomerulonephritis, treatment with IL-18 was shown to increase glomerular production of IFN-γ and glomerular damage.[103] In a mouse kidney transplant model, where recipient mice were major histocompatibility complex-mismatches, IFN-γ expression was significantly lower in IL-18$^{-/-}$ recipient mice and in IL-18BP-treated mice than it was in wild-type and placebo-treated mice, respectively.[33] Hence, there is strong evidence that IL-18 plays a significant role in the development of kidney injury following insult through its induction of the pro-inflammatory cytokine IFN-γ.

1.6.2 IL-18 signalling via JAK-STAT pathways: IL-17 production

Recently, it was demonstrated in a model of experimental autoimmune encephalomyelitis, that IL-18 can also work in concert with IL-23 to induce IL-17 production in both CD4^{+} T cells and gamma-delta T cells.[104] The binding of IL-23 to the IL-23 receptor complex — which comprises the IL-12Rβ1 and IL-23 receptor (IL-23R) subunits — also results in activation of JAK-STAT transcription pathways (Figure 1.4).[105] However, the exact pathway by which IL-18 activates IL-17 production remains unknown.

1.6.3 IL-18 signalling via NFκB pathways

IL-18-mediated activation of the transcription factor NFκB via the IL-18 receptor complex and MyD88/TRAF/IRAK pathway is well characterised and results in the transcription of chemokines such as chemokine (C-C motif) ligand (CCL) 3, CCL4, chemokine (C-X-C motif) ligand (CXCL) 1 and CXCL2, the adhesion molecules intercellular adhesion molecule (ICAM)-1 and vascular adhesion molecule (VCAM)-1, as well as the pro-apoptotic factor Fas (Figure 1.4).[106-108] These pro-inflammatory mediators have all been implicated in the development of kidney disease downstream of IL-18 signalling. IL-18BP-overexpressing transgenic mice were protected from increases in CCL3 and CCL4 gene expression that resulted from UUO,[93] whilst IL-18$^{-/-}$ mice subjected to IRI were similarly protected from the increases in CXCL1 and CXCL2 gene expression that were evident in

WT mice at 24 hours.[91] Notably, CXCL1 and CXCL2 participate in macrophage and neutrophil recruitment to sites of injury and infection, and accordingly both IL-18 deficiency and treatment with IL-18BP reduced macrophage and neutrophil infiltration following IRI.[91]

Similarly, IL-18 is noted for its role in promoting expression of ICAM-1 in glomeruli, such that in a mouse model of glomerulonephritis, treatment with exogenous IL-18 caused an increase in the glomerular expression of ICAM-1.[109] IL-18 also induces the production of VCAM-1, however, in addition to the MyD88/TRAF/IRAK/NFκB pathway, IL-18 is also able to activate Src/ERK and PI3K/AKT pathways to activate the expression of VCAM-1 (Figure 1.4).[68] This is important in the inflammatory context of CKD, as VCAM-1 is expressed on endothelial cells to mediate the tethering of leukocytes to the vascular wall, which ultimately allows them to infiltrate the kidney. Notably, in a preclinical model of autoimmune nephritis associated with upregulation of IL-18, expression levels of ICAM-1 and VCAM-1 were also increased.[36]

IL-18 likely contributes to kidney inflammation via its role in NFκB-mediated FasL expression.[106] A member of the tumour necrosis factor (TNF) family, FasL is a powerful inducer of apoptosis and potently attracts neutrophils to sites of injury.[110, 111] Addition of IL-18 to TECs *in vitro* results in excess collagen production and apoptosis in a concentration-dependent manner,[35] and in hypoxic TECs, stimulation with IL-18 results in the increased expression of FasL.[112] In a model of UUO using IL-18BP-overexpressing transgenic mice, where IL-18 is neutralised, FasL expression is reduced in comparison to WT mice, and mice are protected from renal cell apoptosis and the expression of apoptotic markers caspase-3 and -8.[113] Furthermore, in a model of autoimmune nephritis which is dependent on a mutation in the FasL gene that causes lymphoproliferation (MRL-Fas^{lpr}), IL-18R1 deficiency was associated with reduced leukocyte infiltration and mRNA expression of pro-inflammatory cytokines TNF-α, IFN-γ, IL-10, and IL-12 in the kidney,

when compared to MRL-Fas^{lpr} mice that were not deficient in IL-18R1.[114] Collectively, these findings suggest that in settings of kidney injury, IL-18 causes inflammation, renal cell apoptosis and fibrosis, at least in part via induction of FasL.

1.6.4 IL-18 signalling via Src/ERK pathways

In addition to FasL, IL-18 is also able to induce the expression of another TNF family member, TNF-α, an effect that appears to be mediated via the Src/ERK pathway rather than the NFκB pathway (Figure 1.4).[115] TNF-α is a pro-inflammatory cytokine produced primarily by monocytes and is essential to many cell signalling pathways that result in apoptosis. In a model of renal IRI, IL-18$^{-/-}$ mice had a blunted expression of TNF-α 1- and 3- days post ischemia and were protected from tubular injury.[91] Similar to its role in FasL production, it is likely that IL-18 contributes to renal injury via its induction of TNF-α, resulting in the death of tubular cells in the kidney. Interestingly, TECs isolated from mice with MRL-Fas^{lpr} (which increases FasL activity) displayed increased IL-18 production in response to stimulation with TNFα, which suggests that these pro-inflammatory cytokines operate in synergy.[36]

1.6.5 IL-18 signalling via PI3K/Akt and JNK pathways

IL-18 has been shown to act through PI3K/Akt and JNK leading to activation of NFκB and p38 MAPK, which in turn cause the production of CCL2 and inducible nitric oxide synthase (iNOS), respectively (Figure 1.4). These two pro-inflammatory mediators have been implicated in IL-18-induced renal IRI. Both CCL2 and iNOS were upregulated in WT mice 24 hours post-ischemia, whereas in IL-18$^{-/-}$ mice, expression levels of the two cytokines were markedly blunted at the same time point.[91] CCL2 is a potent chemokine and attracts monocytes to sites of injury, whilst iNOS causes the production of high levels of nitric oxide (NO). NO can readily react with ROS to form peroxynitrite which may cause oxidative damage to cells or activate signalling through the NFκB pathway to induce the production of pro-inflammatory cytokines.[116] Conversely, NO has been shown to inhibit

caspase-1 activity, and prevent the processing and release of IL-18, which indicates that there may be a negative feedback loop between IL-18 and NO.[117]

1.6.6 Autocrine/paracrine IL-18 signalling

Curiously, there is some evidence that IL-18 may act on its own receptor in a positive feedback loop, to cause further production of IL-18, although the cellular signalling pathways underpinning this mechanism remain unclear.[118] This was evident in WT mice subjected to UUO which have increased renal IL-18 and IL-18R1 mRNA expression and increased serum protein levels of IL-18 when compared to sham mice or IL-18R1$^{-/-}$ following UUO. Furthermore, IL-18 and IL-18R1 were co-localised to TECs in wild type mice subjected to UUO.[118] These findings suggest that the actions of IL-18 activating, injurious stimuli on TECs are amplified many-fold via the IL-18-IL-18R1 feed-forward loop.

1.7 Targeting IL-18R1 signalling in preclinical studies

While it is clear that IL-18 plays a key role in the development of inflammation, apoptosis, and fibrosis in the context of kidney disease and injury, it is unclear which signalling pathway(s) downstream of IL-18 activity is the main contributor to IL-18-induced pathophysiology of CKD. Furthermore, it remains unclear if targeting IL-18 signalling at the receptor level (as opposed to the cytokine level with IL-18 monoclonal antibody or IL-18BP) is protective against kidney disease. Recent studies in IL-18R1$^{-/-}$ mice have shown that these mice lack protection against renal dysfunction, pro-inflammatory cytokine expression and leukocyte infiltration in models of cisplatin-induced AKI and bilateral IRI.[112, 119] In fact, IL-18R1$^{-/-}$ mice had greater CD4^{+} T cell, neutrophil and macrophage infiltration into the kidney following bilateral IRI when compared to wild type mice.[112] The deleterious effect of IL-18R1$^{-/-}$ may be explained by a dual role for this receptor subunit which could be crucial for dampening the actions of IL-18 and other pro-inflammatory mediators. In humans, the anti-inflammatory cytokine IL-37 has been shown to signal

through the IL-18R1 to limit inflammation and IL-18 signalling;[86] although neither a mouse homologue of IL-37, nor another murine anti-inflammatory cytokine that signals through this receptor, has been identified.

An alternative approach for inhibiting IL-18 receptor activity, that is unlikely to be confounded by interfering with IL-37 signalling, might involve targeting IL-18RAP, the co-receptor that promotes high affinity binding of the IL-18/IL-18R1/IL-18RAP complex, and only signals in response to IL-18. Currently, there is limited pre-clinical evidence on whether targeting this component of the IL-18 receptor complex would be beneficial in limiting the development of inflammation and fibrosis in CKD. However, Nozaki *et al.* have shown that administration of an IL-18RAP neutralising antibody in a preclinical model of cisplatin-induced AKI attenuated the development of renal dysfunction and injury.[119] It remains to be established whether a similar is effective in other models of acute or chronic kidney injury. Further hampering progress in this area to date has been the lack of an IL-18RAP$^{-/-}$ mouse.

1.8 IL-18 as a biomarker for kidney injury

One of the key challenges in preventing progression of AKI or CKD to ESRD is that kidney disease is often left undetected until symptoms appear, i.e., when over 90% of kidney function has already been lost.[120] Currently, the gold standard for measuring kidney dysfunction is the estimated glomerular filtration rate (eGFR). eGFR is a measurement that acts as a proxy for renal dysfunction and damage and involves measuring circulating levels of creatinine, a product of muscle metabolism which is unable to be filtered out by injured kidneys. The results from this test are input into a formula that estimates GFR.[121] Although this diagnostic method is considered the gold standard in diagnosing kidney dysfunction, it has several significant limitations, namely that: (1) it is not sensitive enough to detect the early stages of kidney dysfunction;[122] (2) it has low accuracy in estimating the extent of kidney damage;[123] (3) changes in circulating creatinine levels that reflect AKI only occur

after injury is initiated;[124] (4) creatinine levels are not consistent between individuals and change with ageing;[124] and (5) diagnosis of CKD beyond stage 3 using eGFR is reliant on the additional measurement of albuminuria, which has poor reliability.[121] Therefore, biomarkers that sensitively and accurately assess kidney disease at its early stages are highly sought after to allow for the earlier detection, and thus intervention for kidney disease treatment.

1.8.1 IL-18 as a biomarker for AKI

There is a wealth of evidence supporting IL-18 as an important mediator of inflammation both in the clinic and in preclinical models of kidney disease.[31, 35, 36, 90-92, 126] Hence, IL-18 has emerged as a diagnostically useful biomarker for kidney injury, as IL-18 may be produced in the kidneys at the time of injury and excreted into the urine or reabsorbed into the circulation.[127] Urine levels of IL-18 were elevated in patients with acute tubular necrosis when compared to healthy controls and patients with other kidney diseases, and increased urinary IL-18 was also predictive of delayed graft function (DGF) following transplant of a cadaveric kidney.[126] In an ICU setting, increased urinary IL-18 levels were associated with AKI upon admission,[128] and increased urinary levels of IL-18 were also predictive of the need for dialysis or patient death in a critically ill patient population.[129] These studies were supported by findings of a meta-analysis which investigated the diagnostic value of IL-18 from 11 studies from 2005-2013 that had reported on the effectiveness of using urinary IL-18 levels to predict AKI.[130] This meta-analysis included studies which demonstrated that IL-18 was detectable in the urine prior to changes in SCr,[131-133] and in some instances increased urinary IL-18 levels were associated with poor patient outcomes.[132, 134, 135] Overall, the meta-analysis found that increased urinary IL-18 levels are likely to have a modest value in predicting AKI in the general population; however, the definition of AKI varied between studies and different cut-off ranges of IL-18 for the diagnostic prediction of AKI were used, making it difficult to draw any overall

conclusions.[130] Nevertheless, the authors of this paper suggested that IL-18 is likely to be an even more accurate predictor of AKI in the paediatric population.[130]

1.8.2 IL-18 as a biomarker for AKI in the paediatric population

Subsequently, several studies have investigated the use of IL-18 as a biomarker of AKI in the paediatric population using Kidney Disease Improving Global Outcomes (KDIGO) guidelines consistently to classify the diagnosis of AKI.[136, 137] In an ICU setting, increased urinary IL-18 levels at 1-day post-admittance could predict the paediatric patients that were most likely to suffer an AKI insult prior to a rise in SCr.[136] Furthermore, in a long-term-follow-up study of paediatric patients who sustained AKI following cardiopulmonary bypass (CPB) surgery, 27% of the patients that were diagnosed with AKI at the time of CPB maintained elevated levels of urinary IL-18 7 years post-surgery despite no clinical signs of CKD.[137] It will be interesting to see if these elevated levels of urinary IL-18 are predictive of future development of CKD.

1.8.3 IL-18 as a biomarker for cardiovascular risk and mortality in CKD

As previously mentioned, it is important to find a biomarker that sensitively and accurately predicts cardiovascular risk and mortality in the CKD patient population, as patients with CKD are more likely to die from CVD-related complications than progress to ESRD.[138] Currently, traditional risk factors for CVD are poor predictors of cardiovascular events in CKD patients in the later stages of the disease.[139, 140] Therefore, novel biomarkers that can predict CVD in CKD patients are also highly sought after. In a cross-sectional study of stage-3 and -4 CKD patients, elevated plasma IL-18 levels were associated with increased coronary artery and thoracic aorta calcification,[141] a strong predictor of cardiovascular risk.[142] Furthermore, in a cohort study of non-diabetic CKD patients who sustained acute myocardial infarction, high serum levels of IL-18 (above a cut-off level of 1584.5 pg/mL) at 2-year follow-up was predictive of death due to a cardiovascular event in the following year.[143] Formanowicz *et al.* also identified that serum levels of IL-18 above this cut-off point were likely to be the best predictor of cardiovascular mortality when compared to

other markers, including eGFR, albumin, carotid intima media thickness, high sensitivity C-reactive protein, ferritin, and N-terminal prohormone of brain natriuretic peptide.[143] Hence, with further study IL-18 may prove to be a useful marker in predicting cardiovascular risk and mortality in CKD patients.

1.8.4 Future directions

While there is a wealth of evidence that suggests that IL-18 could be a useful diagnostic marker for the diagnosis of AKI, especially in ICU and paediatric settings,[136, 137] and that IL-18 could be a good predictor for cardiovascular risk and mortality in CKD,[141, 143] it is unclear what levels of IL-18 in the serum or urine are pathogenic. Moreover, it is unclear whether studies have measured unbound IL-18 versus IL-18 bound to IL-18BP, because — as we mentioned earlier in this review — a higher ratio of unbound to bound IL-18 likely leads to disease pathology.[28] It is also unclear whether high levels of IL-18 are maintained throughout kidney injury, and whether circulating or urinary levels of IL-18 change with treatment for CKD. There are currently several clinical trials assessing the efficacy of treatments in CKD such as probiotics, curcumin supplementation, adipose-derived stem cell treatment; extended release exenatide treatment, and allopurinol treatment (details available at www.clinicaltrials.gov NCT03228563, NCT04413266, NCT02933827, NCT02251431, NCT03865407) that measure serum or urinary IL-18 levels as an endpoint. Hence, it will be interesting to see if increased IL-18 levels are resolved in patients when kidney damage and function is improved.

1.9 Targeting IL-18 in the clinic

Considering the substantial evidence presented in this review on the role of IL-18 in the development of CKD, as well as evidence supporting a role for IL-18 as a mediator of inflammation and fibrosis both in the clinic and in preclinical models of other diseases,[28] it is unsurprising that there is considerable interest in the development of IL-18 inhibitors as novel therapeutics. Currently there are two main drugs in development that directly target

IL-18, the anti-IL-18 monoclonal antibody GSK1070806 and the recombinant human IL-18BP Tadekinig Alfa. Most phase I-II clinical trials investigating the safety and efficacy of these compounds have revealed that they are well tolerated (details available at: www.clinicaltrials.gov NCT02398435, NCT03681067, NCT03512314, NCT01648153, NTC02723786).[144-146] Whole blood analysis also revealed that GSK1070806 had favourable pharmacokinetic and pharmacodynamic profiles in humans in that it could bind IL-18 with high affinity and reduce the ability of IL-12 and LPS to cause IFN-γ production and NK cell activation *in vitro*.[147] Similarly, Tadekinig Alfa administration resulted in an increase in the plasma levels of IL-18BP in patients ~24-32 hours post-administration.[144] To date, the safety and efficacy of GSK1070806 and Tadekinig alfa have been assessed in the settings of DGF, T2DM, Crohn's disease, X-linked inhibitor of apoptosis (XIAP) deficiency and Adult-onset Still's disease (details available at: www.clinicaltrials.gov NTC02723786, NCT02398435, NCT03681067, NCT03512314, NCT01648153).[144-146] In patients with T2DM, no overall changes in blood pressure or blood glucose were reported following anti-IL-18 monoclonal antibody treatment.[145] However, it is unclear whether these patients were hypertensive and the trial was only statistically powered to detect changes associated with the safety profile of GSK1070806.[145] However, in kidney transplant recipients who received GSK1070806 as an intervention to prevent DGF — an insult of AKI experienced by some kidney transplant recipients that can result in premature graft loss — a phase IIa clinical trial was terminated due to increased serum IL-18 levels, adverse events, and the development of DGF in > 50% of the patient population.[146] This resulted in the trial being discontinued before it could reach statistical power. Therefore, it will be interesting to investigate whether recombinant IL-18BP or anti-IL-18 monoclonal antibody are effective at reducing kidney injury and fibrosis in patients with AKI or CKD.

1.10 Conclusion

In conclusion, there is substantial evidence to suggest that the development of CKD is associated with the activation of the inflammasome platform, production of IL-18, and stimulation of downstream pro-inflammatory signalling pathways. Additionally, IL-18, may prove to be a sensitive early biomarker of kidney injury. It remains to be determined if therapeutic targeting of the IL-18 signalling system will ameliorate kidney inflammation and fibrosis, and cardiovascular complications in patients with kidney disease. Therefore, a deeper understanding of this signalling system and its contributions to the development of CKD may serve to determine the therapeutic and diagnostic potential of IL-18 in the clinic.

1.11 Hypothesis and aims of the thesis

As mentioned previously, hypertension is one of the main causes of CKD. Hypertension likely leads to kidney injury by vasoconstriction of/or damage to the blood vessels that supply the kidney.[147] This results in hypoxia within the kidney, which leads to further inflammation and cell death.[147] In turn, elevations in blood pressure accompany the loss of kidney function in CKD, because inflammation in the kidneys can cause glomerular injury and impaired urinary sodium excretion. Ultimately, this disrupts the pressure-natriuresis relationship which controls blood pressure. We hypothesise that the inflammasome-dependent release of IL-18 is a key cause of kidney inflammation and fibrosis, which leads to hypertension in the 1K/DOCA/salt model of high blood pressure and CKD. To test this hypothesis, this thesis will address the following aims:

- To evaluate the impact of genetic inhibition of IL-18 on the development of high blood pressure, renal inflammation, and renal fibrosis in 1K/DOCA/salt-induced hypertension (Chapter 3)

- To determine the cellular source of IL-18 in 1K/DOCA/salt-induced hypertension and kidney injury through a combination of bone marrow transplant and immunolocalisation studies (Chapter 3)
- To use knockout mice to determine the target of IL-18 in 1K/DOCA/salt-induced hypertension and kidney injury, specifically the role of the IL-18 receptor subunits, IL-18R1 (Chapter 4) and IL-18RAP (Chapter 5)

1.12 References

1. Jha V, Garcia-Garcia G, Iseki K, Li Z, Naicker S, Plattner B, Saran R, Wang AY and Yang CW. Chronic kidney disease: global dimension and perspectives. *Lancet*. 2013;382:260-72.
2. Gupta J, Mitra N, Kanetsky PA, Devaney J, et al. Association between albuminuria, kidney function, and inflammatory biomarker profile in CKD in CRIC. *Clin J Am Soc Nephrol*. 2012;7:1938-46.
3. Krishnan SM, Dowling JK, Ling YH, et al Inflammasome activity is essential for one kidney/deoxycorticosterone acetate/salt-induced hypertension in mice. *Br J Pharmacol*. 2016;173:752-65.
4. Vandanmagsar B, Youm Y-H, Ravussin A, Galgani JE, Stadler K, Mynatt RL, Ravussin E, Stephens JM and Dixit VD. The NLRP3 inflammasome instigates obesity-induced inflammation and insulin resistance. *Nat Med*. 2011;17:179-188.
5. Schroder K and Tschopp J. The inflammasomes. *Cell*. 2010;140:821-32.
6. Granata S, Masola V, Zoratti E, Scupoli MT, Baruzzi A, Messa M, Sallustio F, Gesualdo L, Lupo A and Zaza G. NLRP3 Inflammasome Activation in Dialyzed Chronic Kidney Disease Patients. *PLoS One*. 2015;10:e0122272.
7. Vilaysane A, Chun J, Seamone ME, et al. The NLRP3 inflammasome promotes renal inflammation and contributes to CKD. *J Am Soc Nephrol*. 2010;21:1732-44.
8. Hung AM, Ellis CD, Shintani A, Booker C and Ikizler TA. IL-1β receptor antagonist reduces inflammation in hemodialysis patients. *J Am Soc Nephrol*. 2011;22:437-42.
9. Anders HJ, Suarez-Alvarez B, Grigorescu M, et al. The macrophage phenotype and inflammasome component NLRP3 contributes to nephrocalcinosis-related chronic kidney disease independent from IL-1-mediated tissue injury. *Kidney Int*. 2018;93:656-669.

10. Ling YH, Krishnan SM, Chan CT,et al. Anakinra reduces blood pressure and renal fibrosis in one kidney/DOCA/salt-induced hypertension. *Pharmacol Res*. 2017;116:77-86.
11. Hill NR, Fatoba ST, Oke JL, Hirst JA, O'Callaghan CA, Lasserson DS and Hobbs FD. Global Prevalence of Chronic Kidney Disease - A Systematic Review and Meta-Analysis. *PLoS One*. 2016;11:e0158765.
12. Lozano R, Naghavi M, Foreman K, et al. Global and regional mortality from 235 causes of death for 20 age groups in 1990 and 2010: a systematic analysis for the Global Burden of Disease Study 2010. *Lancet*. 2012;380:2095-128.
13. Stevens LA, Viswanathan G and Weiner DE. Chronic kidney disease and end-stage renal disease in the elderly population: current prevalence, future projections, and clinical significance. *Adv Chronic Kidney Dis*. 2010;17:293-301.
14. Vallianou NG, Mitesh S, Gkogkou A and Geladari E. Chronic Kidney Disease and Cardiovascular Disease: Is there Any Relationship? *Curr Cardiol Rev*. 2019;15:55-63.
15. Palmer SC, Maggo JK, Campbell KL, Craig JC, Johnson DW, Sutanto B, Ruospo M, Tong A and Strippoli GF. Dietary interventions for adults with chronic kidney disease. *Cochrane Database Syst Rev*. 2017;4:Cd011998.
16. Hill CJ, Cardwell CR, Patterson CC, Maxwell AP, Magee GM, Young RJ, Matthews B, O'Donoghue DJ and Fogarty DG. Chronic kidney disease and diabetes in the National Health Service: a cross-sectional survey of the UK National Diabetes Audit. *Diabet Med*. 2014;31:448-454.
17. Levey AS and Coresh J. Chronic kidney disease. *Lancet*. 2012;379:165-80.
18. Casas JP, Chua W, Loukogeorgakis S, Vallance P, Smeeth L, Hingorani AD and MacAllister RJ. Effect of inhibitors of the renin-angiotensin system and other antihypertensive drugs on renal outcomes: systematic review and meta-analysis. *Lancet*. 2005;366:2026-33.

19. Roy L, White-Guay B, Dorais M, Dragomir A, Lessard M and Perreault S. Adherence to antihypertensive agents improves risk reduction of end-stage renal disease. *Kidney Int*. 2013;84:570-7.
20. Mann JF, Schmieder RE, McQueen M, et al. Renal outcomes with telmisartan, ramipril, or both, in people at high vascular risk (the ONTARGET study): a multicentre, randomised, double-blind, controlled trial. *Lancet*. 2008;372:547-53.
21. Sarafidis PA, Khosla N and Bakris GL. Antihypertensive therapy in the presence of proteinuria. *Am J Kidney Dis*. 2007;49:12-26.
22. Wang K, Hu J, Luo T, Wang Y, Yang S, Qing H, Cheng Q and Li Q. Effects of Angiotensin-Converting Enzyme Inhibitors and Angiotensin II Receptor Blockers on All-Cause Mortality and Renal Outcomes in Patients with Diabetes and Albuminuria: a Systematic Review and Meta-Analysis. *Kidney Blood Press Res*. 2018;43:768-779.
23. Tobe SW, Clase CM, Gao P, McQueen M, Grosshennig A, Wang X, Teo KK, Yusuf S and Mann JF. Cardiovascular and renal outcomes with telmisartan, ramipril, or both in people at high renal risk: results from the ONTARGET and TRANSCEND studies. *Circulation*. 2011;123:1098-107.
24. Chen RA, Scott S, Mattern WD, Mohini R and Nissenson AR. The case for disease management in chronic kidney disease. *Dis Manag*. 2006;9:86-92.
25. Webster AC, Nagler EV, Morton RL and Masson P. Chronic Kidney Disease. *Lancet*. 2017;389:1238-1252.
26. Jha S and Ting JP. Inflammasome-associated nucleotide-binding domain, leucine-rich repeat proteins and inflammatory diseases. *J Immunol*. 2009;183:7623-9.
27. Schroder K, Zhou R and Tschopp J. The NLRP3 inflammasome: a sensor for metabolic danger? *Science*. 2010;327:296-300.
28. Dinarello CA, Novick D, Kim S and Kaplanski G. Interleukin-18 and IL-18 binding protein. *Front Immunol*. 2013;4:289.

29. Gu Y, Kuida K, Tsutsui H, et al. Activation of interferon-gamma inducing factor mediated by interleukin-1beta converting enzyme. *Science*. 1997;275:206-9.

30. Pirhonen J, Sareneva T, Kurimoto M, Julkunen I and Matikainen S. Virus infection activates IL-1 beta and IL-18 production in human macrophages by a caspase-1-dependent pathway. *J Immunol*. 1999;162:7322-9.

31. Stokman G, Kers J, Yapici Ü,et al. Predominant Tubular Interleukin-18 Expression in Polyomavirus-Associated Nephropathy. *Transplantation*. 2016;100:e88-95.

32. Hewins P, Morgan MD, Holden N, Neil D, Williams JM, Savage CO and Harper L. IL-18 is upregulated in the kidney and primes neutrophil responsiveness in ANCA-associated vasculitis. *Kidney Int*. 2006;69:605-15.

33. Wyburn K, Wu H, Chen G, Yin J, Eris J and Chadban S. Interleukin-18 affects local cytokine expression but does not impact on the development of kidney allograft rejection. *Am J Transplant*. 2006;6:2612-21.

34. Franke EI, Vanderbrink BA, Hile KL, Zhang H, Cain A, Matsui F and Meldrum KK. Renal IL-18 production is macrophage independent during obstructive injury. *PLoS One*. 2012;7:e47417.

35. Liang D, Liu HF, Yao CW, Liu HY, Huang-Fu CM, Chen XW, Du SH and Chen XW. Effects of interleukin 18 on injury and activation of human proximal tubular epithelial cells. *Nephrology*. 2007;12:53-61.

36. Faust J, Menke J, Kriegsmann J, Kelley VR, Mayet WJ, Galle PR and Schwarting A. Correlation of renal tubular epithelial cell-derived interleukin-18 up-regulation with disease activity in MRL-Faslpr mice with autoimmune lupus nephritis. *Arthritis Rheum*. 2002;46:3083-95.

37. Gauer S, Sichler O, Obermüller N, Holzmann Y, Kiss E, Sobkowiak E, Pfeilschifter J, Geiger H, Mühl H and Hauser IA. IL-18 is expressed in the intercalated cell of human kidney. *Kidney Int*. 2007;72:1081-7.

38. Leaf IA, Nakagawa S, Johnson BG, Cha JJ, Mittelsteadt K, Guckian KM, Gomez IG, Altemeier WA and Duffield JS. Pericyte MyD88 and IRAK4 control inflammatory and fibrotic responses to tissue injury. *J Clin Invest*. 2017;127:321-334.
39. Chen H, Zhu J, Liu Y, Dong Z, Liu H, Liu Y, Zhou X, Liu F and Chen G. Lipopolysaccharide Induces Chronic Kidney Injury and Fibrosis through Activation of mTOR Signaling in Macrophages. *Am J Nephrol*. 2015;42:305-17.
40. Kim J, Seok YM, Jung KJ and Park KM. Reactive oxygen species/oxidative stress contributes to progression of kidney fibrosis following transient ischemic injury in mice. *Am J Physiol Renal Physiol*. 2009;297:F461-70.
41. Fang L, Xie D, Wu X, Cao H, Su W and Yang J. Involvement of endoplasmic reticulum stress in albuminuria induced inflammasome activation in renal proximal tubular cells. *PLoS One*. 2013;8:e72344.
42. Zhuang Y, Hu C, Ding G, Zhang Y, Huang S, Jia Z and Zhang A. Albumin impairs renal tubular tight junctions via targeting the NLRP3 inflammasome. *Am J Physiol Renal Physiol*. 2015;308:F1012-9.
43. Zhuang Y, Ding G, Zhao M, et al. NLRP3 inflammasome mediates albumin-induced renal tubular injury through impaired mitochondrial function. *J Biol Chem*. 2014;289:25101-11.
44. Kim SM, Lee SH, Kim YG, et al. Hyperuricemia-induced NLRP3 activation of macrophages contributes to the progression of diabetic nephropathy. *Am J Physiol Renal Physiol*. 2015;308:F993-f1003.
45. Knauf F, Asplin JR, Granja I, Schmidt IM, Moeckel GW, David RJ, Flavell RA and Aronson PS. NALP3-mediated inflammation is a principal cause of progressive renal failure in oxalate nephropathy. *Kidney Int*. 2013;84:895-901.
46. Gilbert KC and Brown NJ. Aldosterone and inflammation. *Curr Opin Endocrinol Diabetes Obes*. 2010;17:199-204.

47. Nangaku M. Chronic hypoxia and tubulointerstitial injury: a final common pathway to end-stage renal failure. *J Am Soc Nephrol*. 2006;17:17-25.

48. Van Beusecum JP, Barbaro NR, McDowell Z, et al. High Salt Activates CD11c(+) Antigen-Presenting Cells via SGK (Serum Glucocorticoid Kinase) 1 to Promote Renal Inflammation and Salt-Sensitive Hypertension. *Hypertension*. 2019;74:555-563.

49. Komada T, Chung H, Lau A, Platnich JM, Beck PL, Benediktsson H, Duff HJ, Jenne CN and Muruve DA. Macrophage Uptake of Necrotic Cell DNA Activates the AIM2 Inflammasome to Regulate a Proinflammatory Phenotype in CKD. *J Am Soc Nephrol*. 2018;29:1165-1181.

50. Venner JM, Famulski KS, Badr D, Hidalgo LG, Chang J and Halloran PF. Molecular landscape of T cell-mediated rejection in human kidney transplants: prominence of CTLA4 and PD ligands. *Am J Transplant*. 2014;14:2565-76.

51. Kim HJ, Lee DW, Ravichandran K,et al. NLRP3 inflammasome knockout mice are protected against ischemic but not cisplatin-induced acute kidney injury. *J Pharmacol Exp Ther*. 2013;346:465-72.

52. Krishnan SM, Ling YH, Huuskes BM, et al. Pharmacological inhibition of the NLRP3 inflammasome reduces blood pressure, renal damage, and dysfunction in salt-sensitive hypertension. *Cardiovasc Res*. 2019;115:776-787.

53. Ludwig-Portugall I, Bartok E, Dhana E, et al. An NLRP3-specific inflammasome inhibitor attenuates crystal-induced kidney fibrosis in mice. *Kidney Int*. 2016;90:525-39.

54. Gong W, Mao S, Yu J, Song J, Jia Z, Huang S and Zhang A. NLRP3 deletion protects against renal fibrosis and attenuates mitochondrial abnormality in mouse with 5/6 nephrectomy. *Am J Physiol Renal Physiol*. 2016;310:F1081-8.

55. Faubel S, Ljubanovic D, Reznikov L, Somerset H, Dinarello CA and Edelstein CL. Caspase-1-deficient mice are protected against cisplatin-induced apoptosis and acute tubular necrosis. *Kidney Int*. 2004;66:2202-13.

56. Guo Y, Zhang J, Lai X, Chen M and Guo Y. Tim-3 exacerbates kidney ischaemia/reperfusion injury through the TLR-4/NF-κB signalling pathway and an NLR-C4 inflammasome activation. *Clin Exp Immunol*. 2018;193:113-129.

57. Gao P, He FF, Tang H, Lei CT, Chen S, Meng XF, Su H and Zhang C. NADPH oxidase-induced NALP3 inflammasome activation is driven by thioredoxin-interacting protein which contributes to podocyte injury in hyperglycemia. *J Diabetes Res*. 2015;2015:504761.

58. Soares JLS, Fernandes FP, Patente TA, Monteiro MB, Parisi MC, Giannella-Neto D, Corrêa-Giannella ML and Pontillo A. Gain-of-function variants in NLRP1 protect against the development of diabetic kidney disease: NLRP1 inflammasome role in metabolic stress sensing? *Clin Immunol*. 2018;187:46-49.

59. Shigeoka AA, Kambo A, Mathison JC, King AJ, Hall WF, da Silva Correia J, Ulevitch RJ and McKay DB. Nod1 and nod2 are expressed in human and murine renal tubular epithelial cells and participate in renal ischemia reperfusion injury. *J Immunol*. 2010;184:2297-304.

60. Lech M, Avila-Ferrufino A, Skuginna V, Susanti HE and Anders HJ. Quantitative expression of RIG-like helicase, NOD-like receptor and inflammasome-related mRNAs in humans and mice. *Int Immunol*. 2010;22:717-28.

61. Zhang W, Cai Y, Xu W, Yin Z, Gao X and Xiong S. AIM2 facilitates the apoptotic DNA-induced systemic lupus erythematosus via arbitrating macrophage functional maturation. *J Clin Immunol*. 2013;33:925-37.

62. Anders HJ and Schaefer L. Beyond tissue injury-damage-associated molecular patterns, toll-like receptors, and inflammasomes also drive regeneration and fibrosis. *J Am Soc Nephrol*. 2014;25:1387-400.

63. Xiang H, Zhu F, Xu Z and Xiong J. Role of Inflammasomes in Kidney Diseases via Both Canonical and Non-canonical Pathways. *Front Cell Dev Biol*. 2020;8:106.

64. Komada T and Muruve DA. The role of inflammasomes in kidney disease. *Nat Rev Nephrol*. 2019;15:501-520.

65. Debets R, Timans JC, Churakowa T, et al. IL-18 receptors, their role in ligand binding and function: anti-IL-1RAcPL antibody, a potent antagonist of IL-18. *J Immunol*. 2000;165:4950-6.

66. Torigoe K, Ushio S, Okura T, et al. Purification and characterization of the human interleukin-18 receptor. *J Biol Chem*. 1997;272:25737-42.

67. Born TL, Thomassen E, Bird TA and Sims JE. Cloning of a novel receptor subunit, AcPL, required for interleukin-18 signaling. *J Biol Chem*. 1998;273:29445-50.

68. Rex DAB, Agarwal N, Prasad TSK, Kandasamy RK, Subbannayya Y and Pinto SM. A comprehensive pathway map of IL-18-mediated signalling. *J Cell Commun Signal*. 2020;14:257-266.

69. Walsh MC, Kim GK, Maurizio PL, Molnar EE and Choi Y. TRAF6 autoubiquitination-independent activation of the NFkappaB and MAPK pathways in response to IL-1 and RANKL. *PLoS One*. 2008;3:e4064-e4064.

70. Garlanda C, Dinarello CA and Mantovani A. The interleukin-1 family: back to the future. *Immunity*. 2013;39:1003-18.

71. Corbaz A, ten Hove T, Herren S, et al. IL-18-binding protein expression by endothelial cells and macrophages is up-regulated during active Crohn's disease. *J Immunol*. 2002;168:3608-16.

72. Kim SH, Eisenstein M, Reznikov L, Fantuzzi G, Novick D, Rubinstein M and Dinarello CA. Structural requirements of six naturally occurring isoforms of the IL-18 binding protein to inhibit IL-18. *Proc Natl Acad Sci U S A*. 2000;97:1190-5.

73. Novick D, Schwartsburd B, Pinkus R, et al. A novel IL-18BP ELISA shows elevated serum IL-18BP in sepsis and extensive decrease of free IL-18. *Cytokine*. 2001;14:334-42.

74. Mühl H, Kämpfer H, Bosmann M, Frank S, Radeke H and Pfeilschifter J. Interferon-gamma mediates gene expression of IL-18 binding protein in nonleukocytic cells. *Biochem Biophys Res Commun*. 2000;267:960-3.

75. Lonnemann G, Novick D, Rubinstein M and Dinarello CA. Interleukin-18, interleukin-18 binding protein and impaired production of interferon-gamma in chronic renal failure. *Clin Nephrol*. 2003;60:327-34.

76. Ye L, Ji L, Wen Z, et al. IL-37 inhibits the production of inflammatory cytokines in peripheral blood mononuclear cells of patients with systemic lupus erythematosus: its correlation with disease activity. *J Transl Med*. 2014;12:69.

77. Li Y, Wang Z, Yu T, Chen B, Zhang J, Huang K and Huang Z. Increased expression of IL-37 in patients with Graves' disease and its contribution to suppression of proinflammatory cytokines production in peripheral blood mononuclear cells. *PLoS One*. 2014;9:e107183.

78. Ye L, Jiang B, Deng J, Du J, Xiong W, Guan Y, Wen Z, Huang K and Huang Z. IL-37 Alleviates Rheumatoid Arthritis by Suppressing IL-17 and IL-17-Triggering Cytokine Production and Limiting Th17 Cell Proliferation. *J Immunol*. 2015;194:5110-9.

79. Nold-Petry CA, Lo CY, Rudloff I, et al. IL-37 requires the receptors IL-18Rα and IL-1R8 (SIGIRR) to carry out its multifaceted anti-inflammatory program upon innate signal transduction. *Nat Immunol*. 2015;16:354-65.

80. Bulau AM, Nold MF, Li S, et al. Role of caspase-1 in nuclear translocation of IL-37, release of the cytokine, and IL-37 inhibition of innate immune responses. *Proc Natl Acad Sci U S A*. 2014;111:2650-5.

81. Wang L, Quan Y, Yue Y, Heng X and Che F. Interleukin-37: A crucial cytokine with multiple roles in disease and potentially clinical therapy. *Oncol Lett*. 2018;15:4711-4719.

82. Dinarello CA, Nold-Petry C, Nold M, Fujita M, Li S, Kim S and Bufler P. Suppression of innate inflammation and immunity by interleukin-37. *Eur J Immunol*. 2016;46:1067-81.

83. Ellisdon AM, Nold-Petry CA, D'Andrea L,et al. Homodimerization attenuates the anti-inflammatory activity of interleukin-37. *Sci Immunol*. 2017;2.

84. Bufler P, Azam T, Gamboni-Robertson F, Reznikov LL, Kumar S, Dinarello CA and Kim SH. A complex of the IL-1 homologue IL-1F7b and IL-18-binding protein reduces IL-18 activity. *Proc Natl Acad Sci U S A*. 2002;99:13723-8.

85. Kumar S, Hanning CR, Brigham-Burke MR, et al. Interleukin-1F7B (IL-1H4/IL-1F7) is processed by caspase-1 and mature IL-1F7B binds to the IL-18 receptor but does not induce IFN-gamma production. *Cytokine*. 2002;18:61-71.

86. Dinarello CA. Overview of the IL-1 family in innate inflammation and acquired immunity. *Immunol Rev*. 2018;281:8-27.

87. Gong J, Wei T, Stark RW, Jamitzky F, Heckl WM, Anders HJ, Lech M and Rössle SC. Inhibition of Toll-like receptors TLR4 and 7 signaling pathways by SIGIRR: A computational approach. *J Struct Biol*. 2010;169:323-330.

88. Yang Y, Zhang Z-X, Lian D, Haig A, Bhattacharjee RN and Jevnikar AM. IL-37 inhibits IL-18-induced tubular epithelial cell expression of pro-inflammatory cytokines and renal ischemia-reperfusion injury. *Kidney Int*. 2015;87:396-408.

89. Melnikov VY, Ecder T, Fantuzzi G, Siegmund B, Lucia MS, Dinarello CA, Schrier RW and Edelstein CL. Impaired IL-18 processing protects caspase-1-deficient mice from ischemic acute renal failure. *J Clin Invest*. 2001;107:1145-52.

90. He Z, Lu L, Altmann C, Hoke TS, Ljubanovic D, Jani A, Dinarello CA, Faubel S and Edelstein CL. Interleukin-18 binding protein transgenic mice are protected against ischemic acute kidney injury. *Am J Physiol Renal Physiol*. 2008;295:F1414-21.

91. Wu H, Craft ML, Wang P, Wyburn KR, Chen G, Ma J, Hambly B and Chadban SJ. IL-18 contributes to renal damage after ischemia-reperfusion. *J Am Soc Nephrol. : JASN*. 2008;19:2331-2341.

92. Melnikov VY, Faubel S, Siegmund B, Lucia MS, Ljubanovic D and Edelstein CL. Neutrophil-independent mechanisms of caspase-1- and IL-18-mediated ischemic acute tubular necrosis in mice. *J Clin Invest*. 2002;110:1083-91.

93. Bani-Hani AH, Leslie JA, Asanuma H, Dinarello CA, Campbell MT, Meldrum DR, Zhang H, Hile K and Meldrum KK. IL-18 neutralization ameliorates obstruction-induced epithelial-mesenchymal transition and renal fibrosis. *Kidney Int*. 2009;76:500-11.

94. Kitching AR, Turner AL, Wilson GR, Semple T, Odobasic D, Timoshanko JR, O'Sullivan KM, Tipping PG, Takeda K, Akira S and Holdsworth SR. IL-12p40 and IL-18 in crescentic glomerulonephritis: IL-12p40 is the key Th1-defining cytokine chain, whereas IL-18 promotes local inflammation and leukocyte recruitment. *J Am Soc Nephrol*. 2005;16:2023-33.

95. Shahzad K, Bock F, Al-Dabet MM, et al. Caspase-1, but Not Caspase-3, Promotes Diabetic Nephropathy. *J Am Soc Nephrol*. 2016;27(8):2270-2275.

96. Okamura H, Kashiwamura S, Tsutsui H, Yoshimoto T and Nakanishi K. Regulation of interferon-gamma production by IL-12 and IL-18. *Curr Opin Immunol*. 1998;10:259-64.

97. Nakahira M, Ahn HJ, Park WR, et al. Synergy of IL-12 and IL-18 for IFN-gamma gene expression: IL-12-induced STAT4 contributes to IFN-gamma promoter activation by up-regulating the binding activity of IL-18-induced activator protein 1. *J Immunol*. 2002;168:1146-53.

98. Hamza T, Barnett JB and Li B. Interleukin 12 a key immunoregulatory cytokine in infection applications. *Int J Mol Sci*. 2010;11:789-806.

99. Okamura H, Tsutsui H, Kashiwamura S, Yoshimoto T and Nakanishi K. Interleukin-18: a novel cytokine that augments both innate and acquired immunity. *Adv Immunol*. 1998;70:281-312.

100. Kalina U, Kauschat D, Koyama N, Nuernberger H, Ballas K, Koschmieder S, Bug G, Hofmann WK, Hoelzer D and Ottmann OG. IL-18 activates STAT3 in the natural killer cell line 92, augments cytotoxic activity, and mediates IFN-gamma production by the stress kinase p38 and by the extracellular regulated kinases p44erk-1 and p42erk-21. *J Immunol*. 2000;165:1307-13.

101. Leite-De-Moraes MC, Hameg A, Arnould A, Machavoine F, Koezuka Y, Schneider E, Herbelin A and Dy M. A distinct IL-18-induced pathway to fully activate NK T lymphocytes independently from TCR engagement. *J Immunol*. 1999;163:5871-6.

102. Daemen MA, van't Veer C, Wolfs TG and Buurman WA. Ischemia/reperfusion-induced IFN-gamma up-regulation: involvement of IL-12 and IL-18. *J Immunol*. 1999;162:5506-10.

103. Garcia GE, Xia Y, Ku G, Johnson RJ, Wilson CB and Feng L. IL-18 translational inhibition restricts IFN-gamma expression in crescentic glomerulonephritis. *Kidney Int*. 2003;64:160-9.

104. Lalor SJ, Dungan LS, Sutton CE, Basdeo SA, Fletcher JM and Mills KH. Caspase-1-processed cytokines IL-1beta and IL-18 promote IL-17 production by gammadelta and CD4 T cells that mediate autoimmunity. *J Immunol*. 2011;186:5738-48.

105. Che Mat NF, Zhang X, Guzzo C and Gee K. Interleukin-23-induced interleukin-23 receptor subunit expression is mediated by the Janus kinase/signal transducer and activation of transcription pathway in human CD4 T cells. *J Interferon Cytokine Res*. 2011;31:363-71.

106. Leyfer D, Bond A, Tworog E, Perron D, Maska S, Brito A, Kamens J, Weng Z and Voss J. cis-Element clustering correlates with dose-dependent pro- and antisignaling effects of IL18. *Genes Immun*. 2004;5:354-62.

107. Morel JC, Park CC, Kumar P and Koch AE. Interleukin-18 induces rheumatoid arthritis synovial fibroblast CXC chemokine production through NFkappaB activation. *Lab invest*. 2001;81:1371-1383.

108. Morel JC, Park CC, Woods JM and Koch AE. A novel role for interleukin-18 in adhesion molecule induction through NF kappa B and phosphatidylinositol (PI) 3-kinase-dependent signal transduction pathways. *J Biol Chem*. 2001;276:37069-75.

109. Kitching AR, Tipping PG, Kurimoto M and Holdsworth SR. IL-18 has IL-12-independent effects in delayed-type hypersensitivity: studies in cell-mediated crescentic glomerulonephritis. *J Immunol*. 2000;165:4649-57.

110. Nagata S and Golstein P. The Fas death factor. *Science*. 1995;267:1449-56.

111. Ottonello L, Tortolina G, Amelotti M and Dallegri F. Soluble Fas ligand is chemotactic for human neutrophilic polymorphonuclear leukocytes. *J Immunol*. 1999;162:3601-6.

112. Yano T, Nozaki Y, Kinoshita K, et al. The pathological role of IL-18Rα in renal ischemia/reperfusion injury. *Lab Invest*. 2015;95:78-91.

113. Zhang H, Hile KL, Asanuma H, Vanderbrink B, Franke EI, Campbell MT and Meldrum KK. IL-18 mediates proapoptotic signaling in renal tubular cells through a Fas ligand-dependent mechanism. *Am J Physiol Renal Physiol*. 2011;301:F171-8.

114. Kinoshita K, Yamagata T, Nozaki Y, Sugiyama M, Ikoma S, Funauchi M and Kanamaru A. Blockade of IL-18 receptor signaling delays the onset of autoimmune disease in MRL-Faslpr mice. *J Immunol*. 2004;173:5312-8.

115. Marotte H, Ahmed S, Ruth JH and Koch AE. Blocking ERK-1/2 reduces tumor necrosis factor alpha-induced interleukin-18 bioactivity in rheumatoid arthritis synovial fibroblasts by induction of interleukin-18 binding protein A. *Arthritis Rheum*. 2010;62:722-31.

116. Yu X, Ge L, Niu L, Lian X, Ma H and Pang L. The Dual Role of Inducible Nitric Oxide Synthase in Myocardial Ischemia/Reperfusion Injury: Friend or Foe? *Oxid Med Cell Longev*. 2018;2018:8364848.

117. Kim YM, Talanian RV, Li J and Billiar TR. Nitric oxide prevents IL-1beta and IFN-gamma-inducing factor (IL-18) release from macrophages by inhibiting caspase-1 (IL-1beta-converting enzyme). *J Immunol*. 1998;161:4122-8.

118. VanderBrink BA, Asanuma H, Hile K, Zhang H, Rink RC and Meldrum KK. Interleukin-18 stimulates a positive feedback loop during renal obstruction via interleukin-18 receptor. *J Urol*. 2011;186:1502-8.

119. Nozaki Y, Kinoshita K, Yano T, et al. Signaling through the interleukin-18 receptor α attenuates inflammation in cisplatin-induced acute kidney injury. *Kidney Int*. 2012;82:892-902.

120. Better Health. Department of Health. Kidney failure: Symptoms of kidney disease. State Government of Victoria. https://www.betterhealth.vic.gov.au. 2018

121. Wouters OJ, O'Donoghue DJ, Ritchie J, Kanavos PG and Narva AS. Early chronic kidney disease: diagnosis, management and models of care. *Nat Rev Nephrol*. 2015;11:491-502.

122. Glassock RJ and Winearls C. Screening for CKD with eGFR: doubts and dangers. *Clin J Am Soc Nephrol*. 2008;3:1563-8.

123. Hallan SI and Orth SR. The KDOQI 2002 classification of chronic kidney disease: for whom the bell tolls. *Nephrol Dial Transplant*. 2010;25:2832-2836.

124. Dennen P and Parikh CR. Biomarkers of acute kidney injury: can we replace serum creatinine? *Clin Nephrol*. 2007;68:269-78.

125. Weinstein JR and Anderson S. The aging kidney: physiological changes. *Adv Chronic Kidney Dis*. 2010;17:302-307.

126. Parikh CR, Jani A, Melnikov VY, Faubel S and Edelstein CL. Urinary interleukin-18 is a marker of human acute tubular necrosis. *Am J Kidney Dis*. 2004;43:405-14.

127. Gracie JA, Robertson SE and McInnes IB. Interleukin-18. *J Leukoc Biol*. 2003;73:213-24.

128. Nisula S, Yang R, Poukkanen M, et al. Predictive value of urine interleukin-18 in the evolution and outcome of acute kidney injury in critically ill adult patients. *Br J Anaesth*. 2015;114:460-8.

129. Siew ED, Ikizler TA, Gebretsadik T, et al. Elevated urinary IL-18 levels at the time of ICU admission predict adverse clinical outcomes. *Clin J Am Soc Nephrol*. 2010;5:1497-505.

130. Lin X, Yuan J, Zhao Y and Zha Y. Urine interleukin-18 in prediction of acute kidney injury: a systemic review and meta-analysis. *J Nephrol*. 2015;28:7-16.

131. Parikh CR, Mishra J, Thiessen-Philbrook H, Dursun B, Ma Q, Kelly C, Dent C, Devarajan P and Edelstein CL. Urinary IL-18 is an early predictive biomarker of acute kidney injury after cardiac surgery. *Kidney Int*. 2006;70:199-203.

132. Parikh CR, Abraham E, Ancukiewicz M and Edelstein CL. Urine IL-18 is an early diagnostic marker for acute kidney injury and predicts mortality in the intensive care unit. *J Am Soc Nephrol*. 2005;16:3046-52.Washburn KK, Zappitelli M, Arikan AA, Loftis L, Yalavarthy R, Parikh CR, Edelstein CL and Goldstein SL. Urinary interleukin-18 is an acute kidney injury biomarker in critically ill children. *Nephrol Dial Transplant*. 2008;23:566-72.

133. Li Y, Fu C, Zhou X, Xiao Z, Zhu X, Jin M, Li X and Feng X. Urine interleukin-18 and cystatin-C as biomarkers of acute kidney injury in critically ill neonates. *Pediatr Nephrol*. 2012;27:851-60.

134. Parikh CR, Coca SG, Thiessen-Philbrook H, et al. Postoperative biomarkers predict acute kidney injury and poor outcomes after adult cardiac surgery. *J Am Soc Nephrol*. 2011;22:1748-57.

135. Palermo J, Dart AB, De Mello A, et al. Biomarkers for Early Acute Kidney Injury Diagnosis and Severity Prediction: A Pilot Multicenter Canadian Study of Children Admitted to the ICU. *Pediatr Crit Care Med*. 2017;18:e235-e244.

136. Cooper DS, Claes D, Goldstein SL, Bennett MR, Ma Q, Devarajan P and Krawczeski CD. Follow-Up Renal Assessment of Injury Long-Term After Acute Kidney Injury (FRAIL-AKI). *Clin J Am Soc Nephrol*. 2016;11:21-9.

137. Subbiah AK, Chhabra YK and Mahajan S. Cardiovascular disease in patients with chronic kidney disease: a neglected subgroup. *Heart Asia*. 2016;8:56-61.

138. Herzog CA, Asinger RW, Berger AK,et al. Cardiovascular disease in chronic kidney disease. A clinical update from Kidney Disease: Improving Global Outcomes (KDIGO). *Kidney Int*. 2011;80:572-586.

139. Sun J, Axelsson J, Machowska A, Heimbürger O, Bárány P, Lindholm B, Lindström K, Stenvinkel P and Qureshi AR. Biomarkers of Cardiovascular Disease and Mortality Risk in Patients with Advanced CKD. *Clin J Am Soc Nephrol*. 2016;11:1163-72.

140. Kiu Weber CI, Duchateau-Nguyen G, Solier C, Schell-Steven A, Hermosilla R, Nogoceke E and Block G. Cardiovascular risk markers associated with arterial calcification in patients with chronic kidney disease Stages 3 and 4. *Clin Kidney J*. 2014;7:167-173.

141. Palit S and Kendrick J. Vascular calcification in chronic kidney disease: role of disordered mineral metabolism. *Curr Pharm Des*. 2014;20:5829-5833.

142. Formanowicz D, Wanic-Kossowska M, Pawliczak E, Radom M and Formanowicz P. Usefulness of serum interleukin-18 in predicting cardiovascular mortality in patients with chronic kidney disease – systems and clinical approach. *Sci Rep*. 2015;5:18332.

143. Gabay C, Fautrel B, Rech J, et al. Open-label, multicentre, dose-escalating phase II clinical trial on the safety and efficacy of tadekinig alfa (IL-18BP) in adult-onset Still's disease. *Ann Rheum Dis*. 2018;77:840-847.

144. McKie EA, Reid JL, Mistry PC, DeWall SL, Abberley L, Ambery PD and Gil-Extremera B. A Study to Investigate the Efficacy and Safety of an Anti-Interleukin-18 Monoclonal Antibody in the Treatment of Type 2 Diabetes Mellitus. *PLoS One*. 2016;11:e0150018.

145. Wlodek E, Kirkpatrick RB, Andrews S, et al. A pilot study evaluating GSK1070806 inhibition of interleukin-18 in renal transplant delayed graft function. *PLoS One*. 2021;16:e0247972.

146. Mistry P, Reid J, Pouliquen I, McHugh S, Abberley L, DeWall S, Taylor A, Tong X, Rocha Del Cura M and McKie E. Safety, tolerability, pharmacokinetics, and pharmacodynamics of single-dose antiinterleukin- 18 mAb GSK1070806 in healthy and obese subjects. *Int J Clin Pharmacol Ther*. 2014;52:867-79.

147. Fu Q, Colgan SP and Shelley CS. Hypoxia: The Force that Drives Chronic Kidney Disease. *Clin Med Res*. 2016;14:15-39.

Chapter 2

General Methods

2.1 Animals

Male mice aged 8-17 weeks and weighing 20-35 g (except where indicated in Table 2.1-2.3), and female mice aged 8-16 weeks weighing 18-30 g were used in this study. These studies were performed on mice of the C57Bl/6 strain. To study the impact of IL-18 signalling on hypertension and other disease parameters, mice genetically deficient in IL-18 (IL-18$^{-/-}$),[1] the IL-18R1 (IL-18R1$^{-/-}$),[2] RAG1 (RAG1$^{-/-}$), and IL-18RAP (IL-18RAP$^{-/-}$) backcrossed onto the C57Bl/6 background were used. Importantly, for the IL-18RAP$^{-/-}$ study, we wanted to examine the gene-dose effect of IL-18RAP, therefore we used sex-matched IL-18RAP$^{+/-}$ littermate controls for each IL-18RAP$^{-/-}$ or IL-18RAP$^{+/+}$ mouse used in this study. Mice were obtained from either the Monash Animal Research Platform (MARP; Monash University, Australia), the Animal Resources Centre (Perth, Australia) the Walter and Eliza Hall Institute (WEHI) or the La Trobe Animal Research and Teaching Facility (LARTF; La Trobe University Australia). Mice were housed in standard boxes, under specific pathogen-free conditions, on a 12 h light-dark cycle, and provided with ad libitum access to normal chow and drinking water. All procedures were conducted according to the Australian Code for the Care and Use of Animals for Scientific Purposes (8th edition) and were approved by the MARP Animal Ethics Committee (Project number: MARP/2013/043) and La Trobe University Animal Ethics Committee (Project number: AEC16-93).

2.2 Generation of IL-18RAP-deficient mice

IL-18RAP$^{-/-}$ mice were designed and generated by the Australian Phenomics Network using the following protocol. The CRISPR design site (crispr.mit.edu) was used to identify guide RNA sites flanking the exon to be removed (ENSMUST00000027237.11). This is the only exon containing the coding sequence and thus deleting this region is likely to produce an IL-18RAP knockout. The sequence of this locus was submitted to the MIT guide design tool to identify suitable guide sites flanking the exon (i.e., guides 5' and 3' to the exon).

The tool identified several guide sites in the 5' and 3' regions and guides were selected according to their score, the higher the score, the less potential off target sites.

5' guide sequence: 5' TGATGTGTGCTGATGCTCGG 3'

3' guide sequence: 3' TGTACACGATATGGCATGCA 5'

Complementary oligonucleotides corresponding to the RNA guide target sites were annealed and cloned into BbsI (NEB, USA) -digested plasmid pX330- U6-Chimeric_BB-CBh-hSpCas9 (Addgene plasmid #42230). Single guide RNAs (sgRNA) were generated using the HiScribe™ T7 Quick High Yield RNA Synthesis Kit (NEB, Australia) according to the manufacturer's instructions and RNAs were purified using the RNeasy Mini Kit (Qiagen, Germany). Cas9 mRNA (30 ng/µl; Sigma-Aldrich, USA), and the 5' and 3' sgRNAs (15 ng/µl) were microinjected into the cytoplasm of C57BL/6 zygotes at the pronuclei stage. Injected zygotes were transferred into the uterus of pseudopregnant F1 females. Founder mice were screened for the correct modification. Three founders were selected for breeding to wild type mice and screened the next generation for the correct modification. These mice were then further bred for > 3 generations and screened for the correct modification.

2.3 Induction of hypertension

All surgeries were performed using aseptic technique under general anaesthesia induced by inhalation of isoflurane (2 L/min, 5% in O_2). Anaesthesia was maintained by 2.5% isoflurane in O_2 (0.4 L/min) and regularly monitored by checking hind-paw withdrawal, blink reflexes and respiratory rate. Hypertension was induced in wild type, IL-18$^{-/-}$, IL-18R1$^{-/-}$, RAG1$^{-/-}$, IL-18RAP$^{+/-}$, and IL-18RAP$^{-/-}$ mice by removal of the left kidney, implantation of a deoxycorticosterone acetate (DOCA; 2.4 mg/day, *s.c.* ; Innovative Research of America, USA) pellet and treatment with 0.9% saline in the drinking water.[3] Normotensive controls for this experiment were mice that also received uninephrectomy

but received a placebo pellet containing the proprietary matrix material without DOCA (Innovative Research of America, USA) and normal drinking water (1K/placebo). Briefly, mice were placed under general anaesthesia, their flank and the nape of their neck were shaved, then their skin was scrubbed with 4% chlorhexidine surgical scrub three times, which was washed off with sterile saline and sterile gauze, before the application of 0.5% chlorhexidine in 70% ethanol. A small incision was made in the skin and muscle layers of the left flank to expose the left kidney. The kidney was gently pulled through the incision and clamped at the artery exit below the renal pelvis with curved haemostats. Forceps were used to peel off the fat around the kidney and renal artery, and the renal artery was then tied off with sterile 5-0 surgical silk sutures (Dynek, Australia). Tissue-cutting scissors were used to detach the kidney from the renal artery, the haemostats were removed, and the muscle layer was closed using continuous stiches with nylon 5-0 sutures (SMI Daclon, Australia). The skin layer was closed by stitching using 5-0 nylon sutures. A separate incision was created at the shaved nape of the neck, and a subcutaneous pouch was created by blunt dissection from the wound site towards the ribcage, into which the DOCA or placebo pellet were inserted. The incision was closed by stitching using 5-0 nylon sutures. Prior to surgery, mice received local anaesthetic (bupivacaine; 2.5 mg/kg, *s.c.*) and analgesic (carprofen; 5 mg/kg, *s.c.*). Carprofen treatment was continued for 3 days post-surgery. After this, mice were maintained on drinking water/saline and normal chow for up to 21 days.

2.4 Bone marrow transplantation

Wild-type and IL-18$^{-/-}$ mice were killed by CO_2 asphyxiation and bone marrow cells were obtained by flushing the femurs and tibias with RPMI 1640 medium (Gibco™, ThermoFisher Scientific, USA). Cells were counted using an automatic cell counter (EVE, NanoEnTek Inc, South Korea) and resuspended in RPMI 1640 medium at a concentration of 5.0 x 10^7 cells per mL. Recipient wild-type and IL-18$^{-/-}$ mice were lethally irradiated

with two separate doses of 5.5 Gy X-ray ionizing radiation (RS-2000 Irradiator, Rad Source, USA), with a resting period of 3 h between each dose.[4] Following the second dose of radiation, the mice were injected via the tail vein with 5.0 x 10^6 bone marrow cells in 100 µL of RPMI. Mice received enrofloxacin (75 mg/kg) in their drinking water for 2 days prior to, and for a further 21 days following bone marrow cell transplantation. Sixteen weeks were allowed for bone marrow engraftment before induction of hypertension by 1K/DOCA/salt treatment.

2.5 Adoptive transfer of T cells

RAG1$^{-/-}$ mice were randomly assigned to receive purified T cells from either WT or IL-18R1$^{-/-}$ mice or vehicle (phosphate buffered saline; PBS) 21 days prior to the induction of hypertension with 1K/DOCA/salt.[8] T cells for adoptive transfer were isolated from the spleens of 10-12-week-old male WT and IL-18R1$^{-/-}$ mice. Spleens were minced with scissors before being passed through a 70 µm cell strainer, and then incubated in red blood cell (RBC) lysis buffer (NH_4Cl, $KHCO_3$, dH_2O) for 5 min at room temperature. Splenic T cells were enriched using a CD90.2 negative pan T cell isolation kit (Miltenyi Biotech, USA) as per manufacturer instructions. Splenic T cells were counted using an automatic cell counter (EVE, NanoEnTek Inc, South Korea) and re-suspended in sterile PBS at a concentration of 5x10^7 cells/mL. A 100 µL volume of either WT or IL-18R1$^{-/-}$ T cells were injected into the tail vein of RAG1$^{-/-}$ mice. Following 21 days of 1K/DOCA/salt-treatment, kidneys of recipient mice were analysed by flow cytometry to confirm successful T cell engraftment.

2.6 Bolus saline challenge to assess renal function and urine metabolites

Renal function and injury were assessed in conscious mice at days 0, 7, 14 and 21 post-surgery from urine volume and concentration of electrolytes and albumin excreted over 4 h following a bolus subcutaneous saline injection (volume equivalent to 10% of body

weight).[5] Briefly, mice were lightly anaesthetised with 2.5% isoflurane in O_2 (0.4 L/min) and urine in the bladder was eliminated by mild suprapubic compression. Mice were then injected subcutaneously across four injection sites with a volume of prewarmed saline (37°C), and immediately placed in metabolic cages for 4 h. Urine volume produced over 4 h was presented as a percentage of the saline volume injected. Measurements of [Na^+] and [Cl^-] were performed by a commercial provider (Monash Pathology Service) using the Synchron LX20 (Beckman Coulter, USA) and albumin concentration was measured by ELISA (Bethyl Laboratories, USA). Note: all mice were acclimatised to the metabolic cages by placing them in the cages for 6 h on three separate occasions during the week prior to the induction of hypertension.

2.7 Blood pressure measurements

2.7.1 Tail cuff plethysmography

Systolic blood pressure (BP) was measured by tail cuff plethysmography using a multi-channel BP analysis system (MC4000; Hatteras Instruments, USA). Mice were restrained on a heated platform (40ºC) and LED light was shone through the tail to a sensor in order to detect a pulse. After a pulse was detected, systolic BP was measured at a point which an inflatable cuff placed around the base of a tail terminated blood flow. Systolic BP was recorded for 30-40 measurement cycles on at least 3 occasions prior to surgery in order to acclimatise the mice to the procedure. Systolic BP was then recorded just prior to surgery (day 0), and again on days 7, 14 and 21. Again, on each occasion mice were subjected to 30-40 measurement cycles with readings from the last 25 cycles averaged to obtain a systolic BP value for each day. Tail cuff plethysmography allows for BP to be measured in a non-invasive manner in conscious mice. While it is a validated technique for assessing systolic BP in rodents, it is not considered to be a reliable means of assessing diastolic BP (and thus mean arterial pressure). Therefore, wherever data from the tail cuff procedure is presented, only the systolic BP estimates are shown.

2.7.2 Radiotelemetry

In a subset of mice, BP was monitored continuously using radiotelemetry. Telemetry is considered to be the gold-standard technique for measuring BP, as it allows for 24 h measurements of systolic and diastolic blood pressure (and thus mean arterial pressure) as well as heart rate and locomotor activity in conscious, unrestrained mice, therefore minimising stress artefacts. Mice were individually housed in standard mouse cages and allowed to acclimatise to their new environment for 1 week.

For radiotelemetry, a telemeter probe (Model TA11PA-C10, Data Sciences International, USA) was surgically implanted into the left carotid artery of mice under 2.5% isoflurane in O_2 (0.4 L/min). The mouse was placed in the prone position with its nose inside a nose cone for delivery of a continuous flow of 2% isoflurane. The mouse was regularly monitored by checking hind-paw withdrawal, blink reflexes and respiratory rate. The neck of the mouse was dampened with 80% ethanol and, using fine scissors, a small (~1 cm in length) midline incision was made. A subcutaneous pouch was created along the right flank using blunt dissection for implantation of the telemeter probe. Fine forceps were used to remove the fat around the thyroid and separate the lobes of the gland to each side. The left carotid artery was exposed by dissecting out the surrounding fascia, and the artery gently lifted by placing curved forceps beneath it. Three pieces of sterile 5-0 surgical silk sutures were used to insert and position the catheter tip: one suture was tied rostral to the forceps with a double knot; a second suture was tied caudal to the forceps with a single knot; and a loose knot was made with the third suture between the other two sutures. A small incision was then made in the carotid artery using Vannas spring scissors (Fine Science Tools, USA) as far rostral as possible, and fine forceps were used to open the incision. The telemeter probe was turned on using a magnet, checked using a radio receiver, and then placed in a stable position beside the mouse. The probe catheter was carefully inserted into the incision made in the artery, and gently passed into the vessel until the notch of the catheter was inserted into the

incision. The middle suture was then secured with a double knot, and the caudal suture was locked in place with a second knot. The radio receiver was again used to ensure that the heart rate was audible. The subcutaneous pouch previously created along the right flank was lubricated with sterile saline using a syringe, and the probe was carefully inserted into the pouch. The left carotid artery was covered by replacing all surrounding tissue, fat, and the thyroid glands, and a sterile 6-0 surgical silk suture was used to make non-continuous stitches to close the incision. Immediately following surgery, mice were treated topically with an antibiotic (Tribactril, Jurox, Australia) and analgesic (carprofen; 5 mg/kg, *s.c.*). Mice received antibiotic in their drinking water for a further 2 days (Baytril; 0.375 mg/mL). Following a 10-day recovery period, the radio transmitter was turned on, allowing for measurement of BP, heart rate and activity as a 10-second average, every 10 minutes for 24 hours every day until the end of the treatment period.

2.8 Measurement mRNA expression levels

At the end of the 21-day treatment period, mice were killed via CO_2 asphyxiation and perfused through the left ventricle with phosphate-buffered saline (PBS) containing 0.2% Clexane (400 IU; Sanofi Aventis, France). The right kidney was excised and cut in half along its transverse plane. One half of the kidney was used immediately for flow cytometric analysis, while the other half was further divided into two transverse sections. One of these sections was fixed in 10% formalin and stored at -4°C for immunohistochemistry, and the other was snap frozen in liquid N_2 and stored at -80°C for later RNA extraction. For this, frozen kidneys were pulverised, and RNA was extracted using a RNeasy Mini Kit (Qiagen, Hilden, Germany). On the day of extraction, frozen kidney samples were pulverised and lysed in an isothiocyanate-based buffer containing β-mercaptoethanol. The lysate was loaded onto an RNA capture column, and, after a series of ethanol washes, total RNA was eluted from the column with 30 µL of RNAse-free water. The yield and purity of the RNA was determined by measuring absorbances at 230, 260 and 280 nm using a NanoDrop

Spectrophotometer (NanoDrop One, Thermo Scientific, USA). A260:A230 and A260:A280 ratios of 2.0 or more were considered suitable for use in reverse transcription and real-time PCR analyses.

Total kidney RNA (2 µg) was converted to cDNA using a High-Capacity cDNA Reverse Transcription kit (Applied Biosystems, USA) as per the manufacturer's instructions. The resulting cDNA was then used as a template in real-time PCR to measure mRNA expression of pro-*Il18*, *Il18r1*, *Il18rap*, *Il18bp*, C-C motif chemokine ligand (*Ccl*) 2, *Ccl*5, intercellular adhesion molecule-1 (*Icam1*), vascular cell adhesion molecule-1 (*Vcam1*), *Il6*, *Il23a*, *Col1a1*, *Col3a1*, *Col4a1*, and *Col5a1*, *Ifnγ*, or the housekeeping gene, *Gapdh* (TaqMan Gene Expression Assays, Applied Biosystems, USA). Briefly, either 2.5-25 ng/µL of cDNA template were loaded in triplicate into the wells of a 96-well plate with TaqMan Universal PCR master mix (Applied Biosystems, USA) and TaqMan primers and probes (Applied Biosystems, USA). Real-time PCR was performed in a Bio-Rad CFX96 Real-Time PCR Detection System (Bio-Rad Laboratories, Hercules, CA, USA) using the following parameters: initial step at 50°C for 2 min; initial denaturation for 10 min at 95°C; followed by 40 cycles of denaturation at 95°C for 15 s and annealing and extension at 60°C for 1 min. Fluorescence was monitored at the end of each cycle. The cycle at which a signal was first detected was defined as the threshold cycle (Ct) and the ΔCt was defined as the difference between the Ct of the gene of interest and the house-keeping gene (*Gapdh*), while the ΔΔCt was defined as the difference between the ΔCts of a given gene in treated vs control samples. Given that each cycle of PCR represents a doubling in DNA product, fold-changes in expression of a gene in treated versus control samples were calculated using the equation[6]:

$$\text{Fold-change} = 2^{-\Delta\Delta Ct}$$

2.9 Flow cytometric analysis

For conventional flow cytometric analysis, cell suspensions were prepared from kidney halves and whole spleens. Kidney halves were minced with scissors and digested in PBS containing collagenase type XI (125 U/mL), collagenase type I-S (460 U/mL) and hyaluronidase (60 U/mL) (Sigma-Aldrich, USA) for 60 mins at 37°C. Following digestion, kidney suspensions were passed through a 70 µm filter (BD Biosciences, USA), and the cells were pelleted by centrifugation at 453 x*g* for 5 min. The cell pellets were further subjected to Percoll™ gradient centrifugation, whereby the pellet was re-suspended in 3 mL of 40% isotonic Percoll™ solution (GE Healthcare Life Science, UK), and carefully under-laid with 3 mL of 70% Percoll™ solution. Samples were centrifuged at 1450 x*g* at 25°C for 25 min with the brakes of the centrifuge turned off. Following centrifugation, adipocytes and debris were aspirated from the top layer, and mononuclear cells were collected from the interface. Mononuclear cells were washed in PBS, centrifuged, and the pellet was re-suspended in PBS. Spleen samples were minced with scissors and passed through a 70 µm filter, and then incubated in red blood cell (RBC) lysis buffer (NH_4Cl, $KHCO_3$, dH_2O) for 5 min at room temperature. Spleen cells were counted using an automatic cell counter (EVE, NanoEnTek Inc, South Korea) and re-suspended in PBS at a concentration of 10^7 cells/mL. Cells were stained for 15 min at room temperature with Live/Dead aqua stain (Life Technologies, USA), followed by an antibody cocktail consisting of anti-mouse CD45 (A700; BioLegend, USA), CD3 (APC; BioLegend, USA), CD8 (PeCy7; BioLegend, USA), CD4 (BV605; BioLegend, USA), CD11b (BV421; BioLegend, USA), F4/80 (APC Cy7; BioLegend, USA), CD69 (BV650; BioLegend, USA), CD44 (PERCP; BioLegend, USA), and IL-18R1 (PE; Invitrogen, USA; see Table 2.4). dissolved in PBS containing 0.5% bovine serum albumin.

For intracellular cytokine/transcription staining, cells were washed in PBS, centrifuged, fixed and permeabilised (eBioscience™ Foxp3/Transcription Factor

Fixation/Permeabilization Concentrate and Diluent; Invitrogen, USA). Cells were then washed in perm wash™ and re-suspended in 1% formalin in PBS containing 0.5% bovine serum albumin and EDTA, prior to analysis on a CytoFlex LS flow cytometer (Beckman Coulter, USA) using CytExpert software (Beckman Coulter). Data were analysed using FlowJo software v10 (FlowJo, USA). For the full gating strategy, see Figure 2.1.

2.9.1 Intracellular Cytokine Detection

To detect renal and splenic T cell-derived IFN-γ, kidney and spleen cell suspensions were prepared as described for flow cytometric analysis. Renal and splenic T cells were enriched using a CD90.2 positive microbead isolation kit (Miltenyi Biotech, USA) as per manufacturer instructions. Enriched T cells were re-suspended in RPMI media containing 10% FBS, penicillin (100 U/mL)/streptomycin (100 µg/mL) and L-glutamine (2 mM) and seeded onto an anti-CD3 (5 ug/mL, Biolegend) coated 96-well plate at a density of $1x10^6$ cells/well for splenic T cells and $1x10^5$ cells/well for renal T cells. In the presence of an anti-CD28 monoclonal antibody (1 ug/mL; BioLegend), T cells were stimulated with various concentrations of IL-18 (0, 0.1, 1, 10 or 100 ng/mL; R&D Systems, USA) for 16 h at 37 °C with 5% CO_2. Cells were further incubated with protein transport inhibitors, golgi-plug (BD Biosciences, USA) and golgi-stop (BD Biosciences), for 6 h. Following incubation, cells were centrifuged at 453 x*g* for 5 min at 4ºC and the supernatant was discarded. Cells were then stained for surface markers including anti-mouse CD45 (A700; BioLegend, USA), CD11b (BV421; BioLegend, USA), TCR-β (APC; BioLegend, USA), CD4 (BV605; BioLegend, USA), CD8 (PerCP-Cy5.5; BioLegend, USA) and IL-18R (PE; Invitrogen, USA) (as described above), before being fixed and permeabilised for intracellular staining with an anti-IFN-γ antibody at room temperature for 15 min. Cells were then washed and re-suspended in PBS for analysis on a CytoFlex LS flow cytometer. Data were analysed using FlowJo software v10 (FlowJo, USA). For the full gating strategy, see Figure 2.2.

2.10 Histopathology staining

Kidneys were fixed in 10% formalin, embedded in paraffin, and cut into 4 µm sections on a microtome. Sections were deparaffinised, rehydrated in 100% xylene, and a series of graded ethanol solutions (70-100%) and stained with either a 0.5% Picrosirius red solution, or haematoxylin and eosin (Amber Scientific, Australia). Excess stain was removed by washing in Scott's tap water (2 g $NaHCO_3$and 20 g $MgSO_4.7H_2O$ in 1 L distilled H_2O) or acidified water (0.5% acetic acid in 1 L distilled H_2O). Following this, the sections were washed with tap water, dehydrated in graded-levels of ethanol (70-100%) and 100% xylene, and finally mounted in Distrene-80 Plasticizer Xylene (DPX; Merck, USA). For measurement of interstitial collagen deposition in $RAG1^{-/-}$ mice, snap frozen transverse kidney sections were embedded in optimal cutting temperature (O.C.T) compound (Tissue-Tek, U. S. A) before being cut into 4 µm sections on a cryostat. Slides were defrosted for 20 mins at room temperature, and then fixed in acetone that had been chilled to -20°C for 10 mins. Slides were washed for 5 mins in 1x PBS and rehydrated in 100% ethanol before being stained with a 0.5% Picrosirius red solution. Excess stain was removed by washing in acidified water (0.5% acetic acid in 1 L distilled H_2O). Following this, the sections were washed with tap water, dehydrated in 100% ethanol and 100% xylene, and finally mounted in Distrene-80 Plasticizer Xylene (DPX; Merck, USA). Seven randomly selected fields of the renal cortex (viewed under a magnification of ×20) per section were imaged using a bright-field microscope (Olympus, Japan). Collagen staining was quantified as a percentage of the total area per field of view using ImageJ software (National Institutes of Health, USA). Changes in renal tubular structure (i.e., tubular dilatation, tubular atrophy and

epithelial brush border integrity) were assessed using a 4-point scoring system as follows: 0 = no damage; 1 = mild damage (< 25% tubules affected); 2 = moderate damage (25–50% of tubules affected); and 3 = severe damage (> 50% of tubules affected). Quantified/scored Picrosirius red and renal histopathology data represent the average values obtained

independently by two investigators who were blinded to the in vivo treatment of each sample.

2.11 Immunohistochemistry

Kidneys were fixed and sectioned as described above, rehydrated and antigen recovery was performed by boiling the slide-mounted tissue sections in sodium citrate buffer (AJAX Finechem; Australia; pH 6) for 6 min. Kidney sections were blocked in 1% goat serum and PBS-Tween for 1 hour, and then incubated with rat anti-CD3 (5 μg/mL; Abcam, USA), rabbit anti-IL-18 (0.2 μg/mL; Abcam, USA) or rabbit anti-IL-18R1 (5 μg/mL; Abcam, USA) diluted in 1% goat serum. For IL-18RAP staining, kidney sections were blocked in 10% goat serum and PBS-Tween for 1 hour, and then incubated with rabbit anti-IL-18RAP (5 μg/mL; Abcam, USA). For staining of aquaporin (AQP)-1 1/22 subunit with mouse anti-AQP1 (1 μg/mL; Santa Cruz, USA), kidney sections were blocked using a Mouse-on-Mouse blocking kit (Vector Laboratories, USA) before staining with secondary antibodies (see Table 2.5). Alexa Fluor 488- or Alexa Fluor 555-conjugated goat secondary antibodies (Invitrogen, USA) were used, and cell nuclei were counterstained with 4′,6-diamidino-2-phenylindole (DAPI; 1:1000, Life Technologies, ThermoFisher Scientific, USA), before being cover-slipped with a fluorescent mounting medium (Dako, USA). Fluorescent images were captured using either a Zeiss 780 confocal microscope (Carl Zeiss, Oberkochen, Germany) or an Olympus BX53 microscope with a light source attached (X-cite series 120Q, Excelitas Technologies, USA).

2.12 Statistics

Unless otherwise stated, results are expressed as mean ± standard error of mean (SEM). For the IL-18RAP$^{-/-}$ mouse study, sample sizes of 6-8 mice were determined a priori in consultation with the La Trobe University Statistics Consultancy Platform to provide 80% power with an alpha-level of 5% for three types of effects based on 2-way analysis of variance (ANOVA): the within effect (time); the between effect (sex); and the between

within effect (differences between the sexes over time). Data were analysed using Student's unpaired t-test, one-way analysis of variance (ANOVA), two-way repeated measures ANOVA or Log-rank (Mantel-Cox) test for Kaplan-Meier survival curve as appropriate. Post hoc analyses (performed when F tests from ANOVA were < 0.05) were performed using Bonferroni's test. Non-parametric data were analysed using Kruskal-Wallis one-way ANOVA. $P < 0.05$ was considered to be statistically significant.

2.13 References

1. Takeda K, Tsutsui H, Yoshimoto T, Adachi O, Yoshida N, Kishimoto T, Okamura H, Nakanishi K and Akira S. Defective NK cell activity and Th1 response in IL-18-deficient mice. *Immunity*. 1998;8:383-90.

2. Nold-Petry CA, Lo CY, Rudloff I, et al. IL-37 requires the receptors IL-18Rα and IL-1R8 (SIGIRR) to carry out its multifaceted anti-inflammatory program upon innate signal transduction. *Nat Immunol*. 2015;16:354-65.

3. Krishnan SM, Dowling JK, Ling YH, et al. Inflammasome activity is essential for one kidney/deoxycorticosterone acetate/salt-induced hypertension in mice. *Br J Pharmacol*. 2016;173:752-65.

4. Duran-Struuck R and Dysko RC. Principles of bone marrow transplantation (BMT): providing optimal veterinary and husbandry care to irradiated mice in BMT studies. *J Am Assoc Lab Anim Sci*. 2009;48:11-22.

5. Trott DW, Thabet SR, Kirabo A, et al. Oligoclonal CD8+ T cells play a critical role in the development of hypertension. *Hypertension*. 2014;64:1108-1115.

6. Schmittgen TD, Lee EJ, Jiang J, Sarkar A, Yang L, Elton TS and Chen C. Real-time PCR quantification of precursor and mature microRNA. *Methods*. 2008;44:31-38.

2.14 Tables

Table 2.1 Mice treated with 1K/DOCA/salt or 1K/placebo.

	Sex	Mouse strain	Origin	# of mice	Age at treatment (weeks)	Weight at treatment (g)	Deaths
IL-18$^{-/-}$ study	M	IL-18$^{-/-}$	LARTF	9	13-14	24-30	
			MARP	8	10-12	20-30	
		C57Bl/6	ARC	10	9-11	26-30	1 *
			MARP	8	10-12	25-30	
Saline bolus challenge	M	IL-18$^{-/-}$	LARTF	24	17-24	21-35	3 †
		C57Bl/6	ARC	20	18-23	25-33	4 *
IL-18R1$^{-/-}$ study	M	IL-18R$^{-/-}$	LARTF	28	13-17	21-36	9 *
		C57Bl/6	ARC	24	11-15	22-32	
IL-18RAP$^{-/-}$ study	M	IL-18RAP$^{+/+}$	LARTF	9	12-19	27-35	3*, 1†
		IL-18RAP$^{+/-}$	LARTF	12	12-19	28-36	7*
		IL-18RAP$^{-/-}$	LARTF	9	12-19	27-38	2*, 1†
	F	IL-18RAP$^{+/+}$	LARTF	11	13-20	21-27	4*
		IL-18RAP$^{+/-}$	LARTF	12	13-20	20-25	
		IL-18RAP$^{-/-}$	LARTF	10	13-21	21-29	2*
WT mice studies	M	C57Bl/6	ARC	69	8-12	22-30	9 *, 9 †, 4
			MARP	63	10-12	24-32	13 *, 2 ‡
			LARTF	15	8-12	24-30	2 *, 2 †
	F		LARTF	15	8-12	18-22	1 *, 1 †
***= Aneurysm †= surgical wound opening/fight wounds ‡= unknown cause**							

Table 2.2 Mice used for bone marrow (BM) transplant study.

Bone marrow transplant study							
	Mouse strain	Origin	# of mice	Age at transplant (weeks)	Age at treatment (weeks)	Weight at treatment (g)	Deaths
Recipient Mice	IL-18$^{-/-}$	LARTF	30	11-14	25-33	21-31	15†, 1 *
	C57Bl/6	LARTF	30	11-13	26-33	20-31	10†
Donor Mice	IL-18$^{-/-}$	LARTF	20	10-15			
	C57Bl/6	LARTF	20	10-13			
*= surgical wound opening/fight wounds †= failure to reconstitute							

Table 2.3 Mice used for T cell transfer study.

RAG1$^{-/-}$ study							
	Mouse strain	**Origin**	**# of mice**	**Age at T cell transfer (weeks)**	**Age at treatment (weeks)**	**Weight at treatment (g)**	**Deaths**
Recipient Mice	Rag1$^{-/-}$	WEHI	29	8-10	12-14	18-28	6*, 2‡
	C57Bl/6	WEHI	14	7-8	10-11	23-32	3*, 1†
Donor Mice	IL-18R1$^{-/-}$	LARTF	8	8-10			
	C57Bl/6	WEHI	16	8-10			
*= Aneurysm †= surgical wound opening/fight wounds ‡= unknown cause							

Table 2.4 Antibody panel for flow cytometry.

Antigen	Host/Isotype	Clone	Tag	Dilution Factor	Company
CD45	Rat IgG2b, κ	30-F11	A700	1:500	BioLegend, USA
CD3e	Hamster IgG	145-2C11	APC	1:500	BioLegend, USA
CD4	Rat IgG2a, κ	RM4-5	BV605	1:500	BioLegend, USA
CD8a	Rat IgG2a, κ	53-6.7	BV605	1:1000	BioLegend, USA
CD11b	Rat IgG2b, κ	M1/70	BV421	1:500	BioLegend, USA
F4/80	Rat IgG2a, κ	BM8	APC Cy7	1:500	BioLegend, USA
CD69	Rat IgG2a, κ	C068C2	BV650	1:500	BioLegend, USA
CD44	Rat IgG2a, κ	XMG1.2	PERCP	1:500	BioLegend, USA
IL-18R1	Rat IgG2a, κ	P3TUNYA	PE	1:500	Invitrogen, USA
FoxP3	Rat IgG2a, κ	FJK-16s	FITC	1:500	eBioscience, USA
TNF-α	Rat IgG1, κ	MP6-XT22	PE	1:1000	BioLegend, USA
TCR-β	Hamster IgG	H57-597	APC	1:500	BioLegend, USA
IFN-γ	Rat IgG2a, κ	DB-1	FITC	1:500	Invitrogen, USA
IL-17	Rat IgG2a, κ	eBio17B7	PE-Cy7	1:500	eBioscience, USA
CD206	Rat IgG2a, κ	C068C2	PE-DAZZLE	1:500	BioLegend, USA
EpCAM	Rat IgG2a, κ	G8.8	PERCPCy5.5	1:500	BioLegend, USA

Table 2.5 Immunohistochemistry antibodies.

Antigen	Host/Isotype	Clone	Dilution Factor	Company
CD3	Rat IgG1	CD3-12	2 µg/mL	Abcam, USA
IL-18	Rabbit IgG	Polyclonal	0.2 µg/mL	Abcam, USA
IL-18R1	Rabbit IgG	Polyclonal	5 µg/mL	Abcam, USA
IL-18RAP	Rabbit IgG	Polyclonal	5 µg/mL	Abcam, USA
AQP1	Mouse IgG2b κ	AQP1 (1/22)	1 µg/mL	Santa Cruz, USA

2.15 Figures

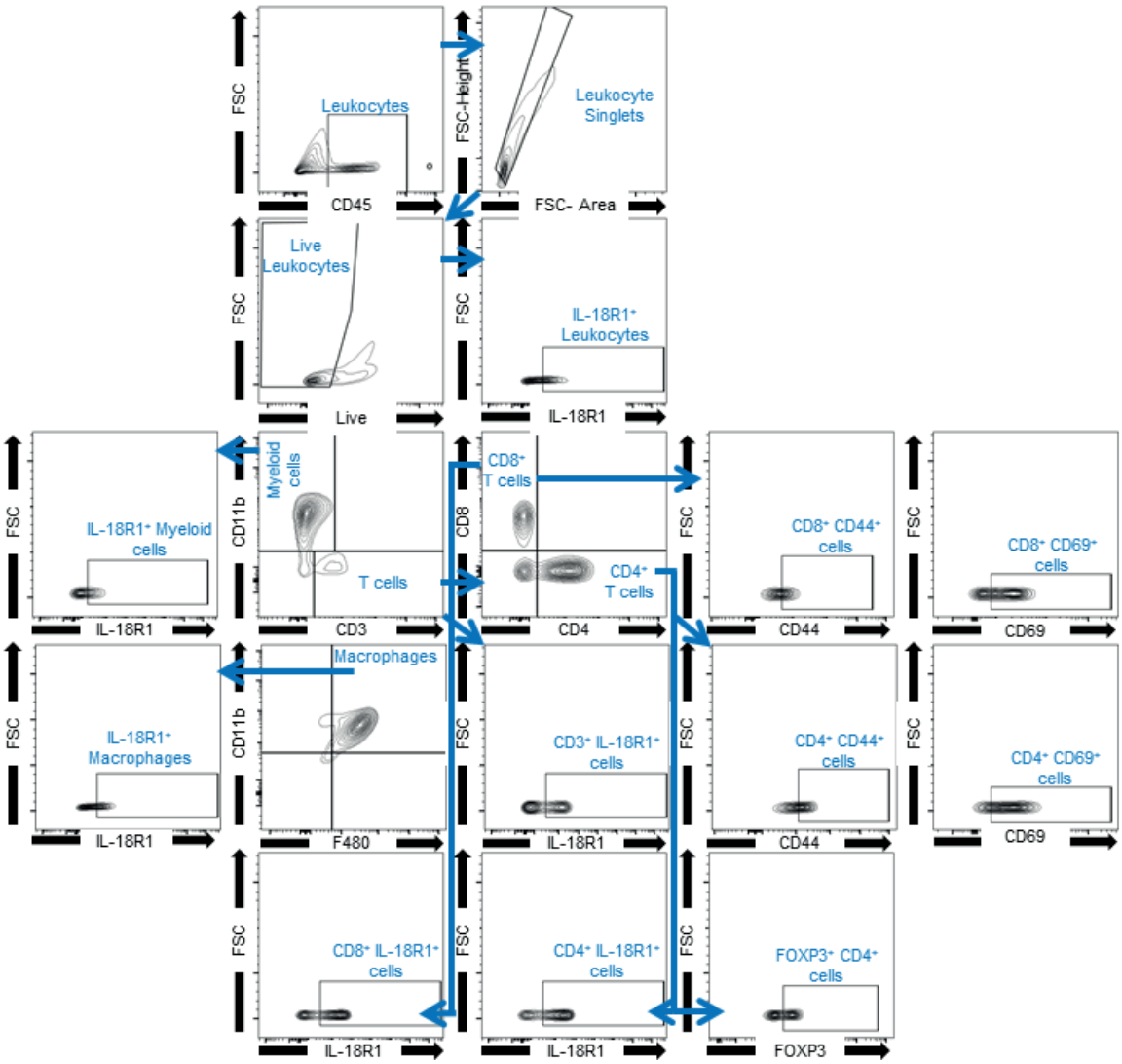

Figure 2.1 Gating strategy for flow cytometric analysis. Leukocytes were gated as $CD45^+$ populations against forward scatter (FSC). Total leukocytes, i.e., live leukocyte singlets, were gated by FSC -height vs FSC-area, and exclusion of dead cells (live/dead stain). Total leukocytes were then divided into myeloid cells ($CD11b^+$) and T cells ($CD3^+$). Some of the myeloid cells were identified as macrophages ($CD11b^+F4/80^+$), and the macrophages were further classified as IL-18R11$^+$. T cells that were positive for CD3 staining were further classified as IL-18R1$^+$, $CD4^+$, or $CD8^+$ T cells. $CD4^+$ and $CD8^+$ cells were further identified as being $CD44^+$, $CD69^+$ or $FOXP3^+$.

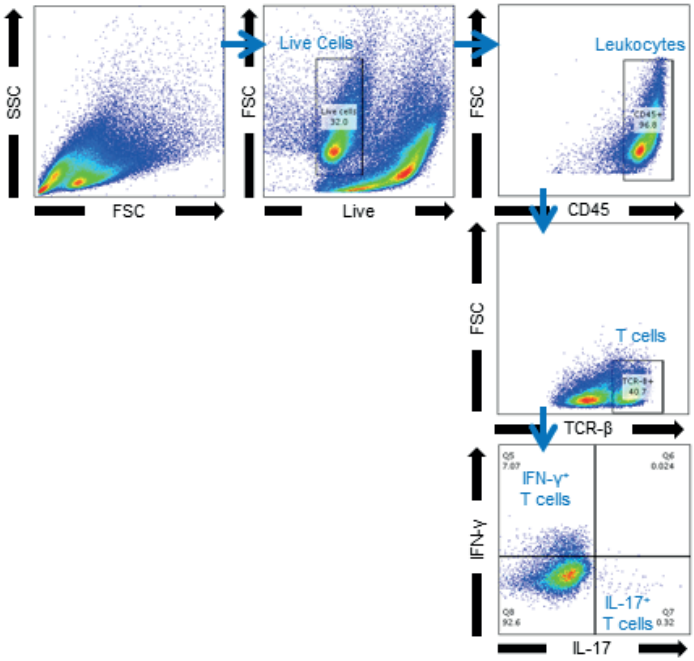

Figure 2.2 Gating strategy for intracellular cytokine detection using flow cytometric analysis. Dead cells (live/dead stain) were excluded before leukocytes were gated as $CD45^+$ populations against forward scatter (FSC). Total leukocytes were classified as being T cells ($TCR\text{-}\beta^+$) and then divided into $IFN\text{-}\gamma^+$ or $IL\text{-}17^+$ populations.

Chapter 3

Interleukin-18 Produced by Renal Tubular Epithelial Cells Promotes Hypertension and Kidney Damage Induced by Deoxycorticosterone Acetate/Salt in Mice

3.1 Summary

Interleukin-18 (IL-18) is elevated in hypertensive patients, but its contribution to high blood pressure (BP) and end-organ damage is unknown. We examined the role of IL-18 in the development of high BP, renal inflammation, and injury in a model of low-renin hypertension. Hypertension was induced in male C57BL6/J (WT) and IL-18$^{-/-}$ mice by uninephrectomy, deoxycorticosterone acetate (2.4 mg/d, *s.c.*) and 0.9% drinking saline (1K/DOCA/salt). Normotensive controls received uninephrectomy and placebo (1K/placebo). BP was measured via tail cuff or radiotelemetry. After 21 days, kidneys were harvested for (immuno)histochemical, quantitative-PCR and flow cytometric analyses of fibrosis, inflammation, and immune cell infiltration. 1K/DOCA/salt-treated WT mice developed hypertension, renal fibrosis, upregulation of pro-inflammatory genes and accumulation of CD3^{+} T cells in the kidneys. They also displayed increased expression of IL-18 on proximal tubular epithelial cells (TECs). IL-18$^{-/-}$ mice were profoundly protected from hypertension, renal fibrosis, and inflammation. Bone marrow (BM) transplantation between WT and IL-18$^{-/-}$ mice revealed that IL-18-deficiency in non-BM-derived cells alone afforded equivalent protection against hypertension and renal injury as global IL-18 deficiency. IL-18 receptor subunits — IL-18R1 and IL-18R accessory protein (IL-18RAP) — were upregulated in kidneys of 1K/DOCA/salt-treated WT mice and localised to T cells and TECs. T cells from kidneys of 1K/DOCA/salt-treated mice produced interferon-γ upon *ex vivo* stimulation with IL-18, whereas those from 1K/placebo mice did not. In conclusion, IL-18 production by TECs contributes to elevated BP, renal inflammation, and fibrosis in 1K/DOCA/salt-treated mice, highlighting it as a promising therapeutic target for hypertension and kidney disease.

3.2 Graphical abstract

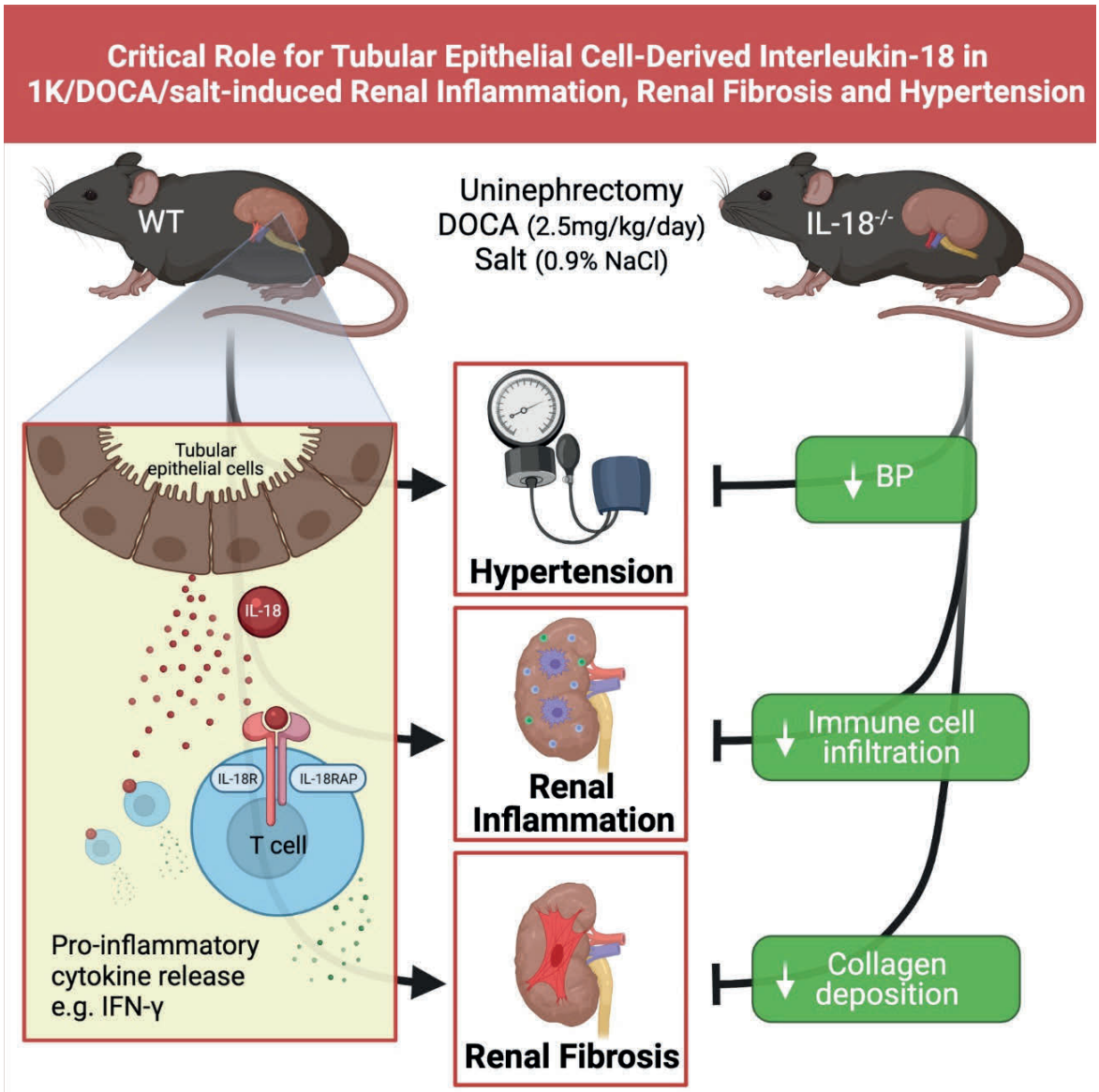

3.3 Introduction

Hypertension is recognised as a chronic inflammatory disease, with the kidneys representing major sites of inflammation.[1,2] Tight control of the pressure-natriuresis relationship by the kidneys — whereby baroreceptors detect changes in pressure and initiate sympathetic signalling pathways that modulate sodium and water reabsorption in the renal tubules — is key to long-term blood pressure homeostasis.[3] During the development of hypertension, infiltration and activation of immune cells in the kidneys, and the ensuing inflammation, fibrosis and tissue injury, disrupts this pressure-natriuresis relationship.[4] Therefore, characterising the mechanisms that promote immune cell activation and inflammation in the kidneys may yield targets for novel antihypertensive therapies.

Plasma levels of the pro-inflammatory cytokine, interleukin (IL)-18, are elevated in hypertensive patients,[5] and there is mounting evidence that IL-18 is increased in the urine and serum of patients with kidney injury.[6,7] IL-18 is initially formed in cells as an inactive precursor, which requires processing into its active form via the proteolytic actions of enzymes called inflammasomes.[8] Inflammasomes are multimeric protein complexes that assemble in response to danger signals such as pathogen-associated molecular patterns (PAMPs) and danger-associated molecular patterns (DAMPs).[9] They are comprised of a pattern recognition receptor linked either directly, or indirectly via the adapter protein ASC (Apoptosis-associated Speck like protein containing a Caspase recruitment domain), to pro-caspase-1.[9] When assembled, pro-caspase-1 undergoes autolytic activation, enabling it to catalyse the maturation of pro-IL-18 — and other cytokine precursors including pro-IL-1β and pro-IL-33 — into their active forms.[8, 10] Following release from its cell of origin, IL-18 acts in a paracrine or autocrine fashion on a cognate receptor complex — the interleukin-18 receptor 1 (IL-18R1) and interleukin-18 receptor accessory protein (IL-18RAP) — to stimulate pro-inflammatory signalling pathways.[11]

Recent work by our group has demonstrated that inhibition of inflammasome activity — either by deletion of the ASC gene or treatment with the NLRP3 inflammasome inhibitor, MCC950 — affords protection against renal inflammation, fibrosis, and high blood pressure in mice with one-kidney/deoxycorticosterone acetate/salt (1K/DOCA/salt) - induced hypertension; a model of low-renin hypertension.[12, 13] However, the role of IL-18 in this model remains to be determined. Therefore, in the present study we examined whether hypertension and renal inflammation in 1K/DOCA/salt-treated mice are associated with upregulation of IL-18 signalling in the kidneys. We identified the cellular sources of renal IL-18 and determined whether genetic deficiency of IL-18 could reduce T cell activation, renal inflammation, fibrosis, and blood pressure following 1K/DOCA/salt treatment.

3.4 Methods

Refer to online supplementary material for an expanded Methods.

3.4.1 Transparency and Openness Promotion

The data that support the findings of this study are available from the corresponding author upon reasonable request.

3.4.2 Animals

A total of 311 wild type or IL-18$^{-/-}$ mice[14], fully backcrossed onto a C57BL6/J background, were used. Male mice were used for direct comparison to related studies in the field[12, 13, 15] and because sex differences in rodent responses to 1K/DOCA/salt have been reported previously.[16] Mice were aged 9-17 weeks and weighed 20-36 g (see Table 3.1 and Table 3.2). Mice were randomly assigned into treatment groups (e.g., hypertensive versus normotensive) using random number generator software (Microsoft Excel, Version 16.36, USA). All procedures were conducted according to the Australian Code for the Care and Use of Animals for Scientific Purposes (8th edition) and were approved by Monash University (Project number: MARP/2013/043) and La Trobe University Animal Ethics (Project number: AEC16-93) Committees.

3.4.3 Induction of hypertension

A low-renin model of hypertension associated with marked fluid volume loading was used wherein mice were uninephrectomised, administered deoxycorticosterone acetate (DOCA; 2.4 mg/day, *s.c.*; Innovative Research of America, USA) and given 0.9% saline drinking water (1K/DOCA/salt).[13] Normotensive controls received uninephrectomy, a placebo pellet containing the proprietary matrix material without DOCA (Innovative Research of America, USA) and normal drinking water (1K/placebo). All surgeries were performed under anaesthesia induced by inhalation of isoflurane (2 L/min, 5% in O_2). Anaesthesia was maintained by 2.5% isoflurane in O_2 (0.4 L/min) and regularly monitored by checking hind

paw withdrawal, blink reflex and respiratory rate. Prior to surgery, mice received local anaesthetic (bupivacaine; 2.5 mg/kg, *s.c.*) and analgesic (carprofen; 5 mg/kg, *s.c.*) and were treated with carprofen for 3 days following surgery.

3.4.4 Bone marrow cell transplantation

Wild-type and IL-18$^{-/-}$ mice were killed by CO_2 asphyxiation and bone marrow cells were obtained by flushing the femurs and tibias with RPMI 1640 medium (Gibco™, ThermoFisher Scientific, USA). Cells were counted using an automatic cell counter (EVE, NanoEnTek Inc, South Korea) and resuspended in RPMI 1640 at 5 x 10^7 cells/mL. Recipient wild-type and IL-18$^{-/-}$ mice were lethally irradiated with two separate doses of 5.5 Gy X-ray ionizing radiation (RS-2000 Irradiator, Rad Source, USA), with a resting period of 3 h between each dose.[17] Following the second dose of radiation, the mice were injected via the tail vein with 5 x 10^6 bone marrow cells in 100 μL of RPMI 1640. Mice received enrofloxacin (75 mg/kg) in their drinking water for 2 days prior to, and for a further 21 days following bone marrow cell transplantation. Sixteen weeks were allowed for bone marrow engraftment before induction of hypertension by 1K/DOCA/salt treatment.

3.4.5 Saline challenge to assess fluid volume loading and renal injury

The extent of fluid volume loading and renal injury were assessed in conscious mice at days 0, 7, 14 and 21 post-surgery using a protocol modified from Trott *et al.* in which urine volume and amount of electrolytes and albumin excreted over 4 h following a bolus subcutaneous saline injection (volume equivalent to 10% of body weight) are monitored.[18] Urine volume produced over 4 h was presented as a percentage of the saline volume injected. Measurements of [Na^+] and [Cl^-] were performed by a commercial provider (Monash Pathology Service) using the Synchron LX20 (Beckman Coulter, USA) and albumin concentration was measured by ELISA (Bethyl Laboratories, USA).

3.4.6 Blood pressure measurements

BP was measured via tail cuff plethysmography or radiotelemetry.

3.4.7 Measurement mRNA expression levels

At the end of the 21-day treatment period, mice were killed by CO_2 asphyxiation and perfused through the left ventricle with phosphate-buffered saline (PBS) containing 0.2% Clexane (400 IU; Sanofi Aventis, France). The remaining right kidney was excised and cut in half along its transverse plane. One half of the kidney was used immediately for flow cytometric analysis, while the other half was further divided into two transverse sections. One of these sections was fixed in 10% formalin and stored at 4°C for immunohistochemistry, and the other was snap frozen in liquid N_2 and stored at -80°C for later RNA extraction. For this, frozen kidneys were pulverised, and RNA was extracted using a RNeasy Mini Kit (Qiagen, Hilden, Germany). RNA was reversed transcribed (High Capacity cDNA Reverse Transcription kit; Applied Biosystems, Lithuania) and the resulting cDNA was then used as a template in real-time PCR to measure mRNA expression of pro-*Il18*, *Il18r1*, *Il18rap*, *Il18bp*, C-C motif chemokine ligand (*Ccl*) 2, *Ccl*5, intercellular adhesion molecule-1 (*Icam1*), vascular cell adhesion molecule-1 (*Vcam1*), *Il6*, *Il23a*, *Col1a1*, *Col3a1*, *Col4a1*, and *Col5a1*, *Ifnγ*, with *Gapdh* used as a housekeeping gene (TaqMan Gene Expression Assays, Applied Biosystems, USA). Real-time PCR was performed in a Bio-Rad CFX96 Real-Time PCR Detection System (Bio-Rad Laboratories, Hercules, CA, USA) and the comparative Ct method used to calculate fold-changes in mRNA expression relative to a reference sample.[19]

3.4.8 Flow cytometric analysis

Flow cytometry was performed on single cell suspensions created from freshly isolated kidney halves via a combination of manual and enzymatic digestion, and a Percoll™ (GE Healthcare Life Science, UK) gradient centrifugation to isolate mononuclear cells. Spleen

samples were minced with scissors and passed through a 70 µm filter, and then incubated in red blood cell (RBC) lysis buffer (NH_4Cl, $KHCO_3$, dH_2O) for 5 min at room temperature. Cells were stained for 15 min at room temperature with Live/Dead aqua stain (Life Technologies, USA), followed by an antibody cocktail to detect various immune cell subsets (see Table 3.3). For intracellular staining of cytokines, cells were permeabilised (eBioscience™ Foxp3/Transcription Factor Fixation/Permeabilization Concentrate and Diluent; Invitrogen, USA) and then fixed by re-suspending in 1% formalin in PBS containing 0.5% bovine serum albumin and EDTA. To detect renal and splenic T cell-derived interferon (IFN)-γ, kidney and spleen cell suspensions were prepared as described for flow cytometric analysis. T cells were enriched using a CD90.2 positive microbead isolation kit (Miltenyi Biotech, USA) and re-suspended in RPMI 1640 containing 10% FBS, penicillin (100 U/mL)/streptomycin (100 µg/mL) and L-glutamine (2 mM) and seeded onto an anti-CD3 (5 ug/mL, Biolegend)-coated 96-well plate at a density of $1x10^6$ cells/well for splenic T cells and $1x10^5$ cells/well for renal T cells. In the presence of an anti-CD28 monoclonal antibody (1 µg/mL; BioLegend), T cells were stimulated with recombinant mouse IL-18 (0, 0.1, 1, 10 or 100 ng/mL; R&D Systems, USA) for 16 h at 37 °C. Cells were further incubated with protein transport inhibitors, golgi-plug (BD Biosciences, USA) and golgi-stop (BD Biosciences) for 6 h. Cells were then stained for surface markers (see Supplementary Figure 3.1 before being fixed and permeabilised for intracellular staining with anti-IFN-γ and anti-IL-17 antibodies at room temperature for 15 min. All samples were analysed on a CytoFlex LS flow cytometer (Beckman Coulter, USA) using CytExpert software (Beckman Coulter). Data were analysed using FlowJo software v10 (FlowJo, USA). For the full gating strategy, see Supplementary Figure 3.2.

3.4.9 Histopathology staining

Fixed, paraffin-embedded kidney sections (4 µm) were stained with either 0.5% Picrosirius red (Polysciences Inc., USA) or haematoxylin and eosin (Amber Scientific, Australia).

Sections were imaged (20x magnification) using either a polarised or bright field microscope (Olympus, Japan) and analysed for percentage collagen area by ImageJ. Changes in renal tubular structure (i.e., tubular dilatation, tubular atrophy and

epithelial brush border integrity) were assessed using a 4-point scoring system as follows: 0 = no damage; 1 = mild damage (< 25% tubules affected); 2 = moderate damage (25–50% of tubules affected); and 3 = severe damage (> 50% of tubules affected). Quantified/scored Picrosirius red and renal histopathology data represent the average values obtained independently by two investigators who were blinded to the *in vivo* treatment of each sample.

3.4.10 Immunohistochemistry

Following sodium citrate antigen retrieval (AJAX Finechem; Australia; pH 6), kidney sections were blocked in 1% goat serum or, where appropriate, Mouse IgG Blocking Reagent (Vector Laboratories, USA), and then incubated overnight at 4°C with rat anti-CD3 (5 µg/mL; Abcam, USA), rabbit anti-IL-18 (0.2 µg/mL; Abcam, USA), rabbit anti-IL-18R1 (5 µg/mL; Abcam, USA), or mouse anti-aquaporin-1 (AQP-1; 1/22; 0.4 µg/mL; Santa Cruz, USA) diluted in 1% goat serum or Mouse on Mouse (M.O.M.) diluent (Vector Laboratories, USA). Alexa Fluor 488- or Alexa Fluor 555-conjugated goat secondary antibodies (Invitrogen, USA) were used following incubation with M.O.M Biotinylated Anti-Mouse IgG Reagent (Vector Laboratories, USA), and cell nuclei were counterstained with DAPI. Fluorescent images were captured using a Zeiss 780 confocal microscope (Carl Zeiss, Oberkochen, Germany).

3.4.11 Statistics

Unless stated otherwise, results are expressed as mean ± standard error of mean (SEM). Data were analysed using either Student's unpaired t-test or two-way repeated measures analysis of variance (ANOVA), as appropriate. Post hoc analyses (performed when F tests

from ANOVA were < 0.05) were performed using Bonferroni's test. Non-parametric data were analysed using Kruskal-Wallis one-way ANOVA. $P < 0.05$ was considered to be statistically significant.

3.5 Results

3.5.1 IL-18$^{-/-}$ mice are protected from 1K/DOCA/salt-induced hypertension

1K/DOCA/salt treatment in WT mice was associated with a marked elevation in systolic BP (by > 20 mmHg as measured by tail cuff) evident by day 7 and persisting throughout the 21-day protocol (Figure 3.1A). By contrast, systolic BP in WT control (1K/placebo) mice remained unchanged (Figure 3.1A). Similar findings were obtained with radiotelemetry in that 1K/DOCA/salt-induced increases in systolic BP were blunted by ~50% in IL-18$^{-/-}$ compared to WT mice (Figure 3.1B). The rise in mean arterial pressure following 1K/DOCA/salt treatment was also reduced in IL-18$^{-/-}$ mice (Figure 3.1C), whereas diastolic BP (Figure 3.1D) and heart rate (Supplementary Figure 3.3) were not significantly different between strains (Figure 3.1D-E).

In WT mice, 1K/DOCA/salt treatment had no effect on mRNA expression of pro-IL-18 in the kidneys (Supplementary Figure 3.4A). However, mRNA expression of other components of the IL-18 signalling pathway, including *Il18r1*, *Il18rap* and *Il18bp*, was higher (by 3- to 6-fold) in kidneys from 1K/DOCA/salt- compared to WT control mice (Supplementary Figure 3.4B-D). As expected, mRNA expression of pro-*Il18* was not detectable in kidneys from IL-18$^{-/-}$ mice (Supplementary Figure 3.4A). By contrast, mRNA for *Il18r1*, *Il18rap* and *Il18bp* was expressed in the kidneys of IL-18$^{-/-}$ mice, at similar basal levels to those in WT mice (Supplementary Figure 3.4B-D). However, after 1K/DOCA/salt-treatment, the increases in expression of *Il18r1* and *Il18rap* were markedly blunted in IL-18$^{-/-}$ compared to WT mice (Supplementary Figure 3.4B-D).

3.5.2 IL-18$^{-/-}$ mice are protected from 1K/DOCA/salt-induced renal inflammation

Flow cytometry was used to determine renal immune cell accumulation in WT and IL-18$^{-/-}$ mice. 1K/DOCA/salt treatment promoted accumulation of CD45^{+} leukocytes in the kidneys of WT mice (Figure 3.2A-B). This comprised increases in total myeloid (CD11b^{+}) and macrophage (CD11b^{+}F4/80^{+}) cells, as well as total T cells (CD3^{+}; Figure 3.2B). Both

$CD4^+$ and $CD8^+$ T cell populations were significantly expanded in kidneys from 1K/DOCA/salt- versus 1K/placebo-treated WT mice (Supplementary Figure 3.5). Compared to WT, the 1K/DOCA/salt-induced increases in total leukocytes, myeloid cells, macrophages, and T cells were all markedly inhibited in IL-$18^{-/-}$mice (Figure 3.2A-B).

IL-18 signalling promotes the expression of the adhesion molecules ICAM-1 and VCAM-1,[20] and can act synergistically with IL-23 and IL-12 to promote the production of various pro-inflammatory chemokines and cytokines.[21, 22] Consistent with the increased immune cell infiltration observed, quantitative PCR revealed increased expression of several pro-inflammatory genes in the kidneys of 1K/DOCA/salt-treated WT mice compared to control WT mice, including *Icam1* (~2.5-fold), *Vcam1* (~6-fold), *Il23a* (~3-fold), *Il6* (~21-fold), *Ccl2* (~26-fold) and *Ccl5* (~6-fold; Figure 3.2C). Although baseline expression of these genes was similar in WT and IL-$18^{-/-}$ mice, the increases in expression following 1K/DOCA/salt treatment were markedly blunted (by 40-80%) in the latter strain, apart from *Ccl5* which was only mildly blunted in IL-$18^{-/-}$ mice and failed to reach statistical significance (Figure 3.2C).

3.5.3 IL-$18^{-/-}$ mice are protected from 1K/DOCA/salt-induced renal fibrosis and histopathology

Semi-quantitative analysis of picrosirius red stained kidney sections from WT mice, using brightfield and polarised microscopy, revealed that expression of renal interstitial collagen was 3- to 4-fold higher in animals treated with 1K/DOCA/salt than in control mice (Figure 3.3A-B). In IL-$18^{-/-}$ mice, basal levels of renal interstitial collagen were similar to those in WT mice yet were virtually unaffected by 1K/DOCA/salt treatment (Figure 3.3A-B).

Consistent with observations at the protein level, mRNA expression of four collagen subtypes (*Col1a1, Col3a1, Col4a1 and Col5a1*) was higher in the kidneys of WT mice treated with 1K/DOCA/salt than in WT controls (Supplementary Figure 3.6). Again, there

was no evidence that 1K/DOCA/salt upregulated collagen gene expression in the kidneys of IL-18$^{-/-}$ mice (Supplementary Figure 3.6).

Histopathological scoring of hematoxylin/eosin-stained kidney sections revealed that 1K/DOCA/salt-treated WT mice exhibited damage to their tubular architecture, evidenced by tubular dilatation, atrophy and loss of epithelial brush borders, compared to control WT mice (Figure 3.3C-D). IL-18$^{-/-}$ mice were protected from all these measures of 1K/DOCA/salt-induced tubular damage (Figure 3.3C-D).

3.5.4 IL-18$^{-/-}$ mice are protected from 1K/DOCA/salt-induced volume overload and kidney dysfunction

The rate at which an acute saline load is excreted by the kidneys is directly related to the volume status of the animal/subject prior to administration of the saline load.[23] Thus, under conditions of volume overload, such as occurs in the 1K/DOCA/salt model, an acute saline bolus would be expected to increase the rate of urine excretion. At baseline, WT mice excreted ~50-60% of a saline bolus within 4 h. The ability of control WT mice to excrete the saline bolus remained relatively unchanged over 21 d. By contrast, mice that received 1K/DOCA/salt displayed enhanced urine output. Thus, after 7 and 14 d, ~100% of the saline bolus was excreted within 4 h, and after 21 d ~80% was excreted (Supplementary Figure 3.7A). At baseline, IL-18$^{-/-}$ mice were similar to WT mice in their ability to excrete a saline bolus within 4 h (40-60%). This was not affected by the 1K/placebo (control) treatment and was only modestly increased following 1K/DOCA/salt (Supplementary Figure 3.7A). Thus, compared to WT, IL-18$^{-/-}$ mice were resistant to 1K/DOCA/salt-induced increases in urine output in response to a saline bolus challenge (Supplementary Figure 3.7A).

Electrolyte excretion (urinary Na^+ and Cl^-) following a saline bolus challenge was also elevated by > 50% in 1K/DOCA/salt-treated WT mice compared to WT controls (Supplementary Figure 3.7B-C), whereas these increases were blunted in 1K/DOCA/salt-treated IL-18$^{-/-}$ mice (Supplementary Figure 3.7B-C).

Elevated urinary albumin is associated with hypertension and is a clinical marker of kidney damage and dysfunction. Following 1K/DOCA/salt-treatment, urinary albumin increased in WT mice by 2- to 4-fold within 7-14 d (Supplementary Figure 3.7D). In contrast, 1K/DOCA/salt treatment had minimal effect on albuminuria in IL-18$^{-/-}$ mice (Supplementary Figure 3.7D).

3.5.5 T cells and tubular epithelial cells are likely targets of IL-18 in hypertensive kidneys

T cells are a known target of IL-18 whereby binding of the cytokine to its cognate receptor complex promotes production of pro-inflammatory cytokines. Flow cytometric analysis revealed a marked accumulation of IL-18R1-expressing leukocytes (CD45^{+}IL-18R1^{+}) in the kidneys of 1K/DOCA/salt-treated WT mice (Figure 3.4A-B). Most of these IL-18R1-expressing cells (i.e., ~55%) were CD3^{+} T cells, including both CD4^{+} and CD8^{+} T cell subsets (Figure 3.4A, C-E). F4/80^{+} and other unidentified cell types comprised 7% and 38% of all CD45^{+} cells expressing IL-18R1 (Supplementary Figure 3.8). Further flow cytometric analysis revealed that ~67% of T cells in the kidneys of 1K/DOCA/salt-treated mice expressed IL-18R1, which was markedly greater than the proportion of IL-18R1-expressing T cells in 1K/placebo mice (~38%; Supplementary Figure 3.8). Consistent with these flow cytometry results, immunofluorescence staining confirmed colocalization of IL-18R1 with some, but not all, CD3^{+} T cells in kidney cross-sections from 1K/DOCA/salt-treated WT mice (Figure 3.4F). IL-18R1 staining was also strongly localised to tubular epithelial cells in 1K/DOCA/salt-treated mice (Figure 3.4F). There was minimal IL-18R1 and CD3 staining in kidney sections of 1K/placebo-treated mice (Figure 3.4F).

Next, we isolated T cells from the kidneys of 1K/DOCA/salt- and 1K/placebo-treated mice and incubated them overnight with IL-18 to test for effects on production of pro-inflammatory cytokines including IFN-γ and IL-17. In the absence of agonist, a small proportion of T cells (4-9%) were found to express IFN-γ, and this did not differ between

groups (Supplementary Figure 3.10). However, whereas overnight incubation with IL-18 had no effect on T cells from control mice, IL-18 caused a concentration-dependent increase in the proportion of IFN-γ-expressing cells in T cells from 1K/DOCA/salt-treated mice (Supplementary Figure 3.10). By contrast, IL-17 expression was not detected in any renally-derived T cells (Supplementary Figure 3.10).

3.5.6 IL-18 is produced by renal tubular epithelial cells

Immunofluorescence staining was performed to determine the cellular source(s) of IL-18 in the kidneys during 1K/DOCA/salt-induced hypertension. IL-18 was frequently detected at the apical surface of tubules within the renal cortex of 1K/DOCA/salt-treated WT mice (Figure 3.5A), whereas no staining was evident in tubules located in the medulla. Faint IL-18 staining was also occasionally observed in glomeruli (Figure 3.5A). Given that the renal cortex is where the proximal portion of the convoluted tubule of most nephrons resides, we stained adjacent kidney sections with the proximal tubule marker, AQP-1.[24] These studies demonstrated that the majority of IL-18 staining was localised to tubules that also stained positive for AQP-1 (Supplementary Figure 3.11). We found no evidence of IL-18 staining on any other structures (e.g., interstitium, blood vessels) within the kidneys of 1K/DOCA/salt-treated WT mice. Moreover, IL-18 immunofluorescence was undetectable in the kidneys of normotensive 1K/placebo-treated mice and, as expected, in those of IL-18$^{-/-}$ mice, regardless of whether they were treated with 1K/DOCA/salt or 1K/placebo (Figure 3.5A).

To provide further insight into the cellular origin of pathogenic IL-18 in 1K/DOCA/salt-induced kidney injury, bone marrow transplant experiments were conducted. WT mice that received WT bone marrow (WT + WT BM) displayed a rapid and sustained increase in systolic BP following 1K/DOCA/salt treatment (Figure 3.5B). Thus, by day 7, systolic BP had risen by ~30 mmHg and was sustained for the rest of the 21-day treatment period

(Figure 3.5B). This hypertensive response was virtually identical to that seen in WT mice receiving IL-18$^{-/-}$ bone marrow and treatment with 1K/DOCA/salt (WT + IL-18$^{-/-}$ BM; Figure 3.5B). Moreover, renal IL-18 expression in WT + IL-18$^{-/-}$ BM mice was similar to that in WT + WT BM mice (Figure 3.5C). This suggests that bone marrow-derived immune cells are not a major source of renal IL-18 expression. By contrast, IL-18$^{-/-}$ mice that received WT bone marrow (IL-18$^{-/-}$ + WT BM) had markedly lower (by 70-80%) expression of renal IL-18 and were largely protected from the development of hypertension in response to 1K/DOCA/salt (Figure 3.5B-C). Notably, IL-18$^{-/-}$ + WT BM and IL-18$^{-/-}$ + IL-18$^{-/-}$ BM mice (the latter being completely devoid of renal IL-18 expression) were equally protected from developing severe hypertension following 1K/DOCA/salt treatment (Figure 3.5B-C).

3.5.7 Non-bone marrow-derived IL-18 causes renal fibrosis and injury in 1K/DOCA/salt-induced hypertension

Following 1K/DOCA/salt treatment, IL-18$^{-/-}$ + WT BM and IL-18$^{-/-}$+ IL-18$^{-/-}$ BM mice exhibited 50% less renal interstitial collagen deposition than WT + WT BM and WT + IL-18$^{-/-}$ BM mice (Figure 3.6A & C). Consistent with these results, we noted that IL-18$^{-/-}$ + WT BM and IL-18$^{-/-}$ + IL-18$^{-/-}$ BM had less tubular dilatation, tubular atrophy, and loss of epithelial brush border integrity than WT + WT BM and WT + IL-18$^{-/-}$ BM mice (Figure 3.6B & D).

3.6 Discussion

This study highlights the crucial role of IL-18 in the development of high blood pressure, kidney damage and dysfunction in the 1K/DOCA/salt model of hypertension in mice. The key novel findings are: (1) 1K/DOCA/salt-dependent hypertension is associated with renal upregulation of several components of the IL-18 signalling system, including IL-18, IL-18R1 and IL-18RAP; (2) IL-18 is predominantly localised to renal tubular epithelial cells, while IL-18R1 is expressed by both renal tubular epithelial cells and T cells; (3) *ex vivo* stimulation of T cells from kidneys of 1K/DOCA/salt-treated mice with IL-18 causes IFN-γ production whereas T cells from normotensive mice are unresponsive to IL-18; (4) mice with global IL-18 deficiency or IL-18-deficiency restricted to non-bone marrow-derived cells are profoundly protected from the development of hypertension, renal inflammation, fibrosis and damage; whereas (5) bone marrow-specific IL-18-deficiency does not result in such protection.

The 1K/DOCA/salt model used herein is characterised by sodium retention, expansion of blood and extracellular fluid volume, and low circulating renin and angiotensin II levels.[25] As such, it bears many similarities to a common form of human primary hypertension, i.e., low-renin hypertension. The model also exhibits other pathophysiological features relevant to human hypertension including sympathetic hyperactivity[26] and, of particular relevance to the present study, inflammation and immune activation in the kidneys.[15] We previously demonstrated that the NLRP3 inflammasome plays a vital role in the development of hypertension and kidney disease in mice subjected to 1K/DOCA/salt.[12, 13] Subsequently, several groups described a crucial role for the NLRP3 inflammasome in other models of hypertension.[27, 28] Collectively, these studies provided a rationale to investigate the relative contributions of the two main inflammasome-derived cytokines — IL-1β and IL-18 — to hypertension. To this end, we recently showed that inhibition of IL-1β signalling with an IL-1 receptor antagonist, anakinra, caused a modest reduction in blood pressure in mice

with established 1K/DOCA/salt-induced hypertension, but provided no protection against renal inflammation[29], indicating the involvement of other pro-inflammatory mediators. Therefore, the current study sought to determine the role of IL-18 in the development of hypertension, with a focus on renal pathophysiology.

IL-18 was first identified as the IFNγ-inducing factor released from monocytes and macrophages and, for many years, these and other myeloid cells were thought to be the primary source of the cytokine.[30-32] However, more recently it has become apparent that the epithelial lining of many tissues, including the oral cavity, colon, and lungs, is a major producer of IL-18 in response to injury and infection.[33-35] In the kidneys, the tubular epithelium has been identified as a major site of IL-18 production in models of bacterial lipopolysaccharide-challenge, obstructive kidney injury and lupus nephritis, and in patients with chronic kidney disease or following renal transplantation.[36-39] Consistent with this, we found IL-18 to be upregulated in the proximal renal tubules of 1K/DOCA/salt-treated WT mice. Moreover, chimeric mice with IL-18 deficiency in non-bone marrow-derived cells were protected from hypertension and renal damage, whereas IL-18 deficiency in the bone marrow alone conferred no protection. Overall, these findings suggest that tubular epithelial cells rather than monocytes/macrophages are the key source of pathogenic IL-18 in the kidneys during 1K/DOCA/salt hypertension.

Interestingly, we observed no increase in mRNA expression of renal *Il18*, whereas *Il18r1*, *Il18rap* and *Il18bp* were all elevated in 1K/DOCA/salt-treated mice. This may suggest that the increased abundance of IL-18 protein detected in the renal tubules was due to altered translational/post-translational mechanisms rather than increased gene transcription. This observation is consistent with the known biology of IL-18. Unlike IL-1β, which is virtually undetectable under physiological conditions and requires rapid, sequential transcriptional and post-translational processing to be activated, the precursor protein for IL-18 (pro-IL-18) is constitutively expressed in many cell types.[40, 41] Thus, the rate-limiting step for

activation and release of IL-18 from tubular epithelial cells is likely to be inflammasome/caspase-1 activation. We previously reported that 1K/DOCA/salt-dependent hypertension in mice is associated with an increase in the expression of cleaved caspase-1 in the kidneys, indicative of inflammasome activation.[12] This raises the question: what is the stimulus for activation of the inflammasome in renal tubules in the setting of 1K/DOCA/salt-induced hypertension? Previous studies highlight albuminuria as a potential culprit in promoting inflammasome activation in renal cells. Incubation of cultured kidney epithelial cells with high concentrations of albumin evoked NLRP3 inflammasome/caspase-1 activation and IL-18 production, downstream of endoplasmic reticulum stress[42] and elevated mitochondrial reactive oxygen species formation.[43, 44] Here we showed that albumin levels were elevated in the urine within 1 week of the 1K/DOCA/salt-treatment, which is consistent with albumin being an early driver of inflammasome activation and IL-18 production in this model. However, as albumin was not elevated in the urine of IL-18$^{-/-}$ mice, it may be that albuminuria occurs downstream of inflammasome activation and IL-18 production. Alternatively, the above observations may suggest a vicious feed-forward cycle where modest increases in albumin in the early stages of hypertension promote inflammasome activation/inflammation which in turn gives rise to further glomerular injury and albumin leakage. Clearly, further studies are needed to determine the temporal and mechanistic relationships between albumin and inflammasome activation in the pathogenesis of renal inflammation and injury in 1K/DOCA/salt-induced hypertension.

Flow cytometric and immunohistochemical analyses showed T cells to be a major site of renal IL-18R1 expression in 1K/DOCA/salt-treated mice. We also showed that *ex vivo* stimulation by IL-18 of T cells isolated from the kidneys of these mice elicited production of the pro-inflammatory cytokine IFN-γ. Together with our previous observation that NLRP3 inflammasome inhibition reduces the proportion of IFN-γ-producing T cells in the

kidneys[13], our findings suggest that IL-18 is an important regulator of T cell function in hypertension. Since the seminal discovery by Guzik *et al.* that the adaptive immune system is a key driver of hypertension[15], multiple studies have shown that T cells accumulate in the kidneys during hypertension and represent an important source of IFN-γ. Furthermore, several mechanisms may operate in parallel to regulate T cell activation and IFN-γ production in the kidneys. For example, Kirabo *et al.* demonstrated that both angiotensin II- and 1K/DOCA/salt-dependent hypertension in mice are associated with the formation of isoketals in dendritic cells.[45] These highly reactive lipid species chemically modify cellular proteins, converting them into neoantigens, which, upon presentation to T cells, promote proliferation and production of IFN-γ.[45] A scavenger of isoketals, 2-hydroxybenzylamine, was highly effective at preventing renal infiltration of T cells, along with kidney fibrosis and damage.[45] Deficiency of the lymphocyte adapter protein, LNK — which functions as a negative regulator of cytokine signalling and proliferation — has also been mooted as a possible contributor to hyperactivation of T cells in hypertension. Genome wide association and gene network analyses in humans demonstrated that a single nucleotide, loss-of-function polymorphism in the *SH2B3* gene that encodes LNK is strongly associated with hypertension.[46, 47] Genetic ablation of *Sh2b3* in mice exacerbated the accumulation of IFN-γ-producing CD8+ T cells in the kidneys and worsened renal dysfunction and hypertension in angiotensin II-infused mice.[48] More recently, Sun *et al* described a pathway whereby the mineralocorticoid receptor (MR) on T cells regulates IFN-γ expression via the transcription factors NFAT1 (nuclear factor of activated T-cells 1) and AP-1 (activator protein-1).[49] Importantly, MR deficiency in T cells mitigated angiotensin II-induced accumulation of IFN-γ-producing T cells in the kidneys and afforded protection against the development of hypertension and renal and vascular damage.[49] Hence, in future studies it will be interesting to explore precisely how these, and

other regulatory mechanisms, act in concert with IL-18 to promote T cell activation and IFN-γ production in the kidneys during hypertension.

A recent study in 1K/DOCA/salt-treated mice showed that once activated, T cells in the kidneys aggregate on the basolateral side of tubules where they interact directly with epithelial cells to cause upregulation of Kir4.1 K^+ channels, and stimulation of ClC-K Cl^- channels.[50] The resultant efflux of Cl^- causes a compensatory influx of Cl^- through the Na-Cl cotransporter located on the luminal surface of the tubular epithelium at the cost of Na^+ retention.[50] Of note, two recent reports suggested that the NCC may couple with IL-18R1 and act as a non-canonical receptor for IL-18.[51, 52] Indeed, we identified the tubular epithelium as another site of IL-18R1 expression within the kidneys. Hence, it is tempting to speculate that IL-18 might represent a master regulator of Na^+ retention in the kidneys via its concerted actions on T cells on the basolateral side of the tubules, and NCC receptors on the luminal side of the tubular epithelium.

The current findings have potential relevance from a therapeutic perspective. Indeed, the IL-18 pathway is emerging more broadly as an attractive target of new therapies for inflammatory diseases. Currently, the main approach for targeting this pathway involves neutralising IL-18 activity, either with a recombinant human IL-18BP (Tadekinig alfa) or anti-IL-18 monoclonal antibodies. Several clinicals trials have recently been completed or are underway to investigate the efficacy of these therapies in autoinflammatory diseases, including adult-onset Still's disease, X-linked inhibitor of apoptosis (XIAP) deficiency and Type 2 Diabetes Mellitus (details available at: NCT02398435, NCT03512314, NCT01648153).[53, 54] Other potential opportunities for intervention in the IL-18 signalling pathway, which are yet to be explored clinically, include inhibition of inflammasome-dependent processing of the cytokine or antagonism of its cognate receptor subunits, IL-18R1 or IL-18RAP. There is also evidence that IL-37 may counteract the actions of IL-18 by binding to IL-18R1 and 'hijacking' it for anti-inflammatory signalling.[55] Future studies

aimed at investigating whether the aforementioned pharmacological interventions mimic the protective effects of genetic ablation of IL-18 in 1K/DOCA/salt, and indeed other animal models of hypertension and chronic kidney disease, will be important next steps towards clinical translation of the current findings.

3.6.1 Perspectives

In summary, we have shown in a model of low-renin hypertension that IL-18 production by renal tubular epithelial cells is an important contributor to the development of high blood pressure, kidney inflammation and fibrosis. Furthermore, we provide evidence that T cells within the kidney are a direct target of IL-18 and likely play a role in propagating inflammation through the production of interferon-γ. These findings highlight the IL-18 signalling pathway as a promising therapeutic target to treat the inflammation that contributes to hypertension and chronic kidney disease. It is envisaged that pharmacological approaches aimed at blocking IL-18 production (e.g., NLRP3 inflammasome inhibitors) or neutralising the actions of the cytokine itself (e.g., anti-IL-18 neutralizing antibodies) may have utility for the future treatment of hypertension and end organ damage, either as stand-alone or adjunct therapies to conventional anti-hypertensive medications.

3.7 References

1. Drummond GR, Vinh A, Guzik TJ and Sobey CG. Immune mechanisms of hypertension. *Nat Rev Immunol*. 2019;19:517-532.
2. Norlander AE, Madhur MS and Harrison DG. The immunology of hypertension. *J Exp Med*. 2018;215:21-33.
3. Ivy JR and Bailey MA. Pressure natriuresis and the renal control of arterial blood pressure. *J Physiol*. 2014;592:3955-67.
4. Rodriguez-Iturbe B and Johnson RJ. Role of inflammatory cells in the kidney in the induction and maintenance of hypertension. *Nephrol Dial Transplant*. 2005;21:260-263.
5. Rabkin SW. The role of interleukin 18 in the pathogenesis of hypertension-induced vascular disease. *Nat Clin Pract Cardiovasc Med*. 2009;6:192-9.
6. Formanowicz D, Wanic-Kossowska M, Pawliczak E, Radom M and Formanowicz P. Usefulness of serum interleukin-18 in predicting cardiovascular mortality in patients with chronic kidney disease--systems and clinical approach. *Sci Rep*. 2015;5:18332.
7. Parikh CR, Jani A, Melnikov VY, Faubel S and Edelstein CL. Urinary interleukin-18 is a marker of human acute tubular necrosis. *Am J Kidney Dis*. 2004;43:405-14.
8. Schroder K and Tschopp J. The Inflammasomes. *Cell*. 2010;140:821-832.
9. Jha S and Ting JPY. Inflammasome-associated nucleotide-binding domain, leucine-rich repeat proteins and inflammatory diseases. *J Immunol*. 2009;183:7623-7629.
10. Martinon F and Tschopp J. Inflammatory caspases and inflammasomes: master switches of inflammation. *Cell Death Differ*. 2007;14:10-22.
11. Dinarello CA, Novick D, Kim S and Kaplanski G. Interleukin-18 and IL-18 binding protein. *Front Immunol*. 2013;4:289-289.
12. Krishnan SM, Dowling JK, Ling YH, et al. Inflammasome activity is essential for one kidney/deoxycorticosterone acetate/salt-induced hypertension in mice. *Br J Pharmacol*. 2016;173:752-65.

13. Krishnan SM, Ling YH, Huuskes BM, et al. Pharmacological inhibition of the NLRP3 inflammasome reduces blood pressure, renal damage, and dysfunction in salt-sensitive hypertension. *Cardiovasc Res*. 2018;115:776-787.
14. Takeda K, Tsutsui H, Yoshimoto T, Adachi O, Yoshida N, Kishimoto T, Okamura H, Nakanishi K and Akira S. Defective NK Cell Activity and Th1 Response in IL-18–Deficient Mice. *Immunity*. 1998;8:383-390.
15. Guzik TJ, Hoch NE, Brown KA, McCann LA, Rahman A, Dikalov S, Goronzy J, Weyand C and Harrison DG. Role of the T cell in the genesis of angiotensin II induced hypertension and vascular dysfunction. *J Exp Med*. 2007;204:2449-60.
16. Karatas A, Hegner B, de Windt LJ, et al. Deoxycorticosterone acetate-salt mice exhibit blood pressure-independent sexual dimorphism. *Hypertension*. 2008;51:1177-83.
17. Duran-Struuck R and Dysko RC. Principles of bone marrow transplantation (BMT): providing optimal veterinary and husbandry care to irradiated mice in BMT studies. *J Am Assoc Lab Anim Sci*. 2009;48:11-22.
18. Trott DW, Thabet SR, Kirabo A, et al. Oligoclonal CD8+ T cells play a critical role in the development of hypertension. *Hypertension*. 2014;64:1108-15.
19. Schmittgen TD and Livak KJ. Analyzing real-time PCR data by the comparative C(T) method. *Nat Protoc*. 2008;3:1101-8.
20. Raeburn CD, Dinarello CA, Zimmerman MA, Calkins CM, Pomerantz BJ, McIntyre RC, Jr., Harken AH and Meng X. Neutralization of IL-18 attenuates lipopolysaccharide-induced myocardial dysfunction. *Am J Physiol Heart Circ Physiol*. 2002;283:H650-7.
21. Yoshimoto T, Takeda K, Tanaka T, Ohkusu K, Kashiwamura S, Okamura H, Akira S and Nakanishi K. IL-12 up-regulates IL-18 receptor expression on T cells, Th1 cells, and B cells: synergism with IL-18 for IFN-gamma production. *J Immunol*. 1998;161:3400-7.

22. Hoeve MA, Savage NDL, de Boer T, Langenberg DML, de Waal Malefyt R, Ottenhoff THM and Verreck FAW. Divergent effects of IL-12 and IL-23 on the production of IL-17 by human T cells. *Eur J Immunol*. 2006;36:661-670.
23. Walser M. Phenomenological analysis of renal regulation of sodium and potassium balance. *Kidney Int*. 1985;27:837-841.
24. Bedford JJ, Leader JP and Walker RJ. Aquaporin expression in normal human kidney and in renal disease. *J Am Soc Nephrol*. 2003;14:2581-7.
25. Lerman LO, Kurtz TW, Touyz RM, et al. Animal Models of Hypertension: A Scientific Statement From the American Heart Association. *Hypertension*. 2019;73:e87-e120.
26. Takeda K and Buñag RD. Augmented sympathetic nerve activity and pressor responsiveness in DOCA hypertensive rats. *Hypertension*. 1980;2:97-101.
27. Shirasuna K, Karasawa T, Usui F, et al. NLRP3 Deficiency Improves Angiotensin II-Induced Hypertension But Not Fetal Growth Restriction During Pregnancy. *Endocrinology*. 2015;156:4281-92.
28. Sun H-J, Ren X-S, Xiong X-Q, et al. NLRP3 inflammasome activation contributes to VSMC phenotypic transformation and proliferation in hypertension. *Cell Death Dis*. 2017;8:e3074-e3074.
29. Ling YH, Krishnan SM, Chan CT, et al. Anakinra reduces blood pressure and renal fibrosis in one kidney/DOCA/salt-induced hypertension. *Pharmacol Res*. 2017;116:77-86.
30. Pirhonen J, Sareneva T, Kurimoto M, Julkunen I and Matikainen S. Virus infection activates IL-1 beta and IL-18 production in human macrophages by a caspase-1-dependent pathway. *J Immunol*. 1999;162:7322-9.
31. Wyburn K, Wu H, Chen G, Yin J, Eris J and Chadban S. Interleukin-18 affects local cytokine expression but does not impact on the development of kidney allograft rejection. *Am J Transplant*. 2006;6:2612-21.

32. Bellora F, Castriconi R, Doni A, Cantoni C, Moretta L, Mantovani A, Moretta A and Bottino C. M-CSF induces the expression of a membrane-bound form of IL-18 in a subset of human monocytes differentiating in vitro toward macrophages. *Eur J Immunol*. 2012;42:1618-26.
33. Sugawara S, Uehara A, Nochi T, et al. Neutrophil proteinase 3-mediated induction of bioactive IL-18 secretion by human oral epithelial cells. *J Immunol*. 2001;167:6568-75.
34. Muñoz M, Eidenschenk C, Ota N, et al. Interleukin-22 induces interleukin-18 expression from epithelial cells during intestinal infection. *Immunity*. 2015;42:321-331.
35. Cameron LA, Taha RA, Tsicopoulos A, Kurimoto M, Olivenstein R, Wallaert B, Minshall EM and Hamid QA. Airway epithelium expresses interleukin-18. *Eur Respir J*. 1999;14:553-9.
36. Franke EI, Vanderbrink BA, Hile KL, Zhang H, Cain A, Matsui F and Meldrum KK. Renal IL-18 production is macrophage independent during obstructive injury. *PLoS One*. 2012;7:e47417.
37. Faust J, Menke J, Kriegsmann J, Kelley VR, Mayet WJ, Galle PR and Schwarting A. Correlation of renal tubular epithelial cell-derived interleukin-18 up-regulation with disease activity in MRL-Faslpr mice with autoimmune lupus nephritis. *Arthritis Rheum*. 2002;46:3083-95.
38. Liang D, Liu HF, Yao CW, Liu HY, Huang-Fu CM, Chen XW, Du SH and Chen XW. Effects of interleukin 18 on injury and activation of human proximal tubular epithelial cells. *Nephrology*. 2007;12:53-61.
39. Stokman G, Kers J, Yapici U, et al. Predominant Tubular Interleukin-18 Expression in Polyomavirus-Associated Nephropathy. *Transplantation*. 2016;100:e88-95.
40. Puren AJ, Fantuzzi G and Dinarello CA. Gene expression, synthesis, and secretion of interleukin 18 and interleukin 1beta are differentially regulated in human blood

mononuclear cells and mouse spleen cells. *Proc Natl Acad Sci U S A*. 1999;96:2256-61.

41. Pizarro TT, Michie MH, Bentz M, Woraratanadharm J, Smith MF, Jr., Foley E, Moskaluk CA, Bickston SJ and Cominelli F. IL-18, a novel immunoregulatory cytokine, is up-regulated in Crohn's disease: expression and localization in intestinal mucosal cells. *J Immunol*. 1999;162:6829-35.
42. Fang L, Xie D, Wu X, Cao H, Su W and Yang J. Involvement of endoplasmic reticulum stress in albuminuria induced inflammasome activation in renal proximal tubular cells. *PLoS One*. 2013;8:e72344.
43. Zhuang Y, Hu C, Ding G, Zhang Y, Huang S, Jia Z and Zhang A. Albumin impairs renal tubular tight junctions via targeting the NLRP3 inflammasome. *Am J Physiol Renal Physiol*. 2015;308:F1012-9.
44. Zhuang Y, Ding G, Zhao M, et al. NLRP3 inflammasome mediates albumin-induced renal tubular injury through impaired mitochondrial function. *J Biol Chem*. 2014;289:25101-11.
45. Kirabo A, Fontana V, de Faria AP, et al. DC isoketal-modified proteins activate T cells and promote hypertension. *J Clin Invest*. 2014;124:4642-56.
46. Levy D, Ehret GB, Rice K, et al. Genome-wide association study of blood pressure and hypertension. *Nat Genet*. 2009;41:677-87.
47. Huan T, Meng Q, Saleh MA, et al. Integrative network analysis reveals molecular mechanisms of blood pressure regulation. *Mol Syst Biol*. 2015;11:799.
48. Saleh MA, McMaster WG, Wu J, et al. Lymphocyte adaptor protein LNK deficiency exacerbates hypertension and end-organ inflammation. *J Clin Invest*. 2015;125:1189-202.
49. Sun XN, Li C, Liu Y, et al. T-Cell Mineralocorticoid Receptor Controls Blood Pressure by Regulating Interferon-Gamma. *Circ Res*. 2017;120:1584-1597.

50. Liu Y, Rafferty TM, Rhee SW, Webber JS, Song L, Ko B, Hoover RS, He B and Mu S. CD8(+) T cells stimulate Na-Cl co-transporter NCC in distal convoluted tubules leading to salt-sensitive hypertension. *Nat Commun*. 2017;8:14037.
51. Wang J, Sun C, Gerdes N, et al. Interleukin 18 function in atherosclerosis is mediated by the interleukin 18 receptor and the Na-Cl co-transporter. *Nat Med*. 2015;21:820-6.
52. Liu CL, Ren J, Wang Y, et al. Adipocytes promote interleukin-18 binding to its receptors during abdominal aortic aneurysm formation in mice. *Eur Heart J*. 2019.
53. McKie EA, Reid JL, Mistry PC, DeWall SL, Abberley L, Ambery PD and Gil-Extremera B. A Study to Investigate the Efficacy and Safety of an Anti-Interleukin-18 Monoclonal Antibody in the Treatment of Type 2 Diabetes Mellitus. *PLoS One*. 2016;11:e0150018.
54. Gabay C, Fautrel B, Rech J, et al. Open-label, multicentre, dose-escalating phase II clinical trial on the safety and efficacy of tadekinig alfa (IL-18BP) in adult-onset Still's disease. *Ann Rheum Dis*. 2018;77:840-847.
55. Dinarello CA. Overview of the IL-1 family in innate inflammation and acquired immunity. *Immunol Rev*. 2018;281:8-27.

3.8 Figures

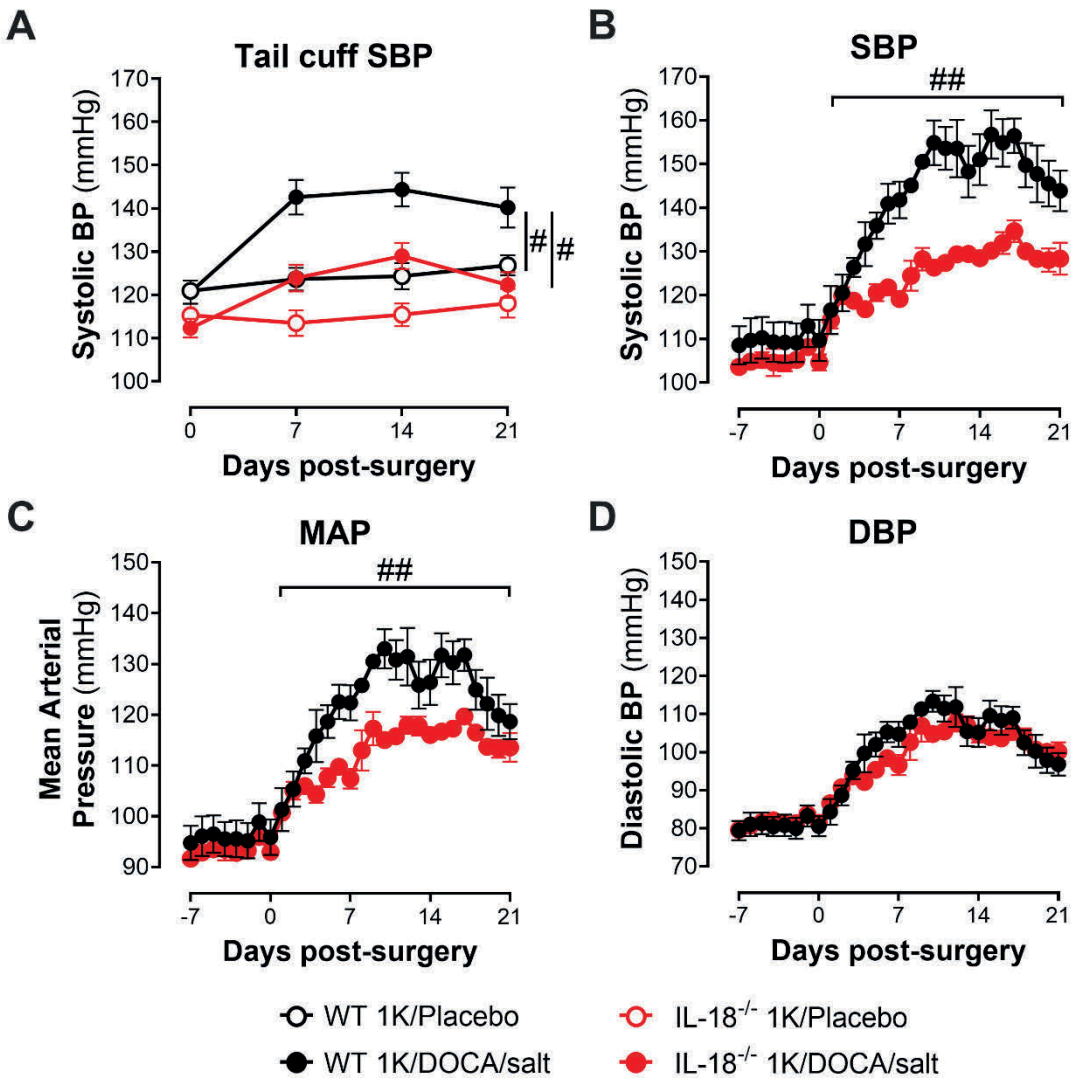

Figure 3.1 1K/DOCA/salt-induced hypertension is blunted in IL-18$^{-/-}$ mice. (A) Tail cuff measurements of systolic BP (n= 10-19). Radiotelemetry measurements of systolic BP (B), mean arterial pressure (C), diastolic BP (D; n=3). All values are expressed as mean ± SEM. ##P ≤ 0.05 and #P < 0.05 vs. WT 1K/DOCA/salt for two-way ANOVA.

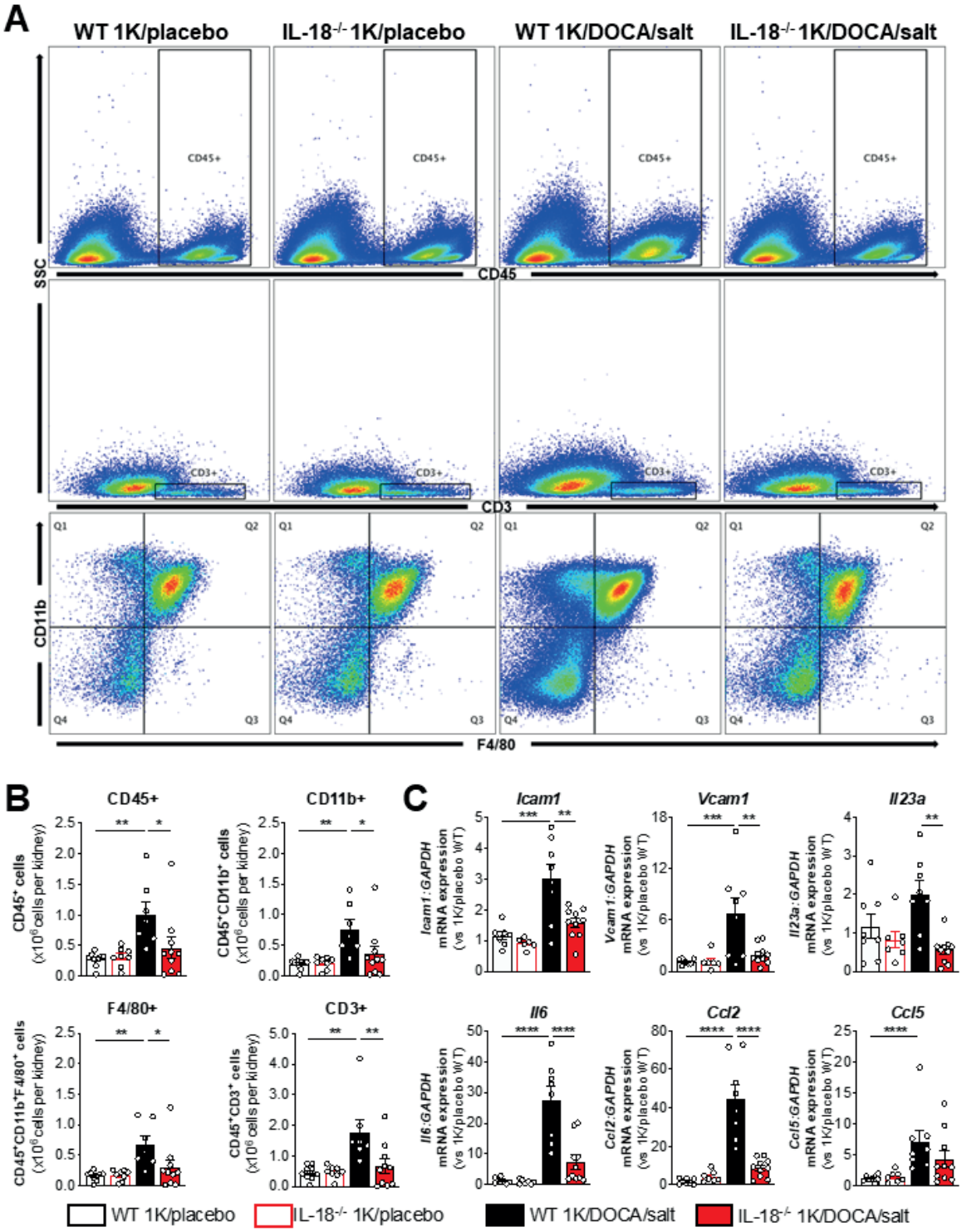

Figure 3.2 IL-18$^{-/-}$ mice are protected from 1K/DOCA/salt-induced renal immune cell infiltration and inflammatory gene expression. (A) Representative flow cytometry plots of renal immune cell infiltration and (B) corresponding group data of total leukocyte (CD45^{+}), myeloid cell (CD45^{+}CD11b^{+}), macrophage (CD45^{+}CD11b^{+}F4/80^{+}) and T cell (CD45^{+}CD3^{+}) populations in the kidney. (C) Renal mRNA expression of *Icam1*, *Vcam1*, *Il23a*, *Il6*, *Ccl2*, and *Ccl5* as measured by real-time PCR. Values are expressed as mean ± SEM from n= 6=10 experiments. ****P ≤ 0.0001, ***P ≤ 0.001, **P ≤ 0.01, *P < 0.05 for two-way ANOVA followed by Bonferroni post-test.

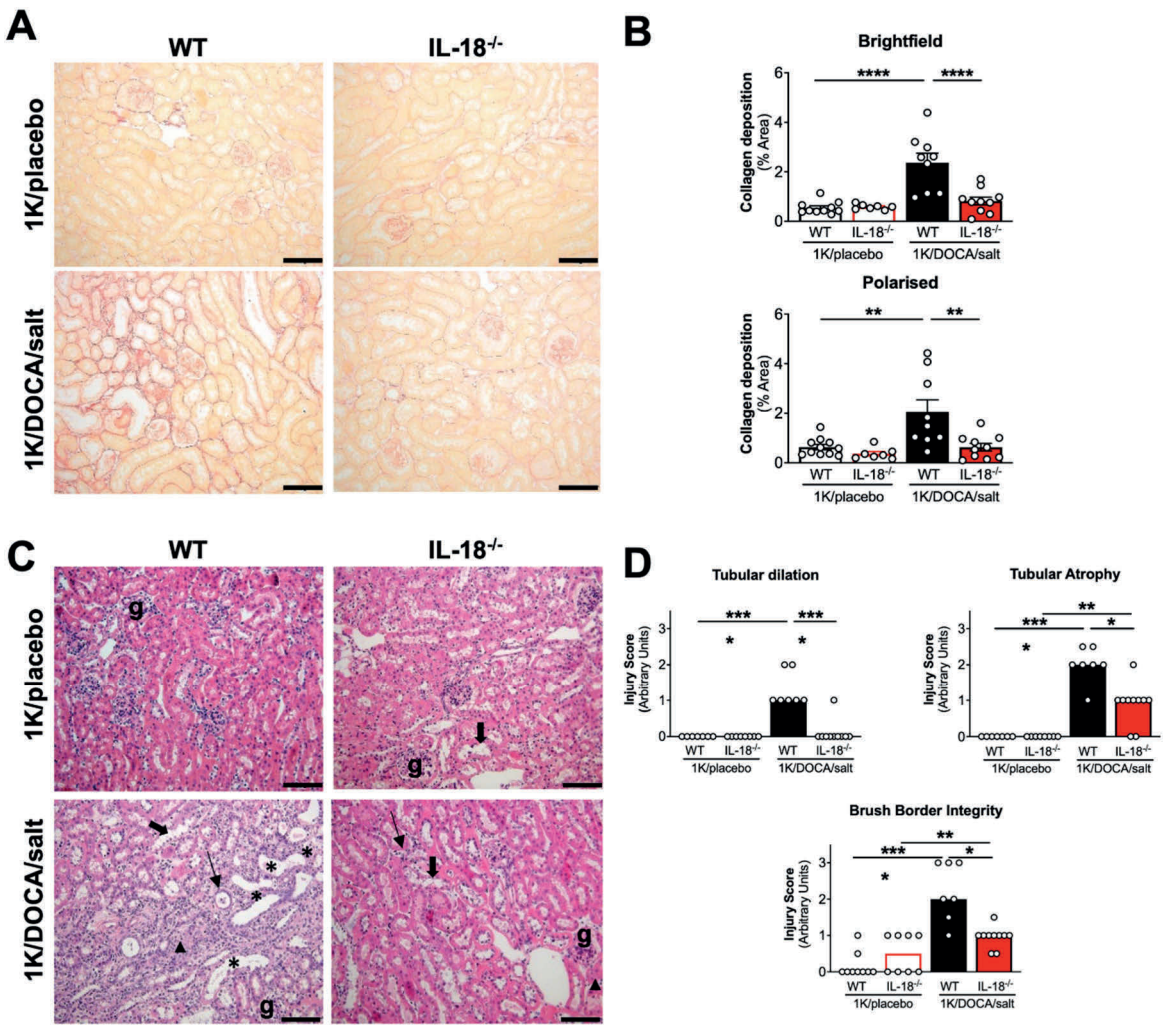

Figure 3.3 IL-18$^{-/-}$ mice are protected from renal fibrosis and damage associated with 1K/DOCA/salt hypertension. (A) Representative brightfield images of kidney sections stained with picrosirius red staining from 1K/placebo- and 1K/DOCA/salt-treated WT and IL-18$^{-/-}$ mice. (B) Percentage area of collagen deposition assessed from brightfield (top) and polarised microscopy (bottom). (C) Representative haematoxylin/eosin-stained kidney sections from 1K/placebo- and 1K/DOCA/salt-treated WT and IL-18$^{-/-}$ mice. (D) Histopathological scoring of tubular dilatation (*), tubular atrophy (arrowhead) and loss of brush border integrity (thick arrow). Thin arrow = inflammatory cell infiltrates; g = glomeruli. Scale bars = 100 µm. Panel B values are expressed as mean ± SEM (n= 6-10) while in panel D values are expressed as the median histological score (n=7-10). ****P ≤ 0.0001, **P ≤ 0.01, *P < 0.05 for one- or two-way ANOVA followed by Bonferroni or Kruskal-Wallis post-tests.

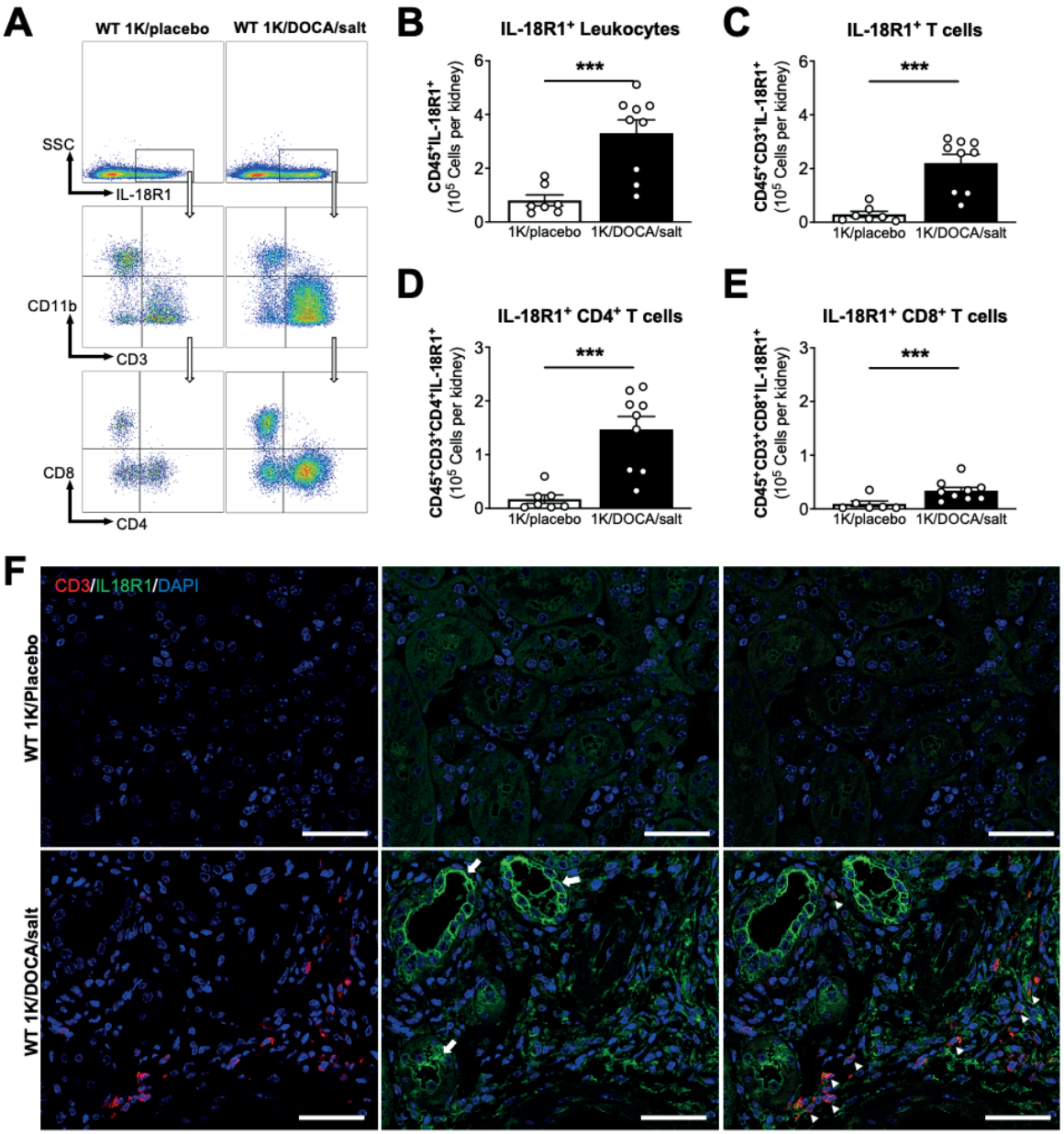

Figure 3.4 IL-18R1 is localised to T cells and tubular epithelial cells in kidneys of 1K/DOCA/salt-treated mice. (A) Representative flow cytometry plots and (B-E) group data showing number of IL-18R1-positive leukocytes ($CD45^+IL\text{-}18R1^+$; B), total T cells ($CD45^+CD11b^-CD3^+IL\text{-}18R1^+$; C), $CD4^+$ T cells (D) and $CD8^+$ T cells (E) in 1K/placebo- and 1K/DOCA/salt-treated WT mouse kidneys. (F) Representative immunofluorescence images showing localisation of $CD3^+$ T cells (red staining; *left*), IL-18R1 (green staining; *middle*) and co-localisation of T cells and IL-18R1 (orange staining; arrowheads in right panels) in kidney sections from 1K/placebo- and 1K/DOCA/salt-treated WT mice. Bold arrows denote tubular epithelial cell staining. Images are representative of n=6 experiments.

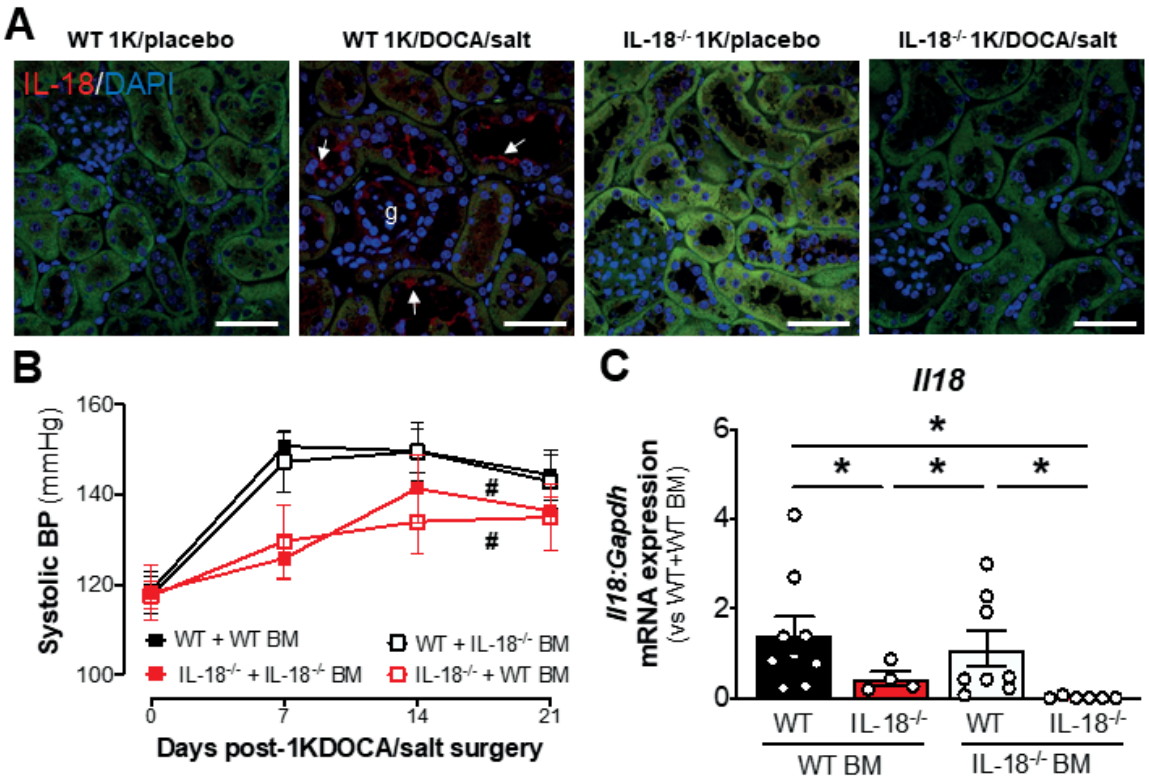

Scale bar = 50 µm. Values are expressed as mean ± SEM from n= 7-9 experiments. ***P ≤ 0.001, **P ≤ 0.01 and *P < 0.05 for Student's unpaired t-test.

Figure 3.5 Tubular epithelial cells are the main source of IL-18 in the kidneys of 1K/DOCA/salt-treated mice. (A) Representative immunofluorescence images showing IL-18 localisation (red staining) to the apical surface of tubular epithelial cells (arrows) and glomeruli (g) in 1K/DOCA/salt-treated but not 1K/placebo-treated WT mice. Scale bar = 50 µm. (B) Systolic BP measurements and (C) renal mRNA expression of *Il18* in 1K/DOCA/salt-treated chimeric WT and IL-18$^{-/-}$ mice that received WT or IL-18$^{-/-}$ bone marrow (BM). Values are expressed as mean ± SEM from n= 4-9 experiments. #P < 0.05 vs. WT + WT BM for two-way ANOVA and *P < 0.05 for two-way ANOVA followed by Bonferroni post-test.

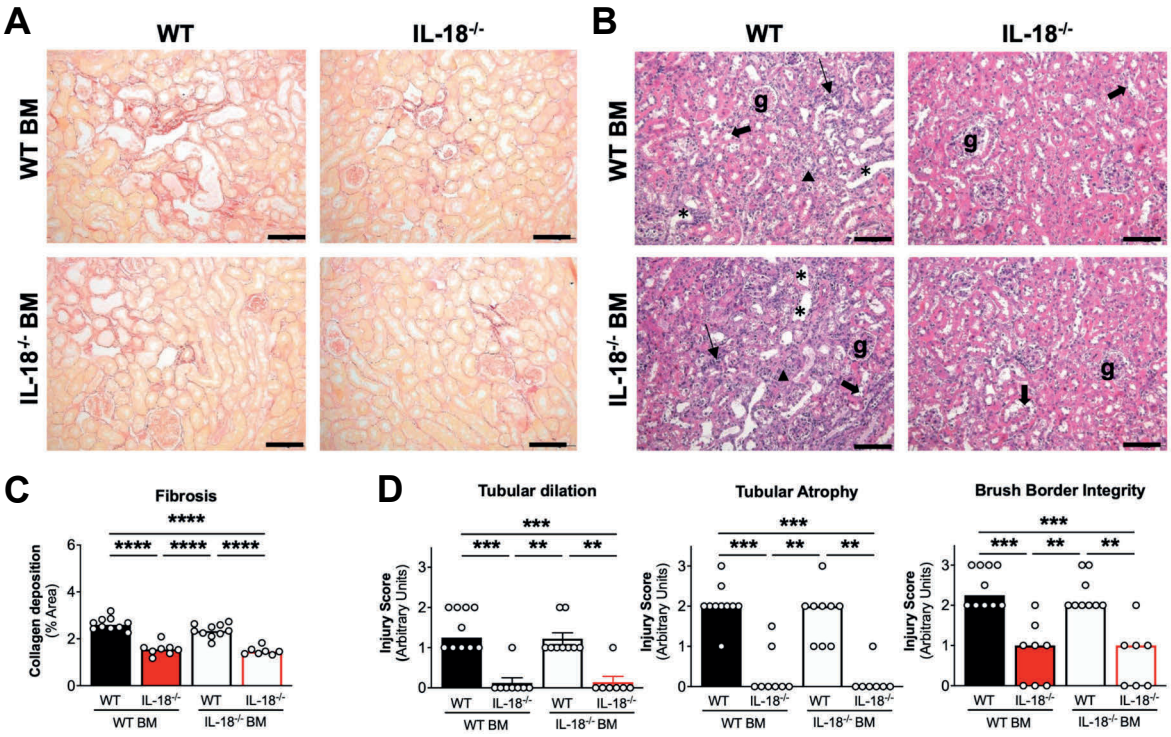

Figure 3.6 Bone marrow-derived cells are not responsible for IL-18-mediated fibrosis and tubular damage in 1K/DOCA/salt-induced hypertension. (A) Representative brightfield images of kidney sections stained with picrosirius red staining from 1K/DOCA/salt-treated chimeric WT and IL-18$^{-/-}$ mice. (B) Representative haematoxylin/eosin-stained kidney sections from 1K/DOCA/salt-treated chimeric WT and IL-18$^{-/-}$ mice. (C) Percentage area of collagen deposition using brightfield microscopy. (D) Histopathological scoring of tubular dilatation (*), tubular atrophy (arrowhead) and loss of brush border integrity (thick arrow) from chimeric mouse experiments. Thin arrow = inflammatory cell infiltrates; g = glomeruli. Scale bars = 100 µm. Panel B values are expressed as mean ± SEM (n= 6-10) while in panel D, values are expressed as the median histological score (n=7-10). ****P ≤ 0.0001, **P ≤ 0.01, *P < 0.05 for one- or two-way ANOVA followed by Bonferroni or Kruskal-Wallis post-tests.

3.9 Supplementary Methods

3.9.1 Animals

A total of 311 male wild type or IL-18$^{-/-}$ mice[14], fully backcrossed onto a C57BL6/J background, were used. Male mice were used for direct comparison to related studies in the field[12, 13, 15] and because sex differences in rodent responses to 1K/DOCA/salt have been reported previously.[16] Mice were aged 9-17 weeks and weighed 20-36 g (see Table 3.1 and Table 3.2). Mice were obtained from either the Monash Animal Research Platform (MARP; Monash University, Australia), the Animal Resources Centre (Perth, Australia) or the La Trobe Animal Research and Teaching Facility (LARTF; La Trobe University Australia). Prior to surgery, mice were housed with littermates in groups of 3-4 animals in Sealsafe Plus GM500 boxes (Tecniplast, USA), under specific pathogen-free conditions, on a 12 h light-dark cycle, and provided with *ad libitum* access to normal chow and drinking water. Mice were randomly assigned into treatment groups (e.g., hypertensive versus normotensive) using random number generator software (Microsoft Excel, Version 16.36, USA). All procedures were conducted according to the Australian Code for the Care and Use of Animals for Scientific Purposes (8th edition) and were approved by the MARP Animal Ethics Committee (Project number: MARP/2013/043) and La Trobe University Animal Ethics Committee (Project number: AEC16-93).

3.9.2 Induction of hypertension

A salt-induced, volume overload model of hypertension was used in this study wherein mice were uninephrectomised at the left kidney and treated with deoxycorticosterone acetate (DOCA; 2.4 mg/day, *s.c.*; Innovative Research of America, USA) and 0.9% saline drinking water (1K/DOCA/salt). Normotensive controls for this experiment were mice that also received uninephrectomy, a placebo pellet containing the proprietary matrix material without DOCA (Innovative Research of America, USA) and normal drinking water (1K/placebo). All surgeries were performed under anaesthesia induced by inhalation of

isoflurane (2 L/min, 5% in O_2). Anaesthesia was maintained by 2.5% isoflurane in O_2 (0.4 L/min) and regularly monitored by checking hind-paw withdrawal, blink reflexes and respiratory rate. Prior to surgery, mice received local anaesthetic (bupivacaine; 2.5 mg/kg, *s.c.*) and analgesic (carprofen; 5 mg/kg, *s.c.*) and were treated with carprofen for 3 days following surgery.

3.9.3 Bone marrow cell transplantation

Wild-type and IL-18$^{-/-}$ mice were killed by CO_2 asphyxiation and bone marrow cells were obtained by flushing the femurs and tibias with RPMI 1640 medium (Gibco™, ThermoFisher Scientific, USA). Cells were counted using an automatic cell counter (EVE, NanoEnTek Inc, South Korea) and resuspended in RPMI 1640 medium at a concentration of 5.0 x 10^7 cells per mL. Recipient wild-type and IL-18$^{-/-}$ mice were lethally irradiated with two separate doses of 5.5 Gy X-ray ionizing radiation (RS-2000 Irradiator, Rad Source, USA), with a resting period of 3 h between each dose.[17] Following the second dose of radiation, the mice were injected via the tail vein with 5.0 x 10^6 bone marrow cells in 100 μL of RPMI. Mice received enrofloxacin (75 mg/kg) in their drinking water for 2 days prior to, and for a further 21 days following bone marrow cell transplantation. Sixteen weeks were allowed for bone marrow engraftment before induction of hypertension by 1K/DOCA/salt treatment.

3.9.4 Saline challenge to assess fluid volume loading and renal injury

The extent of fluid volume loading and renal injury were assessed in conscious mice at days 0, 7, 14 and 21 post-surgery using a protocol modified from Trott *et al.* in which urine volume and amount of electrolytes and albumin excreted over 4 h following a bolus subcutaneous saline injection (volume equivalent to 10% of body weight) are monitored.[18] Briefly, mice were lightly anaesthetised with 2.5% isoflurane in O_2 (0.4 L/min) and urine in the bladder was eliminated by mild suprapubic compression. Mice were then injected subcutaneously across four injection sites with a volume of prewarmed saline (37°C), and

immediately placed in metabolic cages for 4 h. Urine volume produced over 4 h was presented as a percentage of the saline volume injected. Measurements of [Na^+] and [Cl^-] were performed by a commercial provider (Monash Pathology Service) using the Synchron LX20 (Beckman Coulter, USA) and albumin concentration was measured by ELISA (Bethyl Laboratories, USA). Note: all mice were acclimatised to the metabolic cages by placing them in the cages for 6 h on three separate occasions during the week prior to the induction of hypertension.

3.9.5 Blood pressure measurements

BP was measured either via tail cuff plethysmography or radiotelemetry. Tail cuff measurements were performed using a Multichannel BP Analysis System (MC4000; Hatteras Instruments, USA). All mice underwent daily training on the tail cuff device for at least 3 days prior to induction of hypertension. Blood pressures were then recorded on the morning prior to surgery (day 0) and weekly thereafter on days 7, 14 and 21. For radiotelemetry, a telemeter probe (Model TA11PA-C10, Data Sciences International, USA) was surgically implanted into the left carotid artery of mice anaesthetised with 2.5% isoflurane in O_2 (0.4 L/min). Immediately following surgery, mice were treated topically with an antibiotic (Tribactril, Jurox, Australia) and analgesic (carprofen; 5 mg/kg, *s.c.*). Mice also received antibiotic in their drinking water for a further 2 days (Baytril; 0.375 mg/mL). Mice were allowed 10 days to recover, after which time the probes were switched on for 3 days of continuous baseline systolic BP, diastolic BP, mean arterial pressure (MAP), heart rate and locomotor activity recordings. Mice then underwent surgery to induce hypertension as described above and the same parameters were continuously monitored for 21 days.

3.9.6 Measurement mRNA expression levels

At the end of the 21-day treatment period, mice were killed via CO_2 asphyxiation and perfused through the left ventricle with phosphate-buffered saline (PBS) containing 0.2%

Clexane (400 IU; Sanofi Aventis, France). The right kidney was excised and cut in half along its transverse plane. One half of the kidney was used immediately for flow cytometric analysis, while the other half was further divided into two transverse sections. One of these sections was fixed in 10% formalin and stored at -4°C for immunohistochemistry, and the other was snap frozen in liquid N_2 and stored at -80°C for later RNA extraction. For this, frozen kidneys were pulverised, and RNA was extracted using a RNeasy Mini Kit (Qiagen, Hilden, Germany). The yield and purity of the RNA was determined using a NanoDrop Spectrophotometer (NanoDrop One, Thermo Scientific, USA). RNA was reversed transcribed using a High Capacity cDNA Reverse Transcription kit (Applied Biosystems, Lithuania) and the resulting cDNA was then used as a template in real-time PCR to measure mRNA expression of pro-*Il18*, *Il18r1*, *Il18rap*, *Il18bp*, C-C motif chemokine ligand (*Ccl*) 2, *Ccl5*, intercellular adhesion molecule-1 (*Icam1*), vascular cell adhesion molecule-1 (*Vcam1*), *Il6*, *Il23a*, *Col1a1*, *Col3a1*, *Col4a1*, and *Col5a1*, or the housekeeping gene, *Gapdh* (TaqMan Gene Expression Assays, Applied Biosystems, USA). Real-time PCR was performed in a Bio-Rad CFX96 Real-Time PCR Detection System (Bio-Rad Laboratories, Hercules, CA, USA) and the comparative Ct method was used to calculate the fold-change in mRNA expression relative to a reference control sample.[19]

3.9.7 Flow cytometric analysis

For conventional flow cytometric analysis, cell suspensions were prepared from kidney halves and whole spleens. Kidney halves were minced with scissors and digested in PBS containing collagenase type XI (125 U/ml), collagenase type I-S (460 U/ml) and hyaluronidase (60 U/ml) (Sigma-Aldrich, USA) for 60 mins at 37ºC. Following digestion, kidney suspensions were passed through a 70 µm filter (BD Biosciences, USA), and the cells were pelleted by centrifugation at 453 x*g* for 5 min. The cell pellets were further subjected to Percoll™ gradient centrifugation, whereby the pellet was re-suspended in 3 mL of 40% isotonic Percoll™ solution (GE Healthcare Life Science, UK), and carefully

under-laid with 3 mL of 70% Percoll™ solution. Samples were centrifuged at 1450 x*g* at 25°C for 25 min with the brakes of the centrifuge turned off. Following centrifugation, adipocytes and debris were aspirated from the top layer, and the layer containing the mononuclear cells — lying between the Percoll™ gradients — was collected. Mononuclear cells were washed in PBS, centrifuged, and the pellet was re-suspended in PBS. Spleen samples were minced with scissors and passed through a 70 µm filter, and then incubated in red blood cell (RBC) lysis buffer (NH_4Cl, $KHCO_3$, dH_2O) for 5 min at room temperature. Spleen cells were counted using an automatic cell counter (EVE, NanoEnTek Inc, South Korea) and re-suspended in PBS at a concentration of 10^7 cells/mL. Cells were stained for 15 min at room temperature with Live/Dead aqua stain (Life Technologies, USA), followed by an antibody cocktail consisting of anti-mouse CD45 (A700; BioLegend, USA), CD3 (APC; BioLegend, USA), CD8 (PeCy7; BioLegend, USA), CD4 (BV605; BioLegend, USA), CD11b (BV421; BioLegend, USA), F4/80 (APC Cy7; BioLegend, USA), CD69 (BV650; BioLegend, USA), CD44 (PERCP; BioLegend, USA), and IL-18R1 (PE; Invitrogen, USA; see Table 3.) dissolved in PBS containing 0.5% bovine serum albumin.

For intracellular cytokine/transcription staining, cells were washed in PBS, centrifuged, fixed and permeabilised (eBioscience™ Foxp3/Transcription Factor Fixation/Permeabilization Concentrate and Diluent; Invitrogen, USA). Cells were then washed in perm wash™ and re-suspended in 1% formalin in PBS containing 0.5% bovine serum albumin and EDTA, prior to analysis on a CytoFlex LS flow cytometer (Beckman Coulter, USA) using CytExpert software (Beckman Coulter). Data were analysed using FlowJo software v10 (FlowJo, USA). For the full gating strategy, see Supplementary Figure 3.1.

3.9.8 Intracellular Cytokine Detection

To detect renal and splenic T cell-derived IFN-γ, kidney and spleen cell suspensions were prepared as described for flow cytometric analysis. Renal and splenic T cells were enriched

using a CD90.2 positive microbead isolation kit (Miltenyi Biotech, USA) as per the manufacturer instructions. Enriched T cells were re-suspended in RPMI media containing 10% FBS, penicillin (100 U/mL)/streptomycin (100 µg/mL) and L-glutamine (2 mM) and seeded onto an anti-CD3 (5 ug/mL, Biolegend)-coated 96-well plate at a density of $1x10^6$ cells/well for splenic T cells and $1x10^5$ cells/well for renal T cells. In the presence of an anti-CD28 monoclonal antibody (1 µg/mL; BioLegend), T cells were stimulated with various concentrations of IL-18 (0, 0.1, 1, 10 or 100 ng/mL; R&D Systems, USA) for 16 h at 37 °C with 5% CO_2. Cells were further incubated with protein transport inhibitors, golgi-plug (BD Biosciences, USA) and golgi-stop (BD Biosciences), for 6 h. Following incubation, cells were centrifuged at 453 x*g* for 5 min at 4ºC and the supernatant was discarded. Cells were then stained for surface markers (see Table 3.3) before being fixed and permeabilised for intracellular staining with anti-IFN-γ and anti-IL-17 antibodies at room temperature for 15 min. Cells were then washed and re-suspended in PBS for analysis on a CytoFlex LS flow cytometer (Data were analysed using FlowJo software v10 (FlowJo, USA). For the full gating strategy, see Supplementary Figure 3.2.

3.9.9 Histopathology staining

Kidneys were fixed in 10% formalin, embedded in paraffin, and cut into 4 µm sections. Sections were deparaffinised, rehydrated, and stained with either 0.5% Picrosirius red solution (Polysciences Inc., USA), or haematoxylin and eosin (Amber Scientific, Australia). Sections were imaged (20x magnification) using either a polarised or bright field microscope (Olympus, Japan) and analysed for percentage collagen content by ImageJ. Changes in renal tubular structure (i.e., tubular dilatation, tubular atrophy and

epithelial brush border integrity) were assessed using a 4-point scoring system as follows: 0 = no damage; 1 = mild damage (< 25% tubules affected); 2 = moderate damage (25–50% of tubules affected); and 3 = severe damage (> 50% of tubules affected). Quantified/scored Picrosirius red and renal histopathology data represent the average values obtained

independently by two investigators who were blinded to the *in vivo* treatment of each sample.

3.9.10 Immunohistochemistry

Following sodium citrate antigen retrieval (AJAX Finechem; Australia; pH 6), kidney sections were blocked in 1% goat serum or, where appropriate, Mouse IgG Blocking Reagent (Vector Laboratories, USA), and then incubated overnight at 4°C with rat anti-CD3 (5 µg/mL; Abcam, USA), rabbit anti-IL-18 (0.2 µg/mL; Abcam, USA), rabbit anti-IL-18R1 (5 µg/mL; Abcam, USA) or mouse anti-aquaporin-1 (AQP-1, 1/22; 0.4 µg/mL; Santa Cruz, USA). Antibodies were diluted in 1% goat serum or Mouse on Mouse (M.O.M.) diluent (Vector Laboratories, USA). Alexa Fluor 488- or Alexa Fluor 555-conjugated goat secondary antibodies (Invitrogen, USA) were used following incubation with M.O.M Biotinylated Anti-Mouse IgG Reagent (Vector Laboratories, USA), and cell nuclei were counterstained with DAPI. Fluorescent images were captured using a Zeiss 780 confocal microscope (Carl Zeiss, Oberkochen, Germany).

3.9.11 Statistics

Unless otherwise stated, results are expressed as mean ± standard error of mean (SEM). Data were analysed using either Student's unpaired t-test or two-way repeated measures analysis of variance (ANOVA), as appropriate. Post hoc analyses (performed when F tests from ANOVA were < 0.05) were performed using Bonferroni's test. Kruskal-Wallis test was used for non-parametric data analysis. $P < 0.05$ was considered to be statistically significant.

3.10 Supplementary tables

Table 3.1 Mice used for 1K/DOCA/salt vs. 1K/placebo studies.

	Mouse strain	Origin	# of mice	Age at treatment (weeks)	Weight at treatment (g)	Deaths
IL-18$^{-/-}$ study	IL-18$^{-/-}$	LARTF	9	13-14	24-30	
		MARP	8	10-12	20-30	
	C57Bl/6	ARC	10	9-11	26-30	1 *
		MARP	8	10-12	25-30	
Saline bolus challenge	IL-18$^{-/-}$	LARTF	24	17-24	21-35	3 †
	C57Bl/6	ARC	20	18-23	25-33	4 *
Wild type mice studies	C57Bl/6	ARC	69	8-12	22-30	9 *, 9 †, 4
		MARP	63	10-12	24-32	13 *, 2 ‡
*= Aneurysm †= surgical wound opening/fight wounds ‡= unknown cause						

Table 3.2 Mice used for bone marrow transplant studies.

Bone marrow transplant study							
	Mouse strain	Origin	# of mice	Age at BM transplant (weeks)	Age at treatment (weeks)	Weight at treatment (g)	Deaths
Recipient Mice	IL-18$^{-/-}$	LARTF	30	11-14	25-33	21-31	15†, 1 *
	C57Bl/6	LARTF	30	11-13	26-33	20-31	10†
Donor Mice	IL-18$^{-/-}$	LARTF	20	10-15	-	-	-
	C57Bl/6	LARTF	20	10-13	-	-	-
*= surgical wound opening/fight wounds †= failure to reconstitute							

Table 3.3 Antibodies used for flow cytometry.

Antigen	Host/Isotype	Clone	Tag	Dilution Factor	Company
CD45	Rat IgG2b, κ	30-F11	A700	1:500	BioLegend, USA
CD3e	Hamster IgG	145-2C11	APC	1:500	BioLegend, USA
CD4	Rat IgG2a, κ	RM4-5	BV605	1:500	BioLegend, USA
CD8a	Rat IgG2a, κ	53-6.7	PerCP-Cy5.5	1:1000	BioLegend, USA
CD11b	Rat IgG2b, κ	M1/70	BV421	1:500	BioLegend, USA
F4/80	Rat IgG2a, κ	BM8	APC Cy7	1:500	BioLegend, USA
CD69	Rat IgG2a, κ	C068C2	BV650	1:500	BioLegend, USA
CD44	Rat IgG2a, κ	XMG1.2	PERCP	1:500	BioLegend, USA
IL-18R1	Rat IgG2a, κ	P3TUNYA	PE	1:500	Invitrogen, USA

Table 3.4 Antibodies used for flow cytometry experiments to detect T cell-derived IFN-γ.

Antigen	Host/Isotype	Clone	Tag	Dilution Factor	Company
CD45	Rat IgG2b, κ	30-F11	A700	1:500	BioLegend, USA
CD4	Rat IgG2a, κ	RM4-5	BV605	1:500	BioLegend, USA
CD8a	Rat IgG2a, κ	53-6.7	PerCP-Cy5.5	1:1000	BioLegend, USA
CD11b	Rat IgG2b, κ	M1/70	BV421	1:500	BioLegend, USA
IL-18R1	Rat IgG2a, κ	P3TUNYA	PE	1:500	Invitrogen, USA
TCR-β	Hamster IgG	H57-597	APC	1:500	BioLegend, USA
IFN-γ	Rat IgG2a, κ	DB-1	FITC	1:500	Invitrogen, USA
IL-17	Rat IgG2a, κ	eBio17B7	PE-Cy7	1:500	eBioscience, USA
CD206	Rat IgG2a, κ	C068C2	PE-DAZZLE	1:500	BioLegend, USA

3.11 Supplementary Figures

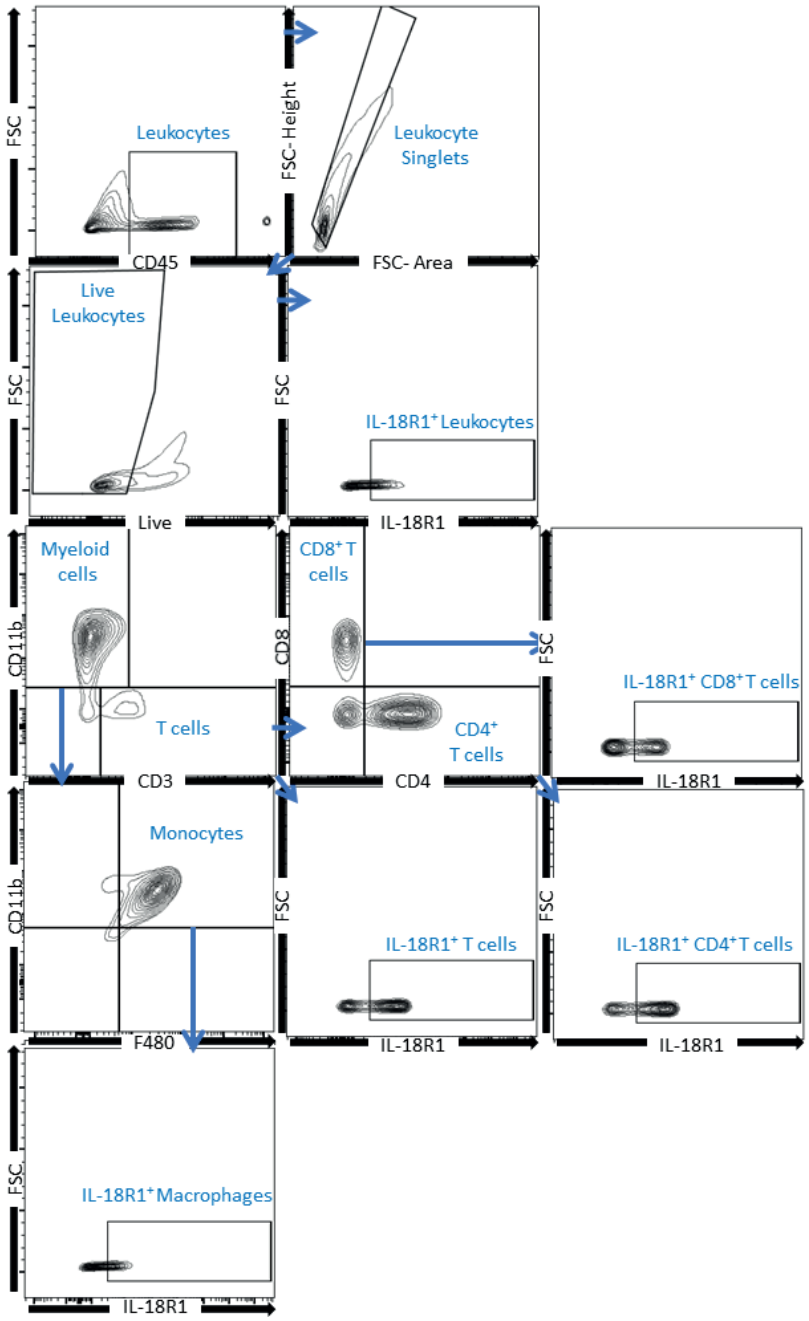

Supplementary Figure 3.1 Gating strategy for flow cytometric analysis. Leukocytes were gated as CD45$^+$ populations against forward scatter (FSC). Total leukocytes, i.e., live leukocyte singlets, were gated by FSC -height vs FSC-area, and exclusion of dead cells (live/dead stain). Total leukocytes were then divided into myeloid cells (CD11b$^+$) and T cells (CD3$^+$). Some of the myeloid cells were identified as macrophages (CD11b$^+$F4/80$^+$), and the macrophages were further classified as IL-18R1$^+$. T cells that were positive for CD3 staining were further classified as IL-18R1$^+$, CD4$^+$, or CD8$^+$ T cells. CD4$^+$ and CD8$^+$ cells were further identified as being IL-18R1$^+$.

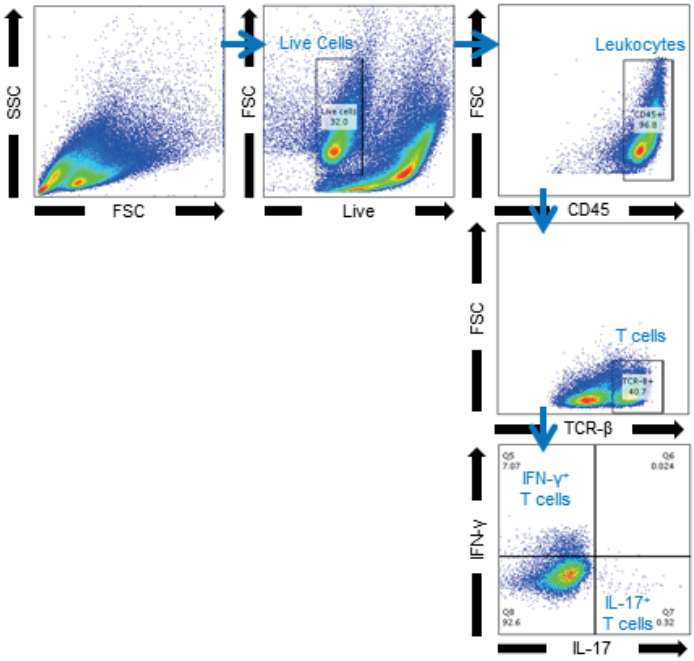

Supplementary Figure 3.2 Gating strategy for intracellular cytokine detection using flow cytometric analysis. Dead cells (live/dead stain) were excluded before leukocytes were gated as $CD45^+$ populations against forward scatter (FSC). Total leukocytes were classified as being T cells ($TCR\text{-}\beta^+$) and then divided into $IFN\text{-}\gamma^+$ or $IL\text{-}17^+$ populations.

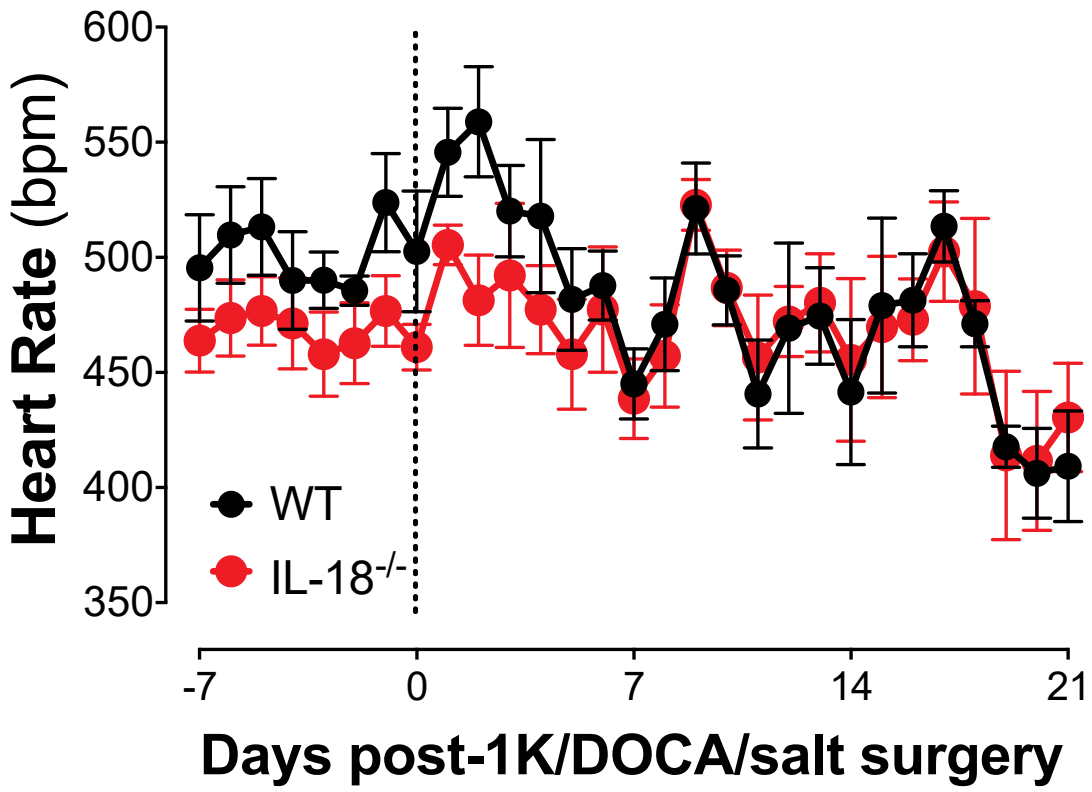

Supplementary Figure 3.3 Radiotelemetry heart rate measurements in 1K/DOCA/salt-treated WT and IL-18$^{-/-}$ mice. All values are expressed as mean ± SEM.

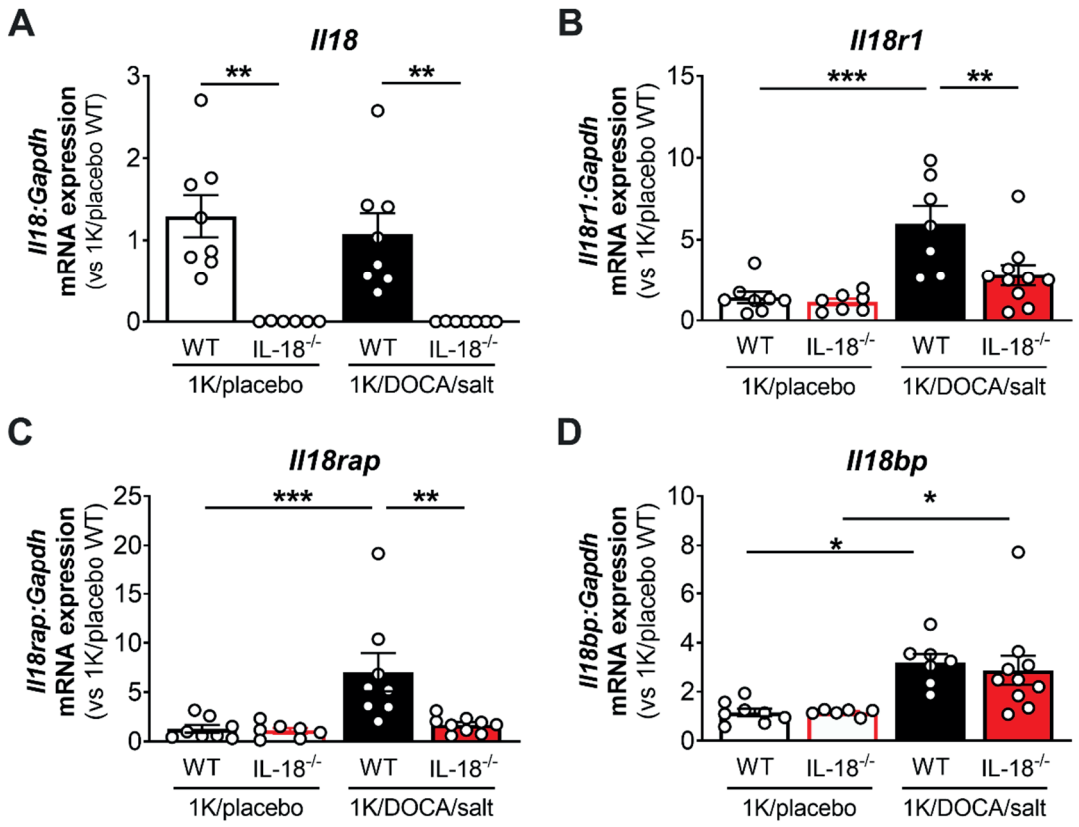

Supplementary Figure 3.4 1K/DOCA/salt-induced upregulation of the IL-18 signalling system is blunted in IL-18$^{-/-}$ mice. Real-time PCR measurements of pro-*Il18* (A), *Il18r1* (B), *Il18rap* (C), and *Il18bp* (D) mRNA expression in the kidneys (n= 6-8). Values are expressed as mean ± SEM. ***P ≤ 0.001, **P ≤ 0.01 and *P < 0.05 for two-way ANOVA followed by Bonferroni post-tests.

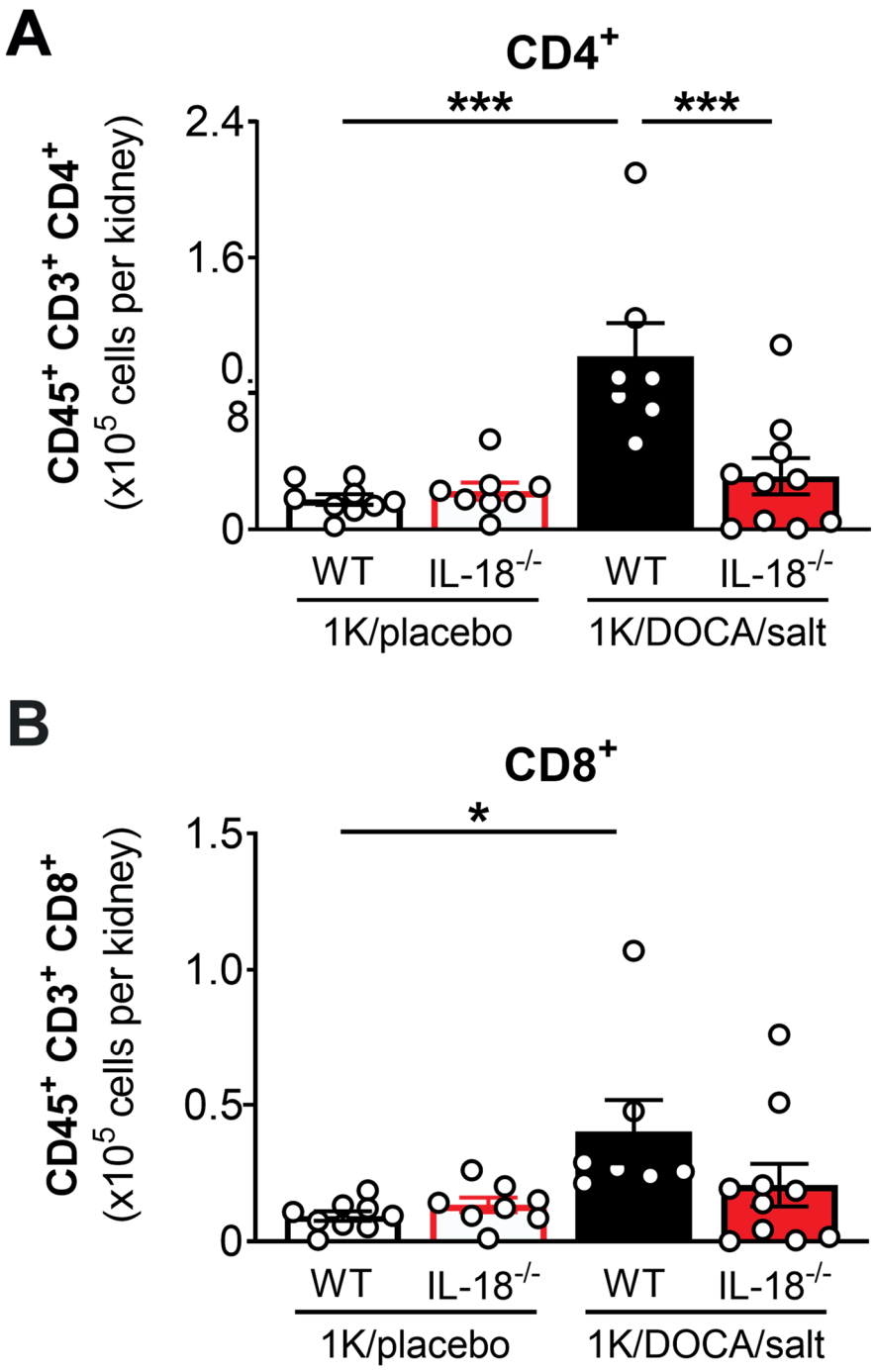

Supplementary Figure 3.5 IL-18$^{-/-}$ mice are protected from 1K/DOCA/salt-induced T cell infiltration of the kidney. Data showing numbers of CD4^{+} T cell (A) and CD8^{+} T cell (B) in the kidneys of mice. Values are mean ± SEM from n= 6=10 experiments. ***P ≤ 0.001 and *P < 0.05 for two-way ANOVA followed by Bonferroni post-test.

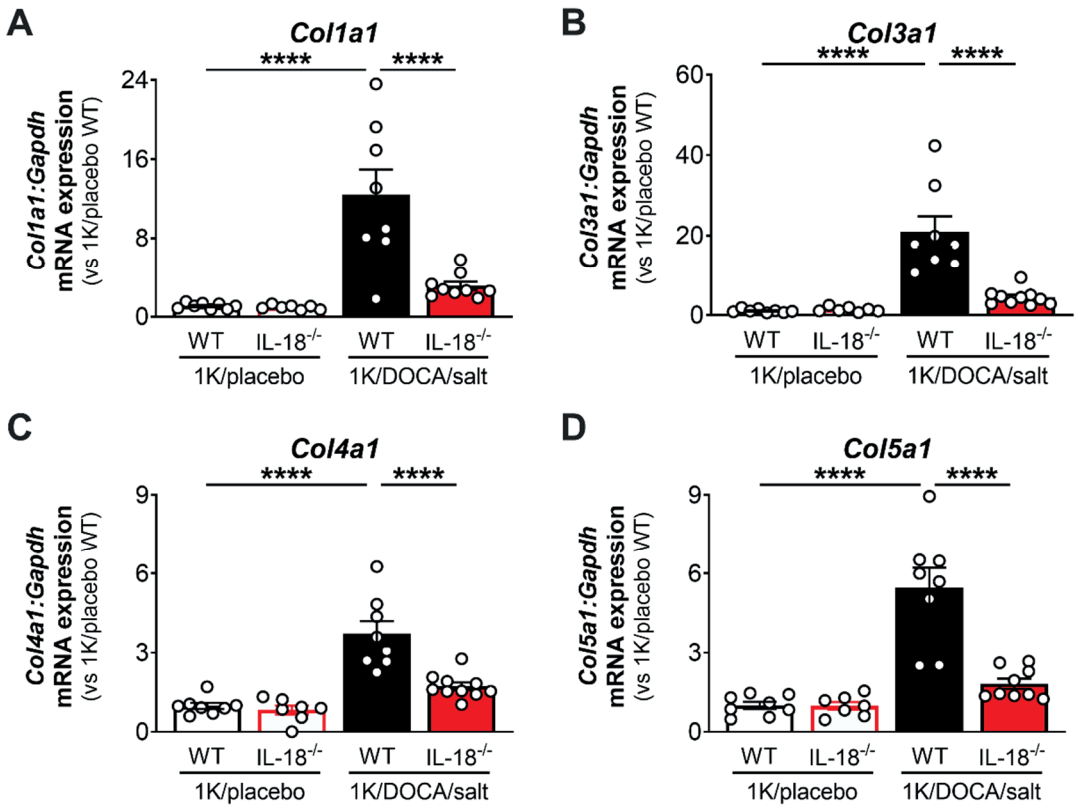

Supplementary Figure 3.6 IL-18$^{-/-}$ mice are protected from 1K/DOCA/salt-induced upregulation of renal collagen gene expression. Renal mRNA expression levels of the collagen α-subunits *Col1a1* (A), *Col3a1* (B), *Col4a1* (C) and *Col5a1* (D) as measured by real-time PCR. Values are expressed as mean ± SEM (n= 6-10). ****P ≤ 0.0001 two-way ANOVA followed by Bonferroni post-tests.

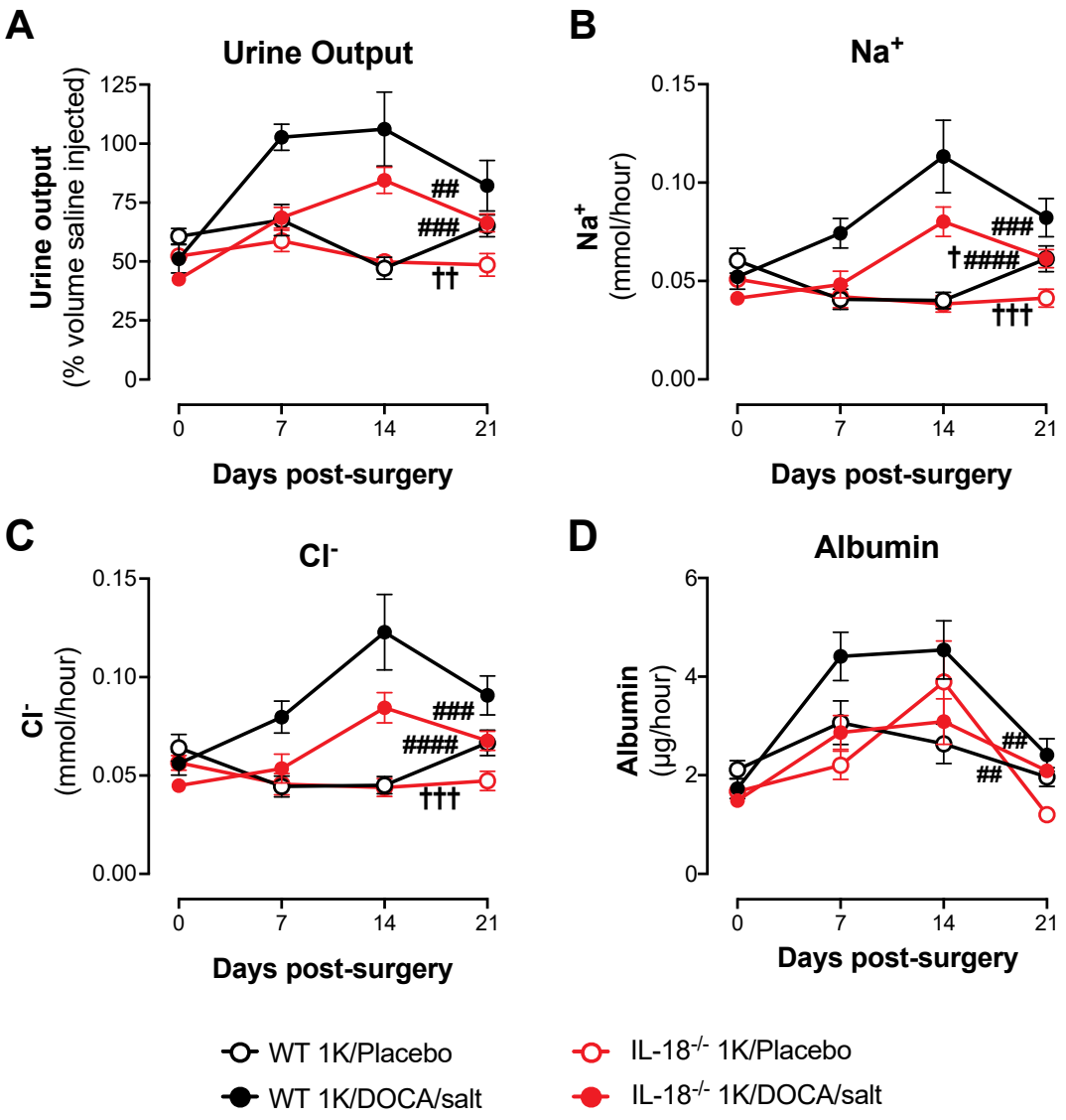

Supplementary Figure 3.7 IL-18-deficiency protects against 1K/DOCA/salt-mediated volume loading and renal injury. IL-18-deficiency protects against 1K/DOCA/salt-mediated volume loading and renal injury. Urine volume (A), Na+ (B), Cl- (C), and albumin (D) excreted by mice over 4 h following a bolus saline challenge. Values are mean ± SEM from n= 7-9 experiments. ###P ≤ 0.001, ##P ≤ 0.01, #P < 0.05 vs. WT 1K/DOCA/salt and ††P ≤ 0.01 and †P < 0.05 vs. IL-18$^{-/-}$ 1K/DOCA/salt for two-way ANOVA.

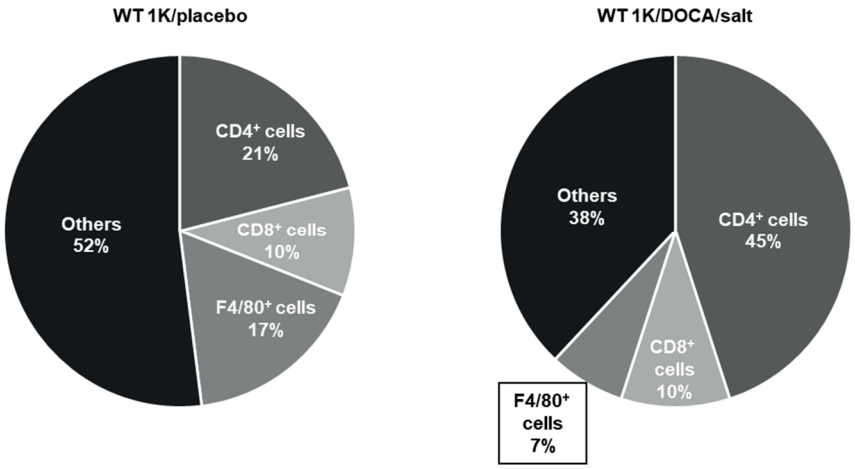

Supplementary Figure 3.8 Proportion of CD45$^+$ immune cell subsets expressing IL-18R1 in 1K/placebo- and 1K/DOCA/salt-treated wild-type mice. (n=8-9 per group).

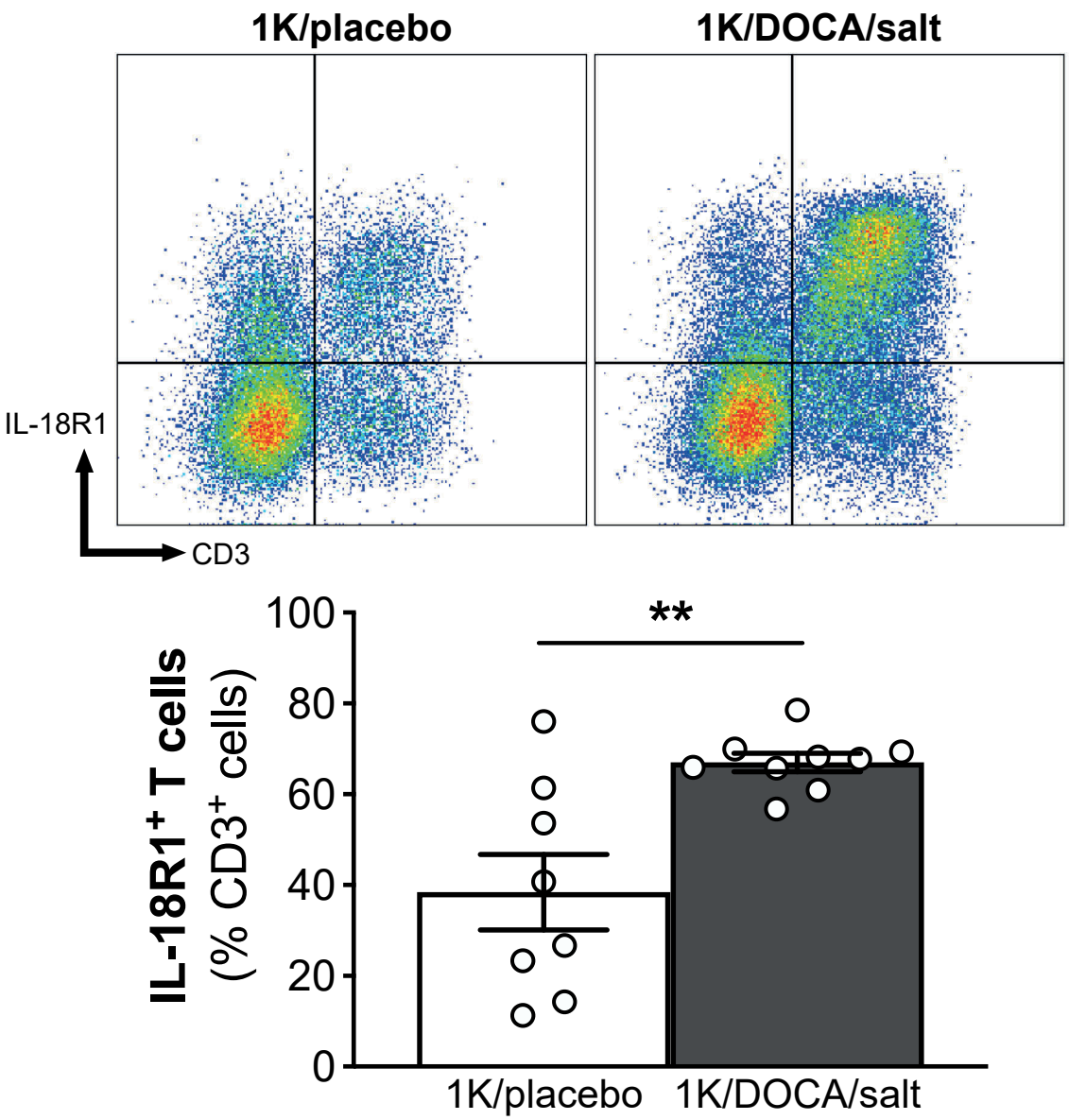

Supplementary Figure 3.9 Percentage of IL-18R1-expressing CD3+ T cells in 1K/placebo- and 1K/DOCA/salt-treated wild-type mice. ** P=0.003, unpaired t-test; n=8-9 per group.

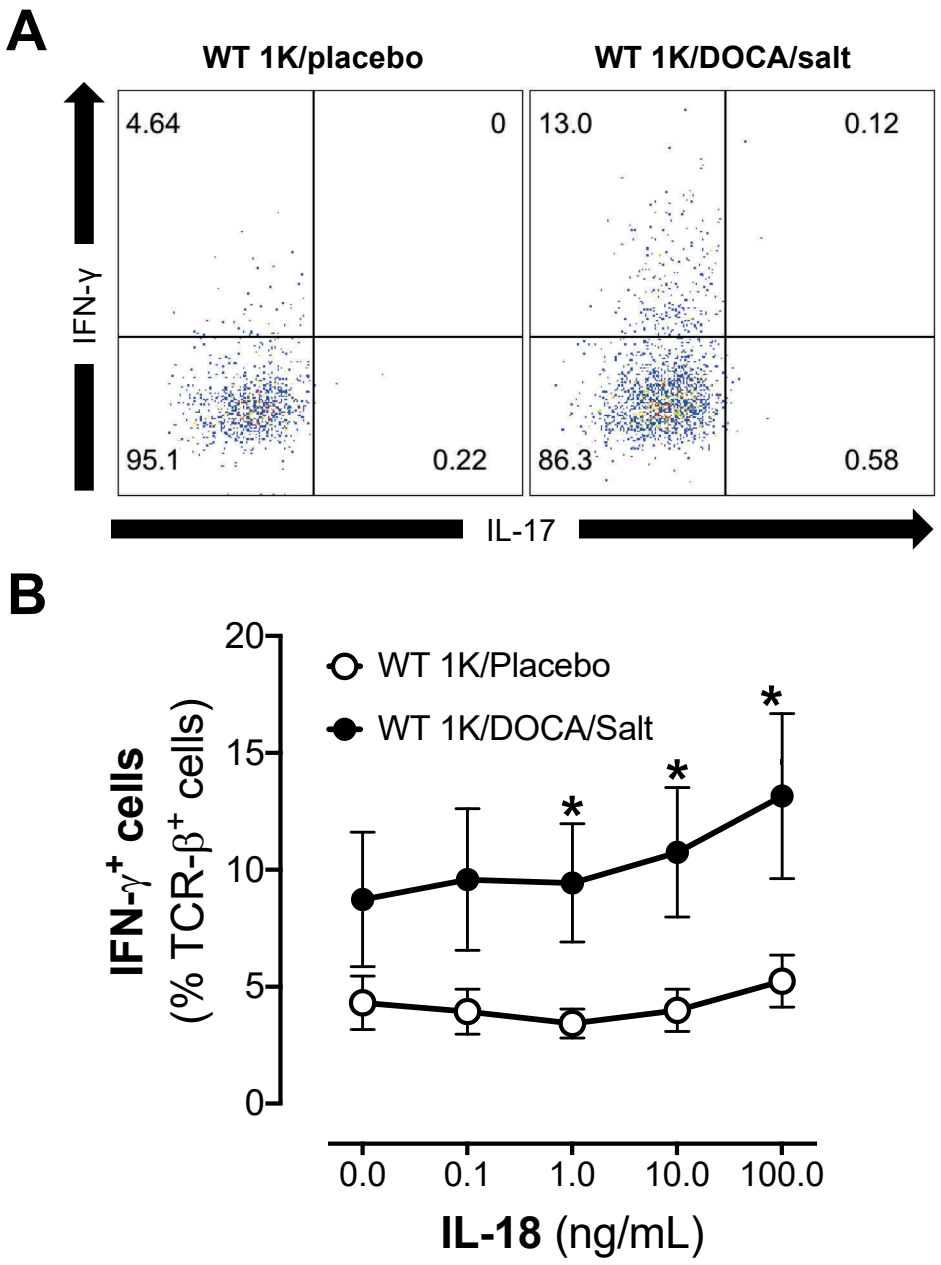

Supplementary Figure 3.10 IL-18-induced IFN-γ production in T cells isolated from 1K/placebo- and 1K/DOCA/salt-treated WT mouse kidneys. (A) Representative flow cytometric plots and (B) group data showing the effect of *ex vivo* stimulation with a combination of increasing concentrations of IL-18 (0-100 ng/mL) and co-stimulatory anti-CD3/CD28 antibodies on the percentage of renally-derived T cells expressing IFN-γ and IL-17. **$P \leq 0.01$ and *$P < 0.05$ for two-way ANOVA followed by Bonferroni post-test.

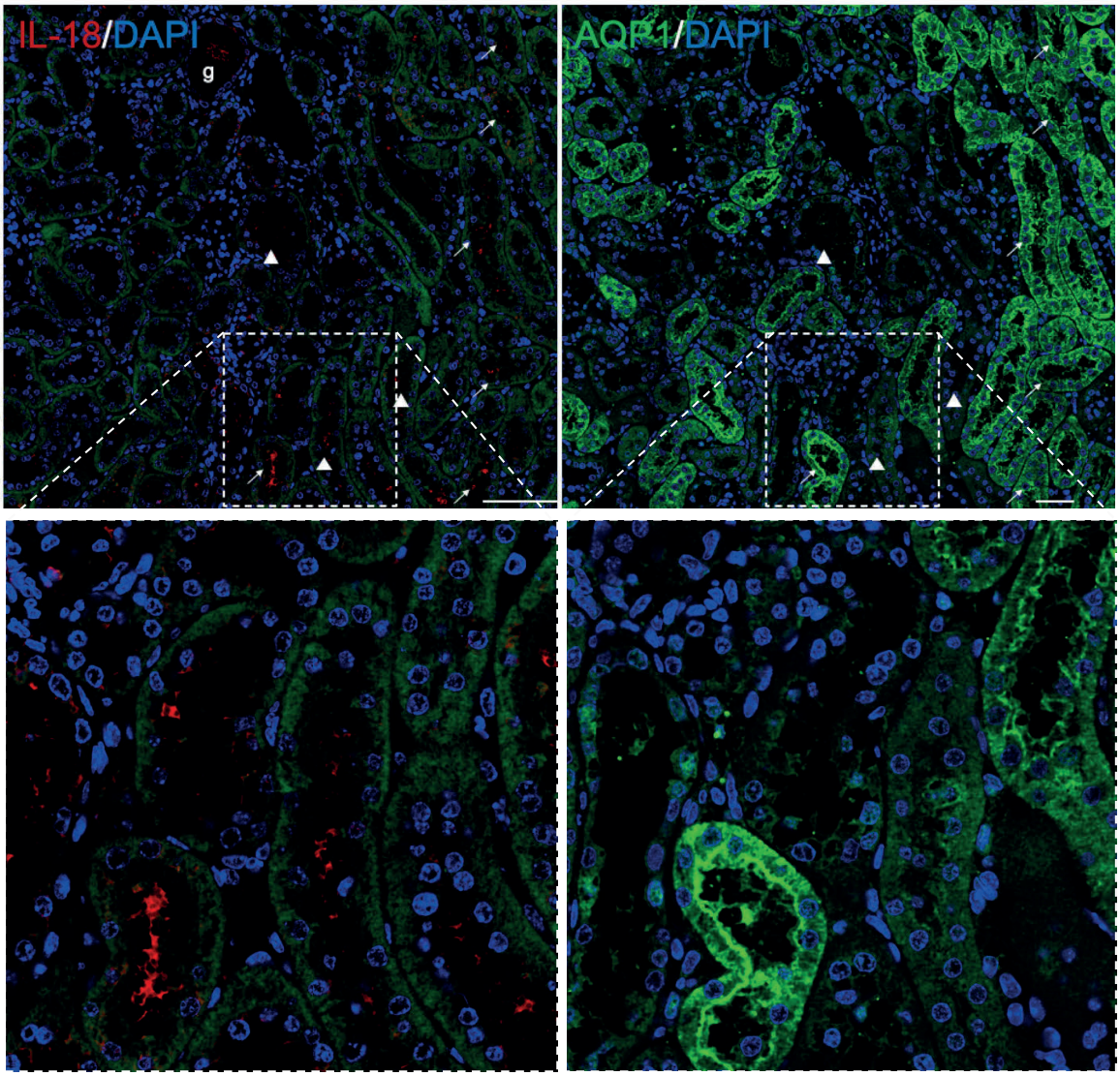

Supplementary Figure 3.11 Immunolocalisation of IL-18 and aquaporin 1 (AQP-1) in 1K/DOCA/salt-treated mouse kidney sections. Tiled (5 x 5 fields of view, 60x magnification; top) and zoomed images of inset box (bottom) of adjacent kidney sections stained with IL-18 (red; left) and AQP-1 (green; right). Arrows denote IL-18-positive tubules that also stained positively for AQP-1; arrowheads show IL-18-positive tubules that were negative for AQP-1. Scale bars = 50µm. Images are representative of n=6 animals

Chapter 4

Interleukin-18 Receptor 1 Positive T Cells are not Essential to Kidney Inflammation and Damage Induced by Deoxycorticosterone Acetate/Salt in Mice

4.1 Summary

Background: Interleukin (IL)-18 is crucial to the development of hypertension and renal inflammation. T cells are a target of IL-18 owing to their expression of a cognate IL-18 receptor complex. We investigated whether global or T cell-restricted deficiency of one of the subunits of this complex, IL-18R1, protects against the development of high BP and kidney inflammation in a model of low-renin hypertension.

Methods: This study used wild-type (WT) and IL-18R1$^{-/-}$ mice. T cell-restricted IL-18R1-deficient mice were created by transplanting T cells from IL-18R1$^{-/-}$ mice into lymphocyte-deficient RAG1$^{-/-}$ mice. Hypertension was induced by uninephrectomy, deoxycorticosterone acetate (2.4 mg/d, *s.c.*) and 0.9% saline for drinking (1K/DOCA/salt). Normotensive controls received uninephrectomy and a placebo pellet (1K/placebo). BP was measured by tail cuff; and, after 21 d, kidneys were harvested for (immuno)histochemical, quantitative-PCR and flow cytometric analysis of fibrosis, inflammation, and immune cell infiltration.

Results: Treatment of WT mice with 1K/DOCA/salt caused hypertension and accumulation of immune cells (CD45^{+}, CD11b^{+}, F4/80^{+} and CD3^{+} cells) in the kidney. IL-18R1$^{-/-}$ mice displayed a blunted hypertensive response to 1K/DOCA/salt (by 50%) but similar renal accumulation of immune cells. Surprisingly, 1K/DOCA/salt-treated IL-18R1$^{-/-}$ mice had a high mortality rate due to rupture of abdominal aortic aneurysms (AAAs;10/15 *cf.* 0/12 In WT mice). T cell-restricted IL-18R1$^{-/-}$ deficiency also afforded protection against 1K/DOCA/salt-induced hypertension without preventing renal immune cell accumulation or upregulation of inflammatory genes (*Il18rap, Ccl5, Icam1 and Vcam1)*. However, in contrast to global IL-18R1-deficiency, T cell-restricted IL-18R1$^{-/-}$ deficiency did not increase the incidence of AAA.

Conclusion: Thus, while inhibition of IL-18 affords protection against both hypertension and renal inflammation, here we demonstrate that global or T cell-restricted IL-18R1

inhibition only protects against the former. Further understanding of IL-18R1-dependent and -independent actions of IL-18 may lead to new therapies for hypertension and kidney disease

4.2 Introduction

Hypertension is a chronic inflammatory disease wherein the kidneys represent major sites of inflammation.[1, 2] Homeostatic control of the pressure-natriuresis relationship by the kidneys is key to the maintenance of blood pressure (BP), and this relationship is thought to be disrupted by inflammation and subsequent renal injury.[3] It is well established that T cells infiltrate the kidneys during hypertension and contribute to inflammation by producing cytokines and cell-death signals.[4, 5] Therefore, characterising the mechanisms that contribute to T cell infiltration and their subsequent activation within the kidneys may yield targets for novel anti-hypertensive therapies.

We previously demonstrated that the inflammasome-derived cytokine interleukin (IL)-18 is essential for the development of renal inflammation, fibrosis, and elevated BP in the 1K/DOCA/salt model of hypertension. The pro-inflammatory actions of IL-18 are typically the result of its binding to a cognate IL-18 receptor complex, which is comprised of two subunits — IL-18R1 and IL-18 receptor accessory protein (IL-18RAP).[6] In our previous study we further demonstrated that 1K/DOCA/salt-induced hypertension is associated with increased expression of IL-18R1 in the kidneys, which was partly due to its upregulation on tubular epithelial cells (TECs), as well as the accumulation of IL-18R1-expressing T cells in the kidneys. Hence, in the present study we investigated whether global or T cell-specific deletion of IL-18R1 affords a similar degree of protection as IL-18-deficiency against the development of 1K/DOCA/salt-induced hypertension and renal pathophysiology.

4.3 Methods

4.3.1 Animals

A total of 119 male wild type, IL-18R1$^{-/-}$ or RAG1$^{-/-}$ mice, backcrossed onto a C57BL6/J background were used. Mice were aged 7-17 weeks and weighed 18-36 g (Table 1). Mice were obtained from either the Walter and Eliza Hall Institute (WEHI; Melbourne, Australia), the Animal Resources Centre (ARC; Perth, Australia) or the La Trobe Animal Research and Teaching Facility (LARTF; La Trobe University Australia). Prior to surgery, mice were housed with littermates in groups of 3-4 animals in Sealsafe Plus GM500 boxes (Tecniplast, USA), under specific pathogen-free conditions, on a 12 h light-dark cycle, and provided with *ad libitum* access to normal chow and drinking water. Mice were randomly assigned into treatment groups (e.g., hypertensive versus normotensive) using random number generator software (Microsoft Excel, Version 16.36, USA). All procedures were conducted according to the Australian Code for the Care and Use of Animals for Scientific Purposes (8th edition) and were approved by the La Trobe University Animal Ethics Committee (Project number: AEC16-93).

4.3.2 Induction of hypertension

A salt-induced, low-renin model of hypertension was used in this study wherein mice were uninephrectomised (left kidney removed) and treated with deoxycorticosterone acetate (DOCA; 2.4 mg/day, *s.c.*; Innovative Research of America, USA) and 0.9% saline drinking water (1K/DOCA/salt).[7, 8] Normotensive controls for this experiment were mice that also received uninephrectomy, a placebo pellet containing the proprietary matrix material without DOCA (Innovative Research of America, USA) and normal drinking water (1K/placebo). All surgeries were performed under anaesthesia induced by inhalation of isoflurane (2 L/min, 5% in O_2). Anaesthesia was maintained by 2.5% isoflurane in O_2 (0.4 L/min) and regularly monitored by checking hind paw withdrawal, blink reflexes and respiratory rate. Prior to surgery, mice received local anaesthetic (bupivacaine; 2.5 mg/kg,

s.c.) and analgesic (carprofen; 5 mg/kg, *s.c.*). Carprofen treatment was continued for 3 days post-surgery.

4.3.3 Adoptive transfer of T cells

RAG1$^{-/-}$ mice were randomly assigned to receive either vehicle (phosphate buffered saline; PBS) or purified T cells from WT or IL-18R1$^{-/-}$ mice. T cells for adoptive transfer were isolated from the spleens of 10-12-week-old male WT and IL-18R1$^{-/-}$ mice. Spleens were minced with scissors before being passed through a 70 µm cell strainer, and then incubated in red blood cell (RBC) lysis buffer (NH_4Cl, $KHCO_3$, dH_2O) for 5 min at room temperature. Splenic T cells were enriched using a CD90.2 negative pan T cell Isolation kit (Miltenyi Biotech, USA). Splenic T cells were counted using an automatic cell counter (EVE, NanoEnTek Inc, South Korea) and re-suspended in sterile PBS at a concentration of 70 x 10^6cells/mL. A 100 µL volume of either vehicle or WT or IL-18R1$^{-/-}$ T cells was injected into the tail vein of RAG1$^{-/-}$ mice and allowed to engraft over a 3-week period. Hypertension was induced by 1K/DOCA/salt-treatment and after 21 days mice were killed via CO_2 asphyxiation and perfused through the left ventricle with PBS containing 0.2% Clexane (400 IU; Sanofi Aventis, France). Kidneys of recipient mice were harvested and analysed by flow cytometry (enabling confirmation of successful T cell engraftment), qPCR, histology, and immunohistochemistry.

4.3.4 Blood pressure measurements

BP was measured via tail cuff plethysmography. Tail cuff measurements were performed using a Multichannel BP Analysis System (MC4000; Hatteras Instruments, USA). All mice underwent daily training on the tail cuff device for at least 3 days prior to induction of hypertension. Blood pressures were then recorded on the morning prior to surgery (day 0) and weekly thereafter on days 7, 14 and 21. On each occasion, mice were subjected to 30-40 measurement cycles with readings from the last 25 cycles averaged to obtain a systolic BP value for each day.

4.3.5 Measurement of mRNA expression levels

At the end of the 21-day treatment period, the right kidney was excised and cut in half along its transverse plane. One half of the kidney was used immediately for flow cytometric analysis, while the other half was further divided into two transverse sections. One of these sections was fixed in 10% neutral buffered formalin and stored at 4°C for immunohistochemistry, and the other was snap frozen in liquid N_2 and stored at -80°C for later RNA extraction. Frozen kidneys were pulverised, and RNA was extracted using a RNeasy Mini Kit (Qiagen, Hilden, Germany). The yield and purity of the RNA was determined using a NanoDrop Spectrophotometer (NanoDrop One, Thermo Scientific, USA). RNA was reversed transcribed using a High Capacity cDNA Reverse Transcription kit (Applied Biosystems, Lithuania) and the resulting cDNA was then used as a template in real-time PCR to measure mRNA expression of pro-*Il18, Il18r1, Il18rap*, C-C motif chemokine ligand (*Ccl*) 2, *Ccl5*, intercellular adhesion molecule-1 (*Icam1*), vascular cell adhesion molecule-1 (*Vcam1*), *Il6*, *Col1a1*, *Col3a1*, *Col4a1*, and *Col5a1*, or the housekeeping gene, *Gapdh* (TaqMan Gene Expression Assays, Applied Biosystems, USA). Real-time PCR was performed in a Bio-Rad CFX96 Real-Time PCR Detection System (Bio-Rad Laboratories, Hercules, CA, USA) and the comparative Ct method was used to calculate the fold-change in mRNA expression relative to a reference control sample.[9]

4.3.6 Flow cytometric analysis

For conventional flow cytometric analysis, cell suspensions were prepared from kidney halves and whole spleens. Kidney halves were minced with scissors and digested in PBS containing collagenase type XI (125 U/ml), collagenase type I-S (460 U/ml) and hyaluronidase (60 U/ml) (Sigma-Aldrich, USA) for 60 min at 37°C. Following digestion, kidney suspensions were passed through a 70 µm filter (BD Biosciences, USA) and the cells were pelleted by centrifugation at 453 x*g* for 5 min. The cell pellets were further subjected to Percoll™ density-gradient centrifugation, whereby the pellet was re-suspended

in 3 mL of 40% isotonic Percoll™ solution (GE Healthcare Life Science, UK), and carefully under-laid with 3 mL of 70% Percoll™ solution. Samples were centrifuged at 1450 x*g* at 25°C for 25 min with the brakes of the centrifuge turned off. Following centrifugation, adipocytes and debris were aspirated from the top layer, and mononuclear cells were collected from the interface. Mononuclear cells were washed in PBS, centrifuged, and the pellet was re-suspended in PBS. Spleen samples were minced with scissors and passed through a 70 µm filter and then incubated in red blood cell lysis buffer for 5 min at room temperature. Spleen cells were counted using an automatic cell counter (EVE, NanoEnTek Inc, South Korea) and re-suspended in PBS at a concentration of 10^7 cells/mL. Kidney and spleen cell suspensions were stained for 15 min at room temperature with Live/Dead aqua stain (Life Technologies, USA), followed by an antibody cocktail consisting of anti-mouse CD45 (A700; BioLegend, USA), CD3 (APC; BioLegend, USA), CD8 (PeCy7; BioLegend, USA), CD4 (BV605; BioLegend, USA), CD11b (BV421; BioLegend, USA), F4/80 (APC Cy7; BioLegend, USA), CD69 (BV650; BioLegend, USA), CD44 (PERCP; BioLegend, USA), and IL-18R1 (PE; Invitrogen, USA; Table 2) dissolved in PBS containing 0.5% bovine serum albumin.

For intracellular cytokine/transcription staining, cells were washed in PBS, centrifuged, fixed and permeabilised (eBioscience™ Foxp3/Transcription Factor Fixation/Permeabilization Concentrate and Diluent; Invitrogen, USA). Cells were then washed in perm wash™ and re-suspended in 1% formalin in PBS containing 0.5% bovine serum albumin and EDTA for analysis on a CytoFlex LS flow cytometer (Beckman Coulter, USA) using CytExpert software (Beckman Coulter). Data were analysed using FlowJo software v10 (FlowJo, USA). For the full gating strategy, see Supplementary Figure 4.1.

4.3.7 Histopathology staining

For measurement of interstitial collagen deposition in RAG1$^{-/-}$ mice, snap frozen transverse kidney sections were embedded in optimal cutting temperature (O.C.T) compound (Tissue-Tek, U. S. A), and cut into 4 µm sections on a cryostat. Sections were defrosted for 20 min at room temperature, and then fixed in acetone that had been chilled to -20°C for 10 min. Slides were washed for 5 min in 1x PBS and rehydrated in 100% ethanol before being stained with a 0.5% Picrosirius Red solution (Polysciences Inc., USA). Sections were imaged (20x magnification) using a polarised microscope (Olympus, Japan) and analysed for percentage collagen content by ImageJ. Quantified Picrosirius Red data represent the average values obtained independently by two investigators who were blinded to the in vivo treatment of each sample.

4.3.8 Immunohistochemistry

Following sodium citrate antigen retrieval (AJAX Finechem; Australia; pH 6), kidney sections were blocked in 1% goat serum, and then incubated overnight at 4°C with rat anti-CD3 (5 µg/mL; Abcam, USA) or rabbit anti-IL-18R1 (5 µg/mL; Abcam, USA) diluted in 1% goat serum. Alexa Fluor 488- or Alexa Fluor 555-conjugated goat secondary antibodies (Invitrogen, USA) were used, and cell nuclei were counterstained with DAPI. Fluorescent images were captured using either a Zeiss 780 confocal microscope (Carl Zeiss, Oberkochen, Germany) or an Olympus BX53 microscope with a light source attached (X-cite series 120Q, Excelitas Technologies, USA).

4.3.9 Statistics

Unless otherwise stated, results are expressed as mean ± standard error of mean (SEM). Data were analysed using either one-way analysis of variance (ANOVA), two-way ANOVA, two-way repeated measures ANOVA or Log-rank (Mantel-Cox) test for Kaplan-Meier survival curves, as appropriate. Post hoc analyses (performed when F tests from

ANOVA were < 0.05) were performed using Bonferroni's test. $P < 0.05$ was considered to be statistically significant.

4.4 Results

4.4.1 IL-18R1$^{-/-}$ mice are protected from 1K/DOCA/salt-induced hypertension but have a higher incidence of abdominal aortic aneurysms.

1K/DOCA/salt treatment induced a marked 40 mmHg elevation in systolic BP in WT mice. Blood pressure elevations were apparent by day 7 and persisted throughout the 21-day treatment protocol (Figure 4.1A). By contrast, BP in 1K/placebo mice remained unchanged across the 21 days (Figure 4.1A). The hypertensive response to 1K/DOCA/salt was blunted by 40-50% in IL-18R1$^{-/-}$ mice, such that systolic BP at day 21 was only ~20 mmHg higher than pre-hypertensive levels (Figure 4.1A). By contrast, IL-18R1 deficiency had no effect on baseline BP in 1K/placebo-treated mice (Figure 4.1A).

Despite being protected against hypertension, 1K/DOCA/salt-treated IL-18R1$^{-/-}$ mice had a profoundly higher incidence of mortality due to AAA. 1K/DOCA/salt-induced hypertension in mice is associated with an increased mortality rate as a result of the formation and rupture of abdominal aortic aneurysms (AAA), and we have previously reported mortality rates of up to 15% in WT mice.[7] In the present study, all of the 1K/DOCA/salt-treated WT mice survived until endpoint with post-mortem analysis confirming AAA in ~35% of the animals used across this entire study. By contrast, there was a 66% (10/15) mortality rate in 1K/DOCA/salt-treated IL-18R1$^{-/-}$ mice (Figure 4.1B) with post-mortem analysis confirming ruptured AAA in all instances. Even in the five 1K/DOCA/salt-treated IL-18R1$^{-/-}$ mice that survived, three were confirmed post-mortem to have AAA. Thus, the incidence of AAA across the entire treatment group was a staggering 87% (13/15; Figure 4. 1C). No deaths or AAA were observed in 1K/placebo-treated WT or IL-18R1$^{-/-}$ mice (Figure 4.1B)

4.4.2 IL-18R1-deficiency does not prevent immune cell accumulation and activation in the kidneys of 1K/DOCA/salt-treated mice

Flow cytometry revealed that 1K/DOCA/salt caused a 4-fold increase in the number of IL-18R1-expressing leukocytes ($CD45^+$IL-$18R1^+$) in the kidneys of WT mice (Figure 4.2A-B). The majority (65%) of these IL-18R1-positive immune cells were T cells ($CD3^+$IL-$18R1^+$; Figure 4.2C), including both $CD4^+$ and $CD8^+$ subsets (Figures 4.2D-E). Macrophages accounted for ~25% of the IL-18R1-positive leukocytes present in the kidneys of WT mice (Figure 4.2F). As expected, kidneys of 1K/DOCA/salt-treated IL-$18R1^{-/-}$ mice, were devoid of IL-18R1-positive leukocytes, T cells and macrophages (Figure 4.2A-F). Yet, despite the lack of IL-18R1 expression on immune cells, 1K/DOCA/salt-treated IL-$18R1^{-/-}$ mice displayed similar overall numbers of total leukocytes ($CD45^+$; Figure 4.3A-B), total ($CD3^+$) T cells (including $CD4^+$ and $CD8^+$ T cells; Figures 4.3C-E) and macrophages ($CD11b^+F480^+$; Figure 4.3F). Importantly, the lack of IL-18R1-expression also had no effect on the overall level of activation of the different T cells subsets as measured by the proportion of cells that expressed FOXP3, CD44, or CD69 within each subpopulation (Figure 4.3G-K).

Co-immunofluorescence staining confirmed $CD3^+$ T cells as major cellular sites of renal IL-18R1 expression in 1K/DOCA/salt-treated WT mice and identified tubular epithelial cells as additional sites of IL-18R1 expression (Figure 4.4A). No IL-18R1-positive cells were detected in 1K/DOCA/salt-treated IL-$18R1^{-/-}$ mice (Figure 4.4A).

4.4.3 T cell-specific IL-18R1 deficiency provides protection against 1K/DOCA/salt-induced hypertension

Previous studies have shown that $RAG1^{-/-}$ mice — which lack T and B cells — are protected from 1K/DOCA/salt-induced hypertension, and that adoptive transfer of WT T cells into these animals recapitulates the hypertensive response.[10] In order to directly assess the role of IL-18R1 signalling in T cells on the development of hypertension and kidney injury, we

isolated T cells from spleens of WT or IL-18R1$^{-/-}$ mice and adoptively transferred them into RAG1$^{-/-}$ recipient mice. RAG1$^{-/-}$ mice that received the vehicle (PBS) served as T cell-deficient controls. All mice were treated with 1K/DOCA/salt.

Baseline BP was lower in T cell-deficient RAG1$^{-/-}$ mice than in WT mice (Figure 4.5A). Therefore, to assess the effect of T cell deficiency/repletion on hypertensive responses to 1K/DOCA/salt, changes in BP from baseline were examined. In WT mice, 1K/DOCA/salt increased systolic BP by ~35 mmHg with the hypertensive response reaching its peak at 14 days (Figure 4.5B). In contrast to previous reports, RAG1$^{-/-}$ mice were not protected from 1K/DOCA/salt-induced hypertension, and adoptive transfer of WT T cells did not appear to affect this response (Figure 4.5B). Interestingly, RAG1$^{-/-}$ mice that received adoptive transfer of IL-18R1$^{-/-}$ T cells had a blunted hypertensive response to 1K/DOCA/salt compared to WT mice (Figure 4.5B). Thus, in these animals, systolic BP rose by no more than 15 mmHg across the 21-day treatment period (Figure 4.5B)

We saw a higher incidence of deaths (~30%) due to AAA in this cohort of 1K/DOCA/salt-treated WT mice (Figure 4.5C) as compared with the earlier cohort (see Figure 4.1A). Similar mortality rates of 25-30% were observed in both T cell-deficient RAG1$^{-/-}$ mice, and in RAG1$^{-/-}$ mice that received WT T cells (Figure 4.5C). Importantly, and in stark contrast to global IL-18R1-deficiency, RAG1$^{-/-}$ mice that received IL-18R1$^{-/-}$ T cells did not display an increase in mortality rate (~10%) compared to the other groups of mice (Figure 4.5C). In other words, by restricting IL-18R1-deficiency to T cells, high rates of mortality were avoided.

To confirm T cell engraftment, we performed flow cytometry on spleens and kidneys of 1K/DOCA/salt-treated RAG1$^{-/-}$ recipient mice. 1K/DOCA/salt-treated RAG1$^{-/-}$ mice that received PBS were completely devoid of splenic CD3^{+} T cells (Figure 4.5D-F). Adoptive transfer of WT T cells into RAG1$^{-/-}$ mice restored both total CD3^{+} and IL-18R1^{+} T cell numbers back to levels similar to those in WT mice (Figure 4.4D-F). Adoptive transfer of

IL-18R1$^{-/-}$ T cells partially reconstituted the splenic CD3^{+} T cell population in RAG1$^{-/-}$ mice, with all T cells present lacking IL-18R1 expression (as expected; Figure 4.5D-F).

Similar to observations in the spleen, kidneys from 1K/DOCA/salt-treated RAG1$^{-/-}$ mice were completely lacking in CD3^{+} T cells (Figure 4.6A-C). Interestingly, 1K/DOCA/salt-treated RAG1$^{-/-}$ mice that received WT T cells had markedly higher numbers (by 5-fold) of total CD3^{+} T cells in their kidneys than WT control mice and moreover, the majority of these cells (> 70%) were IL-18R1^{+} (Figure 4.6A-C). 1K/DOCA/salt-treated RAG1$^{-/-}$ mice that received IL-18R1$^{-/-}$ T cells had a similarly high number of total CD3^{+} T cells in their kidneys but (as expected) these cells were lacking in expression of IL-18R1 (Figure 4.6A-C). Further analysis of T cell subsets showed that the total numbers of CD4^{+} and CD8^{+} T cells in the kidneys were similar in 1K/DOCA/salt-treated RAG1$^{-/-}$ mice whether they received adoptive transfer of WT or IL-18R1$^{-/-}$ T cells (Figure 4.6D-F). Moreover, the numbers of regulatory T cells (CD4^{+}FOXP3^{+}; Figure 4.6G) or activated CD4^{+} and CD8^{+} T cells in the kidneys, as evidenced by expression of CD44 or CD69, were similar regardless of whether the RAG1$^{-/-}$ mice received WT or IL-18R1$^{-/-}$ T cells (Figure 4.6H- K).

There were no obvious differences in total leukocyte or macrophage numbers between 1K/DOCA/salt-treated WT mice and RAG1$^{-/-}$ mice that received WT or IL-18R1$^{-/-}$ T cells (Figure 4.6L-M).

4.4.4 T cell-specific IL-18R1 deficiency does not confer protection against 1K/DOCA/salt-induced renal inflammation

Consistent with the flow cytometry data, qPCR analysis of whole kidneys revealed that 1K/DOCA/salt-treated RAG1$^{-/-}$ mice had lower levels of *Il18r1* expression than 1K/DOCA/salt-treated WT mice (Figure 4.7A). Also consistent with the flow data, 1K/DOCA/salt-treated RAG1$^{-/-}$ mice that received adoptive transfer of WT T cells displayed a rebound response, with markedly elevated expression of *Il18r1* in their kidneys compared to 1K/DOCA/salt-treated WT mice (Figure 4.7A). Expression of *Il18r1* in

1K/DOCA/salt-treated RAG1$^{-/-}$ mice that received IL-18R1$^{-/-}$ T cells was markedly lower than that in either WT mice, or in RAG1$^{-/-}$ mice that received WT T cells (Figure 4.7A).

We also looked at the impact of T cell deficiency and repletion on renal expression of *Il18rap*; the purported partner of IL-18R1 in the IL-18 receptor complex (Figure 4.7B). *Il18rap* expression tended to be lower in 1K/DOCA/salt-treated RAG1$^{-/-}$ than in WT mice (Figure 4.7B). Similar to its effects on *Il18r1* expression, adoptive transfer of WT T cells into RAG1 mice was associated with unusually high levels of *Il18rap* expression in the kidneys; approximately twice that observed in WT mice (Figure 4.7B). However, in contrast to the situation for *Il18r1*, adoptive transfer of IL-18R1$^{-/-}$ T cells was also associated with exaggerated renal expression of *Il18rap* (Figure 4.7B).

Regarding *Il18* and *Il6* expression in the kidneys, levels were similar between WT and RAG1$^{-/-}$ mice, regardless of whether the latter received T cells or not (Figure 4.7C-D), whereas for several other inflammatory markers, adoptive transfer of either WT or IL-18R$^{-/-}$ T cells was associated with an increase in expression in the kidneys. Thus RAG1$^{-/-}$ mice that received adoptive transfer of WT or IL-18R1$^{-/-}$ T cells generally had higher levels of expression of *Ccl2*, *Ccl5*, *Icam1* and *Vcam1* compared to WT mice, or RAG1$^{-/-}$ mice that received no T cells (Figure 4.7E-H).

4.4.5 RAG1$^{-/-}$ mice that receive WT, or IL-18R1$^{-/-}$ T cells are not protected from 1K/DOCA/salt-induced kidney fibrosis

Semi-quantitative analysis of picrosirius red stained kidney sections under polarised light revealed a trend for 50% decreased expression of renal interstitial collagen in RAG1$^{-/-}$ mice compared to WT, although the difference was not significant (Figure 4.8A-B). Similar magnitudes of reduced expression in RAG1$^{-/-}$ compared to WT mice were observed at the mRNA level for *Col1a1*, *Col3a1* and *Col5a1*, but not for *Col4a1* (Figures 4.8C-D). For most of these protein/mRNA measures, adoptive transfer of either WT or IL-18R1$^{-/-}$ T cells into the RAG1$^{-/-}$ mice had no obvious effect in restoring expression back to WT levels,

except for *Col1a1*. For this gene, adoptive transfer of WT T cells did restore expression back to WT levels, whereas adoptive transfer of IL-18R1 T cells had no effect (Figure 4.8C).

4.5 Discussion

The key novel findings of this study are: (1) mice with global IL-18R1 deficiency are protected against 1K/DOCA/salt-induced hypertension but are still prone to a similar amount of renal leukocyte infiltration as 1K/DOCA/salt-treated WT mice; (2) despite being protective against hypertension, global IL-18R1 deficiency made mice more prone to death due to the development and rupture of AAA; (3) T cell restricted IL-18-deficiency also afforded modest protection against 1K/DOCA/salt-induced hypertension without preventing leukocyte infiltration or inflammation of the kidneys; and (4) this was not associated with an increased incidence of AAA. Hence, while this study highlights IL-18R1 as a contributor to the hypertensive response to 1K/DOCA/salt induced hypertension, it seems unlikely that this is due to pro-inflammatory actions within the kidneys.

Using the 1K/DOCA/salt model of hypertension, we previously demonstrated that IL-18 is essential for the development of hypertension, kidney damage and dysfunction. We also demonstrated that 1K/DOCA/salt treatment was accompanied by increased expression of IL-18 signalling components IL-18R1 and IL-18RAP, increased expression of IL-18R1 on T cells, and that there was a concentration-dependent increase in the proportion of T cells from hypertensive mice that produced IFN-γ in response to IL-18 treatment. Collectively, these studies provided a rationale to investigate the contribution of IL-18R1 — especially T cell-derived IL-18R1 — to hypertension and renal inflammation.

An interesting observation from the present study was that although IL-18R1$^{-/-}$ mice were afforded protection from 1K/DOCA/salt-induced increases in BP, they had an equivalent level of immune cell infiltration of their kidneys as WT mice. This means that IL-18R1 likely has little role in immune cell migration into the kidneys. Indeed, leukocytes in the kidneys of 1K/DOCA/salt-treated IL-18R1$^{-/-}$ mice displayed a similar amount of expression of the cell-cell adhesion molecule, CD44, as WT mice. It is, however, possible that IL-18R1-deficiency altered the function of immune cells within the kidney. While this was not

reflected by expression of CD69 — a marker of lymphocyte activation — we cannot rule out the possibility that IL-18R1-deficient leukocytes were alternatively activated. In fact, this idea is supported by the fact that RAG1$^{-/-}$ mice that received IL-18R1$^{-/-}$ T cells were protected from 1K/DOCA/salt-induced hypertension, whereas those that received WT T cells, or PBS (i.e., no T cells) were not. One potential explanation for this finding is that IL-18R1$^{-/-}$ T cells actively promoted protection. If this were the case, it would appear that protection against hypertension was not mediated by suppressing renal inflammation or fibrosis (as T cell-restricted IL-18R1$^{-/-}$ mice had similar levels of inflammatory markers and collagen expression as RAG1$^{-/-}$ mice that received WT T cells). Thus, in future studies it would be interesting to fully characterise the phenotype of IL-18R1-deficient T cells in the kidneys and other organs of 1K/DOCA/salt treated mice to identify novel mechanisms that might mediate protection against hypertension.

A striking finding from the present study was the excessively high incidence of AAA when mice that were globally deficient in IL-18R1 were treated with 1K/DOCA/salt. This high rate of AAA was not observed in similarly treated T cell-restricted IL-18R1$^{-/-}$ mice, suggesting that the loss of IL-18R1 in cells types other than T cells was responsible. Previous studies have shown that AAA formation is a vascular inflammatory process,[11, 12] and thus it is possible that the loss of IL-18R1 was associated with an exaggerated inflammatory response in the vessel wall. Although IL-18R1 is a receptor subunit for pro-inflammatory IL-18 signalling, it can also serve as a subunit for anti-inflammatory signalling mediated by IL-37. IL-18 was initially recognised for its role in IFN-γ production, as IL-18 works in concert with IL-12 to cause the production of IFN-γ by natural killer and T cells.[6] This activity is dependent on IL-18R1, which is initially upregulated following IL-12 signalling, and then activated following interaction with IL-18 itself.[13] Activation of IL-18R1 by IL-18 causes the recruitment of IL-18RAP, and the assembly of this IL-18/IL-18R1/IL-18RAP complex results in contact between the

toll/interleukin receptor (TIR) domain of IL-18R1 and the cytosolic adapter TRAM.[14] This causes the formation of the "Myddosome" complex, where myeloid differentiation primary response 88 (MyD88) forms a complex with IRAK and TRAF6, ultimately resulting in activation of the transcription factor NFκB.[15] NFκB then translocates to the nucleus in order to cause the transcription of pro-inflammatory cytokines, chemokines and adhesion molecules — including IFN-γ. Conversely, IL-18R1 is also the primary binding site of the anti-inflammatory cytokine, IL-37. Engagement of IL-18R1 by IL-37 results in the formation of a receptor complex distinct from the IL-18 signalling complex. Thus, rather than recruiting IL-18RAP, the IL-37/IL-18R1 complex recruits IL-1R8 (also known as SIGRR).[16] IL-1R8 can in turn recruit MyD88, but due to its non-functional TIR domain, cannot promote inflammatory signalling.[17, 18] Although a homologue of IL-37 has not been identified in mice, preclinical studies using IL-37 transgenic mice have demonstrated that IL-18R1 is crucial to IL-37 anti-inflammatory signalling in endotoxemia.[16] Furthermore, the anti-inflammatory proteins suppressors of cytokine signalling (SOCS)-1 and -3 were downregulated in IL-18R1$^{-/-}$ mice in a model of cisplatin-induced acute kidney injury, and the authors suggested that this may account for the lack of protection against kidney inflammation in these mice.[19] To our knowledge, no studies have examined the role of IL-37 as a protective factor against AAA. However, considering the current findings, and with the availability of an IL-37-overexpressing transgenic mouse,[20] there is now a strong rationale for exploring the possibility that IL-37 signalling through IL-18R1 affords protection against AAA.

A seminal study by Guzik *et al.* demonstrated that RAG1$^{-/-}$ mice were protected from the development of angiotensin (Ang) II- and 1K/DOCA/salt-induced hypertension and vascular dysfunction, and this response to Ang II was restored in RAG1$^{-/-}$ mice that received adoptive transfer of T lymphocytes.[10] In Chapter 3, we demonstrated that T cells are the main immune cells that express IL-18R1 and that there is an increase in the proportion of

T cells from hypertensive mice that produce IFN-γ in response to treatment with IL-18. We hypothesised that adoptive transfer of WT T cells into RAG1$^{-/-}$ mice would restore the hypertensive response to 1K/DOCA/salt treatment, whereas adoptive transfer of IL-18R1$^{-/-}$ T cells would prevent the development of 1K/DOCA/salt-induced high BP and kidney inflammation and injury. Thus, it was somewhat surprising in the present study that although RAG1$^{-/-}$ mice were marginally protected from 1K/DOCA/salt-induced renal fibrosis, they were not protected from hypertension. Indeed, similar reports, whereby RAG1$^{-/-}$ mice appear to have 'lost' their apparent resistance to hypertension, have begun to emerge recently.[21] Changes in the phenotype of RAG1$^{-/-}$ mice due to genetic drift, development of compensatory immune mechanisms or environmental changes have all been suggested to contribute to this susceptibility to hypertension.[21, 22] In the current study, we observed that there was a compensatory expansion of innate immune cell populations, including myeloid (CD11b^{+}) and macrophage (F4/80^{+}) populations, in RAG1$^{-/-}$ mice. This accumulation of innate immune cells in the kidney may account for the apparent loss of protection against 1K/DOCA/salt-induced hypertension and kidney fibrosis, as increased renal macrophage infiltration has previously been shown to accompany the development of kidney inflammation, fibrosis and dysfunction that leads to hypertension.[23]

In conclusion, while IL-18R1-deficiency afforded protection against the development of hypertension, factors such as the increased incidence of AAA and potential confounding effects of the loss on an anti-inflammatory signalling pathway mediated by the IL-18R1/IL-8R1 complex, make it difficult to draw any firm conclusions about the role the IL-18 receptor complex plays in the pro-hypertensive and renal damaging actions of IL-18. Hence, an alternative approach might involve targeting the alternative subunit of the IL-18 receptor complex, namely IL-18RAP, which appears to only participate in IL-18 signalling.

4.6 References

1. Norlander AE, Madhur MS and Harrison DG. The immunology of hypertension. *J Exp Med*. 2018;215:21-33.

2. Drummond GR, Vinh A, Guzik TJ and Sobey CG. Immune mechanisms of hypertension. *Nat Rev Immunol*. 2019;19:517-532.

3. Ivy JR and Bailey MA. Pressure natriuresis and the renal control of arterial blood pressure. *J Physiol*. 2014;592:3955-67.

4. Saleh MA, McMaster WG, Wu J, et al. Lymphocyte adaptor protein LNK deficiency exacerbates hypertension and end-organ inflammation. *J Clin Invest*. 2015;125:1189-202.

5. Mathis KW, Wallace K, Flynn ER, Maric-Bilkan C, LaMarca B and Ryan MJ. Preventing Autoimmunity Protects Against the Development of Hypertension and Renal Injury. *Hypertension*. 2014;64:792-800.

6. Okamura H, Tsutsi H, Komatsu T, et al. Cloning of a new cytokine that induces IFN-gamma production by T cells. *Nature*. 1995;378:88-91.

7. Krishnan SM, Ling YH, Huuskes BM, et al. Pharmacological inhibition of the NLRP3 inflammasome reduces blood pressure, renal damage, and dysfunction in salt-sensitive hypertension. *Cardiovasc Res*. 2019;115:776-787.

8. Lerman LO, Kurtz TW, Touyz RM, et al. Animal Models of Hypertension: A Scientific Statement From the American Heart Association. *Hypertension*. 2019;73:e87-e120.

9. Schmittgen TD and Livak KJ. Analyzing real-time PCR data by the comparative CT method. *Nat Protoc*. 2008;3:1101-1108.

10. Guzik TJ, Hoch NE, Brown KA, McCann LA, Rahman A, Dikalov S, Goronzy J, Weyand C and Harrison DG. Role of the T cell in the genesis of angiotensin II induced hypertension and vascular dysfunction. *J Exp Med*. 2007;204:2449-2460.

11. Sonesson B, Sandgren T and Länne T. Abdominal aortic aneurysm wall mechanics and their relation to risk of rupture. *Eur J Vasc Endovasc Surg*. 1999;18:487-93.

12. Bobryshev YV and Lord RS. Vascular-associated lymphoid tissue (VALT) involvement in aortic aneurysm. *Atherosclerosis*. 2001;154:15-21.

13. Yoshimoto T, Takeda K, Tanaka T, Ohkusu K, Kashiwamura S, Okamura H, Akira S and Nakanishi K. IL-12 up-regulates IL-18 receptor expression on T cells, Th1 cells, and B cells: synergism with IL-18 for IFN-gamma production. *J Immunol*. 1998;161:3400-7.

14. Rex DAB, Agarwal N, Prasad TSK, Kandasamy RK, Subbannayya Y and Pinto SM. A comprehensive pathway map of IL-18-mediated signalling. *J Cell Commun Signal*. 2020;14:257-266.

15. Walsh MC, Kim GK, Maurizio PL, Molnar EE and Choi Y. TRAF6 autoubiquitination-independent activation of the NFkappaB and MAPK pathways in response to IL-1 and RANKL. *PLoS One*. 2008;3:e4064-e4064.

16. Nold-Petry CA, Lo CY, Rudloff I, et al. IL-37 requires the receptors IL-18Rα and IL-1R8 (SIGIRR) to carry out its multifaceted anti-inflammatory program upon innate signal transduction. *Nat Immunol*. 2015;16:354-65.

17. Gong J, Wei T, Stark RW, Jamitzky F, Heckl WM, Anders HJ, Lech M and Rössle SC. Inhibition of Toll-like receptors TLR4 and 7 signaling pathways by SIGIRR: A computational approach. *J Struct Biol*. 2010;169:323-330.

18. Dinarello CA. Overview of the IL-1 family in innate inflammation and acquired immunity. *Immunol Rev*. 2018;281:8-27.

19. Nozaki Y, Kinoshita K, Yano T, et al. Signaling through the interleukin-18 receptor α attenuates inflammation in cisplatin-induced acute kidney injury. *Kidney Int*. 2012;82:892-902.

20. Nold MF, Nold-Petry CA, Zepp JA, Palmer BE, Bufler P and Dinarello CA. IL-37 is a fundamental inhibitor of innate immunity. *Nat Immunol*. 2010;11:1014-1022.

21. Ji H, Pai AV, West CA, Wu X, Speth RC and Sandberg K. Loss of Resistance to Angiotensin II-Induced Hypertension in the Jackson Laboratory Recombination-Activating Gene Null Mouse on the C57BL/6J Background. *Hypertension*. 2017;69:1121-1127.

22. Madhur MS, Kirabo A, Guzik TJ and Harrison DG. From Rags to Riches. *Hypertension*. 2020;75:930-934.

23. Blasi ER, Rocha R, Rudolph AE, Blomme EAG, Polly ML and McMahon EG. Aldosterone/salt induces renal inflammation and fibrosis in hypertensive rats. *Kidney Int*. 2003;63:1791-1800.

4.7 Figures

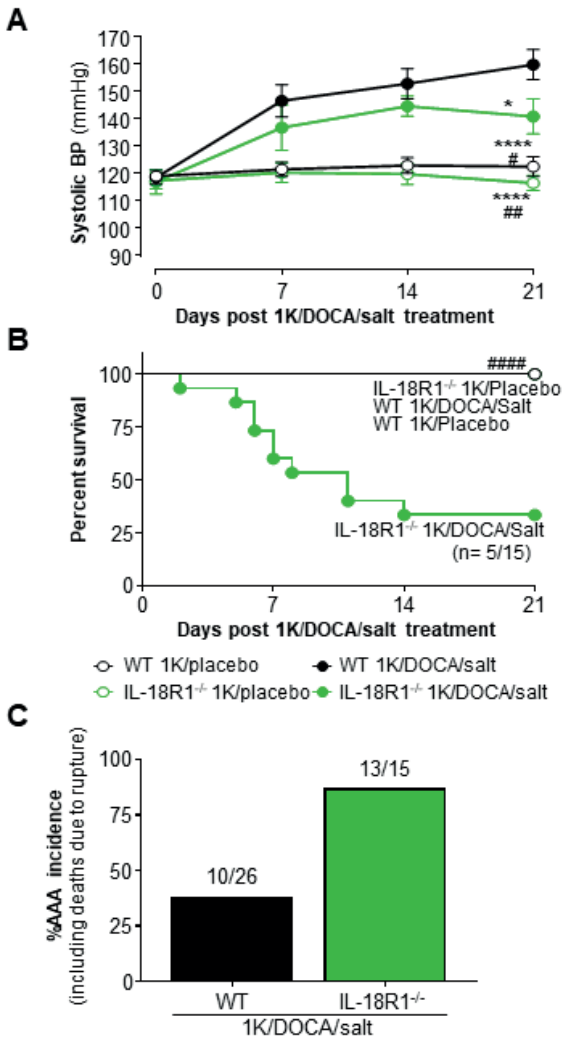

Figure 4.1 1K/DOCA/salt-induced hypertension is blunted in IL-18R1$^{-/-}$ mice at day 21, but IL-18R1$^{-/-}$ mice are more susceptible to abdominal aortic aneurysms. Tail cuff measurements of systolic BP (n= 5-14; A). Kaplan-Meier survival curves of 1K/placebo- and 1K/DOCA/salt-treated WT and IL-18R1$^{-/-}$ mice (B). Incidence of abdominal aortic aneurysms in 1K/DOCA/salt-treated WT and IL-18R1$^{-/-}$ mice (C). Values are mean ± SEM from n= 5-14 experiments. ****P ≤ 0.0001 and *P < 0.05 vs. WT 1K/DOCA/salt and #### P ≤ 0.0001, ##P ≤ 0.01 and #P < 0.05 vs. IL-18R1$^{-/-}$ 1K/DOCA/salt for two-way ANOVA followed by Bonferroni post-hoc tests, or Log-rank (Mantel-Cox) test for Kaplan-Meier survival curve.

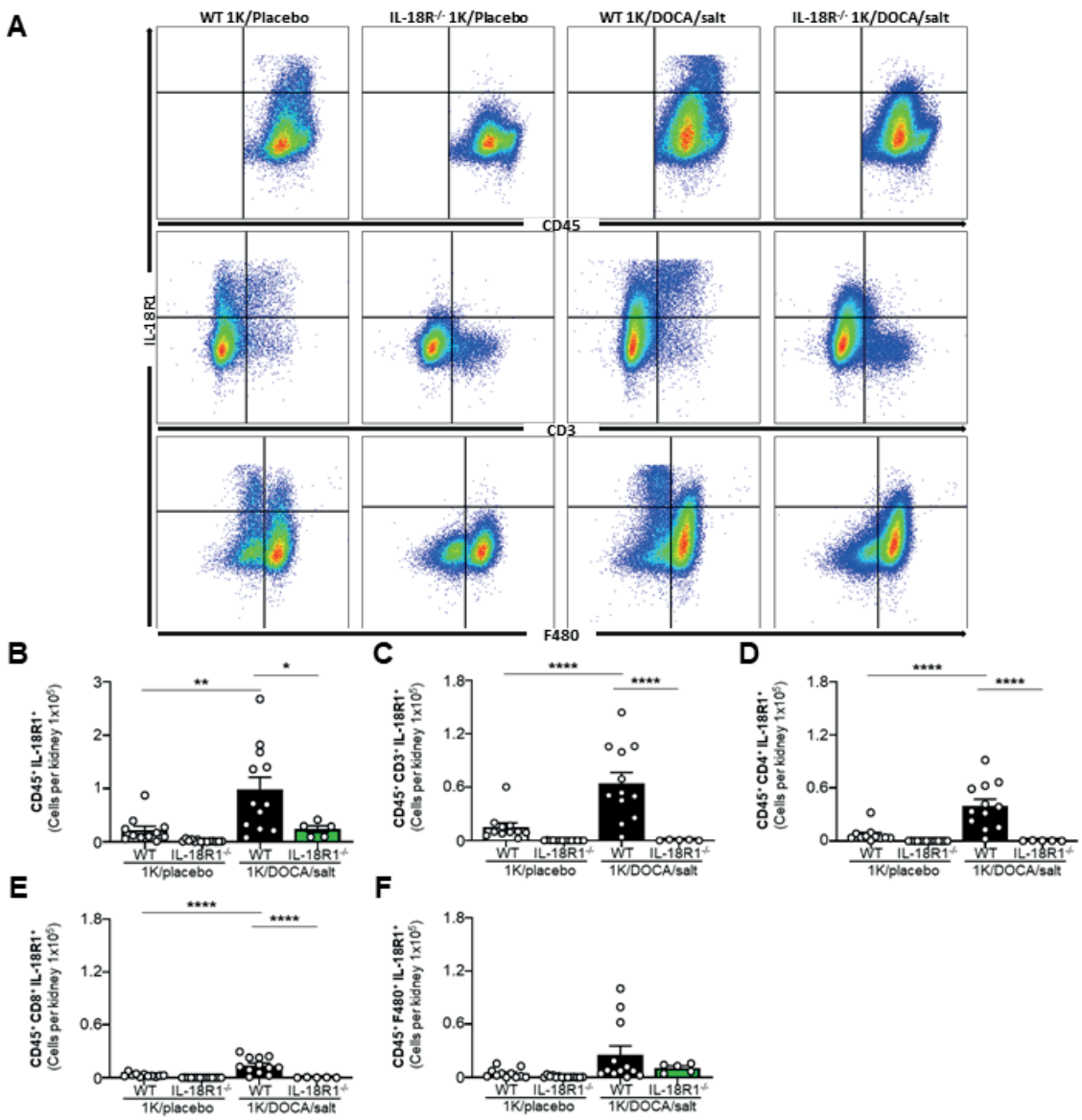

Figure 4.2 IL-18R1-deficiency prevents the accumulation of IL-18R1$^+$ in the kidneys of 1K/DOCA/salt-treated mice. Representative flow cytometry plots (A) and quantified data of IL-18R1$^+$ leukocytes (CD45$^+$; B), total T cell (CD45$^+$CD3$^+$; C), CD4$^+$ T cell (D), and CD8$^+$ T cell (E); and macrophages (F480$^+$; F); populations in the kidney. Values are mean ± SEM from n= 5-14 experiments. ***P ≤ 0.001, **P ≤ 0.01, and *P < 0.05 vs. WT 1K/DOCA/salt for two-way ANOVA followed by Bonferroni post-hoc tests.

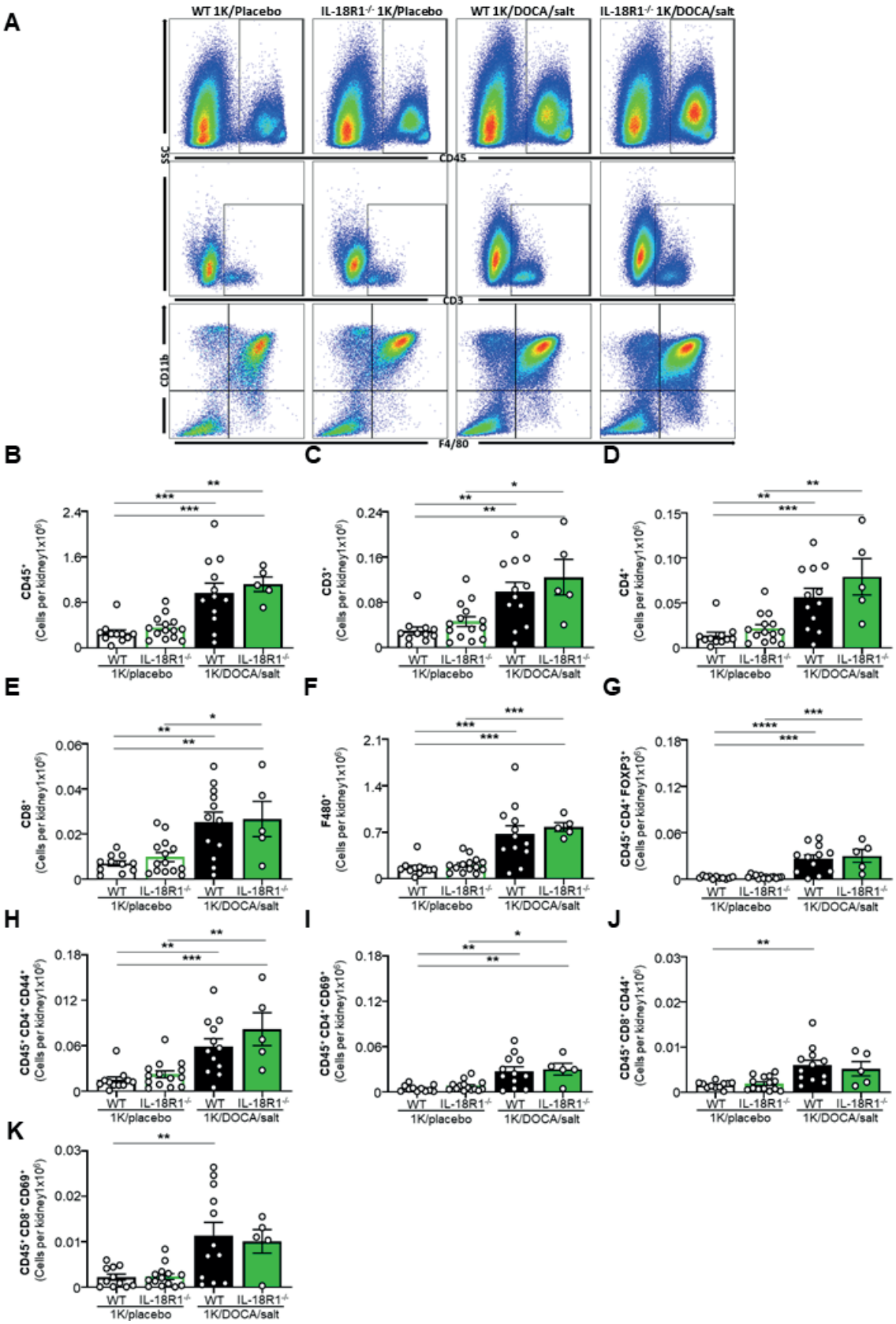

Figure 4.3 IL-18R1$^{-/-}$ mice are not protected from 1K/DOCA/salt-induced renal immune cell infiltration. Representative flow cytometry plots (A) and quantified data of total leukocyte (CD45^{+}; B), total T cell (CD45^{+}CD3^{+}; C), CD4^{+} T cell (D), CD8^{+} T cell

(E), macrophage ($CD45^+CD11b^+F4/80^+$; F), regulatory ($FOXP3^+$) $CD4^+$ T cell (G), activated ($CD44^+$) $CD4^+$ T cell(H), effector ($CD69^+$) $CD4^+$ T cell (I), activated ($CD44^+$) $CD8^+$ T cell (J), and effector ($CD69^+$) $CD8^+$ T cell (K) populations in the kidney. Values are mean ± SEM from n= 5-14 experiments. ****$P \leq 0.0001$, ***$P \leq 0.001$, **$P \leq 0.01$, and *$P < 0.05$ for two-way ANOVA followed by Bonferroni post-hoc tests.

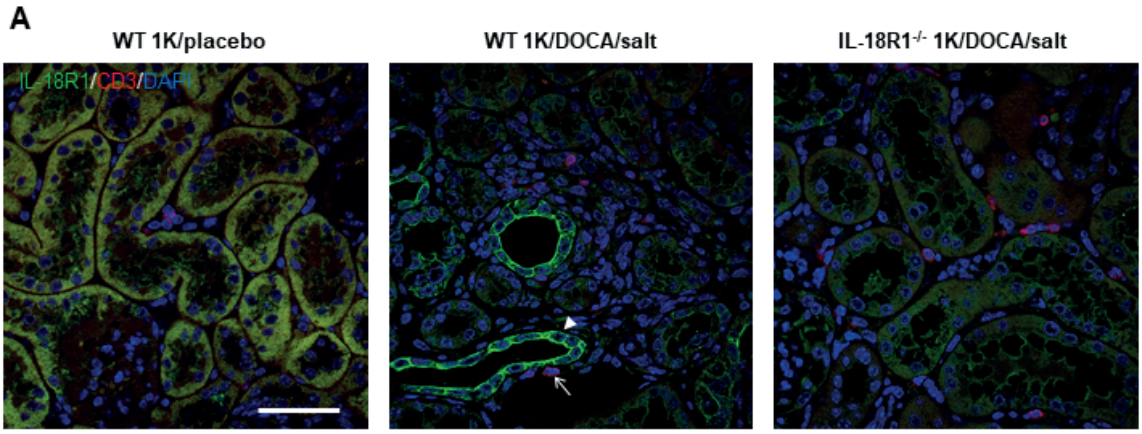

Figure 4.4 IL-18R1 staining is absent in IL-18R1-/- mice and localised to T cells and tubular epithelial cells in the kidney of 1K/DOCA/salt-treated WT mice. Representative immunofluorescence images showing localisation of IL-18R1 (green staining, arrowhead) and $CD3^+$ T cells (red staining), and co-localisation of IL-18R1 and T cells (orange staining; thin arrow) in mouse kidney sections (A). Images are representative of n=4-6 experiments. Scale bar = 50 µm.

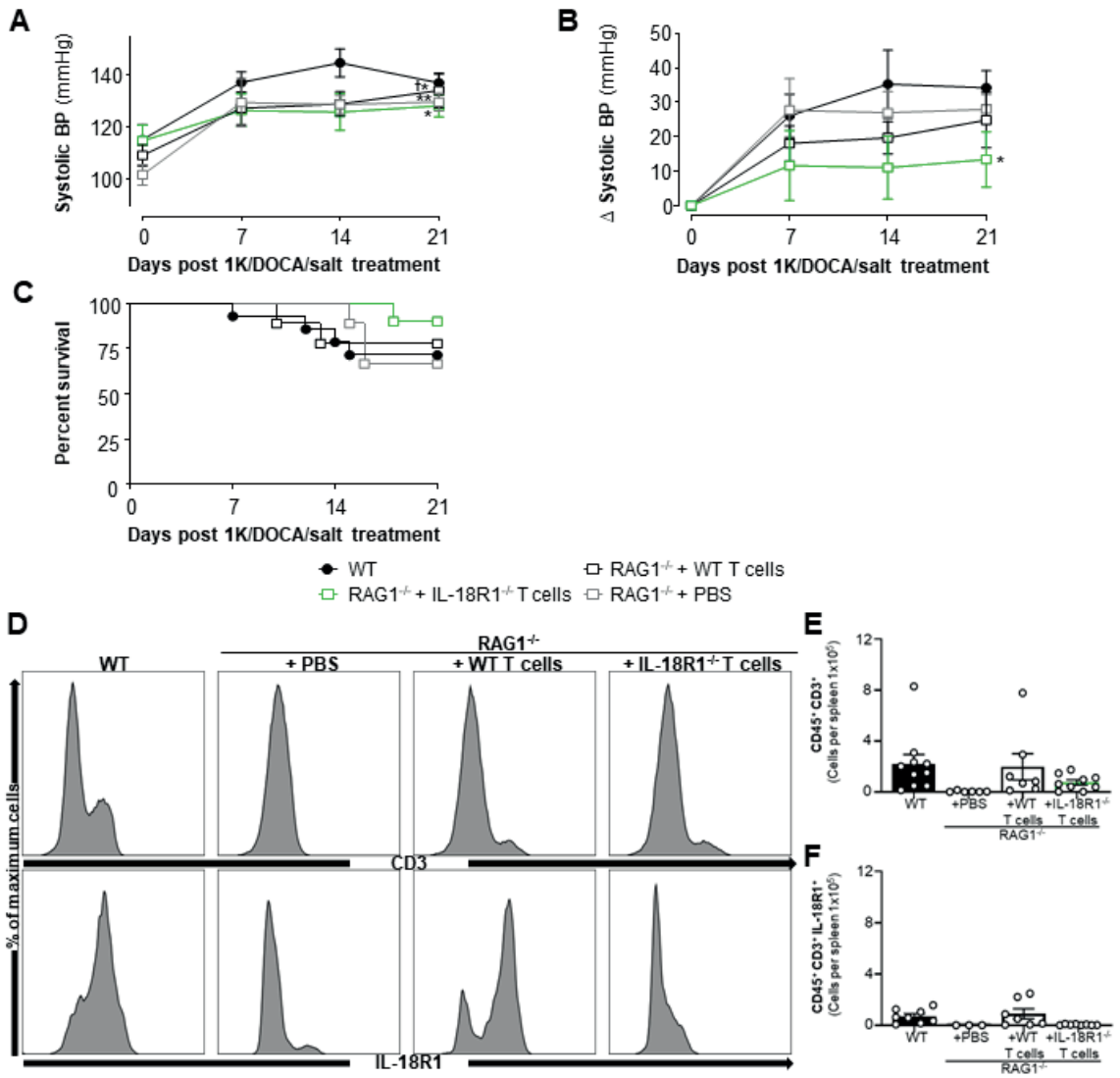

Figure 4.5 1K/DOCA/salt-induced hypertension is blunted in mice with T cell specific IL-18R1-deficiency. Tail cuff measurements of systolic BP (n= 6-10; A), changes in systolic BP from baseline (n= 6-10; B) and Kaplan-Meier survival curves of 1K/DOCA/salt-treated WT and RAG1$^{-/-}$ mice that received PBS, WT and IL-18R1$^{-/-}$ T cells (C). Representative flow cytometry histograms (D) and quantified data of total T cell (CD45^{+}CD3^{+}; E) and IL-18R1^{+} T cell (CD45^{+}CD3^{+}; F) populations in the spleen. Values are mean ± SEM from n= 6-10 experiments. **P ≤ 0.01, and *P < 0.05 vs WT and †P < 0.05 vs RAG1$^{-/-}$ mice + IL-18R1$^{-/-}$ T cells for two-way ANOVA, Log-rank (Mantel-Cox) test for Kaplan-Meier survival curve or one-way ANOVA followed by Bonferroni post-hoc tests.

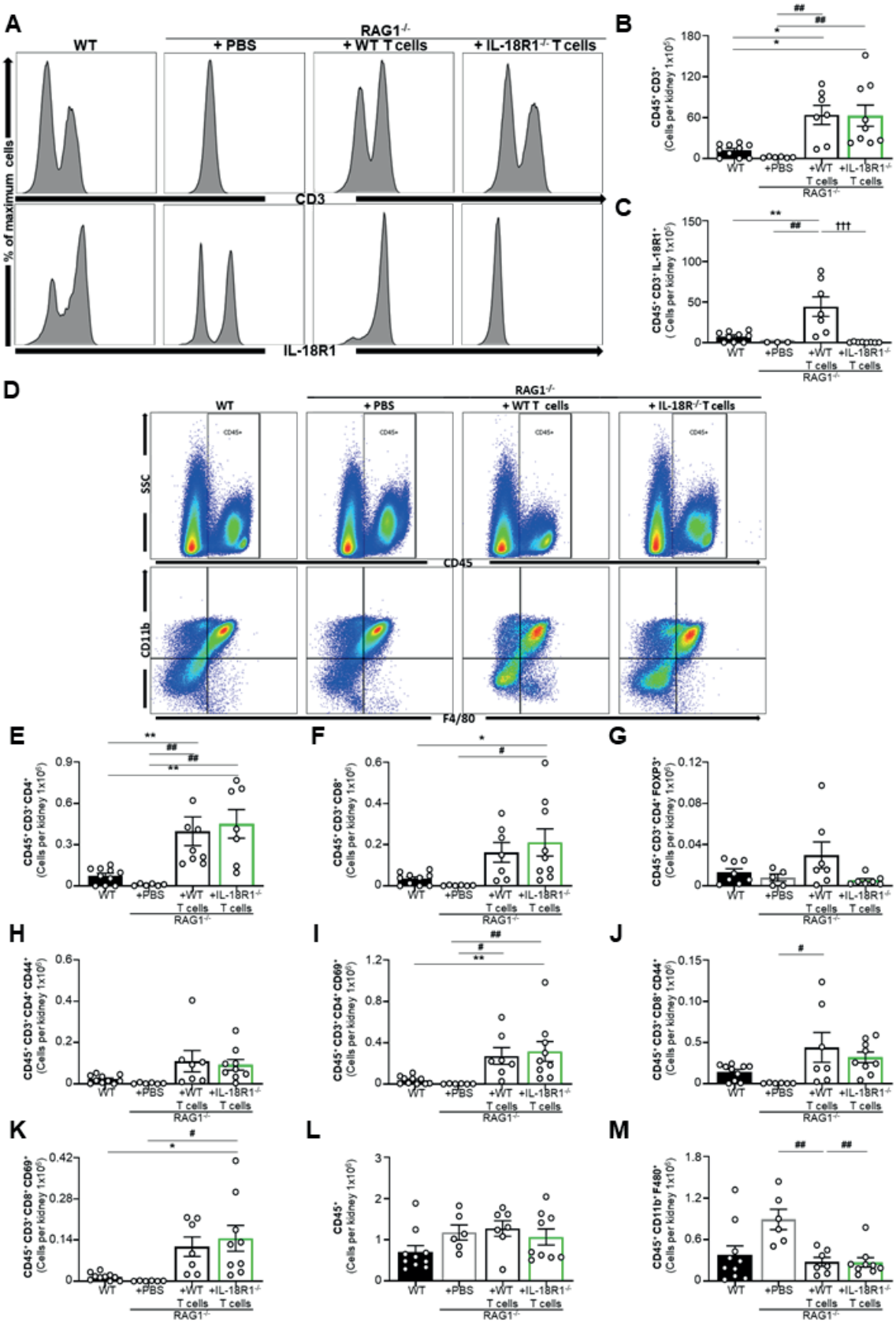

Figure 4.6 Mice with T cell specific IL-18R1-deficiency are not protected from 1K/DOCA/salt-induced renal immune cell infiltration. Representative flow cytometry plots (A) and quantified data of total T cell ($CD45^+CD3^+$; B) and IL-18R1$^+$ T cells

($CD45^+CD3^+$ IL-$18R1^+$; C) in the kidney. Representative flow cytometry plots (D) and quantified data of $CD4^+$ T cell (E), $CD8^+$ T cell (F), activated ($CD44^+$) $CD4^+$ T cell (G), effector ($CD69^+$) $CD4^+$ T cell (H), regulatory ($FOXP3^+$) $CD4^+$ T cell (I), activated ($CD44^+$) $CD8^+$ T cell (J), effector ($CD69^+$) $CD8^+$ T cell (K), total leukocytes ($CD45^+$; L), and macrophage ($CD45^+CD11b^+F480^+$; M), populations in the kidney. Values are mean ± SEM from n= 6-10 experiments. **$P \leq 0.01$ and *$P < 0.05$ vs. WT and ###$P \leq 0.001$, ##$P \leq 0.01$ and #$P < 0.05$ vs. $RAG1^{-/-}$ mice + PBS, and †††$P \leq 0.001$ vs $RAG1^{-/-}$ mice + IL-$18R1^{-/-}$ T cells for one-way ANOVA followed by Bonferroni post-hoc tests.

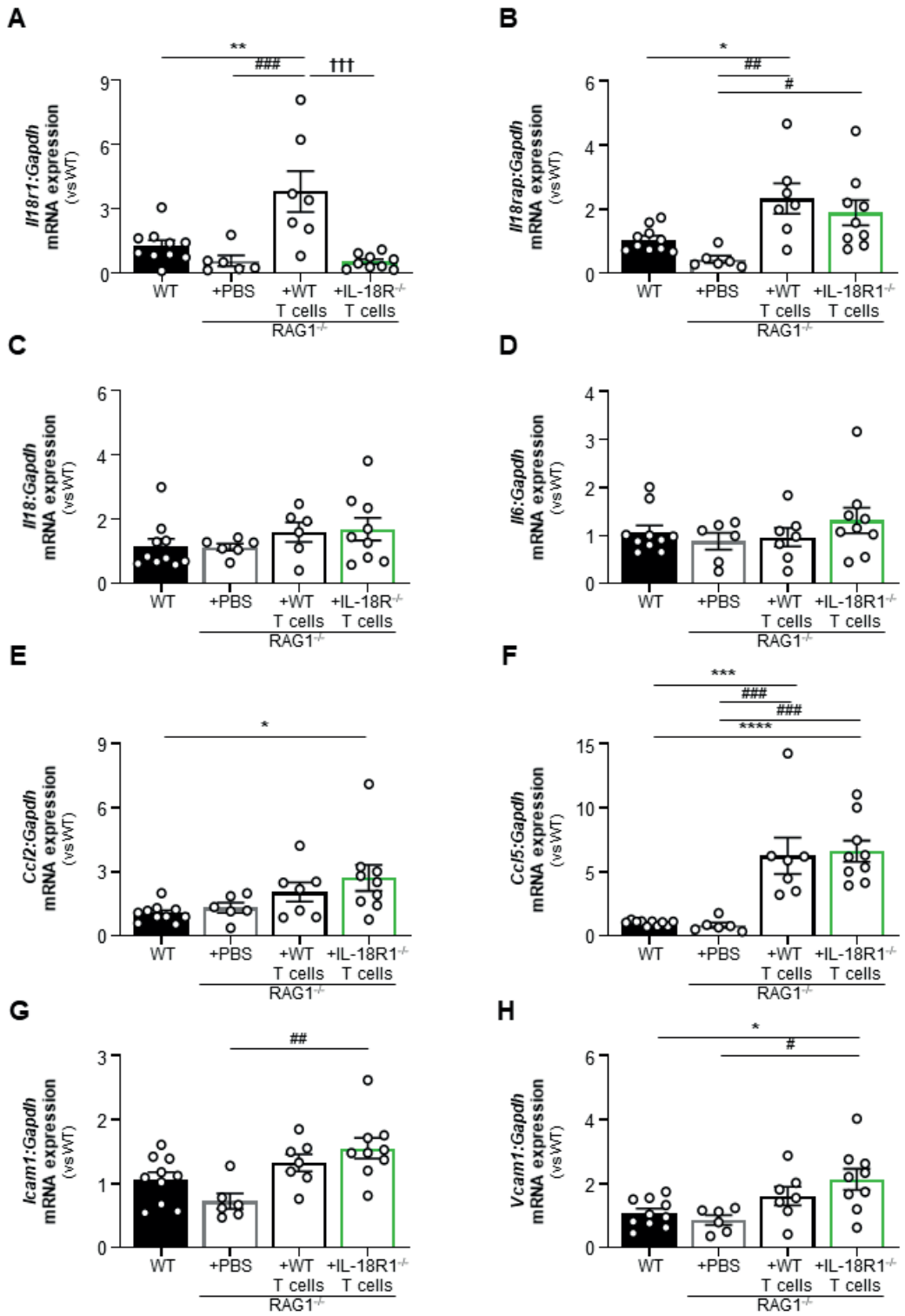

Figure 4.7 Mice with T cell specific IL-18R1-deficiency are not protected from 1K/DOCA/salt-induced renal inflammatory gene expression. Renal mRNA expression levels of the pro-inflammatory genes *Il18r1* (A), *Il18rap* (B) *Il18* (C), *Il6* (D), *Ccl2* (E), *Ccl5* (F), *Icam1* (G), and *Vcam1* (H) as measured by real-time PCR. Values are mean ± SEM from n= 6-10 experiments. ****P ≤ 0.0001, ***P ≤ 0.001, **P ≤ 0.01 and *P < 0. 05

vs. WT and ###P ≤ 0.001, ##P ≤ 0.01, and #P < 0. 05 vs. RAG1$^{-/-}$ mice + PBS for one-way ANOVA followed by Bonferroni post-hoc tests.

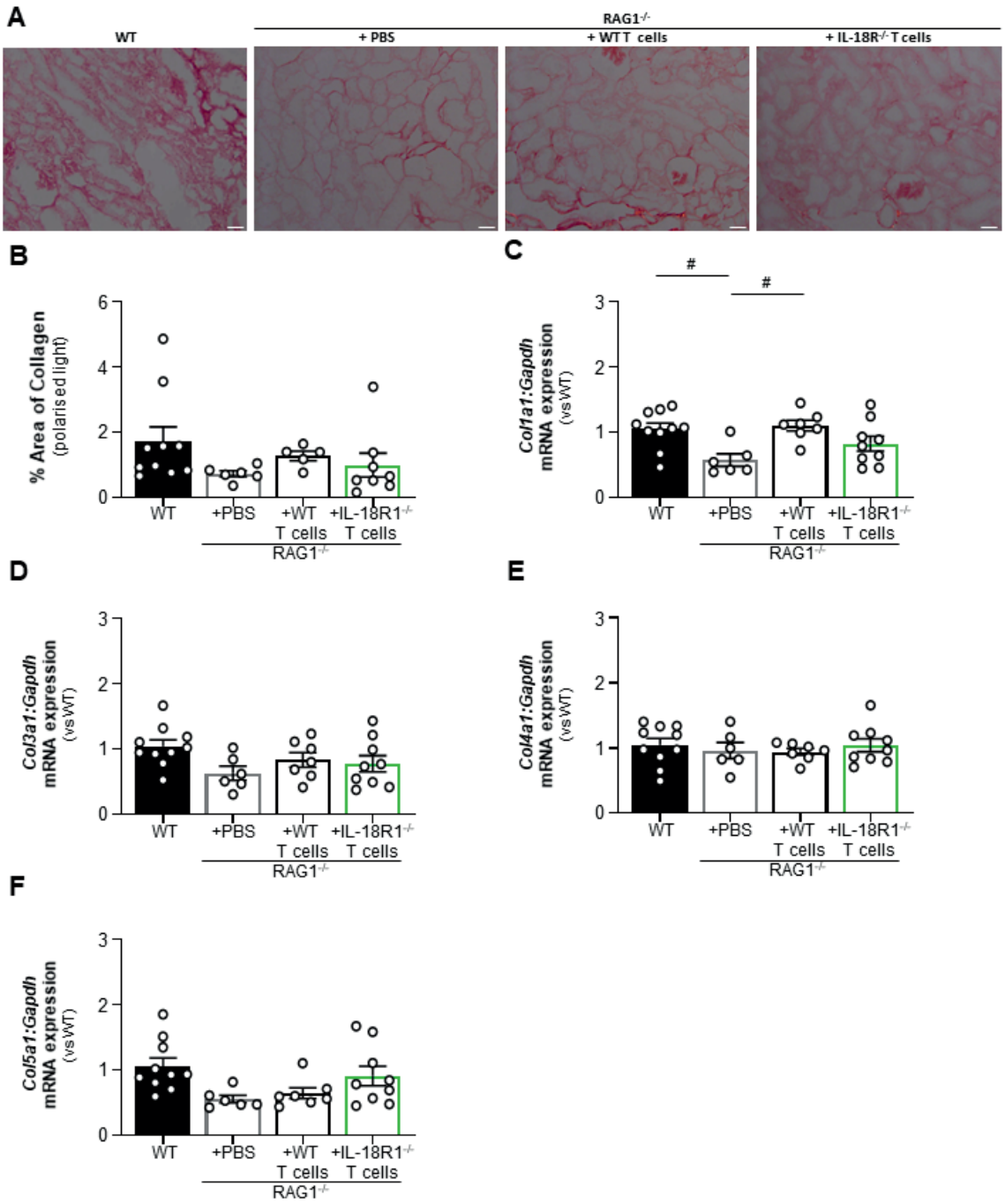

Figure 4.8 Mice with T cell specific IL-18R1-deficiency are not protected from 1K/DOCA/salt-induced renal fibrosis. Renal interstitial collagen deposition as visualised and quantified by polarised picrosirius red staining (A-B) and mRNA expression levels of the collagen α-subunits *Col1a1* (C), *Col3a1* (D), *Col4a1* (E) and *Col5a1* (F) as measured by real-time PCR. Scale bars= 100 µm. Values are mean ± SEM from n= 5-10 experiments. #P < 0. 05 vs. RAG1$^{-/-}$ mice + PBS for one-way ANOVA followed by Bonferroni post-hoc tests.

4.8 Supplementary Tables

Table 4.1. Mice used for this study.

Mice treated with 1K/DOCA/salt or 1K/placebo						
Sex	Mouse strain	Origin	# of mice	Age at treatment (weeks)	Weight at treatment (g)	Deaths
M	IL-18R1$^{-/-}$	LARTF	28	13-17	21-36	9 *
	C57Bl/6	ARC	24	11-15	22-32	

RAG1$^{-/-}$ study							
	Mouse strain	Origin	# of mice	Age at T cell transfer (weeks)	Age at treatment (weeks)	Weight at treatment (g)	Deaths
Recipient Mice	Rag1$^{-/-}$	WEHI	29	8-10	12-14	18-28	6*, 2‡
	C57Bl/6	WEHI	14	7-8	10-11	23-32	3*, 1†
Donor Mice	IL-18R1$^{-/-}$	LARTF	8	8-10			
	C57Bl/6	WEHI	16	8-10			

*= Aneurysm

†= surgical wound opening/fight wounds

‡= unknown cause

Table 4.2. Antibody panel for flow cytometry

Antigen	Host/Isotype	Clone	Tag	Dilution Factor	Company
CD45	Rat IgG2b, κ	30-F11	A700	1:500	BioLegend, USA
CD3e	Hamster IgG	145-2C11	APC	1:500	BioLegend, USA
CD4	Rat IgG2a, κ	RM4-5	BV605	1:500	BioLegend, USA
CD8a	Rat IgG2a, κ	53-6.7	BV605	1:1000	BioLegend, USA
CD11b	Rat IgG2b, κ	M1/70	BV421	1:500	BioLegend, USA
F4/80	Rat IgG2a, κ	BM8	APC Cy7	1:500	BioLegend, USA
CD69	Rat IgG2a, κ	C068C2	BV650	1:500	BioLegend, USA
CD44	Rat IgG2a, κ	XMG1.2	PERCP	1:500	BioLegend, USA
IL-18R	Rat IgG2a, κ	P3TUNYA	PE	1:500	Invitrogen, USA
FoxP3	Rat IgG2a, κ	FJK-16s	FITC	1:500	eBioscience, USA
TCR-β	Hamster IgG	H57-597	APC	1:500	BioLegend, USA
IFN-γ	Rat IgG2a, κ	DB-1	FITC	1:500	Invitrogen, USA

4.9 Supplementary Figures

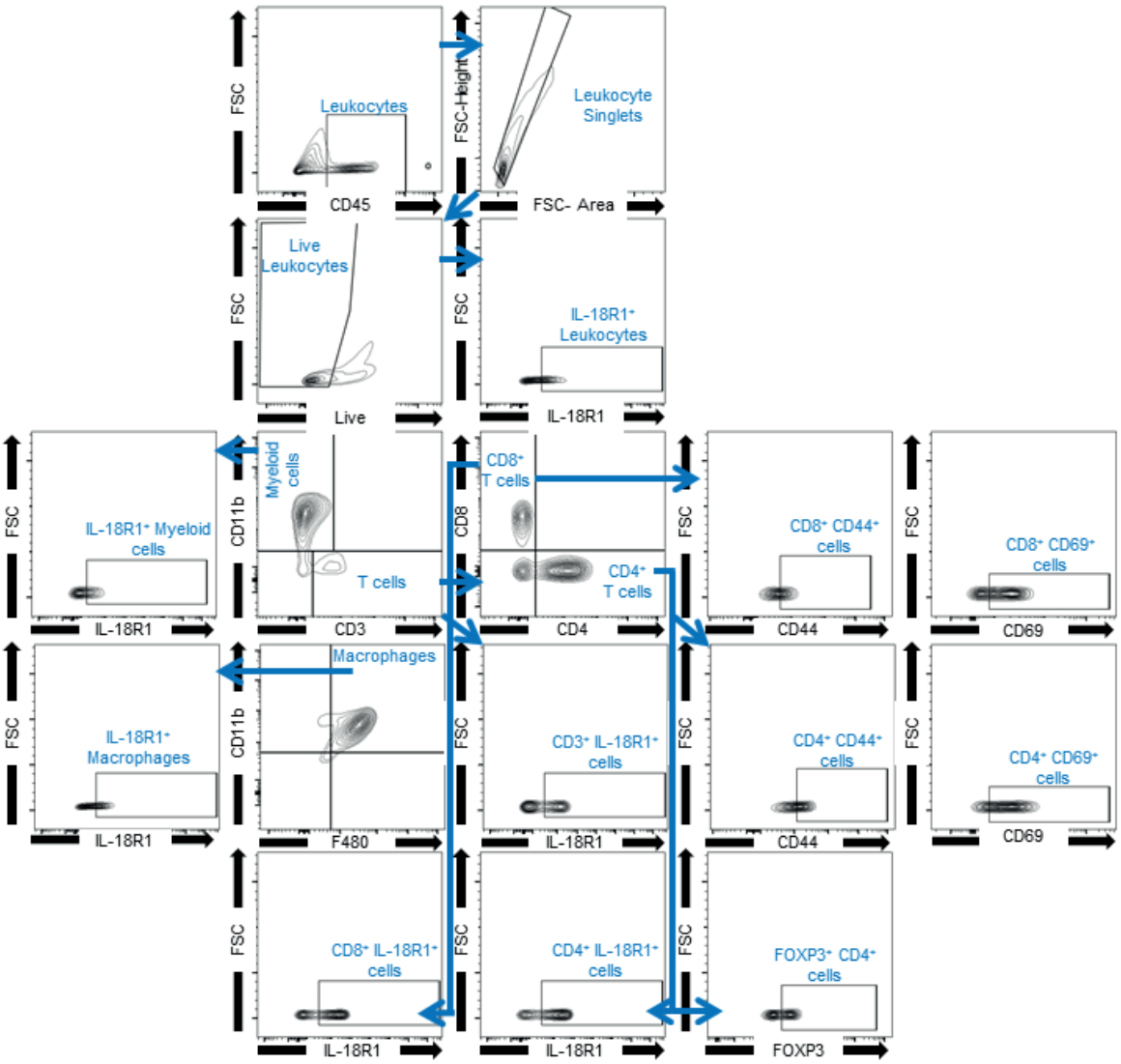

Supplementary Figure 4.1 Gating strategy for flow cytometric analysis. Leukocytes were gated as CD45$^+$ populations against forward scatter (FSC). Total leukocytes, i.e., live leukocyte singlets, were gated by FSC -height vs FSC-area, and exclusion of dead cells (live/dead stain). Total leukocytes were then divided into myeloid cells (CD11b$^+$) and T cells (CD3$^+$). Some of the myeloid cells were identified as macrophages (CD11b$^+$F4/80$^+$), and the macrophages were further classified as IL-18R11$^+$. T cells that were positive for CD3 staining were further classified as IL-18R1$^+$, CD4$^+$, or CD8$^+$ T cells. CD4$^+$ and CD8$^+$ cells were further identified as being CD44$^+$, CD69$^+$ or FOXP3$^+$.

Chapter 5

Interleukin-18 Receptor Accessory Protein Is Not Required for the Development of Renal Inflammation and Elevated Blood Pressure in 1 Kidney /DOCA/Salt-Induced Hypertension in Mice

5.1 Summary

Background: The inflammasome-derived pro-inflammatory cytokine interleukin-18 (IL-18) is a crucial mediator of renal injury during 1K/DOCA/salt-induced hypertension. IL-18 acts through an IL-18 receptor (IL-18R1) complex comprising of two subunits — IL-18R1 and IL-18 receptor accessory protein (IL-18RAP). While IL-18R1 is also known to act as a receptor for other cytokines, some of which may have anti-inflammatory actions, IL-18RAP appears to be exclusively involved in IL-18-mediated signalling. Therefore, we created a novel IL-18RAP knockout mouse using CRISPR-Cas9 to determine whether deletion of this receptor subunit affords protection against the development of kidney inflammation and fibrosis in the 1K/DOCA/salt model of hypertension.

Methods: Hypertension was induced in male and female wildtype (IL-18RAP$^{+/+}$; WT), heterozygous (IL-18RAP$^{+/-}$) and homozygous (IL-18RAP$^{-/-}$) knockout mice by uninephrectomy and treatment with deoxycorticosterone acetate (2.4 mg/d, *s.c.*) and saline (0.9%) drinking water (1K/DOCA/salt). Normotensive control mice were uninephrectomised and received a placebo pellet and normal drinking water (1K/placebo). BP was measured via tail cuff, and, after 21 days, kidneys were harvested for histology, immunofluorescence, qPCR, and flow cytometric analyses.

Results: Deficiency of one (IL-18RAP$^{+/-}$) or both (IL-18RAP$^{-/-}$) alleles of the IL-18RAP gene caused a dose-dependent reduction in renal mRNA and protein expression of IL-18RAP. IL-18RAP deficiency was also associated with impaired T cell function as evidenced by a reduced ability to generate IFNγ following IL-18 stimulation *ex vivo*. 1K/DOCA/salt-treatment was associated with equivalent levels of hypertension, renal inflammation, immune cell infiltration, fibrosis, and tubular injury in male and female wild type mice. Neither partial (IL-18RAP$^{+/-}$) nor complete (IL-18RAP$^{-/-}$) deficiency of IL-18RAP afforded mice — male or female — protection against these pathological effects of 1K/DOCA/salt.

Conclusions: IL-18RAP deficiency does not provide mice with protection against the development of high BP or renal injury following treatment with 1K/DOCA/salt. These findings suggest that the previously documented pro-hypertensive and renal damaging effects of IL-18 are likely to be mediated through an as yet undefined non-cognate signalling pathway.

5.2 Introduction

The kidneys play a major role in blood pressure (BP) homeostasis via tight control of the pressure-natriuresis relationship, whereby renal baroreceptors detect changes in BP and signal via the sympathetic nervous system to modulate sodium and water retention by the tubules.[1] Chronic inflammation in the kidneys occurs during conditions such as hypertension, diabetes, and acute kidney injury, and is thought to disrupt the pressure-natriuresis relationship leading to elevated BP. This inflammation is thought to arise due to the accumulation of host- and/or pathogen-derived danger signals known collectively as danger associated molecular patterns (DAMPs) or pathogen associated molecular patterns (PAMPs). DAMPs and PAMPs can then activate pro-inflammatory signalling platforms termed inflammasomes,[2-4] which in turn drive the production of the pro-inflammatory cytokine interleukin-18 (IL-18).[5, 6] Indeed, IL-18 is known to be increased in patients with hypertension and chronic kidney disease (CKD),[7, 8] and we have previously demonstrated that IL-18 is essential to the development of renal inflammation, fibrosis and dysfunction that occurs during 1K/DOCA/salt-induced hypertension in mice; a model of low-renin hypertension.

IL-18 signals through a receptor complex comprised of an IL-18 receptor (IL-18R1) subunit and an IL-18 receptor accessory protein (IL-18RAP). The IL-18 receptor complex is highly expressed on T cells where it is linked to the production of the pro-inflammatory cytokine interferon-γ (IFN-γ).[9] Indeed, we previously demonstrated that treatment of T cells isolated from the kidneys of hypertensive mice with IL-18 augments the production of IFN-γ, whereas T cells from normotensive mice were unresponsive. These observations imply that inhibition of IL-18-dependent T cell signalling may be a novel approach for limiting renal inflammation and its cardiovascular consequences.

In Chapter 4, we investigated whether IL-18R1 would be a suitable target for novel, anti-hypertensive, pharmacological interventions. However, neither global nor T cell specific

deletion of IL-18R1 afforded protection against the development of renal inflammation and fibrosis during 1K/DOCA/salt-induced hypertension. We hypothesised that this was due to the blockade of additional anti-inflammatory IL-37 signalling that may occur through IL-18R1.[10] In humans, IL-37 can bind to IL-18R1 causing it to recruit IL-1R8 (i.e., instead of IL-18RAP). [10] IL-1R8 has a non-functional toll/interleukin-1 receptor (TIR) domain which does not engage with downstream pro-inflammatory signalling pathways.[10] Therefore, due to the potential protective anti-inflammatory signalling through IL-18R1, IL-18RAP may prove a better and more specific target downstream of IL-18 signalling for novel anti-hypertensive therapies.

Recent studies have demonstrated that IL-18RAP expression is elevated in peripheral monocytes of hypertensive patients, and that IL-18RAP expression is positively associated with mean arterial pressure (MAP) in an African American cohort.[11] Therefore, in the present study we generated a novel strain of IL-18RAP$^{-/-}$ mice using CRISPR-Cas9 to test the hypothesis that inhibition of IL-18 receptor signalling affords protection against hypertension and the development of renal inflammation.

We found that despite being deficient in IL-18RAP mRNA and protein expression in the kidneys, with impaired IL-18-mediated T cell IFN-γ production, IL-18RAP$^{-/-}$ mice were *not* protected from the development of 1K/DOCA/salt-induced hypertension or renal inflammation and damage. These findings suggest that the hypertensive and pro-inflammatory actions of IL-18 in the 1K/DOCA/salt model are mediated through a non-canonical signalling mechanism that remains to be identified.

5.3 Methods

5.3.1 Animals

A total of 49 male and 59 female IL-18RAP$^{+/+}$, IL-18RAP$^{+/-}$ and IL-18RAP$^{-/-}$mice, fully backcrossed onto a C57BL6/J background, were used (Table 5.1). Mice were bred at the La Trobe Animal Research and Teaching Facility (LARTF; La Trobe University Australia) and used for experiments between 8-13 weeks of age. Prior to surgery, mice were housed with littermates in groups of 3-4 animals in Sealsafe Plus GM500 boxes (Tecniplast, USA), under specific pathogen-free conditions, on a 12 h light-dark cycle, and provided with *ad libitum* access to normal chow and drinking water. Mice were randomly assigned into treatment groups (hypertensive or normotensive) using random number generator software (Microsoft Excel, Version 16.36, USA). All procedures were conducted according to the Australian Code for the Care and Use of Animals for Scientific Purposes (8th edition) and were approved by La Trobe University Animal Ethics Committee (Project number: AEC16-93).

5.3.2 Generation of IL-18RAP-deficient mice

The CRISPR design site (crispr.mit.edu) was used to identify guide RNA sites flanking the exon to be removed (ENSMUST00000027237.11). This is the only exon containing the coding sequence and thus it was anticipated that deletion of this region had the greatest likelihood of producing an IL-18RAP knockout. The sequence of this locus was submitted to the MIT guide design tool to identify suitable guide sites flanking the exon (i.e., guides 5’ and 3’ to the exon). The tool identified several guide sites in the 5’ and 3’ regions and guides were selected according to their score, the higher the score, the less potential off target sites.

5’ guide sequence: 5’ TGATGTGTGCTGATGCTCGG 3’

3’ guide sequence: 3’ TGTACACGATATGGCATGCA 5’

Complementary oligonucleotides corresponding to the RNA guide target sites were annealed and cloned into BbsI (NEB, USA)-digested plasmid pX330- U6-Chimeric_BB-CBh-hSpCas9 (Addgene plasmid #42230). Single guide RNAs (sgRNA) were generated using the HiScribe™ T7 Quick High Yield RNA Synthesis Kit (NEB) according to the manufacturer's instructions and RNAs were purified using the RNeasy Mini Kit (Qiagen, Germany). Cas9 mRNA (30 ng/µl; Sigma-Aldrich, USA), and the 5' and 3' sgRNAs (15 ng/µl) were microinjected into the cytoplasm of C57BL/6J zygotes at the pronuclei stage. Injected zygotes were transferred into the uterus of pseudopregnant F1 females. Founder mice were screened for the correct modification. We selected three founders for breeding to wild type mice and screened the next generation for the correct modification. These mice were then further bred for > 3 generations and screened for the correct modification.

5.3.3 Induction of hypertension

A low-renin model of hypertension was used in this study wherein mice were uninephrectomised (left kidney) and treated with deoxycorticosterone acetate (DOCA; 2.4 mg/day, *s.c.*; Innovative Research of America, USA) and 0.9% saline drinking water (1K/DOCA/salt).[12, 13] Normotensive controls for this experiment were mice that also received uninephrectomy, a placebo pellet containing the proprietary matrix material without DOCA (Innovative Research of America, USA) and normal drinking water (1K/placebo). All surgeries were performed under anaesthesia induced by inhalation of isoflurane (2 L/min, 5% in O_2). Anaesthesia was maintained by 2.5% isoflurane in O_2 (0.4 L/min) and regularly monitored by checking hind-paw withdrawal, blink reflexes and respiratory rate. Prior to surgery, mice received local anaesthetic (bupivacaine; 2.5 mg/kg, *s.c.*) and analgesic (carprofen; 5 mg/kg, *s.c.*). Carprofen treatment was continued for 3 days post-surgery.

5.3.4 Blood pressure measurements

BP was measured via tail cuff plethysmography. Tail cuff measurements were performed using a Multichannel BP Analysis System (MC4000; Hatteras Instruments, USA). All mice

underwent daily training on the tail cuff device for at least 3 days prior to induction of hypertension. BPs were then recorded on the morning prior to surgery (day 0) and weekly thereafter on days 7, 14 and 21.

5.3.5 Measurement mRNA expression levels

At the end of the 21-day treatment period, mice were killed via CO_2 asphyxiation and perfused through the left ventricle with phosphate-buffered saline (PBS) containing 0.2% Clexane (400 IU; Sanofi Aventis, France). The remaining right kidney was excised and cut in half along its transverse plane. One half of the kidney was used immediately for flow cytometric analysis, while the other half was further divided into two transverse sections. One of these sections was fixed in 10% formalin and stored at 4°C for immunohistochemistry, and the other was snap frozen in liquid N_2 and stored at -80°C for later RNA extraction. Regarding the latter, frozen kidneys were pulverised, and RNA was extracted using a RNeasy Mini Kit (Qiagen, Hilden, Germany). The yield and purity of the RNA was determined using a NanoDrop Spectrophotometer (NanoDrop One, Thermo Scientific, USA). RNA was reverse transcribed using a High Capacity cDNA Reverse Transcription kit (Applied Biosystems, USA) and the resulting cDNA was then used as a template in real-time PCR to measure mRNA expression of pro-*Il18*, *Il18r1*, *Il18rap*, *Il18* binding protein *(Il18bp)*, C-C motif chemokine ligand (*Ccl*) 2, *Ccl5*, intercellular adhesion molecule-1 (*Icam1*), vascular cell adhesion molecule-1 (*Vcam1*), *Il6*, *Il23a*, *Col1a1*, *Col3a1*, *Col4a1*, and *Col5a1*, or the housekeeping gene, *Gapdh* (TaqMan Gene Expression Assays, Applied Biosystems, USA). Real-time PCR was performed in a Bio-Rad CFX96 Real-Time PCR Detection System (Bio-Rad Laboratories, Hercules, CA, USA) and the comparative Ct method was used to calculate the fold-change in mRNA expression relative to a reference control sample.[14]

5.3.6 Flow cytometric analysis

For conventional flow cytometric analysis, cell suspensions were prepared from kidney halves and whole spleens. Kidney halves were minced with scissors and digested in PBS

containing collagenase type XI (125 U/mL), collagenase type I-S (460 U/mL) and hyaluronidase (60 U/mL) (Sigma-Aldrich, USA) for 60 mins at 37°C. Following digestion, kidney suspensions were passed through a 70 µm filter (BD Biosciences, USA), and the cells were pelleted by centrifugation at 453 x*g* for 5 min. The cell pellets were further subjected to Percoll™ gradient centrifugation, whereby the pellet was re-suspended in 3 mL of 40% isotonic Percoll™ solution (GE Healthcare Life Science, UK), and carefully under-laid with 3 mL of 70% Percoll™ solution. Samples were centrifuged at 1450 x*g* at 25°C for 25 min with the brake of the centrifuge turned off. Following centrifugation, adipocytes and debris were aspirated from the top layer, and the layer containing the mononuclear cells — lying between the Percoll™ gradients — was collected. Mononuclear cells were washed in PBS, centrifuged, and the pellet was re-suspended in PBS. Spleen samples were minced with scissors and passed through a 70 µm filter, and then incubated in red blood cell (RBC) lysis buffer (55 mM NH_4Cl, 10 mM $KHCO_3$, 0.1 mM EDTA, dH_2O) for 5 min at room temperature. Spleen cells were counted using an automatic cell counter (EVE, NanoEnTek Inc, South Korea) and re-suspended in PBS at a concentration of 10^7 cells/mL. Kidney and spleen cell suspensions were stained for 15 min at room temperature with Live/Dead aqua stain (Life Technologies, USA), followed by an antibody cocktail consisting of anti-mouse CD45 (A700; BioLegend, USA), CD3 (APC; BioLegend, USA), CD8 (PeCy7; BioLegend, USA), CD4 (BV605; BioLegend, USA), CD11b (BV421; BioLegend, USA), F4/80 (APC Cy7; BioLegend, USA), CD69 (BV650; BioLegend, USA), CD44 (PERCP; BioLegend, USA), and IL-18R1 (PE; Invitrogen, USA; Table 5.2) dissolved in PBS containing 0.5% bovine serum albumin.

For detection of Foxp3 expression (Treg marker), cells were washed in PBS, centrifuged, fixed and permeabilised (eBioscience™ Foxp3/Transcription Factor Fixation/Permeabilization Concentrate and Diluent; Invitrogen, USA). Cells were then washed in perm wash™ and re-suspended in 1% formalin in PBS containing 0.5% bovine

serum albumin and EDTA, prior to analysis on a CytoFlex LS flow cytometer (Beckman Coulter, USA) using CytExpert software (Beckman Coulter). Data were analysed using FlowJo software v10 (FlowJo, USA). For the full gating strategy, see Supplementary Figure 5.1.

5.3.7 Measurement of T cell IFN-γ production

Spleen cell suspensions were prepared as described for flow cytometric analysis. T cells were enriched using a CD90.2 positive microbead isolation kit (Miltenyi Biotech, USA), suspended in RPMI media containing 10% FBS, penicillin (100 U/mL)/streptomycin (100 µg/mL) and L-glutamine (2 mM), and seeded onto an anti-CD3 (5 ug/mL, BioLegend)-coated 96-well plate at a density of $1x10^6$ cells/well. In the presence of an anti-CD28 monoclonal antibody (1 µg/mL; BioLegend), T cells were stimulated with various concentrations of IL-18 (0, 0.1, 1, 10 or 100 ng/mL; R&D Systems, USA) for 16 h at 37°C. Cells were further incubated with the protein transport inhibitors, golgi-plug (BD Biosciences, USA) and golgi-stop (BD Biosciences), for 6 h. Following incubation, cells were centrifuged at 435 x*g* for 5 min at 4°C and the supernatant was discarded. Cells were then stained for surface markers (see Table 5.2) before being fixed and permeabilised for intracellular staining with an anti-IFN-γ antibody at room temperature for 15 min. Finally, cells were washed and re-suspended in PBS for analysis on a CytoFlex LS flow cytometer (Data were analysed using FlowJo software v10 (FlowJo, USA)). For the full gating strategy, see Supplementary Figure 5.2.

5.3.8 Histopathology staining

Fixed, paraffin-embedded kidney sections (4 µm) were stained with either 0.5% Picrosirius red (Polysciences Inc., USA) or haematoxylin and eosin (Amber Scientific, Australia). Sections were imaged (20x magnification) using either a polarised or bright field microscope (Olympus, Japan) and analysed for percentage collagen area by ImageJ. Changes in renal tubular structure (i.e., tubular dilatation, tubular atrophy and

epithelial brush border integrity) were assessed using a 4-point scoring system as follows: 0 = no damage; 1 = mild damage (< 25% tubules affected); 2 = moderate damage (25–50% of tubules affected); and 3 = severe damage (> 50% of tubules affected). Quantified/scored Picrosirius red and renal histopathology data represent the average values obtained independently by two investigators who were blinded to the *in vivo* treatment of each sample.

5.3.9 Immunohistochemistry

Following sodium citrate antigen retrieval (AJAX Finechem; Australia; pH 6), kidney sections were blocked in 10% goat serum, and then incubated overnight at 4°C with rabbit anti-IL-18RAP (5 µg/mL; Abcam, USA) diluted in 10% goat serum. An Alexa Fluor 555-conjugated goat secondary antibody (Invitrogen, USA) was used, and cell nuclei were counterstained with DAPI. Fluorescent images were captured using either a Zeiss 780 confocal microscope (Carl Zeiss, Oberkochen, Germany) or an Olympus BX53 microscope with a light source attached (X-cite series 120Q, Excelitas Technologies, USA).

5.3.10 Statistics

Unless otherwise stated, results are expressed as mean ± standard error of mean (SEM). Sample sizes of 6-8 mice were determined *a priori* in consultation with the La Trobe University Statistics Consultancy Platform to provide 80% power with an alpha-level of 5% for three types of effects based on 2-way analysis of variance (ANOVA): the within effect (time); the between effect (sex); and the between within effect (differences between the sexes over time). Parametric data were analysed using two-way analysis of variance (ANOVA). Post hoc analyses (only performed when F tests from ANOVA were < 0.05) were conducted using Bonferroni's test. Non-parametric data were analysed using Kruskal-Wallis one-way ANOVA. $P < 0.05$ was considered to be statistically significant.

5.4 Results

5.4.1 Effect of IL-18RAP gene deletion on IL-18 signalling and IL-18 receptor expression in the kidneys

Full and partial deletion of IL-18RAP by CRISPR-Cas9 in homozygous (IL-18RAP$^{-/-}$) and IL-18RAP heterozygous (IL-18RAP$^{+/-}$) knockout mice, respectively, was confirmed by PCR on genomic DNA extracted from tail clips (Supplementary Figure 5.3). Renal *Il18rap* expression was reduced by ~50% and 85% in IL-18RAP$^{+/-}$ or IL-18RAP$^{-/-}$ mice, respectively (Figure 5.1A). We also confirmed a gene-dose effect of IL-18RAP allele deletion on mRNA expression levels of the IL-18 signalling complex in the kidneys of naïve mice. IL-18RAP allele deletion had a dose-dependent inhibitory effect on receptor function such that splenic T cells isolated from IL-18RAP$^{+/-}$ and IL-18RAP$^{-/-}$ mice produced ~50% and ~80% less IFN-γ upon stimulation with IL-18, respectively, than splenic T cells isolated from wild type mice (Figure 5.1D-E). Compared to wild type mice (i.e., IL-18RAP$^{+/+}$), neither *Il18* nor *Il18r1* mRNA expression were different in IL-18RAP$^{+/-}$ or IL-18RAP$^{-/-}$ mice (Figure 5.1B-C).

5.4.2 IL-18RAP gene-deficiency does not protect against 1K/DOCA/salt-induced hypertension

Regardless of sex, baseline systolic BPs were similar between wild-type, IL-18RAP$^{+/-}$ and IL-18RAP$^{-/-}$ mice, measuring around 130 mmHg (Figure 5.2). Similar to our previous reports[15] and again irrespective of sex, 1K/DOCA/salt-treatment caused systolic BP to increase by 25-30 mmHg in wild type mice, reaching this peak at 14 days after surgery (Figure 5.2). Comparable blood pressure profiles following 1K/DOCA/salt-treatment were observed in IL-18RAP$^{+/-}$ and IL-18RAP$^{-/-}$ mice (Figure 5.2). Thus, IL-18RAP-deficiency had no effect on the hypertensive response of mice to 1K/DOCA/salt.

We also measured mRNA expression of *Il18rap* in the kidneys of 1K/DOCA/salt-treated mice and found it to be altered by both sex and genotype. Renal expression of *Il18rap*

following 21 days of 1K/DOCA/salt treatment was approximately 2.5-fold higher in females than in male mice (which were in turn ~2.5-fold higher than levels typically seen in normotensive control mice; Figure 5.3A). For both sexes, mRNA expression of *Il18rap* in the kidneys of 1K/DOCA/salt treated IL-18RAP$^{+/-}$ mice was ~50% of that in similarly treated wild type mice, while no *Il18rap* mRNA was detected in the kidneys of 1K/DOCA/salt treated IL-18RAP$^{-/-}$ mice (Figure 5.3A).

IL-18RAP deficiency also impacted renal mRNA expression of its partner subunit, *Il18r1*. Similar to findings with IL-18RAP, mean expression levels of IL-18R1 in female wild type mice treated with 1K/DOCA/salt appeared to be twice that in similarly treated male wild type mice, although this failed to reach statistical significance (Figure 5.3B). Kidneys from female IL-18RAP$^{+/-}$ and IL-18RAP$^{-/-}$ mice treated with 1K/DOCA/salt expressed lower levels (i.e., by approximately 50-60%) of *Il18r1*, compared to those from wild type mice, with a similar trend observed in males (Figure 5.3B). In contrast to these findings, there was no effect of either sex, or of partial or complete IL-18RAP deficiency on renal mRNA expression of *Il18* or *Il18bp* (Figure 5.3C-D).

Immunofluorescence staining revealed that IL-18RAP was localised (albeit sparsely) on interstitial immune cells in the kidneys of 1K/DOCA/salt-treated IL-18RAP$^{+/+}$ and, to a lesser extent, IL-18RAP$^{+/-}$ mice. As expected, IL-18RAP immunofluorescence was undetectable in the kidneys of IL-18RAP$^{-/-}$ mice (Figure 5.3E).

5.4.3 IL-18RAP-deficiency does not influence the incidence of abdominal aortic aneurysms or mortality rate

1K/DOCA/salt-induced hypertension in mice is associated with an increased mortality rate as a result of the formation and rupture of abdominal aortic aneurysms (AAA). We have previously reported mortality rates of ~10-15% due to AAA in male wild-type mice treated with 1K/DOCA/salt. [12] In the present study, we saw a higher rate of death (i.e., approximately 30%) due to AAA (confirmed post-mortem) in both male and female wild

type mice treated with 1K/DOCA/salt (Figure 5.4A & B). Death rates in male and female IL-18RAP$^{-/-}$ mice following 1K/DOCA/salt treatment tended to be slightly lower than in wild type mice, although these differences were not significant (Figures 5.4A & B). Surprisingly, death rates in 1K/DOCA/salt-treated IL-18RAP$^{+/-}$ mice appeared to differ between sexes. Thus, in male IL-18RAP$^{+/-}$ mice there was a 50% mortality rate due to the development of AAA, whereas in female IL-18RAP$^{+/-}$ mice, no deaths were observed (Figure 5.4A & B). However, it is important to note that within sexes, there were no differences in mortality rates between IL-18RAP$^{+/-}$ and IL-18RAP$^{+/+}$ (Figure 5.4A & B). Overall, there was no significant impact of IL-18RAP-deletion on mortality rates in mice of either sex following 1K/DOCA/salt treatment.

5.4.4 IL-18RAP-deficiency does not alter the expression of inflammatory genes in the kidney of 1K/DOCA/salt-treated mice

We have previously shown that 1K/DOCA/salt treatment causes upregulation of pro-inflammatory cytokines such as *Il23* and *Il6*, chemokines including *Ccl2* and *Ccl5*, and the adhesion molecules *Icam1* and *Vcam1* in the kidneys. In the present study, these inflammatory molecules all appeared to be upregulated in 1K/DOCA/salt-treated wild type mice by approximately 2- to 120-fold compared to historical control value **(**Figure 5.5**).** Although *Ccl2* was moderately more highly expressed in kidneys of males than in female mice —and specifically *Ccl2* was upregulated in male IL-18RAP$^{+/-}$, while female IL-18RAP$^{+/-}$ had decreased expression of Ccl2 when compared to female IL-18RAP$^{+/+}$ —for all other inflammatory genes there was no effect of either sex or genotype on expression (Figure 5.5).

5.4.5 IL-18RAP-deficiency does not alter renal immune cell infiltration in 1K/DOCA/salt-treated mice

Previous studies show that 1K/DOCA/salt treatment of wild type mice is associated with increased infiltration of the kidneys by immune cells.[12, 15] In the present study, IL-18RAP$^{+/-}$

and IL-18RAP$^{-/-}$ mice of both sexes were equally as susceptible as wild type mice to accumulation in the kidneys of: CD45^{+} leukocytes (Figure 5.6A); total myeloid (CD11b^{+}) and macrophage (CD11b^{+}F4/80^{+}) cells (Figure 5.6B-C); total T cells (Figure 5.6D); CD4^{+} and CD8^{+} T cell populations (Figure 5.6E-F); as well as activated (CD44^{+}), effector (CD69^{+}) and regulatory (FOXP3^{+}) T cell subpopulations (Figure 5.6G-K).

5.4.6 IL-18RAP-deficiency does not alter renal fibrosis in 1K/DOCA/salt-treated mice

1K/DOCA/salt treatment of WT (IL-18RAP$^{+/+}$) mice is associated with increased collagen deposition in the renal interstitium and transcriptional upregulation of several collagen genes including *Col1a1, Col3a1, Col4a1* and *Col5a1*. [12] In the present study, picrosirius red staining of kidney sections from 1K/DOCA/salt-treated wild type mice of either sex again revealed substantial interstitial collagen deposition with semi-quantitative analysis indicating that approximately 3.5% of the kidneys were covered by collagen. Picrosirius red staining of kidney sections from IL-18RAP$^{+/-}$ and IL-18RAP$^{-/-}$ mice of both sexes demonstrated they are equally as prone to the development of fibrosis following 1K/DOCA/salt treatment (Figure 5.7A-B). Consistent with these observations, renal mRNA expression levels of collagen subtypes *Col1a1, Col3a1, Col4a1* and *Col5a1*, were comparable between IL-18RAP$^{+/+}$, IL-18RAP$^{+/-}$ and IL-18RAP$^{-/-}$ mice, regardless of sex (Figure 5.7C-F).

5.4.7 Neither male nor female IL-18RAP deficient mice are afforded protection from renal injury associated with 1K/DOCA/salt hypertension

Histopathological scoring of hematoxylin/eosin-stained kidney sections revealed evidence of tubular damage including tubular dilatation, atrophy, and loss of epithelial brush borders in both male and female wild type (IL-18RAP$^{+/+}$) mice following 1K/DOCA/salt treatment (Figure 5.8A-D). Male and female IL-18RAP$^{+/-}$ and IL-18RAP$^{-/-}$ mice exhibited a similar amount of 1K/DOCA/salt-induced damage to their tubular architecture (Figure 5.8A-D).

5.5 Discussion

In this study we generated a novel strain of IL-18RAP-deficient mice to determine the role of this IL-18 receptor subunit in the development of high BP and CKD in a low circulating renin model of hypertension. The key novel findings were: (1) 1K/DOCA/salt-induced hypertension is associated with upregulation of IL-18RAP in the kidney in both male and female mice; (2) deletion of one or both alleles of the IL-18RAP gene caused a gene-dose-dependent reduction in renal mRNA expression and IL-18 signalling in T cells; (3) neither partial (IL-18RAP$^{+/-}$) nor full deletion (IL-18RAP$^{-/-}$) of IL-18RAP affords protection against the development of 1K/DOCA/salt-induced hypertension, renal inflammation, fibrosis and damage in either male or female mice.

We previously demonstrated that IL-18 is essential to the development of hypertension, kidney damage and dysfunction in mice treated with 1K/DOCA/salt. 1K/DOCA/salt treatment of mice was also accompanied by upregulation of both subunits of the IL-18 receptor complex — IL-18R1 and IL-18RAP — in the kidneys. Together, these findings provided a rationale for determining if inhibition of the IL-18 receptor complex would be equally as effective as directly inhibiting the IL-18 cytokine itself at preventing 1K/DOCA/salt-induced hypertension and kidney damage. In an earlier study, we showed that there were inherent challenges with using models of global and T cell specific deletion of IL-18R1. Namely, mice that were globally deficient in IL-18R1 were susceptible to the development and rupture of abdominal aortic aneurysms (AAA), while deficiency of IL-18R1 on T cells alone appeared to cause an exaggerated renal inflammatory response. Although the mechanisms for these paradoxical effects of IL-18R1 deficiency remain to be explored, we speculated that it may be due to the loss of an anti-inflammatory influence of this receptor subunit through its role in IL-37 signal transduction [10] Therefore, the current study sought to determine whether inhibition of IL-18RAP, which is thought to be involved

exclusively in IL-18 signalling,[14, 16] might afford protection against 1K/DOCA/salt-induced hypertension and renal damage.

In support of the concept that IL-18RAP may play a pathogenic role in hypertension, a recent study utilising next generation sequencing of monocytes from normotensive and hypertensive individuals identified IL-18 as one of four genes for which expression was positively correlated with mean arterial pressure.[11] Moreover, IL-18RAP expression was shown to be highly expressed in hypertensive versus normotensive patients.[11] In the present study, we too found that IL-18RAP was more highly expressed in the kidneys of hypertensive versus normotensive mice, regardless of sex. Immunofluorescence studies demonstrated that IL-18RAP was expressed on cells residing within the renal interstitium. Although we did not characterise the nature of these IL-18RAP-expressing cells, their localisation within the renal interstitium suggests that they are probably immune cells. Previously, we showed that IL-18R1 expression is also upregulated in the kidneys of 1K/DOCA/salt-treated mice and that T cells are one of the main IL-18R1-expressing cell types in this organ. While it is possible that infiltrating T cells were also the source of IL-18RAP expression in the renal interstitium of hypertensive mice, the finding in hypertensive humans that circulating monocytes express IL-18RAP raises the possibility that monocyte-derived cells (e.g., macrophages) may also have contributed to the increased IL-18RAP expression. Indeed, we have previously shown that macrophage numbers are markedly higher in kidneys from mice with 1K/DOCA/salt-induced hypertension compared to normotensive control mice.

To enable us to definitively establish whether there is a causative role for IL-18RAP in the development of hypertension and renal injury, we generated a strain of IL-18RAP-deficient mice using CRISPR Cas-9 technology. We showed that these mice were indeed deficient in IL-18RAP at the genome level, and that this was further associated with reduced mRNA and protein expression in the kidneys. Finally, we showed that splenic T cells from these

genetically modified mice failed to produce IFN-γ following *ex vivo* stimulation with IL-18 providing evidence that they were also functional knockouts. Yet, while it was evident that our novel transgenic mice were indeed IL-18RAP-deficient and had impaired T cell function, they displayed an equivalent hypertensive and renal injury response to 1K/DOCA/salt as the wild-type strain. IL-18RAP-deficient mice were also equally susceptible to development of AAA. The logical conclusion from these findings is that IL-18RAP does *not* play a causative role in the development of hypertension and renal damage, and hence, that IL-18 must mediate its effects through a non-cognate signalling pathway. Indeed, recent studies in preclinical models of AAA and atherosclerosis have identified the sodium chloride co-transporter (NCC) as a possible non-cognate target of IL-18 signalling.[17, 18] In AAA, IL-18 was shown to bind to a complex comprising IL-18R1 and NCC on adipocytes and perivascular adipose.[18] IL-18R1 and NCC were also colocalised in atherosclerotic lesions in apolipoprotein E-deficient ($ApoE^{-/-}$) mice,[17] and while either IL-18R1-deficiency (as in $IL\text{-}18R1^{-/-}/ApoE^{-/-}$ double knockout mice) or NCC-deficiency (as in $NCC^{-/}/ApoE^{-/-}$ double knockout mice) alone had no effect on atherosclerotic lesion development in $ApoE^{-/-}$ mice, knocking out both proteins (i.e. in $IL\text{-}18R1^{-/-}/NCC^{-/-}/ApoE^{-/-}$ triple knockout mice) was highly atheroprotective.[17] Furthermore, Wang *et al.* demonstrated *in vitro* that IL-18 could signal through NCC in the absence of IL-18R1 to cause the production of pro-inflammatory cytokines.[17] Overall, these results suggest that IL-18 can signal independently of its cognate receptor via NCC to cause the production of pro-inflammatory cytokines.[17] This may be relevant in the context of 1K/DOCA/salt-induced hypertension and kidney injury, as NCC is highly expressed in the distal convoluted renal tubules and is thought to play an important role in sodium reuptake in response to aldosterone.[19] We previously demonstrated that IL-18 is also localised to proximal tubular epithelial cells in the kidney and hence it is tempting to speculate that the pro-hypertensive actions of IL-18 may be at least partially mediated via paracrine/autocrine signalling through NCC. In future studies it would be interesting to determine if

1K/DOCA/salt-induced hypertension is indeed associated with IL-18 binding to NCC in the renal tubules and whether NCC-deficiency is similarly effective as IL-18-deficiency at providing protection against the development of raised BP and renal injury in this model.

Another important aspect of this study was that we used both male and female mice to determine if there were any sex-specific differences in the development of 1K/DOCA/salt-induced hypertension and kidney damage in mice, and the role of IL-18RAP thereon. We observed no sex differences in the hypertensive, renal inflammatory or fibrosis responses to 1K/DOCA/salt treatment.[20] This contrasts at least two previous studies, one in mice and one in rats, where female animals were protected from the chronic pressor effects of DOCA/salt.[20, 21] For example, *Karatas et al* reported that 1K/DOCA/salt treatment caused greater elevations in BP and a larger renal inflammatory response (as measured by CCL2 expression) in male mice than in female mice.[20] Likewise, male rats had a more pronounced hypertensive response to DOCA/salt treatment than females, with the blunted response in females attributed to a greater accumulation of Tregs and reduced accumulation of Th17 cells in the kidneys.[21] It is unclear why, in the present study, we did not observe sex differences in immune cell accumulation or expression of various inflammatory markers in the kidneys of 1K/DOCA/salt-treated animals. However, with regards to BP, it is possible that the different method we used to measure this parameter provides at least a partial explanation for the discrepancy in findings. While we employed tail cuff plethysmography to measure systolic BP, both previous studies utilised radiotelemetry.[20, 21] Radiotelemetry is generally regarded as the "gold standard" technique for assessing BP in rodents allowing for continuous measurements without the need for restraint of the animals.[13] This minimises the chance of erroneous estimations of resting BP which may arise as a result of stress or moment to moment fluctuations in BP. Thus, while we went to great care to ensure that mice were properly trained on the tail cuff machine and took the average of multiple cycles of BP recordings for each mouse at each timepoint, we cannot rule out the possibility that

subtle differences in BP between sexes went undetected. Thus, in future studies we will employ radiotelemetry to rule out this possibility.

Another potential limitation of the present study is that the mice of interest were deficient in IL-18RAP from birth. Hence, we are unable to exclude the possibility that these mice might have developed compensatory mechanisms to limit the effects of IL-18RAP deficiency. This may have masked any protective effect of IL-18RAP deficiency against 1K/DOCA/salt-induced hypertension and kidney injury. The development of a conditional (i.e., inducible) IL-18RAP knockout model or the use of acute gene silencing or an IL-18RAP neutralising antibody could address this limitation in future studies.

In summary, we have shown that CRISPR-Cas9-mediated deletion of IL-18RAP — a key subunit of the IL-18 receptor complex —— does not protect against the development of hypertension and renal injury in mice treated with 1K/DOCA/salt. These findings suggest that the pro-hypertensive and renal damaging effects of IL-18 (as previously reported) are likely mediated through yet to be defined, non-cognate signalling mechanisms. Thus, future studies aimed at characterising the signalling pathways activated downstream of IL-18 during the development of 1K/DOCA/salt hypertension may unearth targets for novel therapeutic strategies to treat hypertension and chronic kidney disease.

5.6 References

1. Ivy JR and Bailey MA. Pressure natriuresis and the renal control of arterial blood pressure. *J Physiol*. 2014;592:3955-67.

2. Zhu Q, Li X-X, Wang W, Hu J, Li P-L, Conley S and Li N. Mesenchymal stem cell transplantation inhibited high salt-induced activation of the NLRP3 inflammasome in the renal medulla in Dahl S rats. *Am. J. Physiol. Renal Physiol*. 2016;310:F621-F627.

3. Fu H, Chen J-K, Lu W-J, Jiang Y-J, Wang Y-Y, Li D-J and Shen F-M. Inflammasome-Independent NALP3 Contributes to High-Salt Induced Endothelial Dysfunction. *Front Pharmacol*. 2018;9:968-968.

4. Anders HJ and Muruve DA. The inflammasomes in kidney disease. *J Am Soc Nephrol*. 2011;22:1007-18.

5. Martinon F and Tschopp J. Inflammatory caspases and inflammasomes: master switches of inflammation. *Cell Death Differ*. 2007;14:10-22.

6. Schroder K and Tschopp J. The inflammasomes. *Cell*. 2010;140:821-32.

7. Rabkin SW. The role of interleukin 18 in the pathogenesis of hypertension-induced vascular disease. *Nat Clin Pract Cardiovasc Med*. 2009;6:192-9.

8. Gangemi S, Mallamace A, Minciullo PL, Santoro D, Merendino RA, Savica V and Bellinghieri G. Involvement of interleukin-18 in patients on maintenance haemodialysis. *Am J Nephrol*. 2002;22:417-21.

9. Cheung H, Chen NJ, Cao Z, Ono N, Ohashi PS and Yeh WC. Accessory protein-like is essential for IL-18-mediated signaling. *J Immunol*. 2005;174:5351-7.

10. Nold-Petry CA, Lo CY, Rudloff I, et al. IL-37 requires the receptors IL-18Rα and IL-1R8 (SIGIRR) to carry out its multifaceted anti-inflammatory program upon innate signal transduction. *Nat Immunol*. 2015;16:354-65.

11. Alexander MR, Norlander AE, Elijovich F, Atreya RV, Gaye A, Gnecco JS, Laffer CL, Galindo CL and Madhur MS. Human monocyte transcriptional profiling identifies IL-18 receptor accessory protein and lactoferrin as novel immune targets in hypertension. *Br J Pharmacol*. 2019;176:2015-2027.

12. Krishnan SM, Ling YH, Huuskes BM, et al. Pharmacological inhibition of the NLRP3 inflammasome reduces blood pressure, renal damage, and dysfunction in salt-sensitive hypertension. *Cardiovasc Res*. 2019;115:776-787.

13. Lerman LO, Kurtz TW, Touyz RM, et al. Animal Models of Hypertension: A Scientific Statement From the American Heart Association. *Hypertension*. 2019;73:e87-e120.

14. Schmittgen TD and Livak KJ. Analyzing real-time PCR data by the comparative CT method. *Nat Protoc*. 2008;3:1101-1108.

15. Krishnan SM, Dowling JK, Ling YH, et al. Inflammasome activity is essential for one kidney/deoxycorticosterone acetate/salt-induced hypertension in mice. *Br J Pharmacol*. 2016;173:752-65.

16. Tsutsumi N, Kimura T, Arita K, et al. The structural basis for receptor recognition of human interleukin-18. *Nat Commun*. 2014;5:5340.

17. Wang J, Sun C, Gerdes N, et al. Interleukin 18 function in atherosclerosis is mediated by the interleukin 18 receptor and the Na-Cl co-transporter. *Nat Med*. 2015;21:820-826.

18. Liu CL, Ren J, Wang Y, et al. Adipocytes promote interleukin-18 binding to its receptors during abdominal aortic aneurysm formation in mice. *Eur Heart J*. 2020;41:2456-2468.

19. Bostanjoglo M, Reeves WB, Reilly RF, et al. 11Beta-hydroxysteroid dehydrogenase, mineralocorticoid receptor, and thiazide-sensitive Na-Cl cotransporter expression by distal tubules. *J Am Soc Nephrol*. 1998;9:1347-58.

20. Karatas A, Hegner B, Windt LJd, et al. Deoxycorticosterone Acetate-Salt Mice Exhibit Blood Pressure–Independent Sexual Dimorphism. *Hypertension*. 2008;51:1177-1183.

21. Belanger KM, Crislip GR, Gillis EE, et al. Greater T Regulatory Cells in Females Attenuate DOCA-Salt-Induced Increases in Blood Pressure Versus Males. *Hypertension*. 2020;75:1615-1623.

5.7 Figures

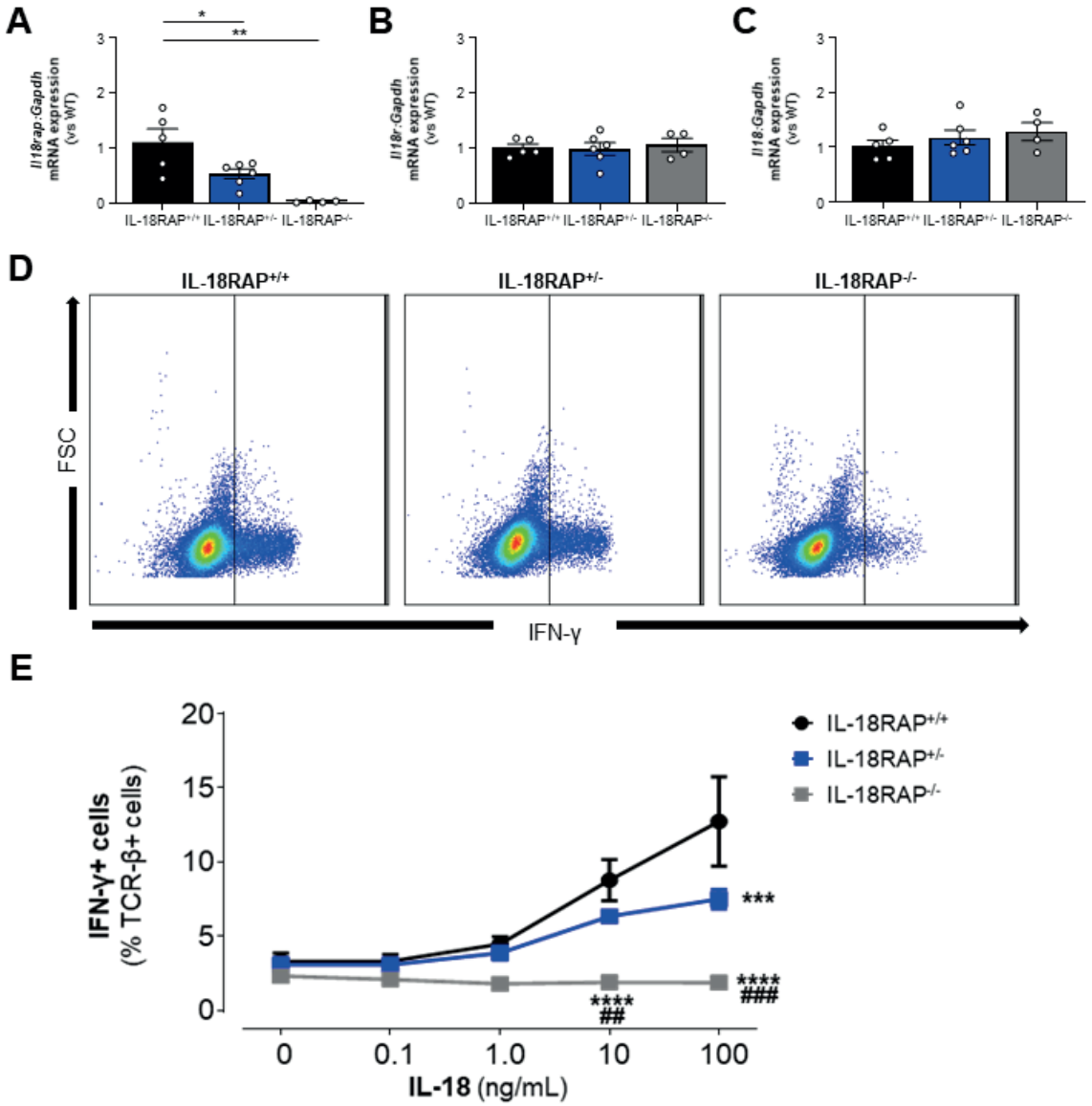

Figure 5.1 IL-18RAP gene dose influences IL-18-mediated cytokine production. Real-time PCR measurements of *Il18rap* (A), *Il18r1* (B) and pro-*Il18* (C) expression in the kidneys. Representative flow cytometric plots (D) and quantitative analysis (E) of intracellular IFN-γ production in T cells isolated from mouse kidneys and stimulated with a combination of anti-CD3/CD28 antibodies and increasing concentrations of IL-18 (0-100 ng/mL). Values are expressed as mean ± SEM from n= 4-6 experiments. ***P ≤ 0.001, **P ≤ 0.01, and *P < 0.05 vs. IL-18RAP$^{+/+}$ or ###P ≤ 0.001 and ##P ≤ 0.01 vs. IL-18RAP$^{+/=}$ for one- or two-way ANOVA followed by Bonferroni post-hoc test.

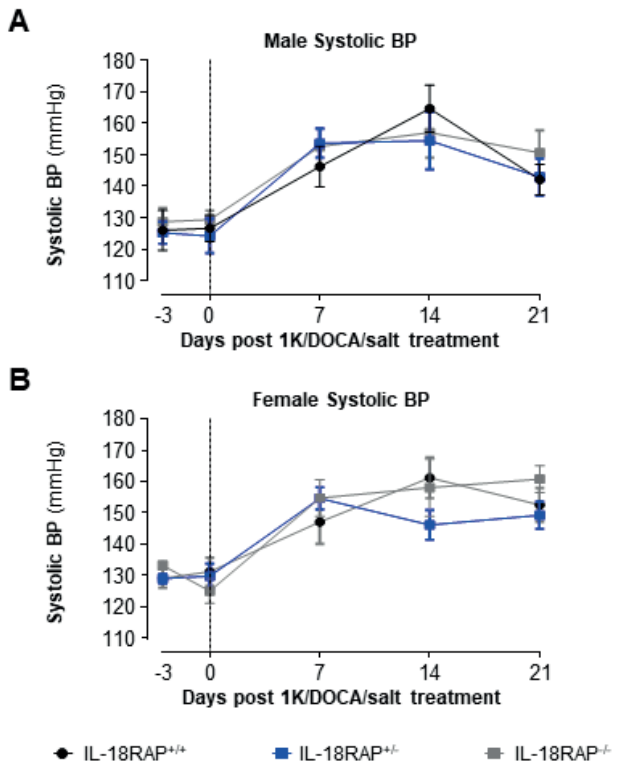

Figure 5.2 Neither male nor female IL-18RAP$^{-/-}$ mice are afforded protection from 1K/DOCA/salt-induced increases in BP. Tail cuff measurements of systolic BP in male (n=6-7; A) and female mice (n=7-13; B). Values are expressed as mean ± SEM for two-way ANOVA followed by Bonferroni post-hoc test.

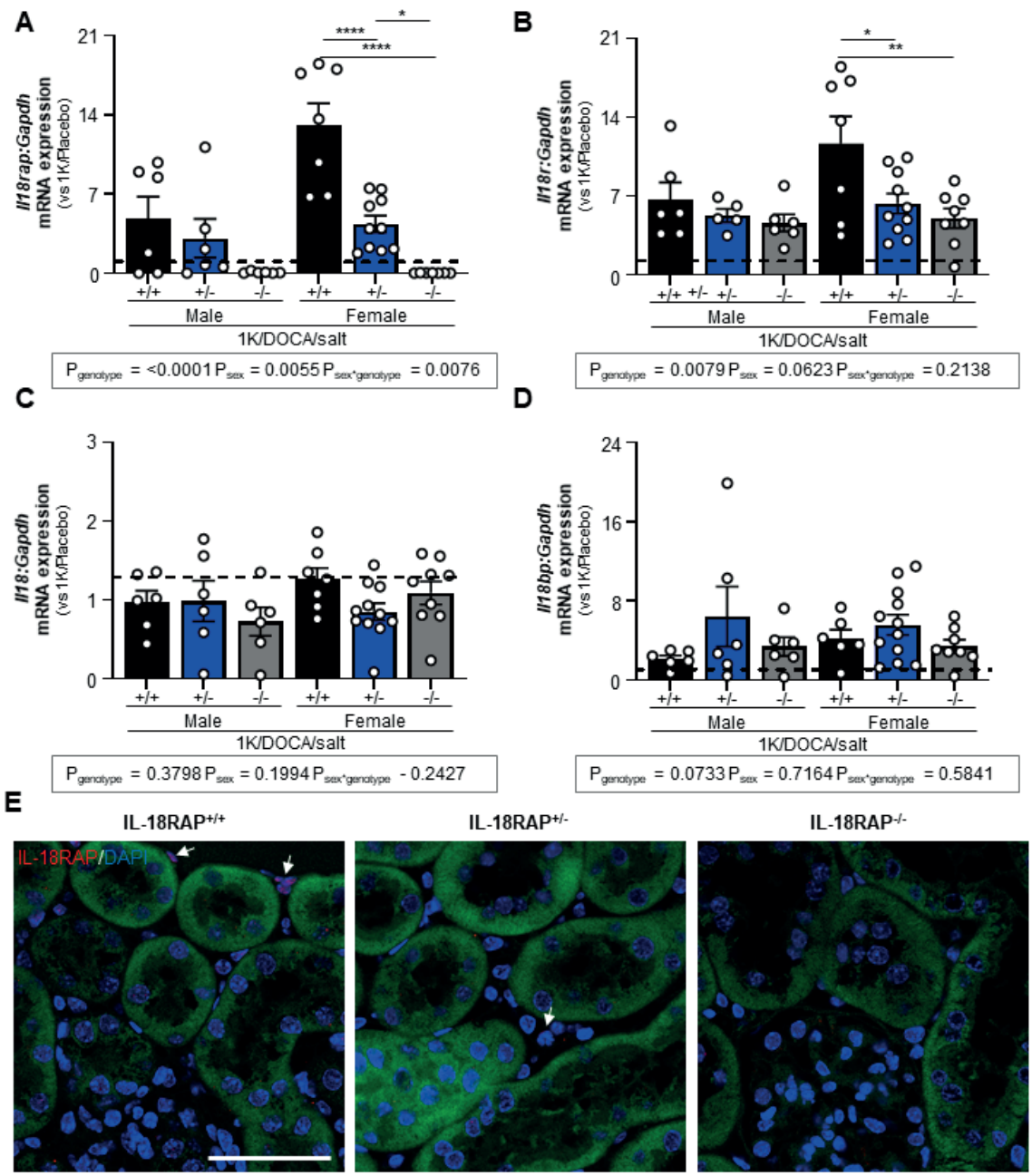

Figure 5.3 Genetic and protein gene dosing effect is present in 1K/DOCA/salt-treated IL-18RAP$^{+/+}$, IL-18RAP$^{+/-}$ and IL-18RAP$^{-/-}$ mice. Real-time PCR measurements of Il18*rap* (A), Il18r1 (B), pro-Il18 (C) and Il18bp (D) expression in the kidneys. mRNA expression is expressed as fold-change from historical placebo, which is indicated by the dotted line. Representative immunofluorescence images showing localisation of IL-18RAP (red staining, thin arrow) in mouse kidney sections (D). Images are representative of n=4-6 experiments. Scale bar = 50 µm. Values are expressed as mean ± SEM from n= 5-12

experiments. ****$P \leq 0.0001$, **$P \leq 0.01$, and *$P < 0.05$ for two-way ANOVA followed by Bonferroni post-hoc test.

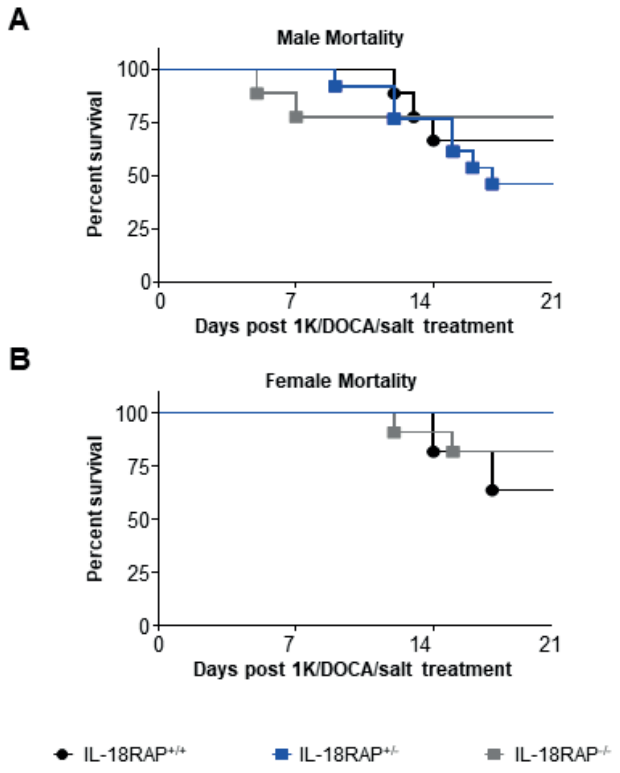

Figure 5.4 Neither male nor female IL-18RAP$^{-/-}$ mice are afforded protection from 1K/DOCA/salt-induced mortality due to the development and rupture of abdominal aortic aneurysms. Kaplan-Meier survival curves of 1K/DOCA/salt-treated IL-18RAP$^{+/+}$, IL-18RAP$^{+/-}$ or IL-18RAP$^{-/-}$ male (n=9-12; A) and female mice (n=10-12; B). Values are expressed as mean ± SEM for Log-rank (Mantel-Cox) test for Kaplan-Meier survival curve.

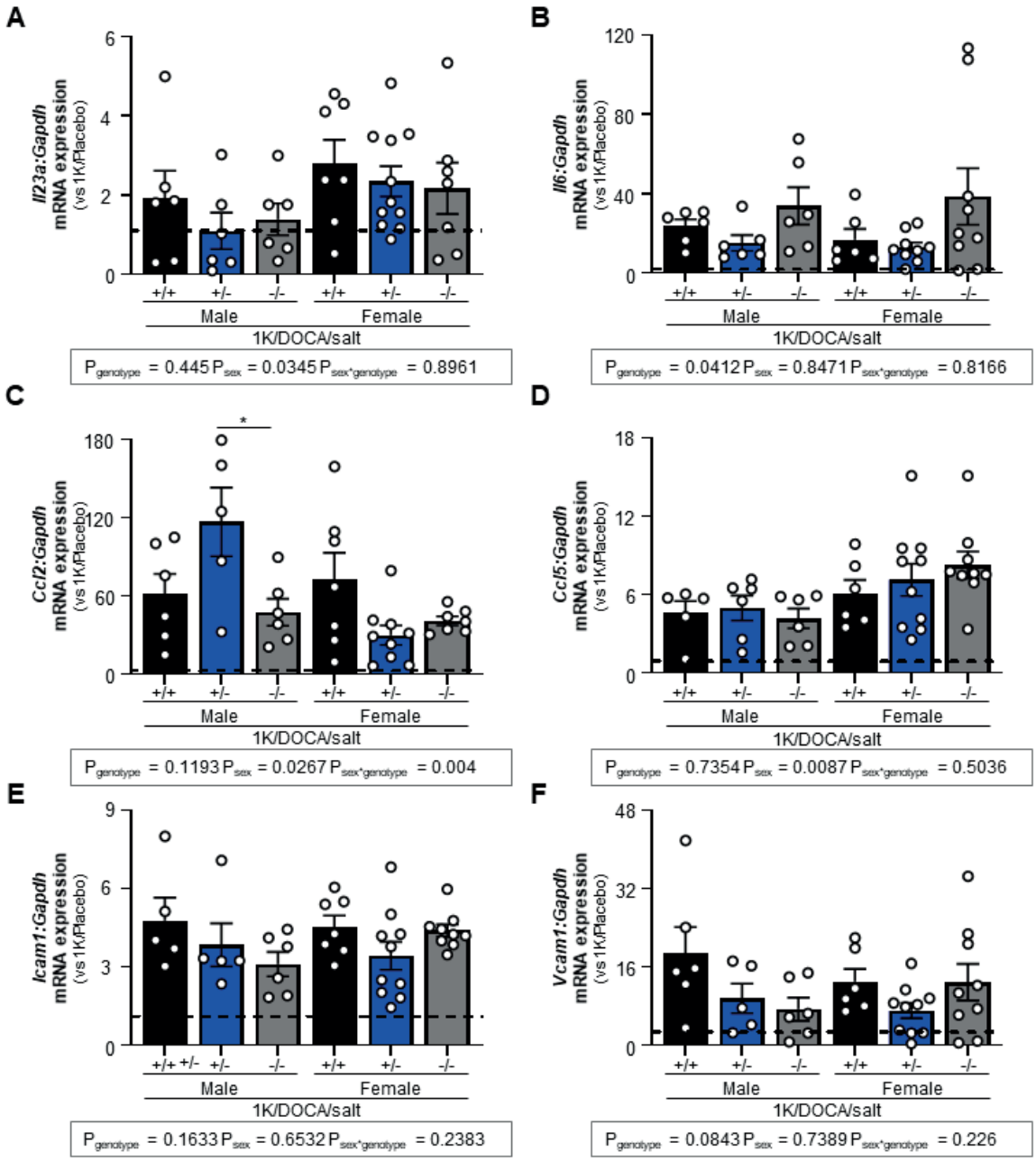

Figure 5.5 Neither male nor female IL-18RAP$^{-/-}$ mice are afforded protection from 1K/DOCA/salt-induced expression of inflammatory genes in the kidney. mRNA expression levels of the pro-inflammatory genes *Il23a* (A), *Il6* (B), *Ccl2* (C), *Ccl5* (D), *Icam1* (E), and *Vcam1* (F) as measured by real-time PCR. mRNA expression is expressed as fold-change from historical placebo, which is indicated by the dotted line. Values are expressed as mean ± SEM from n= 12-20 experiments. *P < 0.05 for two-way ANOVA followed by Bonferroni post-hoc test.

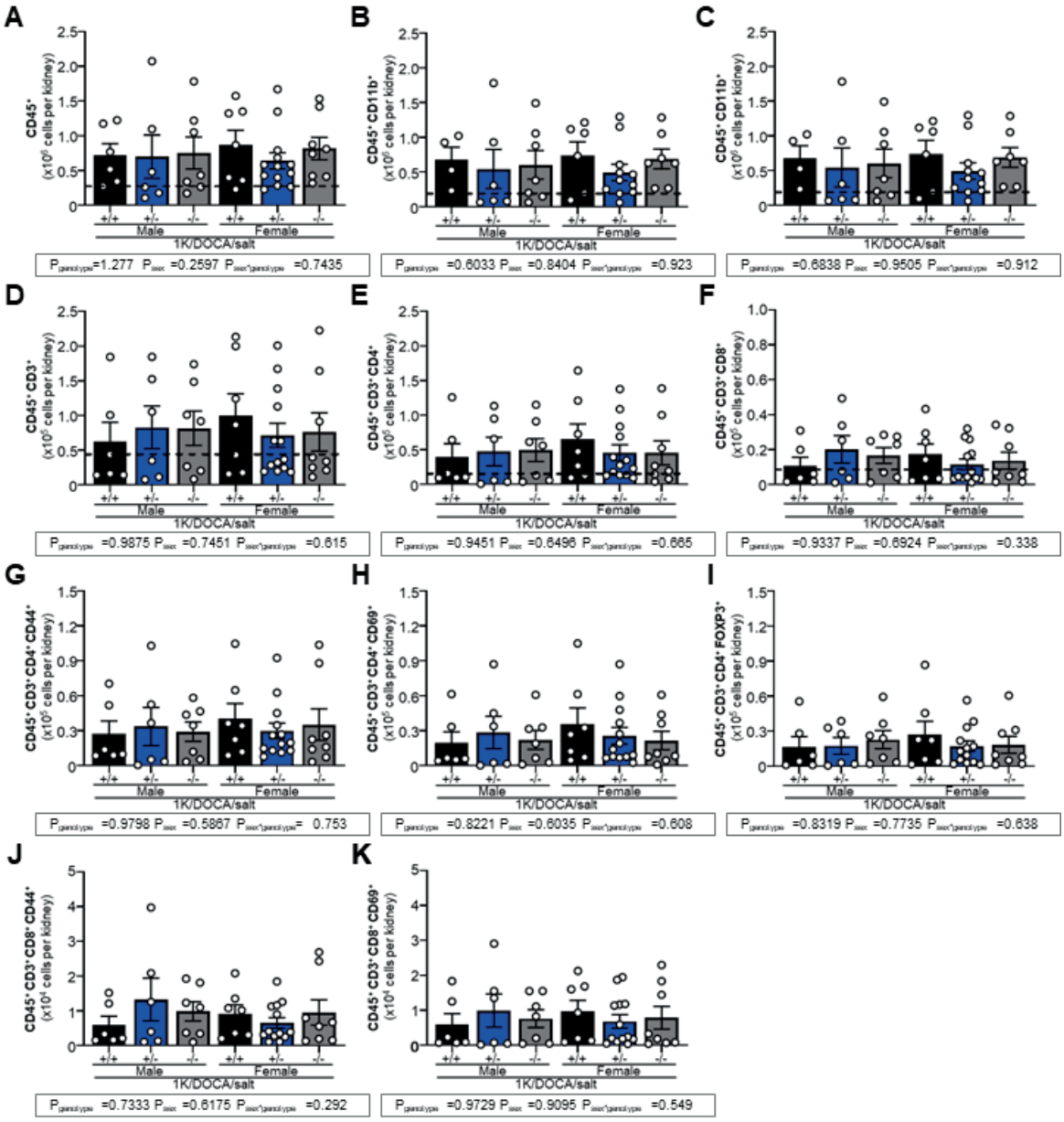

Figure 5.6 Neither male nor female IL-18RAP$^{-/-}$ mice are afforded protection from 1K/DOCA/salt-induced renal immune cell infiltration. Quantified data of total leukocytes (CD45^{+}; A), myeloid lineage cell (CD45^{+}CD11b^{+}; B), macrophage (CD45^{+}CD11b^{+}F4/80^{+}; C), CD3^{+} T cell (D), CD4^{+} T cell (E), CD8^{+} T cell (F), activated (CD44^{+}) CD4^{+} T cell (G), effector (CD69^{+}) CD4^{+} T cell (H), regulatory (FOXP3^{+}) CD4^{+} T cell (I), CD44^{+} CD8^{+} T cell (J), and CD69^{+} CD8^{+} T cell (K) populations in the kidney measured by flow cytometry. Historical placebo mean is indicated by the dotted line. Values are expressed as mean ± SEM from n= 12-20 experiments for two-way ANOVA.

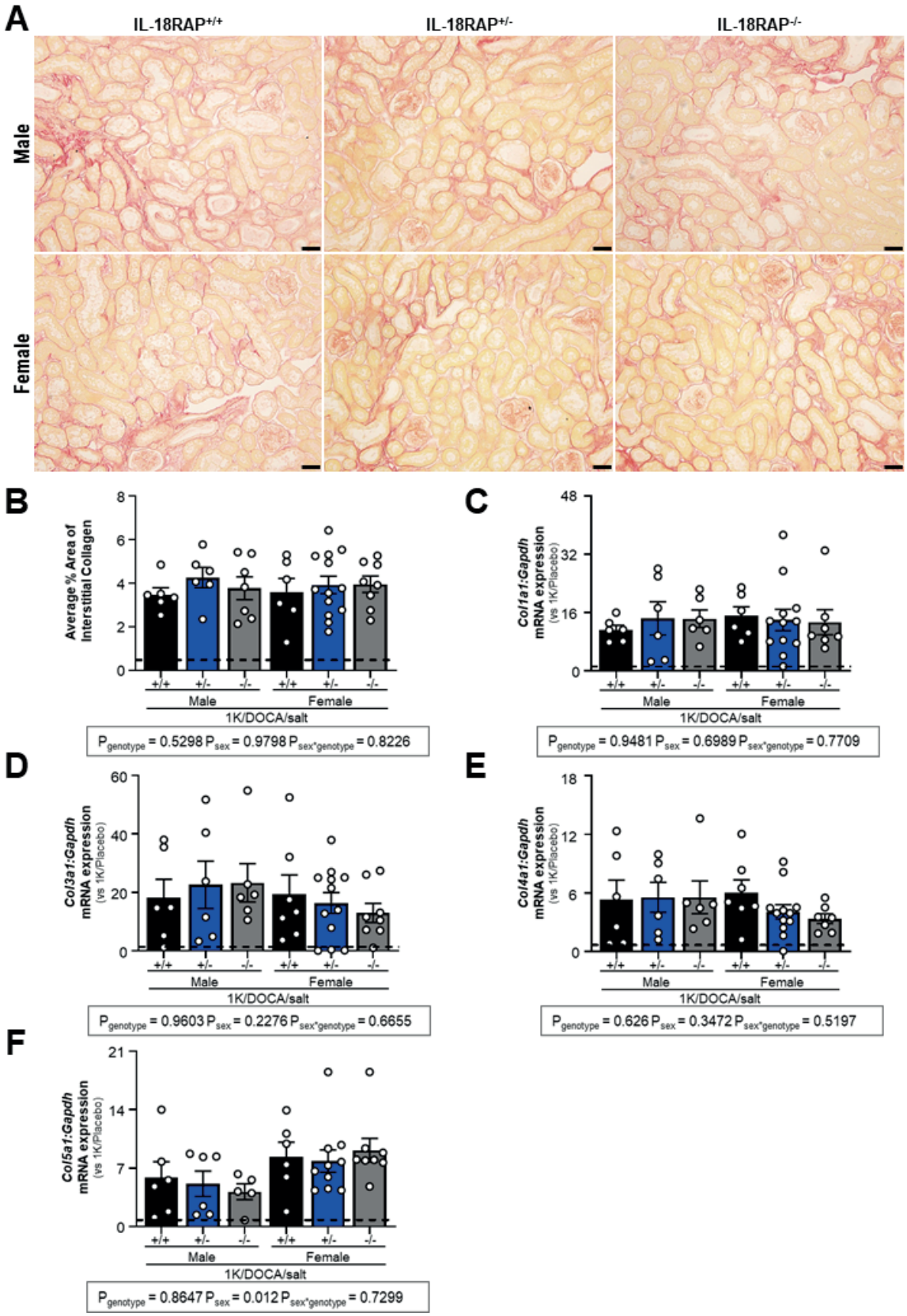

Figure 5.7 Neither male nor female IL-18RAP$^{-/-}$ mice are afforded protection from renal fibrosis associated with 1K/DOCA/salt hypertension. Representative brightfield images of kidney sections stained with picrosirius red staining from 1K/DOCA/salt-treated

male and female IL-18RAP$^{+/+}$, IL-18RAP$^{+/-}$ and IL-18RAP$^{-/-}$ mice (A). Mean area of collagen deposition using brightfield microscopy (B). Scale bars = 100 µm. Renal mRNA expression levels of the collagen α-subunits *Col1a1* (C), *Col3a1* (D), *Col4a1* (E) and *Col5a1* (F) as measured by real-time PCR. mRNA expression is expressed as fold-change from historical placebo mean value and dotted line indicates historical placebo mean value. Values are expressed as mean ± SEM from n= 12-20 experiments for two-way ANOVA.

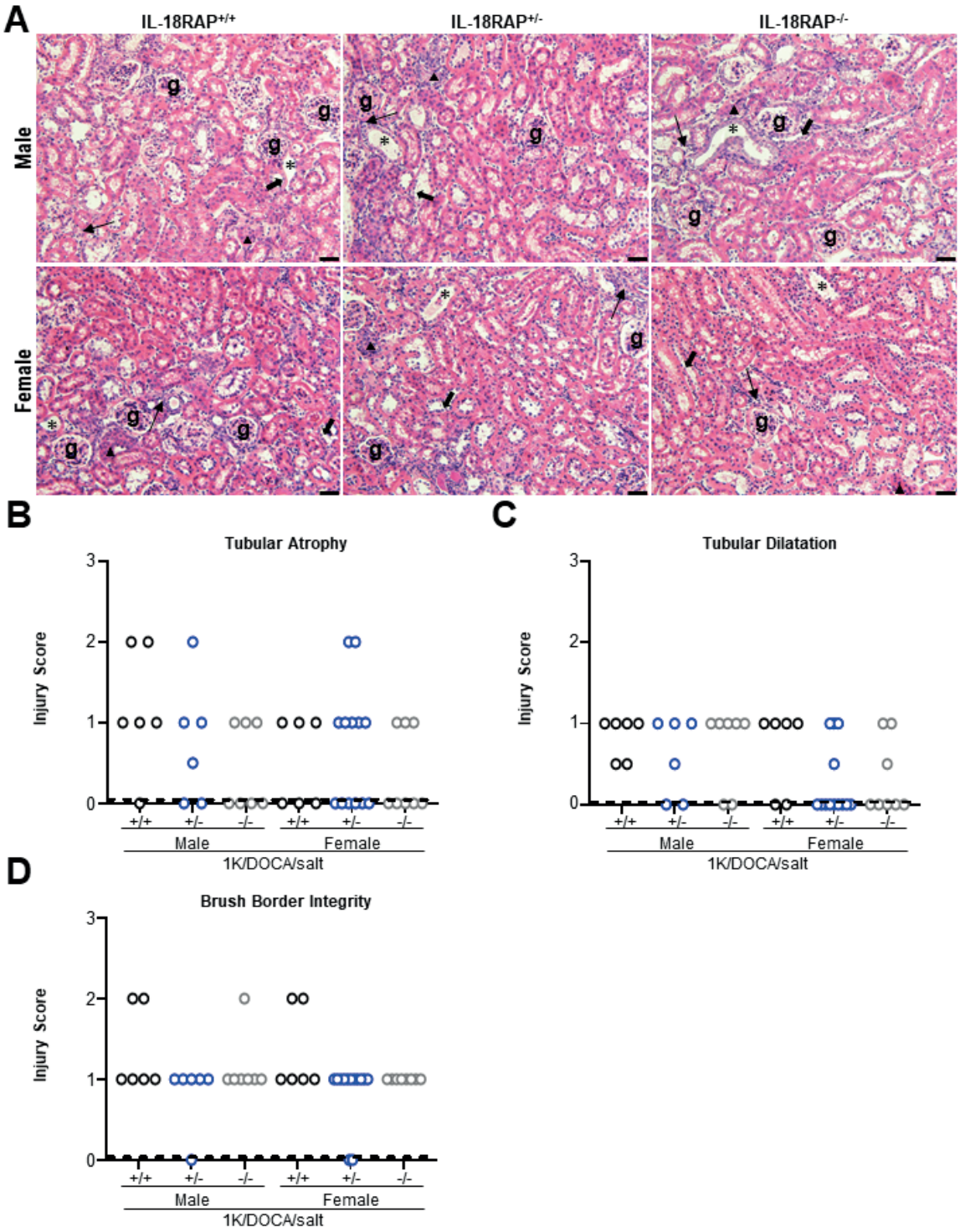

Figure 5.8 Neither male nor female IL-18RAP$^{-/-}$ mice are afforded protection from renal tubular damage in 1K/DOCA/salt-induced hypertension. Representative brightfield images of kidney sections stained with haematoxylin/eosin-stained from 1K/DOCA/salt-treated male and female IL-18RAP$^{+/+}$, IL-18RAP$^{+/-}$ and IL-18RAP$^{-/-}$ mice(A). Historical placebo mean is indicated by the dotted line. Histopathological scoring of tubular atrophy (arrowhead), tubular dilatation (*) and loss of brush border integrity

(thick arrow; B-D). Thin arrow = inflammatory cell infiltrates; g = glomeruli. Scale bars = 100 µm. Values are expressed as the median histological score (n=12-20).

5.8 Supplementary tables

Table 5.1 Mice used for this study

Origin	Sex	Mouse strain	# of mice	Age at treatment (weeks)	Weight at treatment (g)	Deaths
LARTF	Female	IL-18RAP$^{+/+}$	11	13-20	21-27	4*
			5			
		IL-18RAP$^{+/-}$	12	13-20	20-25	
			4			
		IL-18RAP$^{-/-}$	10	13-21	21-29	2*
			2			
	Male	IL-18RAP$^{+/+}$	9	12-19	27-35	3*, 1†
		IL-18RAP$^{+/-}$	12	12-19	28-36	7*
			1			
		IL-18RAP$^{-/-}$	9	12-19	27-38	2*, 1†
			3			
	Male	C57Bl/6	15	8-12	24-30	2 *, 2 †
	Female		15	8-12	18-22	1 *, 1 †
*= Aneurysm †= surgical wound opening/fight wounds						

Table 5.2 Antibody panel for flow cytometry

Antigen	Host/Isotype	Clone	Tag	Dilution Factor	Company
CD45	Rat IgG2b, κ	30-F11	A700	1:500	BioLegend, USA
CD3e	Hamster IgG	145-2C11	APC	1:500	BioLegend, USA
CD4	Rat IgG2a, κ	RM4-5	BV605	1:500	BioLegend, USA
CD8a	Rat IgG2a, κ	53-6.7	BV605	1:1000	BioLegend, USA
CD11b	Rat IgG2b, κ	M1/70	BV421	1:500	BioLegend, USA
F4/80	Rat IgG2a, κ	BM8	APC Cy7	1:500	BioLegend, USA
CD69	Rat IgG2a, κ	C068C2	BV650	1:500	BioLegend, USA
CD44	Rat IgG2a, κ	XMG1.2	PERCP	1:500	BioLegend, USA
IL-18R	Rat IgG2a, κ	P3TUNYA	PE	1:500	Invitrogen, USA
FoxP3	Rat IgG2a, κ	FJK-16s	FITC	1:500	eBioscience, USA
TCR-β	Hamster IgG	H57-597	APC	1:500	BioLegend, USA
IFN-γ	Rat IgG2a, κ	DB-1	FITC	1:500	Invitrogen, USA

5.9 Supplementary Figures

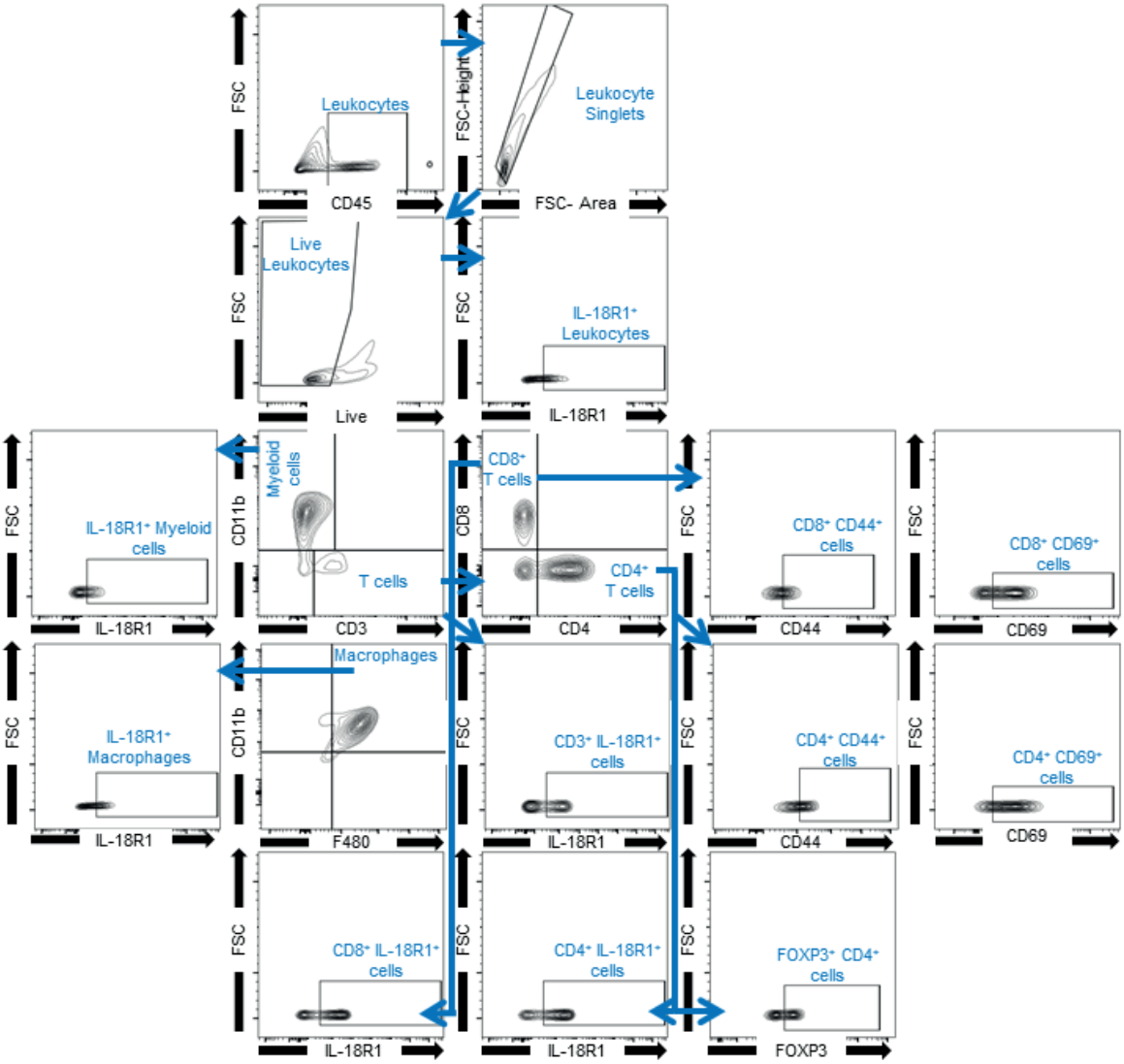

Supplementary Figure 5.1 Gating strategy for flow cytometric analysis. Leukocytes were gated as CD45$^+$ populations against forward scatter (FSC). Total leukocytes, i.e., live leukocyte singlets, were gated by FSC -height vs FSC-area, and exclusion of dead cells (live/dead stain). Total leukocytes were then divided into myeloid cells (CD11b$^+$) and T cells (CD3$^+$). Some of the myeloid cells were identified as macrophages (CD11b$^+$F4/80$^+$), and the macrophages were further classified as IL-18R11$^+$. T cells that were positive for CD3 staining were further classified as IL-18R1$^+$, CD4$^+$, or CD8$^+$ T cells. CD4$^+$ and CD8$^+$ cells were further identified as being CD44$^+$, CD69$^+$ or FOXP3$^+$.

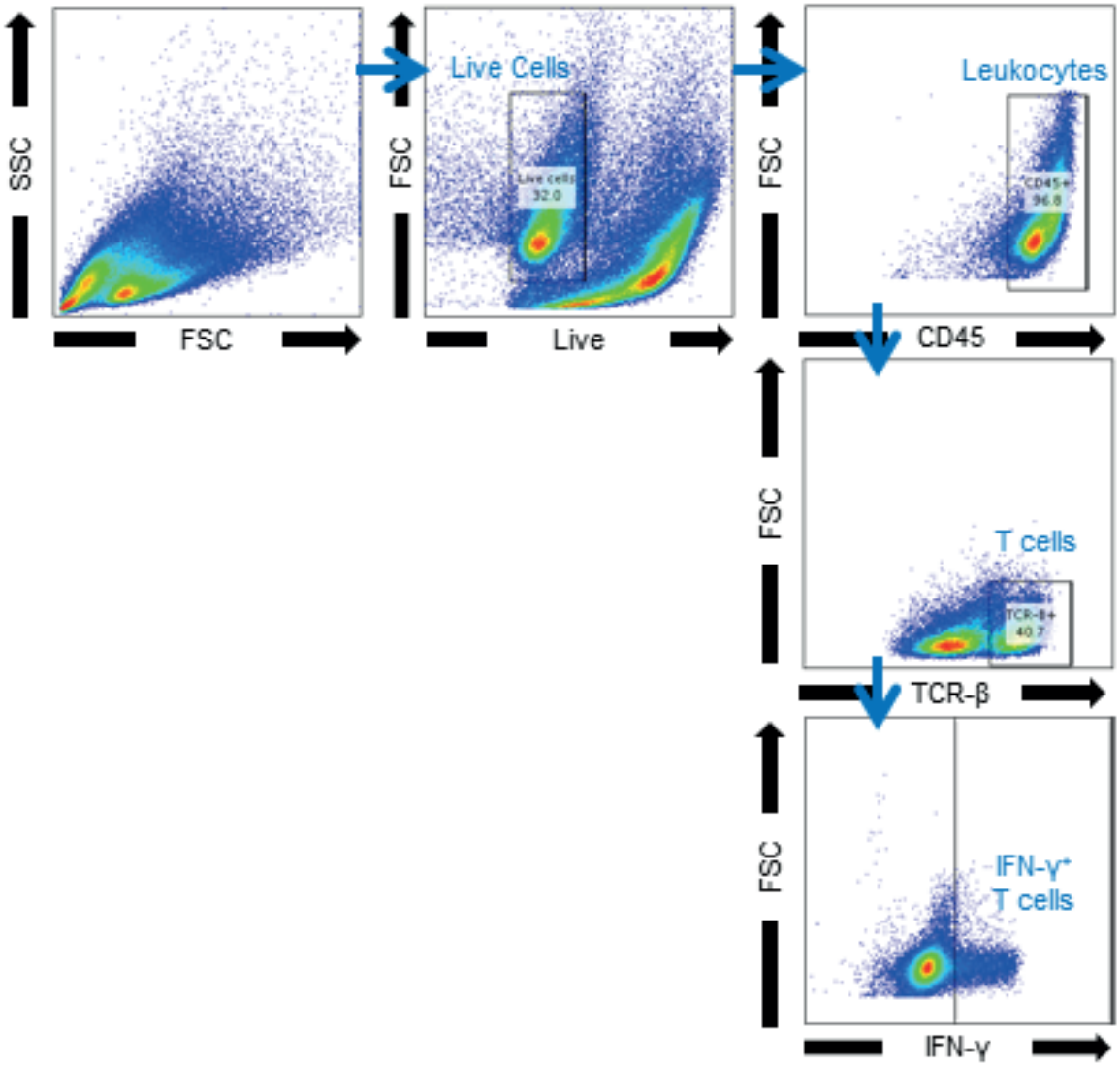

Supplementary Figure 5.2 Gating strategy for intracellular cytokine detection using flow cytometric analysis. Dead cells (live/dead stain) were excluded before leukocytes were gated as $CD45^+$ populations against forward scatter (FSC). Total leukocytes were classified as being T cells ($TCR\text{-}\beta^+$) and then divided into $IFN\text{-}\gamma^+$ or $IL\text{-}17^+$ populations.

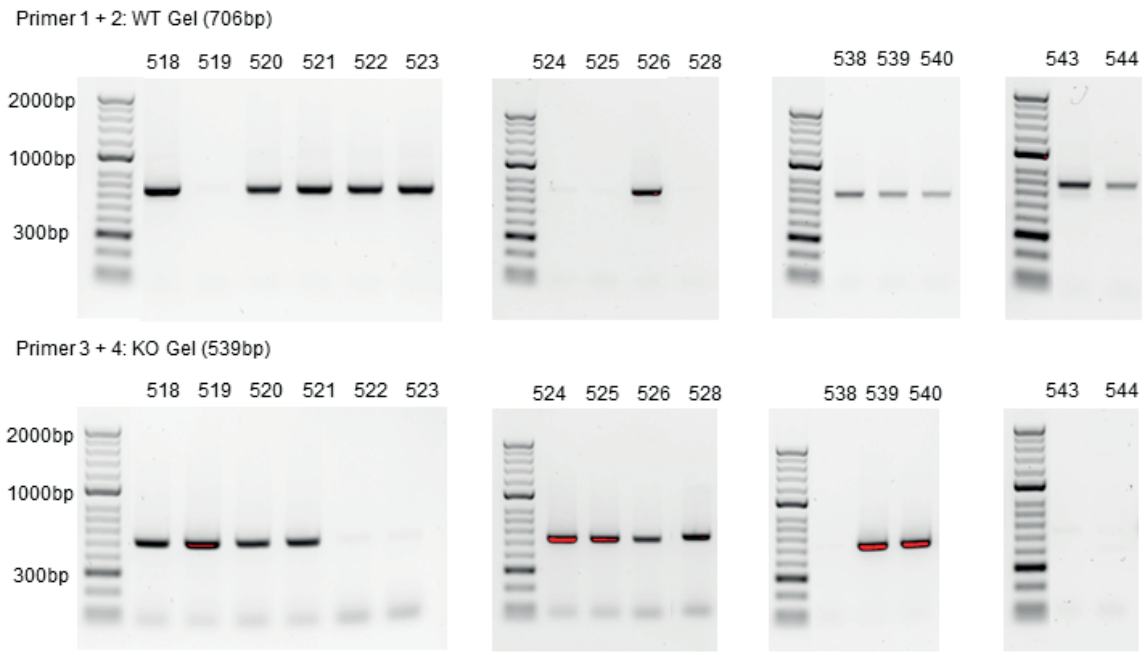

Genotype	WT band	KO band	Mouse IDs
WT homozygote (IL-18RAP$^{+/+}$)	+	-	522, 523, 538, 543, 544
Heterozygote (IL-18RAP$^{+/-}$)	+	+	518, 520, 521, 526, 539, 540
KO homozygote (IL-18RAP$^{-/-}$)	-	+	519, 524, 525, 528

Supplementary Figure 5.3 Genotype results for IL-18RAP knockout mice. A band present at 706bp in gels for primers 1+2 and at 539bp for primers 3+4 indicates that the mouse has a wild type (WT; IL-18RAP$^{+/+}$) genotype, whilst a band present at 706bp in gels for primers 1+2 and no band present at 539bp for primers 3+4 indicates that the mouse has a heterozygous (IL-18RAP$^{+/-}$) genotype. No bands present at 706bp in gels for primers 1+2 and at 539bp for primers 3+4 indicates that the mouse has a homozygous (IL-18RAP$^{-/-}$). Gels are representative of mice used in Figure 1.

Chapter 6

General Discussion

6.1 Summary of key findings

The data presented in this thesis, along with findings by others in models of acute kidney injury (AKI) and chronic kidney disease (CKD), and human patients,[1-6] provides compelling evidence that the inflammasome-derived pro-inflammatory cytokine, interleukin-18 (IL-18), plays a crucial role in the development of kidney inflammation that ultimately manifests as renal dysfunction and hypertension. First, we showed that one kidney/deoxycorticosterone acetate/salt (1K/DOCA/salt)-induced hypertension was associated with upregulation of the IL-18 signalling system in the kidney, with IL-18 generated primarily by tubular epithelial cells (TECs) while the IL-18 receptor (IL-18R1) was localised to both TECs and $CD3^+$ T cells. We showed that *ex vivo* stimulation of T cells isolated from 1K/DOCA/salt-treated mice with IL-18 causes them to produce the pro-inflammatory cytokine interferon-γ (IFN-γ). Global deletion of IL-18 is protective against the development of kidney inflammation, fibrosis, and high blood pressure (BP) in 1K/DOCA/salt-treated mice, and we found that it was likely TEC-derived, and not macrophage-derived IL-18, that was responsible for 1K/DOCA/salt pathology. Surprisingly, deficiency of IL-18R1 — one of two key subunits of the IL-18 receptor — afforded only partial protection, while mice deficient in IL-18 receptor accessory protein (IL-18RAP) — the other subunit of the IL-18 receptor — were not protected. Therefore, this research suggests that IL-18, but not its cognate receptor complex comprising IL-18R1-IL-18RAP, may represent a promising target for the treatment of the kidney inflammation that leads to hypertension.

6.2 IL-18-IL-18R1-IL-18RAP signalling axis in CKD

It is well established that IL-18 plays a key role in initiating the immune response in the kidney by initiating the production of other pro-inflammatory cytokines, chemokines and adhesion molecules[2, 7] via the activation of its receptor complex IL-18R1-IL-18RAP.[8] IL-18 can also directly,[9] and indirectly via these mediators of inflammation, facilitate the

chemoattraction of immune cells into the kidney.[2, 10] Thus, IL-18 production in the kidney causes a feed-forward mechanism that amplifies inflammation and damage in the kidney.

In Chapter 3, we demonstrated that 1K/DOCA/salt treatment caused an increase in the expression of the adhesion molecules intercellular adhesion molecule (ICAM)-1 and vascular adhesion molecule (VCAM)-1, the cytokines IL-23 and IL-6, and the chemokines chemokine (C-C) motif ligand (CCL)2 and CCL5 in the kidney. This was accompanied by an increase in the infiltration of the kidney by leukocytes, myeloid cells, macrophages, and T cells, whereas both pro-inflammatory gene expression and leukocyte infiltration into the kidney were blunted in 1K/DOCA/salt-treated IL-18$^{-/-}$ mice. These results are consistent with inhibition of the IL-18-IL-18R1-IL-18RAP signalling axis.

In Chapters 4 and 5, we aimed to determine whether inhibition of the IL-18 receptor complex was effective in limiting IL-18 induced kidney inflammation and damage in a preclinical model of hypertension and CKD. To our surprise, neither global IL-18R1-deficiency, T cell specific IL-18R1-deficiency, nor IL-18RAP deficiency were effective at reducing inflammation or damage in the kidneys of 1K/DOCA/salt-treated mice. However, consistent with our findings, previous studies have demonstrated that IL-18R1$^{-/-}$ mice developed kidney dysfunction and inflammation in preclinical models of AKI,[11, 12] and that both IL-18R1 and IL-18RAP inhibition were ineffective at limiting cisplatin-induced AKI.[11] However, to date, no studies have compared the effect of the deficiency of each of the components of the IL-18-IL-18R1-IL-18RAP signalling complex on kidney inflammation in the 1K/DOCA/salt model of hypertension and CKD.

Considering the profound protection that IL-18-deficiency affords mice against the development of 1K/DOCA/salt-induced high BP and kidney inflammation, it may seem somewhat surprising that IL-18R1$^{-/-}$ mice were not equally protected from 1K/DOCA/salt-induced immune cell infiltration of the kidney and were susceptible to the development and rupture of abdominal aortic aneurysms (AAAs). Indeed, it seems as though IL-18R1$^{-/-}$ mice

are protected from 1K/DOCA/salt-induced elevated BP at day 21 post-surgery, however these effects are confounded by the high mortality rate due to AAA. This lack of protection conferred by IL-18R1-deficiency may be attributed to the dual pro- and anti-inflammatory role of this receptor subunit. In humans, IL-37 signals through IL-18R1 to limit inflammation by engaging IL-1R8, which has a non-functional TIR domain and prevents the activation of the MyD88 pathway.[13, 14] In a preclinical model of endotoxemia, Nold-Petry *et al*. used human IL-37 transgenic mice to demonstrate that IL-18R1 is essential to the anti-inflammatory signalling of this ligand,[13] however a mouse homologue for IL-37 is yet to be identified. Alternatively, Nozaki *et al*. reported that inhibition of suppressors of cytokine signalling (SOCS) could be a potential explanation for a lack of protection from cisplatin-induced AKI in IL-18R1$^{-/-}$ mice.[11] IL-18R1$^{-/-}$ mice were not afforded protection from the renal expression of pro-inflammatory cytokines following cisplatin treatment because SOCS activity is inhibited in the absence of this receptor, and indeed SOCS-1 and -3 expression in the kidney were downregulated when IL-18R1 is absent.[11] Whether SOCS are inhibited by IL-18R1-deficiency in the 1K/DOCA/salt model of hypertension and CKD remains unclear. Thus, IL-18R1-deficiency not only ablates IL-18-mediated signalling, but also a potential IL-37-like anti-inflammatory pathway, that may be protective, particularly in vascular pathologies such as AAA. The augmented mortality due to AAA confounded the role of IL-18 acting on the IL-18R1.

In order to circumvent the high rate of mortality due to the development and rupture of AAAs in 1K/DOCA/salt-treated IL-18R1$^{-/-}$ mice, we performed adoptive transfer studies, where RAG1$^{-/-}$ mice received IL-18R1$^{-/-}$ T cells. We hypothesised that mice that received IL-18R1$^{-/-}$ T cells would be protected from the development of 1K/DOCA/salt-induced hypertension and kidney inflammation, as 1K/DOCA/salt-treated WT mice have increased T cell accumulation in the kidneys — a large proportion of which were IL-18R1^{+}. Furthermore, stimulation of IL-18R1^{+} T cells enriched from 1K/DOCA/salt-treated mice

caused a dose-dependent increase in IFN-γ production which was absent in 1K/placebo-treated mice. While T cell-restricted IL-18R1-deficiency was found to be protective against the development of elevated BP and the development of AAAs in response to 1K/DOCA/salt treatment, it did not prevent the development of kidney inflammation. A potential explanation for the apparent lack of protection from the development of kidney inflammation and damage in mice with T cell-restricted IL-18R1-deficiency is that other cell types, like TECs in the kidney, express IL-18R1. Preclinical models of unilateral ureteral obstruction (UUO)-induced AKI revealed that IL-18R1 is expressed mainly in TECs in the obstructed kidney,[3, 4] and hypoxia induces IL-18R1 expression in TECs *in vitro*.[15] Furthermore, IL-18R1 was localised to TECs in biopsies from healthy and diseased human kidneys.[16] Indeed, in Chapter 3, we demonstrated that IL-18R1 was also highly expressed on TECs within the kidney, suggesting that these cells may represent an autocrine/paracrine target of IL-18 signalling. Vanderbrink *et al.* revealed that both IL-18 and IL-18R1 were localised to TECs and proposed that IL-18 and IL-18R1 interact in a feed forward mechanism to increase IL-18 production, as IL-18 expression is reduced in IL-18R1$^{-/-}$ mice with UUO-induced AKI.[4] *In vitro* stimulation of neutrophils with endogenous and exogenous IL-18 also revealed that IL-18 acts to increase its own expression.[17] Therefore, future studies should determine whether TECs or bone marrow-derived cells expressing IL-18R1 are the main targets of IL-18 in 1K/DOCA/salt-induced hypertension and kidney disease via bone marrow transplant between WT and IL-18R1$^{-/-}$ mice or via tissue-specific IL-18R1-deficiency.

To bypass the deleterious effects of IL-18R1-deficiency that may have been caused by additional anti-inflammatory pathways mediated by IL-18R1, we developed IL-18RAP$^{-/-}$ mice using CRISPR-Cas9 to ascertain whether inhibiting the IL-18 pathway is successful in limiting IL-18-induced kidney inflammation and damage. IL-18RAP dimerises with IL-18-bound IL-18R1 to form a high affinity receptor complex, which then activates MyD88

signalling pathways, only in response to IL-18 signalling.[18, 19] We hypothesised that, due to its important role in engaging pro-inflammatory pathways in response to IL-18 signalling, IL-18RAP-deficiency would afford mice protection from the development of 1K/DOCA/salt-induced high BP and kidney damage. However, we demonstrated that although there was a gene dosing effect on IL-18RAP mRNA expression, protein expression and the downstream production of IFN-γ in response to full (IL-18RAP$^{-/-}$) and partial (IL-18RAP$^{+/-}$) deficiency, 1K/DOCA/salt-treated mice were not afforded protection from the development of hypertension and kidney injury. In combination with our observations in 1K/DOCA/salt-treated IL-18R1$^{-/-}$ mice, these finding led us to hypothesise that IL-18 may be acting through non-canonical signalling pathways in hypertension and CKD.

There is evidence that IL-18 can activate the sodium chloride cotransporter (NCC) in the presence or absence of IL-18R1 in preclinical models of atherosclerosis and AAA.[20, 21] Mass spectrometry of immunoprecipitated IL-18-treated endothelial cells from ApoE$^{-/-}$IL-18R1$^{-/-}$ mice revealed that IL-18 binds to NCC, and further immunoprecipitation and immunoblotting experiments on peritoneal macrophages from ApoE$^{-/-}$ mice revealed that IL-18R1 and NCC form a complex with IL-18.[20] Triple immunofluorescence staining confirmed that IL-18, IL-18R1 and NCC are colocalised on multiple cell types (macrophages, T cells, vascular smooth muscle cells and endothelial cells) in human AAA lesions.[21] Double deficiency of IL-18R1 and NCC — but not deficiency in just one of IL-18R1 or NCC — was protective against atherosclerotic progression, immune cell infiltration of the atherosclerotic lesion and increased plasma levels of pro-inflammatory cytokines in ApoE$^{-/-}$ mice. [20] Further *in vitro* studies using IL-18-stimulated macrophages demonstrated that this protection from pro-inflammatory cytokine production was due to inhibition of downstream ERK1/2 or p38 signal kinases which were unable to undergo phosphorylation in the absence of IL-18R1 and NCC. [20] Similar to the *in vivo* results,

phosphorylation of these signal kinases still occurred in cells that were only deficient in one of these receptors. [20] Altogether, these results suggest that IL-18R1 and NCC are both required for IL-18-dependent pro-inflammatory signalling and injury in models of atheroscelrosis and AAA. [20, 21]

The involvement of NCC in IL-18 signalling may be particularly relevant in the context of 1K/DOCA/salt hypertension and CKD, given that one of the main NCC-expressing cell types are epithelial cells from the distal convoluted tubule, which are highly sensitive to aldosterone.[22] In Chapter 3, we observed that IL-18R1 was also expressed on TECs, and — although not shown in Chapter 3 — immunofluorescent imaging of the inner medulla revealed that IL-18R1 is highly expressed on collecting ducts in this region as well (Figure 6.1). It is curious that IL-18 is produced in proximal TECs in the kidney, yet its putative receptor complex, IL-18R1-NCC, is expressed on collecting ducts. This raises the hypothesis that IL-18 is involved in the homeostatic control of salt reabsorption by the kidney. That is, that high concentrations of salt in the proximal tubule leads to upregulation of NLRP3 and production of IL-18. IL-18 is detectable in the urine in patients with kidney injury,[6, 23, 24] and it is tempting to speculate that the urinary transport of IL-18 may allow for its paracrine signalling along the nephron. IL-18 may then be able to stimulate IL-18R1/NCC on the distal tubules and thereby cause increased Na^+ reabsorption (Figure 6.2). Therefore, future studies could focus on understanding the interactions between IL-18 and NCC within the tubules using tissue-specific IL-18/IL-18R1/NCC knockout mice and *ex vivo* models to determine how IL-18 interacts to influence physiological and pathophysiological processes within the kidneys including sodium (Na^+) reabsorption, inflammation, and interstitial collagen deposition.

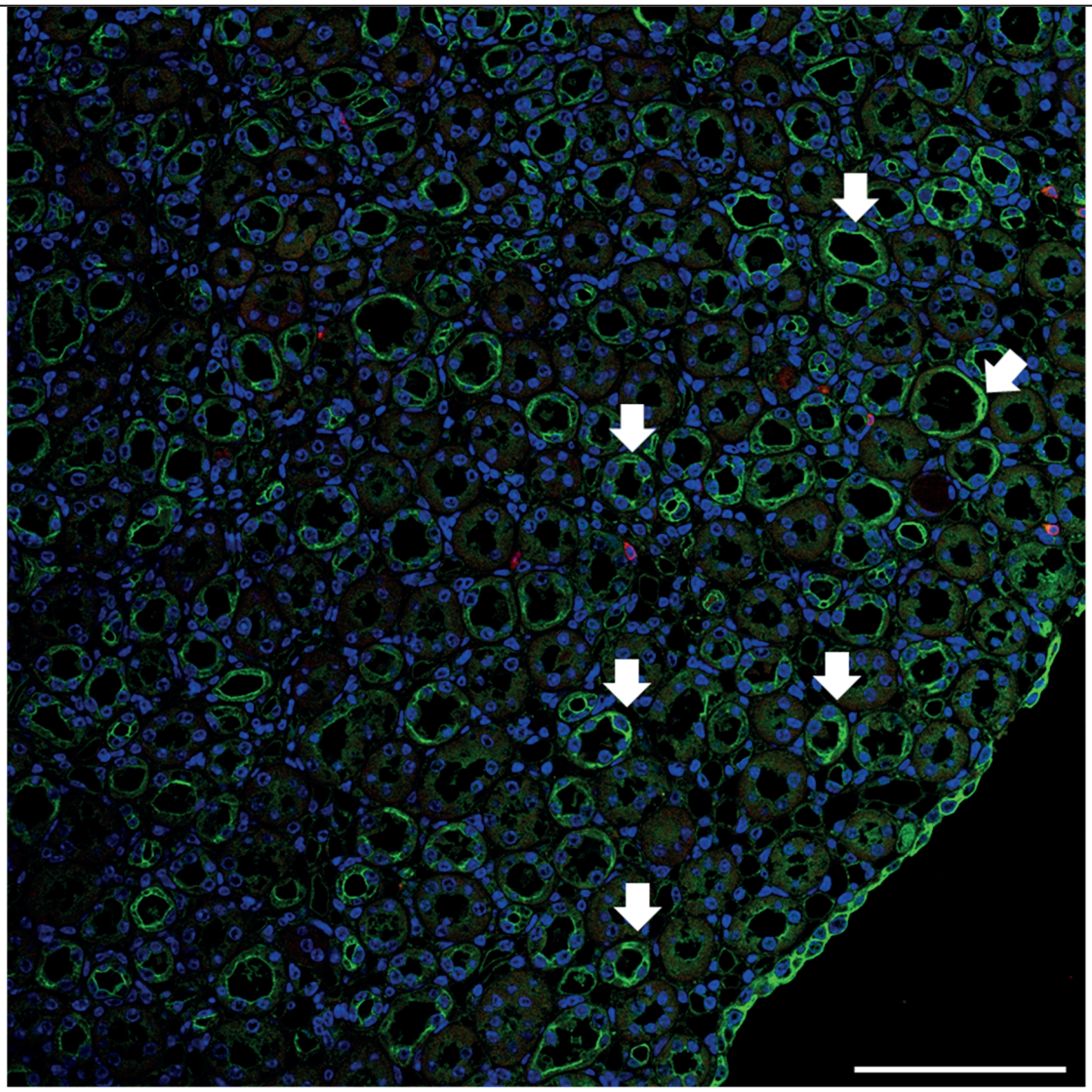

Figure 6.1 Immunolocalisation of IL-18R1 in the papilla of 1K/DOCA/salt-treated mouse kidney sections. Representative immunofluorescence images showing localisation of CD3+ T cells (red staining), IL-18R1 (green staining) and co-localisation of T cells and IL-18R1 (orange staining) in the papilla of kidney sections from 1K/DOCA/salt-treated WT mice. Bold arrows denote tubular epithelial cell staining. Images are representative of n=6 experiments. Scale bar = 100 µm

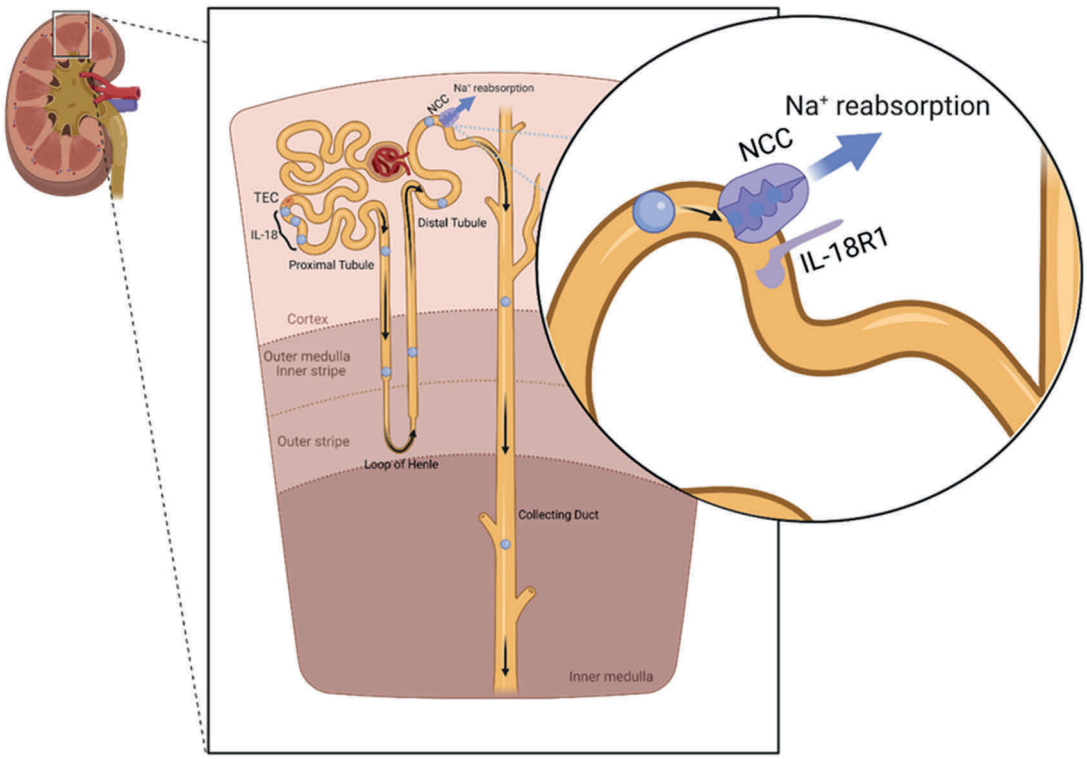

Figure 6.2 Hypothetical mechanism by which IL-18 regulates sodium (Na+) homeostasis in the kidney. We have shown that 1K/DOCA/salt-treatment causes the production of IL-18 in tubular epithelial cells. IL-18R1 and NCC are expressed in tubules and distal tubule cells respectively, and IL-18 may act on them in a paracrine fashion, transported via the urine, to regulate Na+ reabsorption in the kidney. Created with BioRender.com.

6.3 Stimuli for IL-18 production

Previous research from our lab and others has demonstrated that the NOD-like receptor family pyrin domain-containing protein (NLRP3) inflammasome and its adaptor protein apoptosis-associated speck like protein containing a caspase recruitment domain (ASC) are essential for the development of kidney disease and hypertension in preclinical models.[25-29] The data presented in this thesis suggests that the pro-inflammatory cytokine, IL-18, is an important mediator of the pro-inflammatory effects of inflammasome activity in the kidney. Furthermore, a combination of reciprocal bone marrow transplant and immunohistochemistry studies revealed that TECs, rather than immune cells, are the main source of IL-18 in the 1K/DOCA/salt model of hypertension and CKD. However, the current study did not investigate the stimulus for IL-18 production in TECs.

The NLRP3 inflammasome is a multimeric signalling platform that requires both a priming and activation step to ultimately cause the production of the pro-inflammatory cytokines IL-18 and IL-1β. At baseline, inflammasome subunits (NLRP3, ASC and caspase-1) and the pro-forms of IL-1β and IL-18 are expressed at low levels to prevent aberrant activation and autoinflammation but are upregulated in response to priming stimuli [30] This priming step involves activation of the nuclear factor κB (NFκB) transcription pathway via toll like receptor (TLR) 4 activation, lipopolysaccharides from gram positive bacteria, or endogenous factors including hyaluronan, biglycan, low density lipoproteins and heat shock proteins.[31] Alternatively, IL-1β or tumour necrosis factor (TNF)-α -mediated signalling can also induce the NFκB transcription pathway to cause inflammasome activation.[30]

Following inflammasome priming, activation of the inflammasome requires the oligomerisation of the inflammasome subunits NLRP3, ASC, and pro-caspase-1, into a multimeric platform that ultimately results in the autocleavage of pro-caspase-1 into its active form (Figure 6.3).[32] Caspase-1 then cleaves pro-IL-18 and pro-IL-1β into their

mature forms (Figure 6.3).[32, 33] Unlike the signals for inflammasome priming, which are detected by pattern recognition receptors (PRRs) on the cell surface, inflammasome activation occurs after the detection of either pathogen associated molecular patterns (PAMPs) or endogenously produced danger associated molecular patterns (DAMPs) in the cytosol by the PRR domain of the NLRP3 subunit. In the context of chronic inflammation, danger signals generated in disease settings have been highlighted as the main culprits of NLRP3 inflammasome activation.

In CKD, several DAMPs have been proposed as activators of the inflammasome in kidney TECs, including uric acid, albumin, and glucose.[20, 34-38] Each of these DAMPs have been associated with either mitochondrial ROS production or potassium (K^+) efflux, leading to inflammasome activation. Indeed, *Tschopp & Schroder* proposed that the induction of these mechanisms is the unifying feature of DAMPs that causes inflammasome activation (Figure 6.3).[39]

Uric acid is increased in the serum of patients with CKD and may contribute to both the priming and activation of the inflammasome. Indeed, uric acid treatment was shown to increase expression of NLRP3 in human epithelial cells via TLR4.[34] Further studies in rats showed that uric treatment caused the expression of Caspase-1, and localisation of NLRP3 and ASC to the mitochondria and cellular matrix of TECs, which suggests that uric acid likely activates the inflammasome via the production of mitochondrial ROS formation.[35] Furthermore, in a model of streptozotocin-induced diabetic nephropathy, allopurinol treatment reduced serum uric acid levels and supressed the renal expression of inflammasome subunits (Figure 6.3).[40]

Albuminuria is a key feature of CKD, and is positively associated with increased renal expression of caspase-1, IL-1β and IL-18 in nephritic patients.[36, 37] *In vitro,* bovine serum albumin treatment causes the maturation of caspase-1, IL-1β and IL-18 in TECs,[36] whilst NLRP3 and caspase-1 deficiency confers protection against kidney injury in a mouse model

of albumin overload.[37] NLRP3 and caspase-1$^{-/-}$ mice were also protected from mitochondrial dysfunction in this albumin overload model, and protection from albumin-induced mitochondrial damage was confirmed using NLRP3 silencing RNA to inhibit the inflammasome in TECs *in vitro* (Figure 6.3).[37]

High glucose has also been shown to activate the inflammasome, likely via a P2X4 receptor-dependent mechanism.[38] P2X4 expression in TECs was positively correlated with urinary levels of IL-18 and IL-1β in patients with type 2 diabetes mellitus (T2DM)-related nephropathy, and further *in vitro* experiments revealed that inflammasome activation in glucose-treated TECs was suppressed with P2X4 inhibition. [38] Inflammasome activation in this model is likely due to K^+ efflux via the P2X4 receptor (Figure 6.3).[38]

In the current study, we demonstrated that urinary albumin was elevated in wild type mice by 1-week post-1K/DOCA/salt-treatment. However, urinary albumin was not elevated in IL-18$^{-/-}$ mice treated with 1K/DOCA/salt, so it is unclear whether albumin precedes inflammasome activation or is a product of IL-18-induced kidney injury. While it is evident that TEC-derived IL-18 is crucial to the development of kidney inflammation, fibrosis, and dysfunction in the 1K/DOCA/salt model of hypertension and CKD, we have not evaluated the stimulus for IL-18 production by TECs. Future studies should focus on uncovering which DAMP activates the inflammasome in TECs to cause the production of IL-18. This information could help to develop biomarkers to predict IL-18 production and kidney injury, and to inhibit inflammasome activation upstream of IL-18 production in order to prevent or reverse kidney injury and inflammation.

While the question of whether IL-18 could be used as a blood or urine biomarker of hypertension and hypertension-related kidney damage is an interesting and important one, this study was not designed to test this. Rather, the aim of this study was to determine if IL-18 plays a pathogenic role in hypertension and kidney disease and could thus represent a therapeutic target. Future studies that establish a time course analysis of IL-18 expression

in the kidneys would also be worthwhile but would require a different study design and large numbers of mice that would need to be killed at various timepoints.

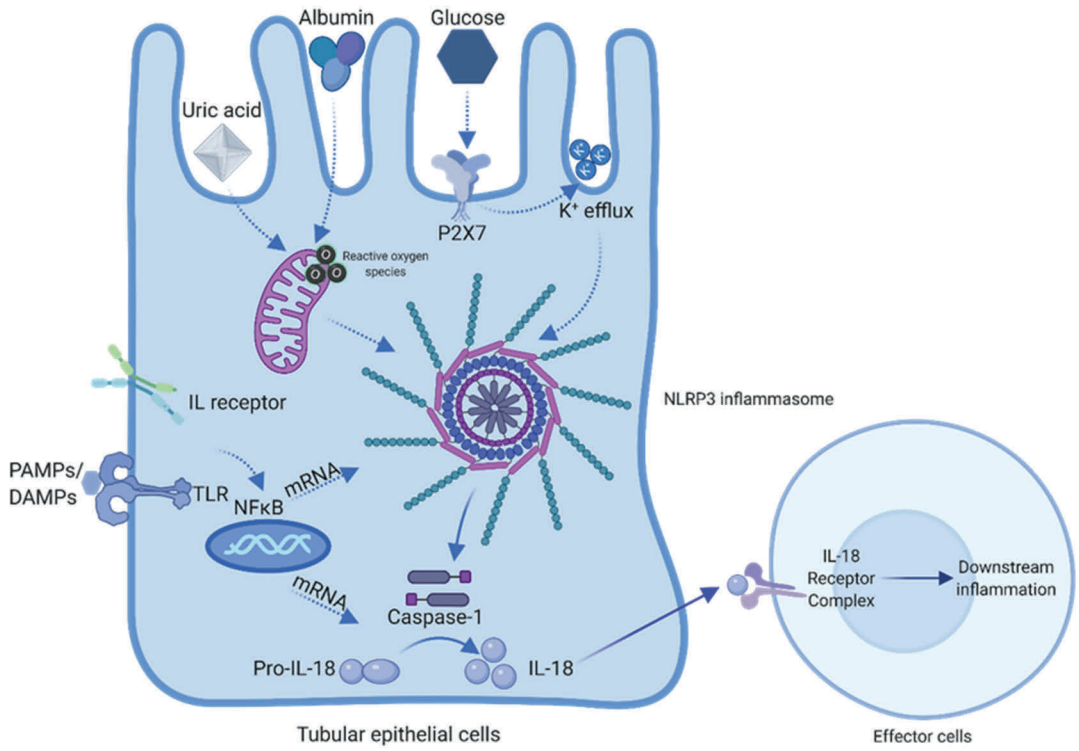

Figure 6.3 Schematic representation of DAMPs/PAMPs that initiate inflammasome activation in tubular epithelial cells (TECs). Inflammasomes are comprised of a pattern recognition receptor (PRR) domain, the adapter protein ASC and pro-caspase 1. Danger signals or danger associated molecular patterns (DAMPs), including uric acid, albumin, and glucose, cause mitochondrial ROS production or potassium (K^+) efflux which initiate inflammasome activation in TECs. This causes the production of mature IL-18. Created with BioRender.com.

6.4 Potential mechanisms for IL-18-mediated Na^+ reabsorption and increase in BP

In Chapter 3, we demonstrated that IL-18 is a key mediator of renal inflammation in 1K/DOCA/salt-treated mice. However, the key questions that remain are (1) is this renal inflammation a cause of the ensuing hypertension and, if so, (2) what are the mechanisms involved? Recent evidence has emerged to suggest that IL-18 and IL-1β, and pro-inflammatory cytokines produced downstream thereof, including IFN-γ, IL-6 and IL-17, can modulate sodium (Na^+) reabsorption in the kidneys (Figure 6.4).

Both the inflammasome derived-cytokine IL-1β, and the product of IL-1β signalling, IL-6, have been implicated in the development of hypertension and increased Na^+ reabsorption by the kidney. Our lab has previously demonstrated that inhibition of IL-1 receptor (IL-1R1) signalling using the receptor antagonist anakinra is effective at reducing 1K/DOCA/salt-induced high BP.[41] Similarly, Zhang *et al.* showed that IL-1R1-deficiency and inhibition were effective at lowering angiotensin II-induced high BP.[42] These authors also demonstrated that the BP-lowering effect of IL-1R1-deficiency was at least partly due to the inhibition of IL-1R1 signalling on nitric oxide (NO)-producing macrophages, which prevents their maturation and hence the production of NO in the kidney. Nitric oxide has been shown to inhibit Na^+ reabsorption in the kidney by supressing the activity of the sodium-potassium-two chloride (NKCC2) cotransporters in the loop of Henle.[42] Therefore, IL-1R1 inhibition appears to facilitate increased production of NO by macrophages in the kidney, thus preventing the reabsorption of Na^+ in the loop of Henle that contributes to high BP (Figure 6.4).[42]

IL-6 can also be produced as a result of IL-1β signalling, and both genetic ablation and pharmacological inhibition of IL-6 have been demonstrated to afford protection against the development of high BP and kidney dysfunction in pre-clinical models of hypertension.[43, 44] *In vitro* administration of IL-6 caused increased expression of the epithelial sodium

channel (ENaC) on mouse collecting duct cells and was also shown to activate this Na^+ reabsorbing channel.[45] IL-6 may also contribute to Na^+ reabsorption indirectly via angiotensin II, as IL-6 is able to stimulate the production of the angiotensin II precursor angiotensinogen *in vitro* (Figure 6.4).[46]

Likewise, previous studies have suggested that the classical IL-18-derived cytokine IFN-γ, and IL-17 which is produced downstream of IL-18 in $CD4^+$ T cells and γδ-T cells,[47] may promote Na^+ and water retention in the kidneys and in so doing give rise to hypertension. In a model of angiotensin II induced hypertension, IFN-$\gamma^{-/-}$ mice were protected from the development of high BP and reabsorbed less Na^+ and water in response to a saline challenge than WT mice.[48] Further investigation revealed that IFN-$\gamma^{-/-}$ mice had reduced expression of sodium/hydrogen exchanger 3 (NHE3) in their proximal tubules, and equivalent reductions in NKCC2 and NCC in their distal tubules, which together likely contributed the enhanced excretion of water and Na^+ in these mice.[48] Also, IFN-γ stimulation of proximal tubule cells can cause the production of angiotensinogen, which could indirectly modulate Na^+ and water retention (Figure 6.4).[49]

Similar to observations in IFN-$\gamma^{-/-}$ mice, IL-$17^{-/-}$ mice were shown to be afforded protection against angiotensin II-induced hypertension,[50] and Na^+ and water reabsorption. In WT mice, renal expression of NHE3 was increased following 2 weeks of angiotensin II treatment, with further increases in NCC and ENaC activity after 4 weeks of angiotensin II treatment.[48] These increases in NHE3, NCC and ENaC were blunted in IL-$17^{-/-}$ mice. [48] Further *in vitro* experiments revealed that these IL-17-dependent increases in expression and activity of NHE3 and NCC in kidney tubule cells were mediated via phosphorylation of serum- and glucocorticoid-regulated kinase 1 (SGK1; Figure 6.4).[51]

Our findings in IL-18R$1^{-/-}$ mice and mice with T cell restricted IL-18R1-deficiency support a role for the contribution of IFN-γ downstream of IL-18 signalling to sodium handling in 1K/DOCA/salt-induced hypertension. BP is reduced in these settings of IL-18R1

deficiency even though these mice are still susceptible to T cell recruitment in the kidney to the same or greater extent than in WT mice. Although there is still T cell infiltration, we did not measure function of these T cells (i.e., IFN- γ production) and this difference in function could account for the reduction in BP independent of kidney inflammation. Kidney inflammation could also be explained in these mice due to the removal of the additional anti-inflammatory pathway in mice that are IL-18R1 deficient. Future studies should focus on whether T cell function, i.e., IFN- γ production, is altered in these mice, and whether this contributes to the protection from elevated BP that we observe in global and T cell specific IL-18R1 deficiency.

The previous discussion suggests that the pro-hypertensive effects of IL-18 in the 1K/DOCA/salt model could have been mediated indirectly via the actions of its downstream pro-inflammatory cytokines IFN-γ and IL-17a on renal Na transport mechanisms, or directly via its interactions with the IL-18R1-NCC complex (Figure 6.4).[20, 21] While we did not measure NCC localisation or expression in the current study, investigation of the localisation and expression profile of this transporter in 1K/DOCA/salt-treated IL-18$^{-/-}$ mice should be explored in future studies. Furthermore, this thesis focussed on the role of IL-18 in the kidneys during hypertension, and although we saw no evidence of IL-18 localisation to vascular structures within this organ, we cannot rule out the possibility that hypertension is associated with upregulation of IL-18 in non-immune cell types in other blood pressure-regulating organs.

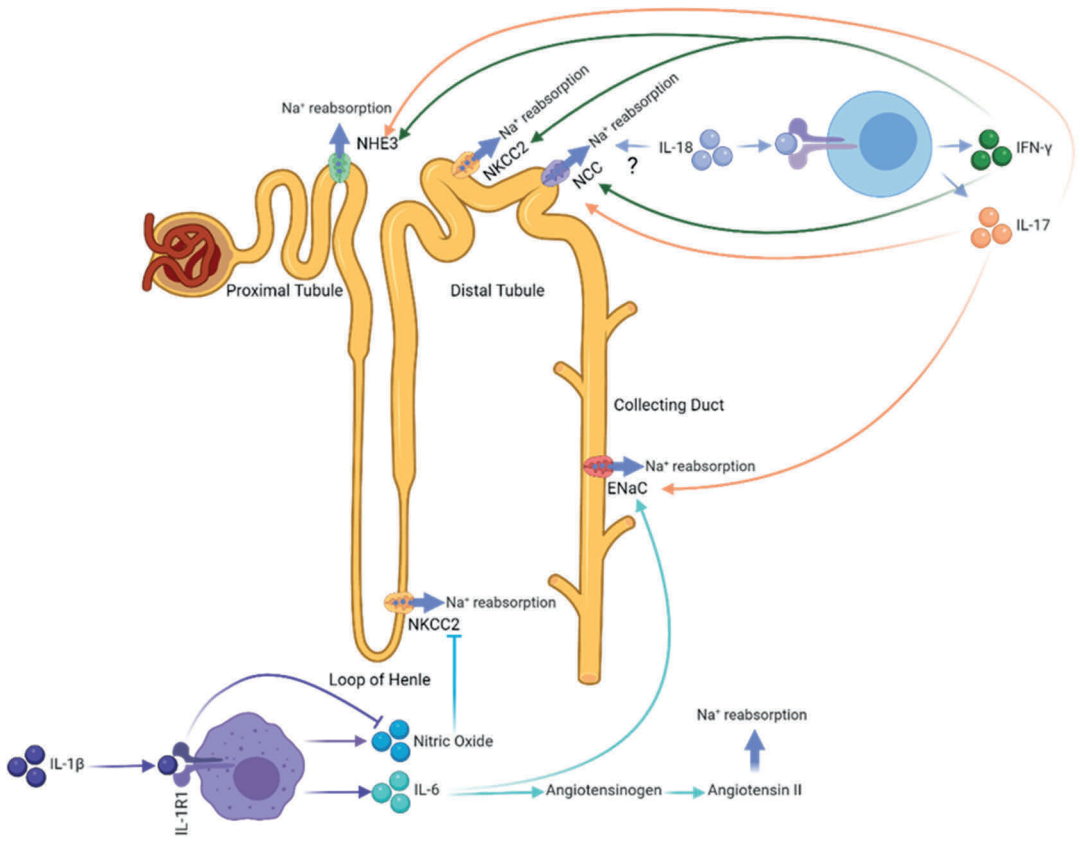

Figure 6.4 Mechanisms by which pro-inflammatory cytokines regulate sodium (Na+) reabsorption in the kidney. Pro-inflammatory cytokines IL-1β, IL-6, IFN-γ and IL-17 have all been demonstrated to regulate Na+ reabsorption in the kidney in experimental models of hypertension. This occurs via sodium-potassium-two chloride (NKCC2) cotransporter, sodium chloride cotransporter (NCC), epithelial sodium channel (ENaC) and sodium/hydrogen exchanger 3 (NHE3) channels along the nephron. Created with BioRender.com.

6.5 Inhibition of IL-18

The data presented in this thesis, combined with previous findings from our lab, suggests that pharmacological inhibition of IL-18, or inhibition of IL-18 production, could be an effective target for reducing BP and end organ damage in hypertension and CKD. Future studies in our lab will investigate whether inhibition of IL-18 with a neutralising monoclonal antibody (mAb), in mice with established hypertension and kidney injury (i.e., reflecting the clinical situation where patients present with established disease) can halt or reverse cardiovascular and renal damage. In these studies, it will be imperative to establish the extent of 1K/DOCA/salt-induced kidney injury just prior to initiation of anti-IL-18 mAb therapy (i.e., the baseline level of damage) and the ideal timeframe for commencing anti-IL-18mAb treatment (i.e., whether this is upon diagnosis of hypertension/kidney damage or when urinary or circulating IL-18 levels are increased). Furthermore, it will be important to measure kidney function using sensitive measures that are translatable to human studies. For example, serum creatinine (SCr) and glomerular filtration rate (GFR) are commonly used measures for assessing kidney function in humans,[52] and inclusion of these measures in assessing the efficacy of pharmacological inhibition of IL-18 in preclinical studies could provide insight into the translatability of this therapy for use in the treatment of CKD.

Although, IL-18 levels in the serum and urine are becoming recognised as biomarkers for kidney damage in clinical trials in patients with CKD and T2DM (details available at: www.clinicaltrials.gov NCT02251431, NCT02933827, NCT03865407, NCT04413266), no studies have investigated whether pharmacological inhibition of IL-18 is effective at reducing BP and kidney injury in hypertensive patients, or patients with CKD. Phase I/IIa clinical trials investigating agents that neutralise the effects of IL-18 inhibitors — including an anti-IL-18 mAb (GSK1070806) and the recombinant IL-18BP, Tadekinig alfa — in disease settings such as T2DM, delayed graft function (DGF) following kidney transplant, Crohn's disease, and X-linked inhibitor of apoptosis (XIAP) deficiency and Adult-onset

Still's disease, have so far mainly focussed only on assessing the safety of these compounds (details available at: www.clinicaltrials.gov NCT02398435, NCT03681067, NCT03512314, NCT01648153).[53-55] In most instances the IL-18 inhibitory agents were reported to be well tolerated. Of note, in patients with T2DM, no overall changes in BP were reported following anti-IL-18 mAb treatment.[54] However, this trial was only powered to assess the safety profile of the compound, and not efficacy in terms of BP lowering or renal protection.[54] In kidney transplant recipients, GSK1070806 was administered post-transplant to prevent DGF — an AKI insult that can result in early graft loss — the phase IIa clinical trial was terminated early because serum levels of IL-18 were elevated, there were instances of adverse events, and > 50% of the patient population developed DGF which exceeded the expected rate of DGF.[55] Therefore, the trial was discontinued before it reached statistical power.[55] Hence, further studies are required to assess the effectiveness of inhibiting IL-18 to reverse high BP and kidney inflammation in CKD.

Previous studies in our lab demonstrated that the small molecule NLRP3 inhibitor, MCC950, is effective in reducing kidney inflammation, reversing elevated BP and ameliorating renal dysfunction in mice with established 1K/DOCA/salt-dependent hypertension.[56] Although MCC950 had also shown efficacy in preclinical models of disease, including cardiovascular diseases such as: atherosclerosis, myocardial infarction and diabetes-induced atherosclerosis,[57-66] clinical trials for rheumatoid arthritis using MCC950 (then named CRID3) were terminated in Phase I due to its hepatotoxic effects.[67] In fact, a total of 9 structurally and/or mechanistically distinct inflammasome inhibitors are either currently in Phase I-II clinical trials or have been examined in clinical trials previously, in a wide range of inflammatory disease. These inhibitors and their mechanisms are summarised in Table 6.1.

Table 6.1 Drugs that inhibit inflammasome activity

Compound name	Mechanism	Disease context	Clinical trial number
IZD334	MCC950-related[67]	Cardiovascular disease (trial terminated October 2020)	EudraCT-2020-000942-32
		Cryoporin-associated periodic syndrome	NCT04086602
Inzomelid	MCC950-related[67]	Cryoporin-associated periodic syndrome	NCT04015076
Tranilast	Prevents NLRP3 oligomerisation by acting on ATP-ase in NACHT domain[68]	Cryoporin-associated periodic syndrome	NCT03923140
glyburide	Inhibits NLRP3 downstream of P2X7 receptor[69]	Traumatic brain injury	NCT01454154
MCC950	Targets ATP binding pocket of NACHT domain in NLRP3[70]	Discontinued due to liver toxicity in Phase I	
VX-765	Inhibits Caspase-1[71]	Resistant partial epilepsy, terminated due to hepatotoxicity	NCT01501383
depansutrile (OLT1177)	Prevents NLRP3 oligomerisation[72]	Acute gout	NCT02134964
Somalix	MCC950-related, peripherally distributed	Arthritis and cardiovascular disease	unlisted
IFM-2427	undisclosed	Gout, atherosclerosis, and non-alcoholic steatohepatitis (NASH)	

The majority of inflammasome inhibitors currently being trialled target the NACHT domain of the NLRP3 inflammasome, and prevent oligomerisation of the inflammasome,[67] thus preventing the downstream production of pro-inflammatory cytokines IL-1β and IL-18.[73] This includes three MCC950-related compounds. One of these, IZD334, was

withdrawn from a trial in a cohort of patients at high-risk of cardiovascular disease due to coronary artery disease (details available at: www.clinicaltrialsregister.eu EudraCT-2020-000942-32). Of the other two, Inzomelid remains under investigation in a clinical trial on patients with the inflammatory disease cryoporin-associated periodic syndrome (details available at: www.clinicaltrials.gov NCT04086602), while Somalix is in an ongoing Phase I clinical trial, with the intention to use this compound in patients with arthritis and cardiovascular disease.[74] Overall, there have been no studies to date investigating inflammasome inhibitors in patients with hypertension or kidney disease, and for that matter, no reports on whether these compounds influence BP or renal function in other disease states. The announcement that Somalix will be assessed for its effectiveness in treating patients with cardiovascular disease is exciting, as it is highly likely that BP and possibly kidney function — both major risk factors for cardiovascular disease[75, 76] — will be included as end point measures. Therefore, we should have a better understanding of whether blocking inflammasome activity, and by extension the production of IL-18, reduces BP and improves kidney function in the very near future.

6.6 Overall conclusion

The work presented in this thesis provides strong evidence that IL-18, produced by renal tubular epithelial cells, ~~and~~ acting via a non-cognate signalling mechanism that is independent of IL-18RAP, plays a crucial role in the development of high BP, kidney inflammation, dysfunction and fibrosis in a volume-overload, low-renin model of hypertension and kidney injury. Our findings suggest that targeting IL-18 directly with pharmacological therapies that neutralise its activity (such as with recombinant human IL-18BP or anti-IL-18 mAbs) or by inhibiting its production by blocking inflammasome activity has the potential for future use in the treatment of hypertension and kidney inflammation. Future studies aimed at characterising the non-cognate signalling pathway

activated by IL-18 in the kidneys during the development of hypertension, may reveal further targets for future therapies.

6.7 References

1. Liang D, Liu HF, Yao CW, Liu HY, Huang-Fu CM, Chen XW, Du SH and Chen XW. Effects of interleukin 18 on injury and activation of human proximal tubular epithelial cells. *Nephrology*. 2007;12:53-61.

2. Wu H, Craft ML, Wang P, Wyburn KR, Chen G, Ma J, Hambly B and Chadban SJ. IL-18 contributes to renal damage after ischemia-reperfusion. *J Am Soc Nephrol. : JASN*. 2008;19:2331-2341.

3. Franke EI, Vanderbrink BA, Hile KL, Zhang H, Cain A, Matsui F and Meldrum KK. Renal IL-18 production is macrophage independent during obstructive injury. *PLoS One*. 2012;7:e47417.

4. VanderBrink BA, Asanuma H, Hile K, Zhang H, Rink RC and Meldrum KK. Interleukin-18 stimulates a positive feedback loop during renal obstruction via interleukin-18 receptor. *J Urol*. 2011;186:1502-8.

5. Bani-Hani AH, Leslie JA, Asanuma H, Dinarello CA, Campbell MT, Meldrum DR, Zhang H, Hile K and Meldrum KK. IL-18 neutralization ameliorates obstruction-induced epithelial-mesenchymal transition and renal fibrosis. *Kidney Int*. 2009;76:500-11.

6. Parikh CR, Jani A, Melnikov VY, Faubel S and Edelstein CL. Urinary interleukin-18 is a marker of human acute tubular necrosis. *Am J Kidney Dis*. 2004;43:405-14.

7. Faust J, Menke J, Kriegsmann J, Kelley VR, Mayet WJ, Galle PR and Schwarting A. Correlation of renal tubular epithelial cell-derived interleukin-18 up-regulation with disease activity in MRL-Faslpr mice with autoimmune lupus nephritis. *Arthritis Rheum*. 2002;46:3083-95.

8. Rex DAB, Agarwal N, Prasad TSK, Kandasamy RK, Subbannayya Y and Pinto SM. A comprehensive pathway map of IL-18-mediated signalling. *J Cell Commun Signal*. 2020;14:257-266.

9. Rabkin SW. The role of interleukin 18 in the pathogenesis of hypertension-induced vascular disease. *Nat Clin Pract Cardiovasc Med*. 2009;6:192-9.

10. Wyburn K, Wu H, Chen G, Yin J, Eris J and Chadban S. Interleukin-18 affects local cytokine expression but does not impact on the development of kidney allograft rejection. *Am J Transplant*. 2006;6:2612-21.

11. Nozaki Y, Kinoshita K, Yano T, et al. Signaling through the interleukin-18 receptor α attenuates inflammation in cisplatin-induced acute kidney injury. *Kidney Int*. 2012;82:892-902.

12. Nozaki Y, Hino S, Ri J, Sakai K, Nagare Y, Kawanishi M, Niki K, Funauchi M and Matsumura I. Lipopolysaccharide-Induced Acute Kidney Injury Is Dependent on an IL-18 Receptor Signaling Pathway. *Int J Mol Sci*. 2017;18:2777.

13. Nold-Petry CA, Lo CY, Rudloff I, et al. IL-37 requires the receptors IL-18Rα and IL-1R8 (SIGIRR) to carry out its multifaceted anti-inflammatory program upon innate signal transduction. *Nat Immunol*. 2015;16:354-65.

14. Gong J, Wei T, Stark RW, Jamitzky F, Heckl WM, Anders HJ, Lech M and Rössle SC. Inhibition of Toll-like receptors TLR4 and 7 signaling pathways by SIGIRR: A computational approach. *J Struct Biol*. 2010;169:323-330.

15. Yang Y, Zhang Z-X, Lian D, Haig A, Bhattacharjee RN and Jevnikar AM. IL-37 inhibits IL-18-induced tubular epithelial cell expression of pro-inflammatory cytokines and renal ischemia-reperfusion injury. *Kidney Int*. 2015;87:396-408.

16. Liang D, Liu HF, Yao CW, Liu HY, Huang-Fu CM, Chen XW, Du SH and Chen XW. Effects of interleukin 18 on injury and activation of human proximal tubular epithelial cells. *Nephrology*. 2007;12:53-61.

17. Fortin CF, Ear T and McDonald PP. Autocrine role of endogenous interleukin-18 on inflammatory cytokine generation by human neutrophils. *FASEB J*. 2009;23:194-203.

18. Born TL, Thomassen E, Bird TA and Sims JE. Cloning of a novel receptor subunit, AcPL, required for interleukin-18 signaling. *J Biol Chem*. 1998;273:29445-50.

19. Debets R, Timans JC, Churakowa T, et al. IL-18 Receptors, Their Role in Ligand Binding and Function: Anti-IL-1RAcPL Antibody, a Potent Antagonist of IL-18. *J Immunol*. 2000;165:4950.

20. Wang J, Sun C, Gerdes N, et al. Interleukin 18 function in atherosclerosis is mediated by the interleukin 18 receptor and the Na-Cl co-transporter. *Nat Med*. 2015;21:820-826.

21. Liu CL, Ren J, Wang Y, et al. Adipocytes promote interleukin-18 binding to its receptors during abdominal aortic aneurysm formation in mice. *Eur Heart J*. 2020;41:2456-2468.

22. Bostanjoglo M, Reeves WB, Reilly RF, et al. 11Beta-hydroxysteroid dehydrogenase, mineralocorticoid receptor, and thiazide-sensitive Na-Cl cotransporter expression by distal tubules. *J Am Soc Nephrol*. 1998;9:1347-58.

23. Parikh CR, Mishra J, Thiessen-Philbrook H, Dursun B, Ma Q, Kelly C, Dent C, Devarajan P and Edelstein CL. Urinary IL-18 is an early predictive biomarker of acute kidney injury after cardiac surgery. *Kidney Int*. 2006;70:199-203.

24. Washburn KK, Zappitelli M, Arikan AA, Loftis L, Yalavarthy R, Parikh CR, Edelstein CL and Goldstein SL. Urinary interleukin-18 is an acute kidney injury biomarker in critically ill children. *Nephrol Dial Transplant*. 2008;23:566-72.

25. Krishnan SM, Dowling JK, Ling YH, et al. Inflammasome activity is essential for one kidney/deoxycorticosterone acetate/salt-induced hypertension in mice. *Br J Pharmacol*. 2016;173:752-65.

26. Komada T, Chung H, Lau A, Platnich JM, Beck PL, Benediktsson H, Duff HJ, Jenne CN and Muruve DA. Macrophage Uptake of Necrotic Cell DNA Activates the AIM2 Inflammasome to Regulate a Pro-inflammatory Phenotype in CKD. *J Am Soc Nephrol*. 2018;29:1165-1181.

27. Kim SM, Lee SH, Kim YG, et al. Hyperuricemia-induced NLRP3 activation of macrophages contributes to the progression of diabetic nephropathy. *Am J Physiol Renal Physiol*. 2015;308:F993-f1003.

28. Kadoya H, Satoh M, Sasaki T, Taniguchi S, Takahashi M and Kashihara N. Excess aldosterone is a critical danger signal for inflammasome activation in the development of renal fibrosis in mice. *FASEB J*. 2015;29:3899-910.

29. Shirasuna K, Karasawa T, Usui F, et al. NLRP3 Deficiency Improves Angiotensin II-Induced Hypertension But Not Fetal Growth Restriction During Pregnancy. *Endocrinology*. 2015;156:4281-92.

30. Bauernfeind FG, Horvath G, Stutz A, et al. Cutting edge: NF-kappaB activating pattern recognition and cytokine receptors license NLRP3 inflammasome activation by regulating NLRP3 expression. *J Immunol* 2009;183:787-791.

31. Brubaker SW, Bonham KS, Zanoni I and Kagan JC. Innate immune pattern recognition: a cell biological perspective. *Annu Rev Immunol*. 2015;33:257-290.

32. Schroder K and Tschopp J. The inflammasomes. *Cell*. 2010;140:821-32.

33. Martinon F and Tschopp J. Inflammatory caspases and inflammasomes: master switches of inflammation. *Cell Death Differ*. 2007;14:10-22.

34. Xiao J, Zhang XL, Fu C, Han R, Chen W, Lu Y and Ye Z. Soluble uric acid increases NALP3 inflammasome and interleukin-1β expression in human primary renal proximal tubule epithelial cells through the Toll-like receptor 4-mediated pathway. *Int J Mol Med*. 2015;35:1347-54.

35. Romero CA, Remor A, Latini A, De Paul AL, Torres AI and Mukdsi JH. Uric acid activates NRLP3 inflammasome in an in-vivo model of epithelial to mesenchymal transition in the kidney. *J Mol Histol*. 2017;48:209-218.

36. Fang L, Xie D, Wu X, Cao H, Su W and Yang J. Involvement of endoplasmic reticulum stress in albuminuria induced inflammasome activation in renal proximal tubular cells. *PLoS One*. 2013;8:e72344.

37. Zhuang Y, Ding G, Zhao M, et al. NLRP3 inflammasome mediates albumin-induced renal tubular injury through impaired mitochondrial function. *J Biol Chem*. 2014;289:25101-11.

38. Chen K, Zhang J, Zhang W, Zhang J, Yang J, Li K and He Y. ATP-P2X4 signaling mediates NLRP3 inflammasome activation: a novel pathway of diabetic nephropathy. *Int J Biochem Cell Biol*. 2013;45:932-43.

39. Tschopp J and Schroder K. NLRP3 inflammasome activation: The convergence of multiple signalling pathways on ROS production? *Nat Rev Immunol*. 2010;10:210-5.

40. Wang C, Pan Y, Zhang Q-Y, Wang F-M and Kong L-D. Quercetin and allopurinol ameliorate kidney injury in STZ-treated rats with regulation of renal NLRP3 inflammasome activation and lipid accumulation. *PLoS One*. 2012;7:e38285-e38285.

41. Ling YH, Krishnan SM, Chan CT, et al. Anakinra reduces blood pressure and renal fibrosis in one kidney/DOCA/salt-induced hypertension. *Pharmacol Res*. 2017;116:77-86.

42. Zhang J, Rudemiller NP, Patel MB, et al. Interleukin-1 Receptor Activation Potentiates Salt Reabsorption in Angiotensin II-Induced Hypertension via the NKCC2 Co-transporter in the Nephron. *Cell Metab*. 2016;23:360-8.

43. Lee DL, Sturgis LC, Labazi H, Osborne JB, Jr., Fleming C, Pollock JS, Manhiani M, Imig JD and Brands MW. Angiotensin II hypertension is attenuated in interleukin-6 knockout mice. *Am J Physiol Heart Circ Physiol*. 2006;290:H935-40.

44. Hashmat S, Rudemiller N, Lund H, Abais-Battad JM, Van Why S and Mattson DL. Interleukin-6 inhibition attenuates hypertension and associated renal damage in Dahl salt-sensitive rats. *Am J Physiol Renal Physiol*. 2016;311:F555-61.

45. Li K, Guo D, Zhu H, Hering-Smith KS, Hamm LL, Ouyang J and Dong Y. Interleukin-6 stimulates epithelial sodium channels in mouse cortical collecting duct cells. *Am J Physiol Regul Integr Comp Physiol*. 2010;299:R590-5.

46. Satou R, Gonzalez-Villalobos RA, Miyata K, Ohashi N, Katsurada A, Navar LG and Kobori H. Costimulation with angiotensin II and interleukin 6 augments angiotensinogen expression in cultured human renal proximal tubular cells. *Am J Physiol Renal Physiol*. 2008;295:F283-9.

47. Lalor SJ, Dungan LS, Sutton CE, Basdeo SA, Fletcher JM and Mills KH. Caspase-1-processed cytokines IL-1beta and IL-18 promote IL-17 production by gammadelta and CD4 T cells that mediate autoimmunity. *J Immunol*. 2011;186:5738-48.

48. Kamat NV, Thabet SR, Xiao L, Saleh MA, Kirabo A, Madhur MS, Delpire E, Harrison DG and McDonough AA. Renal transporter activation during angiotensin-II

hypertension is blunted in interferon-γ-/- and interleukin-17A-/- mice. *Hypertension*. 2015;65:569-576.

49. Satou R, Miyata K, Gonzalez-Villalobos RA, Ingelfinger JR, Navar LG and Kobori H. Interferon-γ biphasically regulates angiotensinogen expression via a JAK-STAT pathway and suppressor of cytokine signaling 1 (SOCS1) in renal proximal tubular cells. *FASEB J*. 2012;26:1821-30.

50. Madhur MS, Lob HE, McCann LA, Iwakura Y, Blinder Y, Guzik TJ and Harrison DG. Interleukin 17 promotes angiotensin II-induced hypertension and vascular dysfunction. *Hypertension*. 2010;55:500-7.

51. Norlander AE, Saleh MA, Kamat NV, et al. Interleukin-17A Regulates Renal Sodium Transporters and Renal Injury in Angiotensin II-Induced Hypertension. *Hypertension*. 2016;68:167-174.

52. Nelson A, Mackinnon B, Traynor J and Geddes CC. The Relationship Between Serum Creatinine and Estimated Glomerular Filtration Rate: Implications for Clinical Practice. *Scott Med J*. 2006;51:5-9.

53. Gabay C, Fautrel B, Rech J, et al. Open-label, multicentre, dose-escalating phase II clinical trial on the safety and efficacy of tadekinig alfa (IL-18BP) in adult-onset Still's disease. *Ann Rheum Dis*. 2018;77:840-847.

54. McKie EA, Reid JL, Mistry PC, DeWall SL, Abberley L, Ambery PD and Gil-Extremera B. A Study to Investigate the Efficacy and Safety of an Anti-Interleukin-18 Monoclonal Antibody in the Treatment of Type 2 Diabetes Mellitus. *PLoS One*. 2016;11:e0150018.

55. Wlodek E, Kirkpatrick RB, Andrews S, et al. A pilot study evaluating GSK1070806 inhibition of interleukin-18 in renal transplant delayed graft function. *PLoS One*. 2021;16:e0247972.

56. Krishnan SM, Ling YH, Huuskes BM, et al. Pharmacological inhibition of the NLRP3 inflammasome reduces blood pressure, renal damage, and dysfunction in salt-sensitive hypertension. *Cardiovasc Res*. 2019;115:776-787.

57. Gordon R, Albornoz EA, Christie DC, et al. Inflammasome inhibition prevents α-synuclein pathology and dopaminergic neurodegeneration in mice. *Sci Transl Med*. 2018;10.

58. Voet S, Srinivasan S, Lamkanfi M and van Loo G. Inflammasomes in neuroinflammatory and neurodegenerative diseases. *EMBO Mol Med*. 2019;11.

59. Coll RC, Robertson AAB, Chae JJ, et al. A small-molecule inhibitor of the NLRP3 inflammasome for the treatment of inflammatory diseases. *Nat Med*. 2015;21:248-255.

60. van der Heijden T, Kritikou E, Venema W, van Duijn J, van Santbrink PJ, Slütter B, Foks AC, Bot I and Kuiper J. NLRP3 Inflammasome Inhibition by MCC950 Reduces Atherosclerotic Lesion Development in Apolipoprotein E-Deficient Mice-Brief Report. *Arterioscler Thromb Vasc Biol*. 2017;37:1457-1461.

61. van Hout GP, Bosch L, Ellenbroek GH, et al. The selective NLRP3-inflammasome inhibitor MCC950 reduces infarct size and preserves cardiac function in a pig model of myocardial infarction. *Eur Heart J*. 2017;38:828-836.

62. Primiano MJ, Lefker BA, Bowman MR, et al. Efficacy and Pharmacology of the NLRP3 Inflammasome Inhibitor CP-456,773 (CRID3) in Murine Models of Dermal and Pulmonary Inflammation. *J Immunol*. 2016;197:2421-33.

63. Perera AP, Fernando R, Shinde T, et al. MCC950, a specific small molecule inhibitor of NLRP3 inflammasome attenuates colonic inflammation in spontaneous colitis mice. *Sci Rep*. 2018;8:8618.

64. Dempsey C, Rubio Araiz A, Bryson KJ, et al. Inhibiting the NLRP3 inflammasome with MCC950 promotes non-phlogistic clearance of amyloid-β and cognitive function in APP/PS1 mice. *Brain Behav Immun*. 2017;61:306-316.

65. Sharma A, Choi JSY, Stefanovic N, et al. Specific NLRP3 Inhibition Protects Against Diabetes-Associated Atherosclerosis. *Diabetes*. 2020.

66. Qu J, Yuan Z, Wang G, Wang X and Li K. The selective NLRP3 inflammasome inhibitor MCC950 alleviates cholestatic liver injury and fibrosis in mice. *Int Immunopharmacol*. 2019;70:147-155.

67. Mullard A. NLRP3 inhibitors stoke anti-inflammatory ambitions. *Nat Rev Drug Discov*. 2019; 18:405-407.

68. Chauhan D, Vande Walle L and Lamkanfi M. Therapeutic modulation of inflammasome pathways. *Immunol Rev*. 2020;297:123-138.

69. Huang Y, Jiang H, Chen Y, et al. Tranilast directly targets NLRP3 to treat inflammasome-driven diseases. *EMBO Mol Med*. 2018;10.

70. Lamkanfi M, Mueller JL, Vitari AC, Misaghi S, Fedorova A, Deshayes K, Lee WP, Hoffman HM and Dixit VM. Glyburide inhibits the Cryopyrin/Nalp3 inflammasome. *J Cell Biol*. 2009;187:61-70.

71. Coll RC, Hill JR, Day CJ, et al. MCC950 directly targets the NLRP3 ATP-hydrolysis motif for inflammasome inhibition. *Nat Chem Biol*. 2019;15:556-559.

72. Maroso M, Balosso S, Ravizza T, Iori V, Wright CI, French J and Vezzani A. Interleukin-1β biosynthesis inhibition reduces acute seizures and drug resistant chronic epileptic activity in mice. *Neurotherapeutics*. 2011;8:304-315.

73. Marchetti C, Swartzwelter B, Gamboni F, et al. OLT1177, a β-sulfonyl nitrile compound, safe in humans, inhibits the NLRP3 inflammasome and reverses the metabolic cost of inflammation. *Proc Natl Acad Sci U S A*. 2018;115:E1530-e1539.

74. Coll RC, Robertson A, Butler M, Cooper M and O'Neill LAJ. The cytokine release inhibitory drug CRID3 targets ASC oligomerisation in the NLRP3 and AIM2 inflammasomes. *PLoS One*. 2011;6:e29539-e29539.

75. Nature Research Custom Media and The University of Queensland. Switching off chronic inflammation. [Advertisement] *Nature.* 2021.

76. Gansevoort RT, Correa-Rotter R, Hemmelgarn BR, Jafar TH, Heerspink HJ, Mann JF, Matsushita K and Wen CP. Chronic kidney disease and cardiovascular risk: epidemiology, mechanisms, and prevention. *Lancet*. 2013;382:339-52.

77. Global Burden of Metabolic Risk Factors for Chronic Diseases Collaboration. Cardiovascular disease, chronic kidney disease, and diabetes mortality burden of cardiometabolic risk factors from 1980 to 2010: a comparative risk assessment. *Lancet Diabetes Endocrinol*. 2014;2:634-647.